Hydraulics of Reservoir Sedimentation

October 1996

Author: Gerrit Roux Basson

Dissertation presented for the Degree of Doctor of Philosophy
at the University of Stellenbosch

Promoter: Professor A Rooseboom

Declaration

I, the undersigned, hereby declare that the work contained in this dissertation is my own original work and has not previously in its entirety or in part been submitted at any university for a degree.

26/11/96

DATE

SUMMARY

Reservoirs generally have a limited life span due to sedimentation. The replacement of lost storage capacity is a worldwide problem and the need therefore exists to limit reservoir sedimentation as much as possible.

The hydraulics of reservoir sedimentation has been studied in this dissertation. Since sediment transporting capacity is the dominant parameter in determining both sediment deposition and re-entrainment patterns, the theoretical analysis of turbulent suspended sediment and density current sediment transport processes has been studied in detail. The stream power theory provides the basis for accurate descriptions of all the hydraulic processes involved in reservoir sedimentation.

Key theoretical developments and findings from the study are:

- *A new sediment transport equation has been derived, based on applied stream power. Calibration and verification with laboratory, river and reservoir data has been carried out successfully. The new total load equation provides the interrelationship between sediment concentration, energy dissipation and bed roughness in the lower and upper flow regimes. Comparison of the prediction accuracy of the new sediment transport equation with other generally used equations, indicates a high degree of accuracy.*

- *A new bed roughness predictor has been developed, based on the new sediment transport equation.*

- *Non-uniform sediment transport processes and reservoir sediment deposition patterns were evaluated and found to be important as the sorting process is interrelated with re-entrainment, consolidation, cohesion etc.*

- *Non-equilibrium sediment transport of fine sediment was found to be very important in the accurate description of deposition processes. A new methodology, calibrated with canal and reservoir data, has been developed.*

- *The density current velocity, shear stress and suspended sediment distributions were described theoretically in terms of stream power principles. A mathematical expression for the layer thickness of a density current was calibrated with laboratory and field data.*

- *Sediment transport by means of density currents was verified with Chinese and South African reservoir data.*

- *The formation of a density current can be predicted in terms of the minimum stream power concept. Verification with laboratory data was successful.*

- *Density current velocities were described by using a Chezy type equation, which was calibrated with laboratory data.*

- *Densities of sediment deposits and consolidation of fine sediments were described by means of a new method, by combining the methods of Miller (1953) and Rooseboom (1975), as well as by incorporating an effective time approach to predict consolidation with variable sediment yield/deposition or erosion/re-entrainment rates.*

- *Width-depth relationships for South African reservoir flushing channels were found to be similar to those in China.*

- *Critical conditions for mass erosion of cohesive sediments can be related to shear strength, sediment density and clay content.*

- *By combining the theory in an existing mathematical model (MIKE 11), it is possible to model reservoir sedimentation comprehensively. Calibration and verification of the model for flood flushing at Welbedacht Reservoir were carried out successfully. Long-term sustainable reservoir capacities were also determined for changed reservoir operation rules and modified outlets.*

- *A database on reservoir sediment transport through a number of South African reservoirs was established. The data were obtained under conditions of flushing, sluicing and storage operation, while density current data were also gathered.*

OPSOMMING

Damme het 'n beperkte leeftyd as gevolg van toeslikking wat 'n wêreldwye probleem skep. Daar bestaan dus die behoefte om damtoeslikking te beperk.

Die hidroulika van damtoeslikking is in hierdie proefskrif bestudeer, met die klem op sedimentvervoer aangesien dit die dominante faktor is in damtoeslikkingprosesse. Turbulente gesuspendeerde sedimentvervoer sowel as digtheidstroming sedimentvervoer-prosesse is in detail ondersoek. Die stroomdrywingteorie vorm die basis vir die akkurate beskrywing van hidrouliese prosesse betrokke by damtoeslikking.

Die hoofresultate van die navorsing is:

- *'n Nuwe sedimentvervoerformule, gebaseer op aangewende stroomdrywing, is ontwikkel. Kalibrasie en stawing met laboratorium-, rivier- en damdata is suksesvol uitgevoer. Die nuwe sedimentvervoerformule beskryf die verwantskap tussen sedimentkonsentrasie, energiedissipering en bodemruheid, beide vir laer en hoër vloeiregimes. Vergelyking van die akkuraatheid van die nuwe vergelyking met die van ander algemeen gebruikte vergelykings, dui op die hoë relatiewe betroubaarheid.*

- *'n Nuwe bodemruheidvergelyking is ontwikkel wat op die nuwe sedimentvervoervergelyking gebaseer is.*

- *Nie-uniforme sediment-vervoerprosesse en sediment neerlating-prosesse is ontleed. Die belangrikheid van nie-uniforme sediment-vervoer en die verwantskap met sediment-kohesie, konsolidasie, uitskuring, ens. is bevestig.*

- *Nie-ewewigs sedimentvervoer van fyn sediment is ondersoek en het geblyk om baie belangrik in die akkurate beskrywing van sedimentneerlatingprosesse in damme te wees. 'n Nuwe metode is ontwikkel om nie-ewewigs sedimentvervoer te beskryf wat gekalibreer is met kanaal- en damdata.*

- *Die vloeisnelheid, sleurspanning en gesuspendeerde vertikale sedimentkonsentrasie verspreidings van 'n digtheidstroom is teoreties beskryf met stroomdrywingbeginsels. Die wiskundige beskrywing van diktes van digtheidstrome is met laboratorium- en damdata bevestig.*

- *Sedimentvervoer in digtheidstrome is met Chinese en Suid-Afrikaanse damdata geverifieer.*

- *Die vorming van 'n dighteidstroom kan beskryf word volgens die beginsel van minimum stroomdrywing, soos gestaaf met laboratoriumdata.*

- *Digtheidstrome se vloeisnelhede is beskryf met 'n Chezy-tipe vergelyking en gekalibreer met laboratoriumdata.*

- *Digthede en die konsolidasie van fyn sediment afsettings is beskryf met 'n nuwe metode soos ontwikkel uit die metodes van Miller (1953) en Rooseboom (1975). 'n Effektiewe tydskaal is ook gebruik om konsolidasie te voorspel met wisselende sedimentlewering/sedimentneerlating en erosie/uitskuringtempo's.*

- *Wydte-diepte-verhoudings vir Suid-Afrikaanse dam spoelkanale het ooreengestem met soortgelyke data vir Chinese damme.*

- *Kritiese toestande vir massa-uitskuring van kohesiewe sediment is in verband gebring met sediment-skeursterkte, - digtheid en -klei-inhoud.*

- *Die teorie is saamgevoeg in 'n bestaande rekenaarmodel (MIKE 11) wat dit moontlik maak om verskeie aspekte van damtoeslikking saam te ondersoek. Kalibrasie en stawing van die model is suksesvol uitgevoer vir sediment spoeling uit Welbedachtdam tydens vloedtoestande. Langtermyn damkapasiteite wat behou kan word onder veranderde bedryfstoestande en met aangepaste damuitlate is ook ontleed.*

- *'n Databasis vir sedimentvervoer deur damkomme is opgebou wat verskillende bedryfs- en vloedtoestande insluit.*

ACKNOWLEDGEMENTS

To complete a research project of this nature is impossible without the support of family, friends and colleagues, but above all the mercy of God, who opened the door to some of the mysteries of nature.

To my wife, Karin, and children, thank you very much for your support.

To my promoter, Professor Albert Rooseboom, thank you for stimulating my interest in hydraulics already at graduate level. The basic theory regarding stream power derived by prof. Rooseboom in 1975, formed the platform on which the theoretical developments of this dissertation were built.

I wish to thank the South African Water Research Commission for funding a research project from which data and information could be used for this dissertation.

The South African Department of Water Affairs (DWAF) played an instrumental role in the successful completion of this dissertation, and I wish to thank especially Dr JM Jordaan for his positive contributions.

I wish to express my gratitude to the many Regional Offices of the DWAF, together with the Phalaborwa Water Board, Umgeni Water Board, Tescor, Bloem Water Board, Ladysmith City Council, who were involved in field sampling, often under the most difficult conditions. In particular I want to thank Mr P Grobler, B Wallace and L van Oudtshoorn.

To the Institute of Geoscience who had to endure the winter temperatures of the Free State, thank you for an excellent job, especially with all the uncertainties that formed part of the core sampling.

Thanks are also due to the laboratories of the University of Stellenbosch and the Agricultural Research Institute for meticulously analysing thousands of samples.

A special thanks to the BKS Engineering team involved: Mrs F Jooste and S Whiteman (word processing), A van der Merwe (graphics), M Mertz for obtaining the literature from all over the world, and dr J Lourens for his inputs in the soil mechanical aspects. Mr EE Kuschke deserves a special thanks for his involvement in field work. A near accident such as almost washed over a waterfall, or bleeding hands could not stop him from continuing with the sampling programme. Without your support the excellent field database established would not be possible.

Prof D Wu of IRTCES, China, thank you for explaining the reservoir sedimentation problems encountered in China in great detail, and for providing invaluable information on density currents.

I also wish to acknowledge the excellent work done by dr Kim Wium Olesen of the Danish Hydraulic Institute, incorporating the theory into the MIKE 11 program so that various aspects of sedimentation could be tested jointly by using the model. I am also greatful for the Danish Hydraulic Institute for partially sponsoring the model changes.

Thanks are also due to dr Wolmarans of the University of Pretoria, involved in reviewing the statistical analyses.

KEYWORDS

Hydraulics; reservoir sedimentation; sediment transport; density current; sluicing; flushing; sediment deposition; cohesive sediment; non-cohesive sediment; re-entrainment; bedforms; retrogressive erosion.

CONTENTS

LIST OF FIGURES

LIST OF PHOTOGRAPHS

2071H/sw

LIST OF TABLES

DEFINITIONS

Sluicing

Sluicing is an operational technique whereby sediment-laden inflows are released through a reservoir before the sediment particles can settle, thereby reducing the sediment trap efficiency of the reservoir.

Flushing

Flushing during floods, or high flow periods during the rainy season, with water level drawdown, is used to re-entrain previously deposited sediments and to remove these sediments from the reservoir via (large) bottom outlets.

Density Current

Density currents associated with suspended sediment transport may develop under special conditions. A density current consists of the movement of a fluid, of higher density, underneath a fluid of lower density, through a reservoir.

Retrogressive erosion

During water level drawdown flood flushing, when critical conditions for mass erosion are exceeded, sediment is scoured and a flushing channel is eroded in an upstream direction, starting at the dam. The frontset slope within this channel is reduced to the original river bed slope under ideal conditions.

Turbulent transport

Transportation of sediment through turbulent suspension in open channel flow.

Reservoir trap efficiency

That percentage of the average sediment load which enters a reservoir that is trapped within the reservoir.

Colloidal sediment transport

Very small sediment particles which are electrically charged are kept in suspension due to these charges.

Sediment

Elements with higher densities than that of the transporting medium which can be entrained and transported by the given transporting medium.

LIST OF SYMBOLS

a	adaptation coefficient representing mean settling depth
α	dimensionless exponent
α	coefficient
A	coefficient used in Ackers and White equation
A	integration constant
A	channel cross-section area
b	constant
B	bed width of flushing channel
B	top width of flow
B_o	buoyancy flux
β	constant
βi	% of i-th sediment fraction in the bed
c	integration constant
c'	coefficient used in Ackers and White equation
C_{eq}	equilibrium concentration
C	sediment concentration
C_{vy}	average sediment concentration at a distance y above the bed (in percent by volume)
C_{eq}^*	relative equilibrium concentration
C_v	average sediment concentration
C_t	sediment concentration by weight
C_s	suspended sediment concentration
C_o	initial sediment concentration
C_{fo}	resistance coefficient
C_d	drag coefficient
C_i	actual sediment transport per fraction
C_{ci}	transport capacity of the i-th class
C_1	near bed sediment concentration
C_a	reference concentration
C^*	equilibrium sediment concentration
C_H	Chezy coefficient
C_b	bed load concentration
C''	Chezy type coefficient for density current
C_o	sediment concentration at the bed where $v = o$ at y_o
Δz	depth of recent deposits

d	sediment particle diameter
d_{90}	sediment size for which 90 % of particles is finer
d_{50}	median sediment particle size
d_{gr}	sediment particle size
d_s	representative particle size
δ_b	saltation height
D	flow depth
D	dispersion coefficient
D_*	dimensionless particle diameter
D1..4	density current layer depths
e_b	efficiency coefficient
ϵ	coefficient of turbulence exchange
η	parameter as function of sediment particle size, settling velocity and water viscosity
E	erosion rate
E	applied stream power
E	specific energy
E_o	empirical erosion rate coefficient
f	Lacey's silt factor
f	Darcy Weisbach resistance coefficient
f_k	resistance coefficient with equilibrium sediment transport
f_o	Darcy Weisbach resistance coefficient where $C_v = 0$
F	mean shear force
Fr	Froude number
Fr_D	densimetric Froude number
F_{gr}	mobility number
F_o	inflow Froude number
Fv_a	shear box power
g	gravitational acceleration
g'	gravitational acceleration adjusted for density difference ratio
γ'	specific weight of density current
γ	specific weight of water
γ_d	specific weight of deposits
γ_s	specific weight of sediment
G_{gr}	sediment transport function
h	depth of uniform density current flow
h	depth of water above density current

h'	density current depth
h_p	density current depth at plunge point
h_L	maximum climbing height of a density current
h_5	density current layer depth
h_o	density current depth at plunge point
h_n	depth of density current head
H	bed form height
H	depth of flushing channel
H	water depth
I	moment of inertia of element around axis 0
J_n	water surface slope
J_i	density current interface slope
J_o	density current bed slope
k	roughness coefficient
k_s	roughness coefficient
k_1	dimensionless coefficient
κ	Von Kármán coefficient
K_1, K_2	constants
K_T	reservoir capacity - sediment inflow ratio
K_3	constant related to sediment concentration
K,K_1,K_2	coefficient
K_W	reservoir capacity - inflow ratio
ℓ	Prandtl's mixing length
ℓ_o	mixing length
λ	rate of erosion
λ_m	mean friction coefficient of the underflow
λ_o; λ_i	coefficients of friction at bed and interface
L_i^*	adaptation length for each fraction
m	coefficient used in Ackers and White equation
m	coefficient related to sediment concentration
m	morphological channel stability coefficient
m_c	stable bank slope
μ	dynamic viscosity
η	coefficient of rigidity
M	constant
M	erosion rate

M	mass of element
υ	kinematic viscosity
n	coefficient used in Ackers and White equation
N	coefficient
p	total pressure
p_c, p_m, p_s	percentages of clay, silt and sand
ψ	suspension parameter correction coefficient
$\propto$	angle
$\propto$	empirical erosion rate coefficient
$\propto$	erosion constant
$\propto$	coefficient for non-equilibrium density current sediment transport
$\propto_1$; $\propto_2$	coefficients
$\propto_3$; $\propto_4$	constant and coefficient
$\propto_5$; $\propto_6$	constant and coefficient
P	wetted perimeter
P	applied power
q	discharge per unit width
q_{so}	sediment inflow per unit width
q_{st}	suspended load transport rate
q_t	total load transport rate
q_{bw}	bed load transport rate
q_T	total sediment load
q_{st}	sediment transport capacity
q_d, q_e	fluxes of deposition and erosion of sediment
q_s	sediment discharge per unit width
Q	flow rate
Q_s	total sediment discharge
r	ratio of predicted to observed sediment transport rate
r^2	correlation coefficient
ρgsv	unit input stream power
ρ_c, ρ_m, ρ_s	densities of clay, silt and sand fractions
ρ_T	sediment density after T years
ρ_s	sediment density
ρ_m	density of sediment laden water
ρ_2	density in density current
ρ_∞	long-term sediment density

ρ_o	initial sediment density
R_o	radius of eddies near bed
R	hydraulic radius
R_p	hydraulic radius at plunge point
s	slope
ss	sediment source/sink term
s_f	energy slope
s^*	sediment transport capacity
S_2	energy slope for sediment laden water
S_1	energy slope for clear water
s_o	bed slope
s_s	water surface slope
$\tan\alpha$	ratio of tangential shear to normal force
θ	coefficient used in Engelund Hansen equation
τ_{ce}	critical shear stress for surface erosion
τ	bed shear stress
τ_{cme}	critical bed shear stress for mass erosion
τ_o	bed shear stress
τ_*	shear velocity to the power 2
τ_o	shear stress at bed
$\tau\frac{dv}{dy}$	applied stream power
τ_i	shear resistance at the interface
τ_B	yield shear stress
τ_o	mean bed shear stress
τ_c	critical shear stress
τv	stream power
τ_{oc}	critical shear stress for incipient motion (Shields)
τ_o'	grain shear stress
T	time scale in non-equilibrium sediment transport
T	transport stage parameter
T	width
u_{bs}	particle velocity
u_g'	bed shear velocity
u_a	effective particle velocity at reference level a
u_g'	effective bed shear
$u_{f,cr}'$	Shields critical bed shear velocity

$\bar{u}$	average velocity in x direction
u',u''	first and second derivations of velocity
U_x,U_y	fluctuating components of velocity in x and transverse directions
U_x	mean shear velocity
u',v'	fluctuating part of velocities in the x and y directions
v	flow velocity
v_y	flow velocity at distance y above the bed
v_{max}	maximum flow velocity
v_p	velocity at plunge point
v_f	front velocity of a laminar density current
v_*	shear velocity
v_o	rotation centre point velocity
v_n	density current head (nose) velocity
$\bar{v}$	average flow velocity
vs_{cr}	critical input streampower for incipient motion
$\bar{v}s$	average input unit streampower
V	reservoir capacity
V_t	reservoir capacity after t years of operation
V_o	density current flow velocity at plunge point
w	particle settling velocity
w	distance from centre point of a sphere
w_{50}	settling velocity of median particle diameter
x	Einstein correction coefficient
y_1	distance from bed where laminar velocity distribution equals that of turbulent flow
y_o	mathematical distance from bed where flow velocity is zero
z	suspension theory coefficient
z_d	depth of previously deposited sediment
z_1	suspension theory coefficient as revised by Rooseboom (1975)
ζ	non-equilibrium sediment transport parameter

1. INTRODUCTION

1.1 The domain of this dissertation

This dissertation addresses the hydraulics of reservoir sedimentation. Sediment transport is the dominant parameter in reservoir sedimentation processes and is analysed in detail. Turbulent suspended sediment and density current sediment transport have been identified as the main sediment transport processes through reservoirs. Related to turbulent sediment transport is the description of bed roughness for different flow regimes and energy dissipation.

Non-uniform sediment transport and its importance in the sediment sorting process during sediment deposition processes is analysed. Non-equilibrium sediment transport of fine sediments is evaluated and calibrated with data.

Apart from depositional processes normally encountered in reservoir sedimentation, the hydraulics of sediment re-entrainment is analysed for non-cohesive and cohesive sediments including surface and mass erosion. The flood flushing channel shape determines the long-term reservoir capacity and the critical condition for mass erosion is used to describe the depth of scour. Width-depth relationships for the flushing channel are also evaluated.

Sediment density and consolidation are addressed for variable rates of sediment deposition and re-entrainment.

The vertical distribution of velocity, shear stress and sediment concentration of a density current are described mathematically. The formation of a density current, its velocity, sediment transport and venting through a dam, are analysed.

By integrating the various sedimentation processes in a mathematical model, the hydraulics of reservoir sedimentation can be evaluated comprehensively.

1.2 History of dam development and reservoir sedimentation

Water development through the construction of dams or weirs to regulate or divert river flows has been with us since the ancient civilisations before the time of Christ in China, Japan, the Middle East, Central and South America, and the Mediterranean *(Li Eding, 1987)*. It was, however, only after the turn of this century that reservoir construction escalated considerably on a worldwide scale. According to the ICOLD register, which started in 1950, the total number of registered large dams (dam heights > 15 m or capacity > 1 million m^3) increased from 5 268 in 1950 to 36 226 in 1986 **(Figure 1.2-1)**.

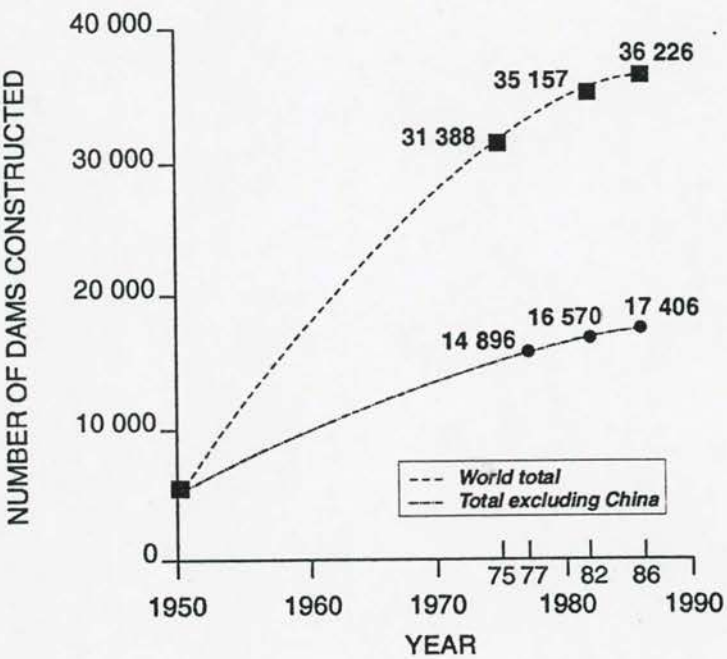

Figure 1.2 - 1 History of dam development

During the period 1950 to 1986, the annual growth rate of reservoirs world wide was 5,5 %. These statistics are, however, dominated by events in China, where dam construction experienced an enormous surge. Based on the ICOLD statistics, the average age of reservoirs is now estimated to be in the order of only 30 years. *(ICOLD, 1989)*

The problem of sedimentation had been encountered by river engineers even before the time of Christ. It would seem that engineers even then had a very good understanding of hydraulics and sedimentation; a number of hydraulic structures which were designed and constructed more than 2 200 years ago are still being operated successfully. One of the best examples of such a project is the Dujiangyan irrigation diversion scheme in China, which has operated within its design parameters of diverting 300 to 700 m^3/s of flows for irrigation whilst limiting sediment diversion, as the original design had envisaged. A physical model study of this project carried out in 1972 confirmed the original design parameters within an accuracy of 3 % . *(Xu Muju, 1990)*

At the beginning of the present century, a number of large dams were constructed such as Aswan Dam on the Nile River (1902) and Elephant Butte Dam on the Rio Grande (1916). By 1936, the seriousness of the sedimentation problem of reservoirs had been realised. *Stevens (1936)* wrote: "Man cannot hope to halt the processes of mountain erosion and plains building. The land he cultivates could not exist except for these forces. He must expect that rains will gully his fields, or cover them with debris, and that streams will continue to carry sediments that will fill the canals and reservoirs. An empire exists below the reservoir that has been created by the Elephant Butte Dam. The land is phenomenally rich. The reservoir ... is slowly being deprived of its ability to store water. Silt is being deposited at the rate of 20 000 acre-feet per year. Its original capacity will be so depleted in two or three generations that the civilisations now dependent on it will have to seek other sources of water supply and storage."

Referring to the Boulder Dam project, Stevens remarked:

"... Unless remedial measures are adopted, the reservoir will become virtually useless by the fifth generation. Fortunately, sites are available where other reservoirs may be constructed; and, after these are gone, others will undoubtedly be found ... but what of the ultimate future, when all available storage sites have been exhausted? Must these fertile areas revert,

ultimately, to the sage-brush and the cactus? Will sedimentation, that made possible this vibrant civilisation, ultimately sound its death knell? The menace exists, it is real, and unless something constructive can be evolved, civilisation in these regions must eventually decline."

An interesting array of attitudes towards the sedimentation problem were evidenced in the discussions to Steven's paper. Waggener proposed that "The answer to the question of preventing silting of a reservoir is to build another above it, to impound the silt." Bisschop, an irrigation engineer from South Africa, remarked that "There appears to be only one solution, namely to recognise frankly that some irrigation projects are doomed to a definite life span and will have to revert back to the original type and manner of flood irrigation ..." Bonner observed that "The capital outlays will be amortised long before sedimentation of the reservoirs seriously impairs their usefulness. When the time comes, any desirable restoration of capacity will be a problem for the engineer of that far distant day ..." O'Brien noted that "... the time may come when perhaps channels and other silt-controlling works, costing perhaps more than the dam itself, will be found to be economically justified."

Although the rate of dam construction seems to have levelled off slightly in recent years, the existing dams have become critical and essential elements in the different regional economies. Hydropower now accounts for 21 % of the world's electricity output, while storage reservoirs augment the cultivation of 17 % of the world's irrigated crop land, thus accounting for one third of the world's agricultural output *(Le Moigne, 1990; Postel, 1989)*.

1.3 Reservoir sedimentation rates

The estimate of global reservoir capacity loss due to sedimentation is 1% of the original capacity per annum, which converts into US $6 billion when expressed in terms of replacement cost *(Mahmood, 1987)*. In South Africa, *Jordaan (1989)*, found an annual sedimentation rate of 0,5%, which converts into the loss of roughly 150 million m^3 reservoir storage capacity each year. If a conservatively low estimate of the construction cost of large dams is taken as R2,00/m^3 of storage capacity, the annual loss of storage in South Africa amounts to R300 million (with many other indirect costs not even accounted for), which emphasises the seriousness of the problem. The current sedimentation status of a number of South African reservoirs most seriously affected are indicated in **Figures 1.3-1**. (The data used in **Figure 1.3-1** have been obtained from the South African Department of Water Affairs

and Forestry (DWAF) data base of reservoir basin surveys *(DWAF, 1995)* and it is possible that a number of especially smaller reservoirs not included in this data base have been affected even more by sedimentation).

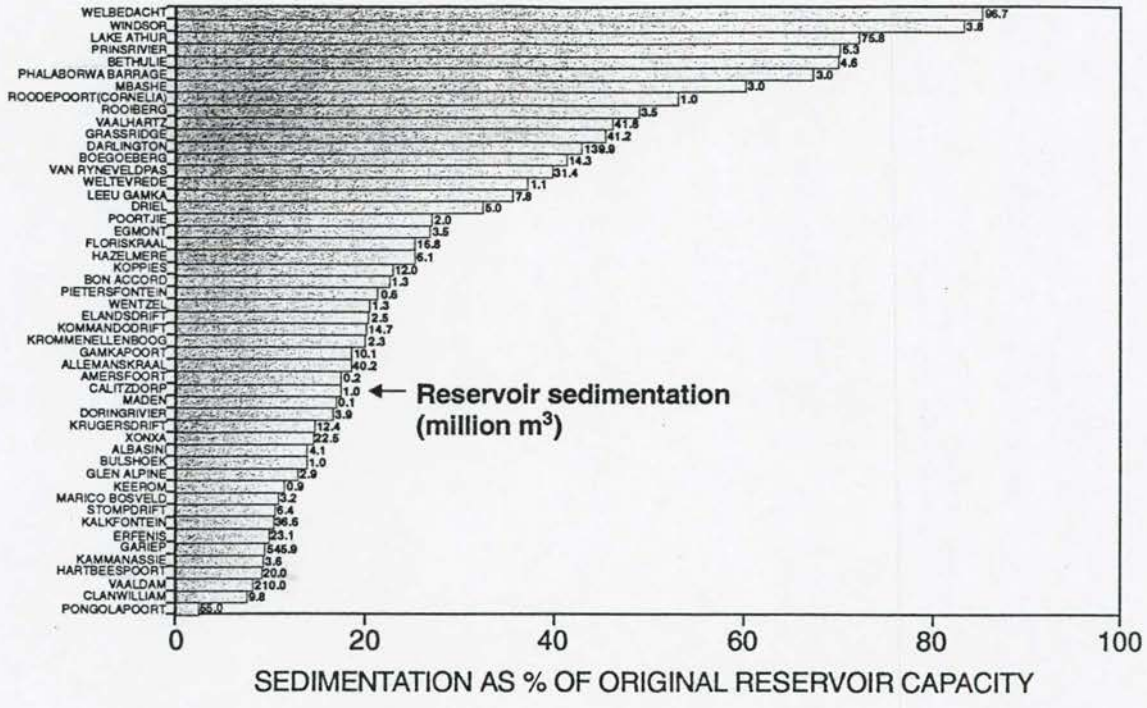

Figure 1.3 - 1 Reservoir sedimentation in South Africa

Worldwide, it has been found that reservoirs with small storage: run-off ratios in relatively small catchments in semi-arid areas with high sediment yield ratios are highly vulnerable to rapid sedimentation. The same is true in South Africa: the Mbashe weir in the Eastern Cape Province (former Transkei) silted up almost completely within 2 years after completion (*Wallace, 1994*), and the Welbedacht Reservoir on the Caledon River lost 85 % of its capacity within 20 years (*DWAF, 1996*).

Although the total capacity of small reservoirs (according to ICOLD classification) amounts to less than 20 % of the total estimated gross world capacity of 5 000 km^3, their estimated number of over 300 000 far outstrips that of the larger dams *(Delft, 1992)*.

1.4 Underestimation of sedimentation rates

Sediment yields can be determined based on long-term records of sediment loads in rivers, a database of reservoir basin surveys which is used to establish regional sediment yield maps, and/or modelling of the catchment erosion processes.

In the past, sedimentation has often been underestimated, which resulted in sediment problems being experienced in reservoirs long before their "economic life" had come to an end *(Smil, 1987; Goldsmith, 1985; Walling, 1989; Blanton, 1980)*.

In many reservoir designs the sedimentation aspect has been dealt with in a marginal manner. Engineering designs are still focused on the control of clean water rather than the sediment carried by the water, which is more difficult to predict and control. Reasons for reservoir sedimentation underestimates can be related to a number of "misconceptions and miscalculations" at the time of reservoir design, and can be grouped into sediment yield misjudgments and engineering problems.

Sediment yields have in the past been underestimated due to:

- small and short (or non-existent) data bases (derived from reservoir surveys and/or river sediment transport data)

- limited information on regional sediment yields linked to soil types, topography and other climatic variables;

- land use changes and increased erosion and sediment yields. In small catchments in the developing world, sediment yield increases of 4 % to 5 % per annum have been experienced due to informal settlements, overgrazing etc. Planning of water resources developments should be carried out with great care under these conditions.

Many engineering problems have occurred owing to incorrect prediction of reservoir sediment trap efficiency resulting from:

- overestimation of sediment transporting capacity through reservoirs,
- overestimation of the efficiency of outlet structures to sluice/flush sediment from reservoirs,
- changed operation during the life of reservoirs, and
- overestimation of the effectiveness of soil conservation schemes, especially in large catchments.

Most of the reservoir construction activity during this century has taken place in the so-called developing countries and outside the climatologically temperate zones. Many of these massive investments (dams are typically high-investment but low-maintenance structures) were undertaken after short study periods (*Bolton, 1984*). Often little time was allowed for proper hydrological studies as well as the more difficult question of sediment yield determination.

The massive and almost worldwide expansion of man-made reservoirs from the 1930s onwards was largely based on the optimistic assessment by scientists, engineers and policy makers of man's ability to modify and control river regimes on a sustainable basis. Assumptions were made not only regarding the ability to control water, but equally man's ability to predict and to control the production of sediment as well as its transportation in rivers and through reservoirs *(Bolton, 1984)*.

Apart from storage losses, reservoir sedimentation also impacts on a number of other important issues.

1.5 Operational and maintenance problems

Sediment deposition in reservoirs causes not only loss of water storage capacity, but also impairment of navigation, loss of flood control benefits, increased flooding upstream, sediment entrainment in hydropower equipment, blockage of gates etc.

In the planning and design of a reservoir, engineers must anticipate and predict sedimentation problems and incorporate into the design measures to regulate/limit sediment accumulation within the reservoir. If the problem of sedimentation is neglected, the designers may fail to adopt appropriate measures for the release of sediment such as adequately sized deep bottom sluices for sediment flushing. Dams constructed without adequate bottom outlets may require extensive and costly reconstruction and the operational rules for the reservoir will probably require substantial alteration to facilitate sediment regulation. Serious environmental concerns may be linked to the discharge of the sediments accumulating in reservoirs.

Design and operational measures which are required to balance sediment inflows and outflows through the impounded river have been implemented at only a limited member of reservoirs across the world to date. These measures will, however, have to become increasingly commonplace worldwide as reservoirs age and sediment accumulates to a point where reservoir performance becomes unacceptably impaired.

1.6 Economic impact of sedimentation

In analysing the total costs of sedimentation, direct as well as indirect costs should be considered.

Direct costs include:

- increase in maintenance costs of irrigation schemes and power stations,
- water losses due to reduced storage capacity, resulting in reduced power generation, agricultural output and fishery opportunities etc.,
- additional chemical treatment costs due to higher turbidity. At the Welbedacht Dam water purification plant, high turbidity levels have been exceeding the plant design limits for a number of years and a pre-treatment plant will most likely have to be added to treat the reservoir water.

Indirect costs include:

- damage to agricultural land due to aggradation and related swamping, deposition of infertile material and impairment of natural drainage,

- impacts on infrastructure such as roads, bridges and water distribution systems. Approximately 50 km upstream of Welbedacht Dam, sedimentation of the Caledon River caused the bridge opening of a main route to become too small, and the bridge will have to be reconstructed in the near future in order to allow the safe passage of the design flood with sufficient freeboard allowance,

- higher energy costs due to the use of alternative sources of power (thermal) versus hydropower (Mbashe weir), (*Wallace, 1994*),

- remedial measures to alleviate a sedimentation problem such as the reconstruction of an outlet (Mbashe weir). Estimates of annual indirect costs amount to US $ 175 million in the United States (1969) *(Crowder, 1987)* and US $ 40 million in South Africa (1988) *(Braune and Looser, 1988)*.

1.7 Environmental impacts of sedimentation of reservoirs

Reservoir sedimentation impacts on fish, bird and animal habitats both upstream and downstream of the dam due to aggradation and degradation of the original river bed. The smaller nutrient loads associated with reduced sediment loads downstream of the reservoir can impact seriously on the local fishing industry (*Delft, 1992*). Sediment-attachment is an important carrying mechanism for phosphorus.

Inside a reservoir, sediment deposition affects the aquatic ecology and provides nutrients. The interrelationship between sedimentation and fisheries is complex and should be considered when assessing sediment control measures.

Shoreline nourishment diminishes with reservoir sedimentation. Toxic chemicals can build up in reservoirs, and with measures taken such as flushing of sediment, relatively high concentrations of toxic material might be flushed downstream during a single flood event.

The water quality may be affected by sedimentation due to phosphorus and other sediment-carried pollutants. Under stratified conditions, when the hypolimnion becomes anaerobic, bottom sediments release attached phosphorus, iron and manganese compounds leading to water treatment problems. Soil nutrients which are washed into reservoirs could eventually lead to algal growth and eutrophic conditions.

River channel degradation is caused by reservoir sedimentation. Sediment concentrations along river reaches directly downstream of reservoirs tend to be lower than the transport capacity and the grain size distribution changes (containing more coarse particles and less intermediate size particles). Together with the discharge regime modification (flood peak attenuation), this leads to erosion of the downstream channel, undercutting of the banks and eventual widening of the river channel.

The new equilibrium, with a transport capacity corresponding to the released sediment load, will be achieved by decreasing the bed slope. The bed degradation and accompanying lowering of water levels downstream of a reservoir may have many effects that include: *(Han and Tong, 1982; Sloff, 1991; Zhang and Qian, 1985; Delft, 1992)*:

- excessive drainage of flood plains
- headward erosion in tributaries
- groundwater table lowering
- reduction of flood plain flooding
- increase of bed roughness due to coarsening of the bed and growth of vegetation
- threats to the stability and efficiency of structures in and along the river
- failure of the dam through head cutting of the downstream river
- increased bank erosion
- improved navigation and
- silting of harbours and increased coastal erosion
- In cases where the reservoir capacity is so large that it reduces the outflow peaks considerably, the sediment transport capacity downstream could be limited and aggradation of the river may occur (*Delft, 1992*).
- Due to modifications in discharge and sediment regime, planform changes can occur.

River bed degradation and channel slope adjustment are often limited because of river bed armouring and the presence of non-erodible layers *(Delft, 1992)*.

1.8 Social and political issues

Reservoir sedimentation causes increased flooding levels upstream of the dam which require more land to be expropriated and impacts on people who have to be relocated. Relocation could be on the enormous scale of more than 1 million people in the case of the Three Gorges project on the Yangtze River, China, to only a few families being involved *(Delft, 1992)*. In all cases the same social issues apply with the need for housing, new jobs, change of family lifestyle etc. impacting on the individual.

Water rights of riparian farmers often need to be re-evaluated due to sedimentation. Riparian farmers in South Africa are often allowed to use the reservoir basin for planting crops, but at their own risk.

The social and political impacts on the catchment and project beneficiaries due to reservoir sedimentation need to be considered.

Perhaps the most important aspect of reservoir sedimentation is the fact that many reservoirs have limited life spans. Major economic interests develop with a reservoir. Irrigation schemes often result in areas of rapid economic development. Industries and communities become dependent on power supply, all leading to enormous social and economic impacts as the reservoir storage capacity is depleted by sedimentation.

1.9 Development of theory

Since the 1930's, sediment transport theory has been developed greatly and a large amount of theoretical work has been carried out on erosion and deposition of sediment. Although the "tools" available to the practising engineer today make it much easier to assess sedimentation problems, many of the problems which the engineers had to cope with earlier this century still prevail today.

With the aid of theories, which in many cases have been specifically developed for reservoir

sedimentation conditions, as well as practical field experience, it is now possible to readdress the problem of reservoir sedimentation and to provide guidelines for the future design and operation of reservoirs. Concern about the long-term viability and sustainable use of reservoirs has led to worldwide efforts to evaluate and develop techniques to deal with reservoir sedimentation. The main objective of reservoir design and operation to control reservoir sedimentation is to identify suitable sediment control techniques which minimize the impacts of reservoir sedimentation, thereby ensuring a longer lifespan for a reservoir.

1.10 Measures to deal with reservoir sedimentation

There are various options for reservoir sedimentation control:

a) minimize sediment loads entering reservoirs through

- soil and water conservation programmes
- upstream trapping of sediment (debris dams or vegetation screens)
- bypassing of high sediment loads

b) minimize deposition of sediment within a reservoir through

- sluicing: passing of sediment-laden floodwaters through the reservoir by creating high sediment transport capacities in the reservoir by means of water level draw down
- density current venting

c) remove accumulated sediment deposits through

- flushing by means of drawing the water level down during the rainy season
- excavation by means of dredging or other mechanical means

d) compensating for reservoir sedimentation

- maintain long-term storage capacity by raising the dam
- abandon/decommission the reservoir and construct a new reservoir or import

water from elsewhere

The technical, economical and environmental feasibility of the above measures depends on a number of site-specific factors such as:

- availability of suitable bottom outlet facilities
- availabilities of surplus water for flushing
- characteristics of the sediments and reservoir basin
- purpose of storage and water demand
- consequences of flushing/dredging sediment disposal
- consequences of control measures interfering with reservoir operation
- environmental impact
- institutional-political limitations.

Limited success has been achieved with sediment control strategies for existing reservoirs. There seems to be a lack of measures/policies which have been implemented, which tends to indicate that economically feasible means to maintain reservoir capacities in the long run are limited. Reasons for this can be found in:

- a lack of quantitive information on sediment control techniques and the hydraulic processes involved;
- appraisal methods which have taken little account of long-term environmental or social impacts;
- the lack of an integrated approach to sedimentation policies, and
- a lack of technological development of monitoring and control techniques.

1.11 Purpose of this dissertation and methodology followed

Having reviewed the history of dam development, the effects of reservoir sedimentation, the development of theory and measures to limit reservoir sedimentation, it is evident that many sedimentation-related problems are due to an incomplete knowledge of the hydraulic processes involved. Although many design tools have been developed, such as numerical and physical modelling techniques for the analysis of reservoir sedimentation processes, many are not based on a sound theoretical base and in fact contain numerous empirical relationships. The

approach followed in this dissertation was therefore not to develop another empirical "design tool", but rather to investigate reservoir sedimentation from basic theoretical hydraulic and sediment transport principles. Sediment transport forms the basis of reservoir sedimentation processes and was therefore investigated in detail, with laboratory and field data being used for the verification of mathematically sound relationships which describe the dominant sediment transport mechanisms of turbulent and density current flows.

Included under the sediment transport theory are sediment deposition, the sediment sorting process and non-equilibrium sediment transport. This research did not only concentrate on depositional processes. Hydraulic measures of sediment control, such as flushing/sluicing and re-entrainment of previously deposited sediment both non-cohesive and cohesive, with surface and mass erosion, were also investigated.

Apart from establishing the theory for different sedimentation processes, it was also important to integrate the theory in order to predict long-term equilibrium sedimentation processes. This has been done for both depositional and erosive processes such as flood flushing. The theory was therefore tested under highly variable hydraulic conditions, including the evaluation of the impacts of changed reservoir operation and outlet configurations.

2. RESERVOIR SEDIMENTATION PROCESSES

2.1 Introduction

When a river enters a reservoir, the sediment transport capacity is reduced and the sediment load is no longer dependent on sediment availability but can be related directly to hydraulic conditions in the reservoir. While coarser sediment is generally deposited in the upstream part of a storage reservoir, fine sediments (silt and clay fractions, $d < 60\mu m$), are transported further towards the dam through turbulent suspension, density currents or colloidal suspension. Deposition occurs in the main (original river) channel and overbank areas of the reservoir. Typical flow and deposition patterns within large reservoirs are indicated in **Figure 2.1-1** *(Graf, 1983)*.

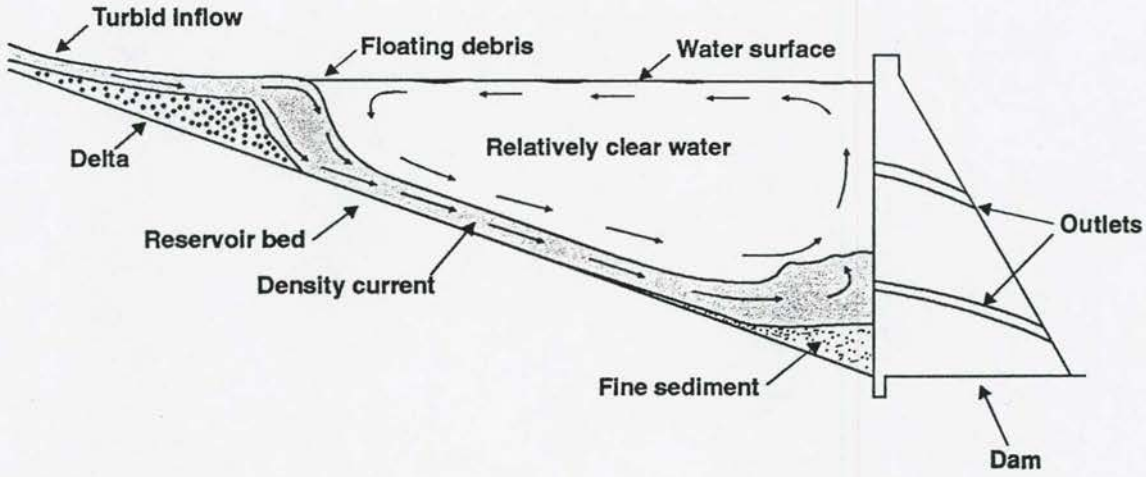

Figure 2.1 - 1 Schematic diagram of reservoir sedimentation processes

2.2 Sediment transport

Three main mechanisms of sediment transport can be identified within reservoirs, namely turbulent suspended sediment transport, density currents and colloidal suspension.

- Turbulent suspension is the dominant mechanism of sediment transport through most reservoirs (as in rivers), and is discussed in detail in **Chapter 3**.

- A density current may be defined as the movement under gravity of a stream of fluid under, through, or over another fluid, the density of which differs by a small amount from that of the primary fluid. Differences in temperature, salinity or suspended sediment concentration can provide the mechanism by which a denser fluid "dives" below the upper fluid. Different types of density currents have been observed, such as overflow, interflow and underflow, and while the first two are often more related to temperature or salinity density difference systems, the latter is the means of sediment transport often found in reservoirs.

  Field data on the ratios of outflowing sediment load to incoming load during density current venting for different reservoirs are presented in **Table 2.2-1** *(Bruk, 1985; Delft, 1992; Tan, 1994; Mahmood 1987)*.

Table 2.2-1: Recorded ratios of outflow to inflow sediment load during density current venting

Reservoir	Location	Storage capacity (million m^3)	Reservoir length (km)	Ratio: sediment outflow to incoming load
Eril Emda	Algeria	160		0,25 - 0,60
Lake Mead	USA	38 400	128	0,18 - 0,39
Guanting	China	2 270		0,19 - 0,34
Heisonlin	China	8,6	2	1,16 - 0,59
Sanmenxia	China	9 640	80 (1961)	0,18 - 0,21
Sefid-Rud	Iran	1 800 (original)		0,20 - 0,37
Fengjiashan	China	398	12 - 14	0,23 - 0,65
Bajiazui	China	525 (original)	10	0,46
Liujiaxia	China	5 720 (original)		0,57 - 0,84
Nebeur	Tunisia	300		0,59 - 0,64

Density currents have been observed in several reservoirs such as Lake Mead, USA, Sautet Reservoir in France, Metha and Groshnitza Reservoirs in the former Yugoslavia, and the Nulele Reservoir in the former USSR *(Wu, 1994)*.

The hydraulics of density currents are discussed in **Chapter 4.**

- Colloidal suspensions are due to electrostatic forces on the small particles, and their transport is therefore not related to the effect of gravity. Such suspensions not only depends on particle size, but is largely influenced by water quality. Colloidal sediments fall in the size range of approximately 10^{-3} to 1 micron, between dissolved particles on the one hand and sediments suspended by turbulent/laminar flow conditions on the other.

  The so-called wash load (normally not considered in laboratory calibrated standard sediment transport equations), should not be mistaken for colloidal suspension. The research conducted for this dissertation has shown that the transport of silt and clay sediment fractions as found in South African reservoirs can be described by relationships which are also valid for coarse sediments.

  Colloidal suspensions normally would be present in reservoirs at concentrations of less than 100 ppm, and due to their estimated low contribution to total sediment transport through a reservoir (maximum of 3 percent), such suspensions will not be considered further in this dissertation.

2.3 Sediment deposition

Coarser fractions (sand sizes and larger) are normally deposited in the upstream reaches of a reservoir and are conducive to the formation of a delta. Deltas may extend up to the reservoir full supply level (FSL) (and above) and are in many cases covered with vegetation. Delta formation leads to increased flood hazard along the river reaches upstream of a reservoir, with decreased clearances at bridges, and formation of marshes and swamps.

The delta may cut off the storage capacity in side valleys (Gaunting Reservoir, China; Yongding and Grinshu Rivers, China) *(Feng et al, 1989)*.

The headward extension of backwater deposits depends on the following:

- The average annual sediment yield and the storage capacity-runoff ratio of the reservoir, which give the long-term deposition patterns.

- Discharge patterns. Variation in discharge leads to the propagation of backwater deposits upstream and downstream in the so-called reach of changing backwater effects. This is a dynamic process. At the Danjiankou Reservoir, China, water level variation has been 18 m since 1973 but has resulted in changing backwater effects over a distance of 90 km. *(Zhang and Qian, 1985).*

  The upstream and downstream migration of the zone of backwater deposits only takes place in the main channel, because the erosive power of flow over the floodplain is generally too small to cause re-entrainment of sediments. This leads to continuous upstream propagation of the zone of backwater deposits of the flood plain as recorded upstream of Sanmenxia Reservoir, China *(Zhang and Qian, 1985).*

- The original slope of the river bed *(Zhang and Qian, 1985).*
- Stream adjustment within the deposits by the elimination of meanders, forming optimum width-depth ratios and varying the bed roughness *(Bondurant, 1973).*
- Reservoir basin geometry.
- Sediment particle size distribution.
- Reservoir operation.

Different delta shapes have been identified:

- In narrow reservoirs, delta deposits are distributed evenly across the width, and depending on the average capacity, the incoming sediment load as well as reservoir operation, "real" (deltaic) or wedge-shaped deposits will form. With wedge-shaped deposits the delta front reaches the dam and sediment is deposited uniformly across the reservoir.

  Zhang and Qian (1985) proposed an empirical relationship to distinguish between deltaic and wedge shaped deposits:

Deltaic: $V/S\Delta t > 2$ *and* $\frac{\Delta h}{h_o} < 0{,}15$

Wedge: $V/S\Delta t < 2$ *and* $\frac{\Delta h}{h_o} > 0{,}15$

with V = average reservoir capacity during time interval Δt

$S\Delta t$ = incoming sediment load during the interval Δt

h_o = average water depth from base of outlet at the dam

Δh = fluctuation of water level during Δt

- In wide reservoirs delta formation is more complicated and difficult to predict. An underwater ridge of deposits forms along the line of the jet introduced by the flow *(Vanoni, 1977)*. During high flows the ridge may be bridged and a new channel formed which transports fine sediment closer to the dam. This avulsion causes a new delta to be built up over the previously deposited fine sediment. *Chang (1982)* showed that for increasing discharges the stream develops into a single channel instead of forming branches.

Chang (1982) found that the channel pattern in a depositional area of the delta is characterized by multiple distributary channels. This situation occurs when the base water level is raised, discharge increased, sediment load increased, grain size increased, or the channel elongated. On the other hand a single channel usually develops as a result of channel degradation when reservoir water levels are lowered. Drying, clayey areas consolidate and crack, and with rising water levels new deposits fill the cracks and gullies resulting in a very densely packed deposit of coarse and fine sediments *(Breusers et al, 1982)*.

The delta is often divided into different zones *(Zhang and Qian, 1985)* (refer to **Figure 2.3-1)**

a) Tail reach: Transition between the natural stream and the delta. The tail reach is usually short, and its slope is approximately the mean of the bed and top-set slopes *(Delft, 1992)*.

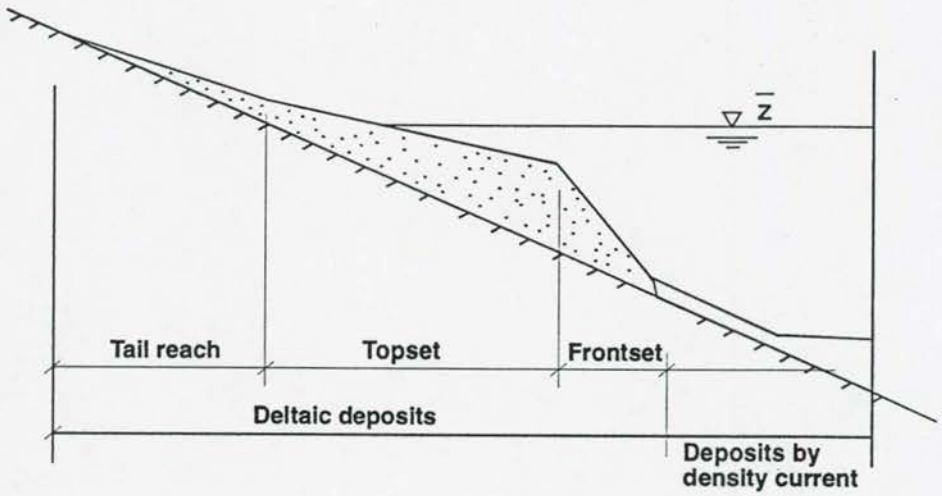

Figure 2.3 - 1 Schematic diagram of delta regions

b) Top-set zone or top of delta: this reach is essentially in equilibrium and deposition on the front-set leads to parallel deposition on the top-set. The slope of the top-set zone depends on:

- the mean concentration of bed sediment transport during flood seasons
- the median sediment grain diameter
- the mean discharge during the flood season
- the width of flow

Normally the top set slope is ½ to ⅔ times the original bed slope *(Borland, 1971)*.

c) fore-set or front-set zone: downstream of the apex point (transition between top-set and front-set zones) the water depth increases abruptly. The slope of the fore-set is slightly less than the angle of repose of the sediment particles. *Borland (1971)* indicated from USA reservoir surveys that this slope was 6,5 times the top-set slope. *Chien (1982)* proposed a factor of 1,6 times the top-set slope for Chinese reservoirs, which could be due to the existence of turbidity currents in many Chinese reservoirs.

Schälchi (1987) concluded from experiments that the front-set becomes steeper until a certain angle is reached, whereafter slumping of the whole front occurs.

d) A fourth zone, the bottom-set zone, is formed by deposition of fine sediments transported by colloidal, turbulent suspension and/or turbidity currents.

A delta is also subjected to the smoothing influence of wave action. Top-set parts of a delta extending above the highest water levels are often covered by vegetation which prevents water circulation, reduces erosion potential and increases evapotranspiration.

In flood-detention reservoirs the flood plains are only inundated during the filling of the reservoir in flood season and therefore the flood plain profile within these basins is essentially parallel to backwater curves in the high flows.

In South Africa, the above-mentioned rules of thumb to describe delta types and slopes have been found unreliable *(Annandale, 1984)*, mainly because the hydraulics of reservoir sedimentation has not been included in these highly empirical relationships.

The rate of advance of the apex point within the reservoir depends on:

- the river discharge
- sediment inflow and characteristics
- catchment characteristics
- reservoir geometry.

In Lake Mead **(Figure 2.3-2)** the delta advanced at a rate of approximately 3 000 m per year (1939 to 1948) *(Sundborg, 1964)*, while in the Lillboet River of British Columbia the rate is 10 m per year *(Gilbert, 1975)*.

Sediment depositional patterns are mostly determined by storage operation of reservoirs. This means that reservoirs are operated to maximize water yield, without considering operational changes to limit storage capacity loss due to sedimentation. Hydraulic operational techniques, namely sluicing, flood flushing, density current venting and bypassing of high sediment loads can however be implemented to limit reservoir sedimentation.

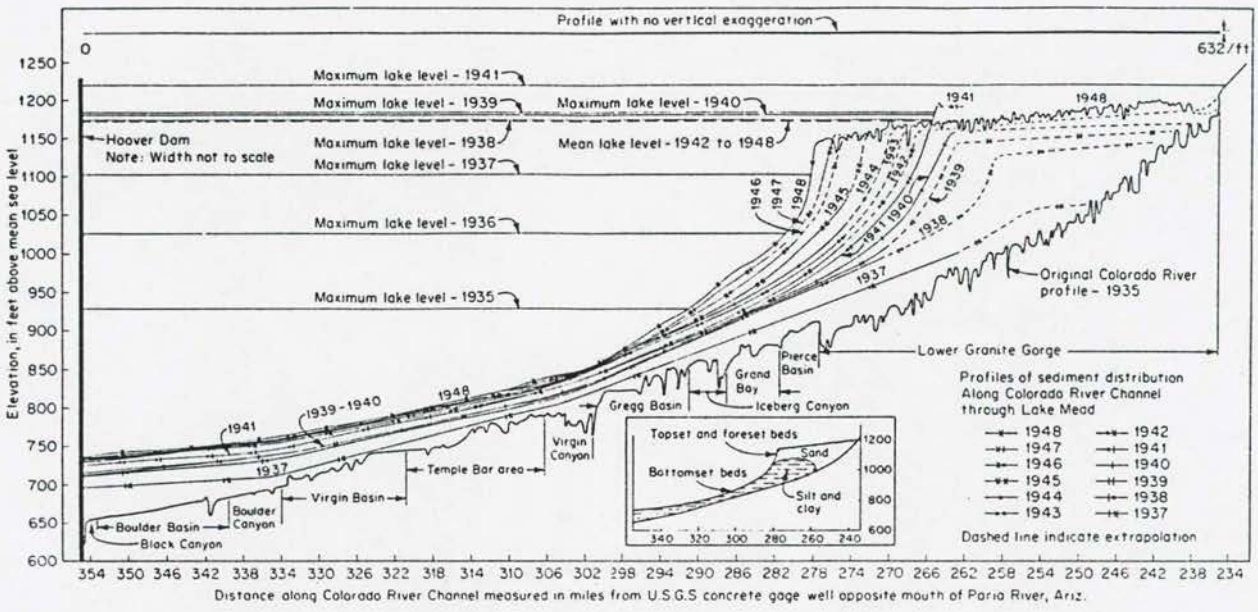

Fig. 12.16 Deposition pattern along the Colorado River through Lake Mead. [*After* SMITH *et al.* (*1954*).]

Figure 2.3 - 2 Delta formation in Lake Mead

It is sometimes possible to maintain the original bed slope of the river in a reservoir through seasonal flushing. Flood plane deposits will, however, not be eroded. An example of such operation and the impact on delta formation is illustrated with the Sanshenggong Barrage, China. This barrage with 18 gates was completed in 1961, with impoundment only from June to October. While the main channel slope remained unchanged, the flood plane slope changed from 0,00017 to 0,00013 after construction **(Figure 2.3-3)**. Very important is the fact that the outlets are at the original riverbed and the barrage did not change the rating curve for discharges below 800m³/s *(Fan, 1992)*.

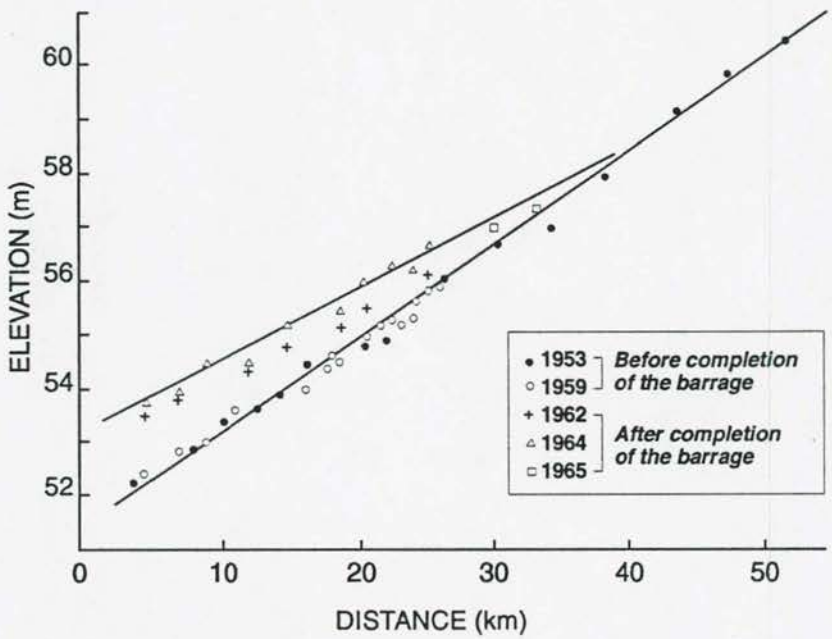

Figure 2.3 - 3 Floodplain profiles before and after construction of Sanshenggong Barrage (Fan, 1992)

2.4 Passing incoming sediment loads through the reservoir by sluicing

Sluicing is an operational technique whereby sediment-laden inflows are released through a dam before the sediment particles can settle, thereby reducing the trap efficiency of the reservoir. This is accomplished in most cases by operating the reservoir at a lower water level during the flood season in order to maintain sufficient sediment transport capacity (turbulent and colloidal) through the reservoir. After the flood season, the pool level is raised to store relatively clear water. This operating strategy has been based more on experience than on quantifying the physical processes, and this research has aimed to provide more insight into the theory.

Sediment concentrations of finer sediments carried by inflows into reservoirs tend to vary greatly during a single flood event, because the initial run-off, especially after a dry season, encounters more transportable material than subsequent run-offs. The sediment concentrations therefore also tend to be much higher during the rising stages of a flood than during the corresponding falling stages. In sluicing operation it is therefore wise to start impoundment as late as possible so as to trap only water which contains relatively little sediment.

While it is possible to scour non-cohesive sediments from reservoirs (by flushing) long after deposition has occurred, this is not the case with highly cohesive sediment. Overbank deposition, in most cases, cannot be removed by flushing operation and it is therefore imperative that deposition of sediment is limited through sluicing operation. Velocities required to keep sediment in suspension are normally much lower than those required to erode deposited sediment, especially consolidated cohesive sediment *(Hu, 1990; Rooseboom, 1985)*. This means that sluicing of sediments is often more efficient than scouring by flushing operation.

Numerous reservoirs are operated to pass sediments through, with varying degrees of success as described by *Ackers and Thompson (1987), Brabben (1988), Brown (1943), Bruk (1985), Mahmood (1987), Pitt and Thompson (1984), Scheuerlein (1987), Sloff (1991), Zhang and Qian (1985), and Delft (1992)*.

Successful sluicing operations depend on the following:

- Enough surplus inflow must be available for discharging sediment.
- Outlet works must possess adequate capacity and preferably be located near the original river-bed level.
- Judicious operation (time, duration) by properly trained operators is essential and is often the most critical part of sediment discharge operations.
- The reservoir basin should have a narrow configuration throughout.
- The river should transport mainly suspended sediments.

- The river flows must possess excess capacity to transport sediment through the reservoir.

- The flow hydrograph must be predictable with confidence at the dam site. This is important for operation in order to re-fill the reservoir in time after the sluicing operation.

- Training walls within the reservoir can enhance the efficiency of sluicing.

2.5 Re-entrainment of previously deposited sediments through flood flushing

Sediment flood flushing is a technique whereby the flow velocities in a reservoir are increased to such an extent that deposited sediments are re-mobilised and transported through bottom outlets. In many cases sluicing and flushing are used in combination or alternatingly.

During the flushing process a river channel is eroded through the sediment deposits. The width and slope of the channel with periodic flushing operations will approach those which existed under the original regime conditions. The erosion process during drawdown flushing is described by *Zhang and Qian, (1985)*: When the reservoir water level is drawn down below the apex point of the delta, retrogressive erosion will result until the fore-set and top-set slopes of the delta are equal. Thereafter progressive erosion takes place with decreasing intensity as the bottom slope decreases. Retrogressive erosion is usually more dominant than progressive erosion and therefore more important in reservoir desiltation.

The main difference between sluicing and flushing requirements for gates is that the gates for flushing operation should be close to the original river-bed level. As in the case of sluicing, excess run-off is required for successful flushing operation. In semi-arid and arid regions flushing operation often results in unacceptably high water losses. Flushing/sluicing operation therefore increases the risk of failure of water supply during critical hydrological periods *(Brabben, 1988; White and Bettess, 1984)*. Flushing operation cannot be implemented in reservoirs with over-year storage either, or where periodic interruptions in the use of the reservoir cannot be tolerated *(White and Bettess, 1984)*. In such cases the risks can be reduced by operating reservoirs in combination with each other.

The efficiency of flood flushing depends on:

- the geometry of the reservoir (slope, width, length, storage ratio)
- outlet discharge capacity, location and elevation
- characteristics of inflowing and deposited sediment
- mode of operation (degree of water level drawdown and duration)
- duration of flushing and flushing discharge.

Favourable conditions for effective flushing are *(Bruk, 1985; Paul and Dhillon, 1988; Delft, 1992)*:

- Low head on the outlets, preferably free flow conditions. Sediment flushing is most effective when the reservoir is drawn down to the extent that the flow conditions over the deposits approach that of the original river (free surface flow) *(White and Bettess, 1984; Mahmood, 1987)*. The best condition for starting the flushing operation is therefore an empty reservoir. Flushing without water level drawdown is practised where localized scour of sediment at intakes is required. A crater develops which terminates as soon as the slope of the crater is equal to the angle of repose. Flushing without drawdown has only this local effect because velocities decrease approximately proportional to the square of the distance from the outlets *(Scheuerlein, 1993)*.
- High discharges
- Unconsolidated deposits, no gravel and no armouring
- Wide bottom outlet(s) are essential for low reservoir water levels in order to obtain maximum sediment tranpsort capacities through the reservoir when emptying the reservoir during flushing

- Deep outlet location, preferably at the original river-bed level.

- Long duration of flushing and intermittent flushing. In a long reservoir an appreciable drawdown for several months is needed to complete the flushing action, because of the low rate of bed changes *(De Vries, 1959)*. Generally, outflow concentrations are high at the beginning of retrogressive erosion and gradually decrease with time. Flushing should be stopped when outflow concentrations are low in order to save water. In semi-arid regions flushing of single flood events (few hours to days) is possible if excess water is available and the inflow volume is monitored in order to end with a full reservoir after the flood. In such cases impounding only during the falling stage of the flood hydrograph will limit sedimentation.

- Small ratio of reservoir capacity to inflow storage to provide excess run-off for flushing.

- A steep bottom slope. Bed slopes are approximately 2 % in most reservoirs where flushing has been practised successfully *(Singh, 1987)*.

- A narrow reservoir. *Singh (1987)* concludes that a maximum reservoir width of 300 m is found in reservoirs where flushing is successfully used. With periodic flushing the scoured channel will approach the original river width. In flood-plain type of reservoirs (wide basin characteristics) therefore, it is only possible to recover storage capacity up to the extent of the original channel *(Mahmood, 1987)*.

- A climate with distinct dry and wet seasons, allowing flushing operation in the early wet season when flows are highly charged with sediments, and storing water during the dry season.

- Frequent flushing. Flushing should be undertaken frequently to prevent excessive consolidation of deposits *(Delft, 1992)*. *Krumdieck and Chamot (1979)* recommended a flushing frequency of at least once every year for the Santa Domingo reservoir, Venezuela. When sluicing and flushing are used in combination, the frequency of flushing may be less *(Bruk, 1985)*. In China annual sedimentation is restricted by sluicing while flushing is applied every 3 to 5 years, for example in the Hengshan Reservoir *(Zhou et al., 1989)*.

It may be necessary to flush even more frequently if possible. In the Russian Rioni series of hydro-electric stations a flushing frequency of twice a year was adopted. In late autumn the reservoirs are flushed before winter, when power demand is high, and again after winter to remove the lighter consolidated deposits. *(Kereselidze et al., 1985)*. At the Hengshan Reservoir, China, the flushing efficiency was high even when the main channel eroded in a previous flushing had been silted by sediments during a period of several (4 or 5) years *(Zhou et al., 1989)*.

- A water supply rather than hydropower system. Hydropower generation will be decreased considerably due to water level drawdown, and unless originally planned for, this could be unacceptable in terms of power requirements. At Sanmenxia Reservoir, China, power generation was reduced to one third of what was originally planned due to sedimentation which necessitated a change in reservoir operation rules.

- Combination with other measures such as dredging.

Apart from loss of water, flushing could also have other negative effects *(Qian, 1982; Yoon, 1991; Mahmood, 1987)*:

- Rapid pool drawdown could lead to sediment slides which can block the outlets or reduce storage as well as jeopardize the safety of especially earth dams.

- High sediment releases may cause aggradation of the downstream river channel *(Qian et al., 1993)*.

- Sediment being discharged may cause abrasion of the outlets.

- High-concentration sediment releases may affect the water quality and ecological environment along downstream reaches.

The water-detritus ratio (W-D), the ratio between the volume of water wasted and the volume of deposits flushed out, is one of the indicators of flushing efficiency. The W-D ratio typically varies between 20 to 50 as indicated by field data in **Table 2.5-1** *(Qian 1982, Fan 1985, Yoon, 1991)*.

Table 2.5-1: Recorded W-D ratios

Reservoir	Location	Mode of operation	W-D ratio
Grimsel	Switzerland	Bottom outlets, drawdown	16-22
Gebiden	Switzerland	Bottom outlets, drawdown	42
Gebiden	Switzerland	Bottom outlets, no drawdown	18
Nebour	Tunis	Bottom outlet flushing with drawdown and density current	9
Sefid Rud	Iran	Bottom outlets	13-34
Khashm El Girba	Sudan	-	35-44
Zemo-Afchar	Russia	-	8-83
Gurnsey	USA	Overflow spillway	400-820
Santa Domingo	-	Emptying	7-11
Shincaozi	China	Overflow spillway	23-86
Warsak	Pakistan	Overflow spillway	590

A special case of flushing is found in flood detention operation. Normally the sediment deposition caused by flood detention can be flushed out during the receding flood phase or during the next flood through large bottom outlets with or without gates. Most of the resulting headward retrogressive erosion occurs in the main channel, however, and not in the flood plain deposits. *(Fan, 1985).*

Two rates of drawdown are discussed by *Lu Xiuzhen (1991)*: quick or gradual. A radial erosion process is caused by the former in which the bed profile 'revolves around' an axis near the outlet. The bed slope gradually decreases to the original bed slope as was observed in the Sanmenxia Reservoir, China, in 1962. A gradual drawdown induces a layered erosion process with the revolving axis located near the upstream end of the reservoir, as observed in Sanmenxia Reservoir in 1964.

Takasu (1982) found that an increased outflow rate during flushing resulted in an increased flushed sediment load due to increased bank erosion in the main channel in the reservoir, although the concentration decreased.

2.6 Density currents

Under exceptional conditions, sediment-induced density currents develop which would cause more sediment to be transported towards the dam than the relationships for turbulent suspension would indicate. If suitable outlets are provided, the stream containing high sediment concentrations can be discharged through dams. Density current venting is an

attractive way of releasing sediment-laden flows from a storage reservoir, particularly as unlike with flushing/sluicing operations, it is not necessary to lower reservoir pool levels.

Favourable conditions for the formation and venting of sediment-laden density currents are *(Bruk, 1985; Lu Xinzhen, 1990; Rooseboom, 1985; Scheuerlein, 1987)*:

- A steep bed slope and a narrow basin configuration. Density currents will then have higher sediment transport capacity.

- When a main channel exists at the bottom of a reservoir, the release ratio of the turbidity current has been found to be twice the ratio without a channel (Hengshan Reservoir, China) *(Zhou et al., 1989; Bruk, 1985)*. Turbidity current venting in a new reservoir is therefore desirable and can reduce sedimentation of the main channel *(Singh, 1987)*. Advanced sediment build-up in a reservoir works against the development of a turbidity current because the topside slope of the deposit is smaller than the original river-bed slope *(Mahmood, 1987)*.

- A large incoming discharge with high sediment load. Field data at Guanting Reservoir, China indicated that when the discharge per unit width, $q > 0,2$ to $0,3\ m^2/s$, a density current formed. *(Wu, 1994)*

- Large density differences between the density created by suspended sediment transport in the density current and that of the overlaying clear water.

- Long duration of incoming flood. The flood duration should be longer than the travel time of the density current from the plunge point to the dam in order to vent the density current effectively.

- Large flow depths, often associated with steep bed slopes.

- Low flow velocities in the reservoir. With high velocities through the reservoir turbulent suspended sediment transport will dominate.

- A high concentration of fine particles in the density current. According to *Mahmood (1987)*, field and laboratory studies indicate that flocculation of clay particles does not induce settlement of clay out of the density current.

- Large, low level outlets and correct timing of opening and closing of outlets. A sampling pipe in the reservoir could be used to monitor sediment concentrations *(Lu, 1990)*. If the turbidity current is not vented, a muddy pool will develop which can block inlets and gates. If the elevation of the top of the bottom outlet is lower than the top of the density current, the ratio of outflow to inflow concentration increases.

- Releases should not be in excess of the mass transfer rate of the density current, the reason being that larger discharge rates could cause turbulent interaction to dominate in the transport mechanism. As a result mixing and dilution would take place *(Un Groupe ..., 1982; Rooseboom, 1985)*.

2.7 Bypassing of sediment

Bypassing of sediment involves the storing of sediment-free water (usually low flows), while high sediment loads are bypassed around the reservoir. The bypassing system can consist of a canal/tunnel around the reservoir, or by having a so-called off-channel storage reservoir fed under gravity from the main river or by pumped flow. For a bypassing system to be effective in the long-term, it must be correctly sized (with related high cost) and operated. Systems for bypassing sediments along the full length of a reservoir can only be economical under very special conditions *(Rooseboom, 1985)*. The topography around a reservoir seldom lends itself to making bypassing feasible, but there are a number of smaller reservoirs which have been constructed with bypasses.

In arid areas, bypassing of sediment-laden water could be in conflict with the need for water, and the long-term operation must be carefully planned. Sediment excluders (sand traps) can be used in such circumstances to desilt flood-water, and/or the falling stage of the flood hydrograph which normally has lower sediment concentrations than the rising stage could be utilized for storage. Sediment excluders are less effective in removing silt and clay, but half of the sand load can be removed with one tenth of the flow *(Mahmood, 1987; FAO, 1975)*.

At Nagle Dam, South Africa, the main reservoir (storage capacity 21 million m^3) is situated on a horseshoe bend in the river, while a small flood diversion weir was constructed upstream to bypass turbid water *(Annandale, 1987)*. The bypass canal was cut into rock and has a steep gradient. No significant sedimentation has occurred in the reservoir since 1950 (See **Photograph 2.7-1**). During the 1980's discharges up to 2 000 m^3/s were bypassed during major floods.

Two small reservoirs, Shongweni and Henley, South Africa, also have bypasses consisting of tunnels and concrete-lined canals.

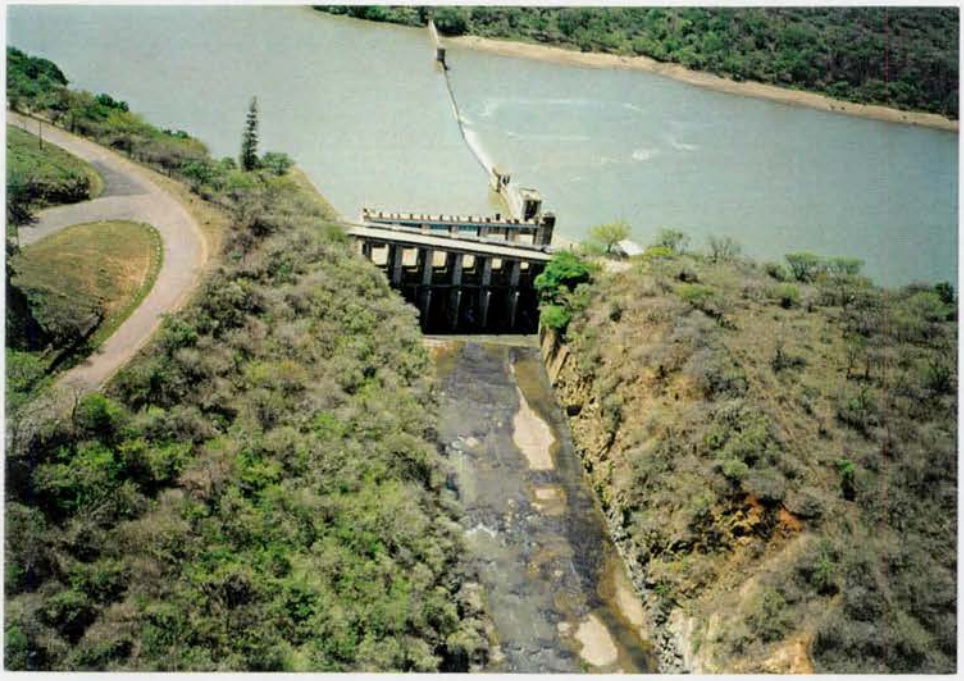

Photograph 2.7 - 1 Nagle Dam bypass canal

2.8 Reservoir operation and sediment transport through reservoirs

In order to understand how efficiently the above hydraulic methods can deal with reservoir sedimentation, their respective impacts on sediment loads and on trapping of sediment need to be considered. Over the long term, a discharge-sediment load relationship as indicated in **Figure 2.8-1** is obtained for a "natural" river.

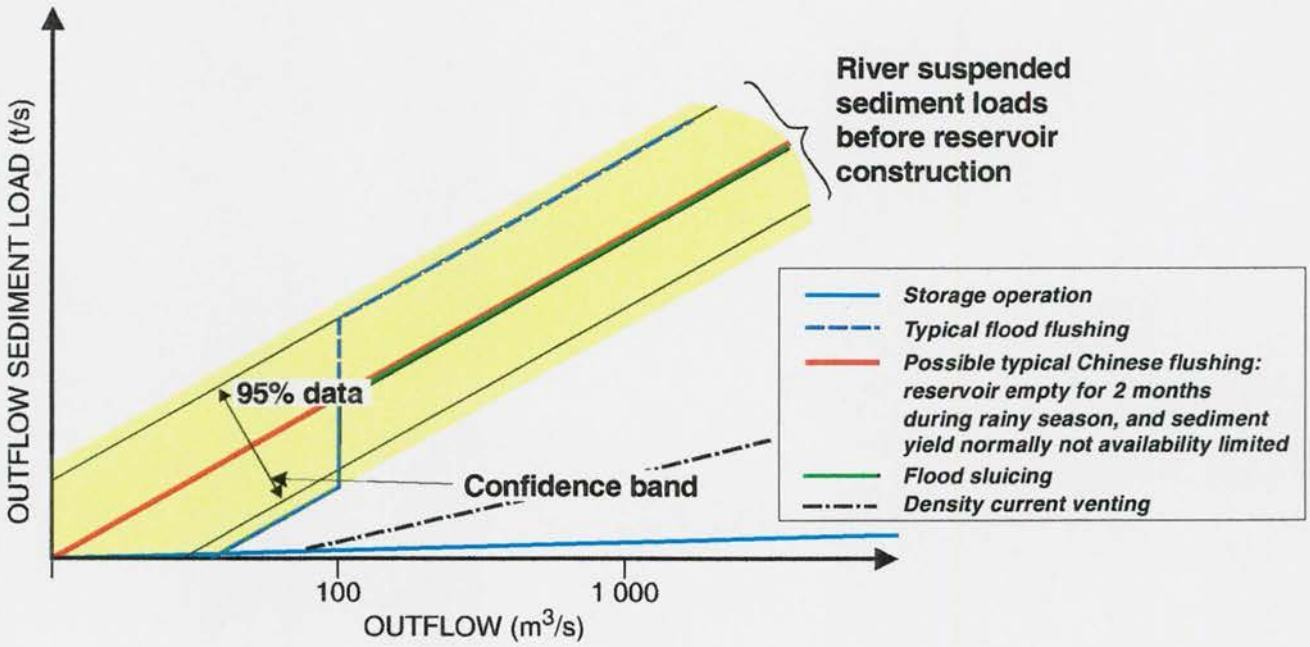

Figure 2.8 - 1 Reservoir operation and sediment transport

The one extreme option is storage operation, allowing almost no through flow of suspended sediment. Almost clear water will be released from storage operated reservoirs, resulting in channel degradation downstream of the dam. With regular flood hydrograph flushing (normally practised in semi-arid areas such as in South Africa), the operational method is only efficient above a certain discharge. At high discharges, sediment loads higher than the mean seasonal sediment loads can be expected, but sediment equilibrium can be established. Regular flushing with suitable bottom outlets will also ensure that the flushed sediment loads approach the mean background value. Sluicing is another method of operation (partial water level drawdown during high inflows) which can limit the outflowing sediment loads to those for typical natural river conditions, but a long-term equilibrium in sediment inflow and outflow cannot be established, since low inflow conditions will normally not be sluiced in arid conditions in order to avoid risking failure in water supply. Under such conditions, sluicing only delays the rate of reservoir sedimentation and it needs to be used in conjunction with flood flushing to maintain substantial long-term equilibrium reservoir capacity.

Lastly, reservoir emptying and flushing as practised on a regular basis in China with enough excess water during the whole summer rainy season will impact least on the aquatic environment. It should be possible to obtain the seasonal mean sediment load discharge relationship as for river conditions from low to high flows, although with somewhat increased variability in the suspended sediment loads discharged from the reservoir.

Figure 2.8-1 shows that reservoir operation with combined sluicing and flushing operation should in the long term least impact on the riverine ecology if practised regularly, coinciding with high inflow conditions. Rapid changes in water quality with low concentrations of dissolved oxygen and high suspended sediment loads during flood flushing/sluicing/ (uncharacteristic of the natural river) need to be considered, however, in order to protect the aquatic ecosystem downstream of the reservoir.

Flushing/sluicing of a reservoir will alter the relationship between water flow and sediment load released from the reservoir, but the degree of alteration is not as large as that under the operating rule of impoundment *(Zhou, 1994)*. If a reservoir is first operated for storage, followed by flushing later, the discharged sediment load will, however, induce new problems as compared with the former equilibrium established under "clear" water flow in the river.

For sluicing/flushing operation the major constraint is excess water availability, which means that the reservoir has to be small in relation to the runoff. In practice, the most efficient passing through of sediment is obtained when the reservoir capacity is less than 5% of the mean annual runoff, although larger reservoirs are also sluiced successfully. The *Churchill (1948)* and *Brune (1953)* trap efficiency curves indicate why reservoirs need to be so small **(Figure 2.8-2)**. Reservoirs significantly reduce sediment transport capacity and it is only when near-riverine (small trap efficiency), high sediment transport conditions can be established in a reservoir by water level drawdown, and with high flow conditions, that sediment sluicing/flushing is effective.

The experience gained at Sanmenxia Reservoir (*Delft, 1992*) with different reservoir operating rules is further illustrated in **Table 2.8-1**. It was only after reconstruction of the outlets that sediment sluicing could be optimized, with much reduced operating water levels, but with the advantage of maintaining long-term reservoir capacity.

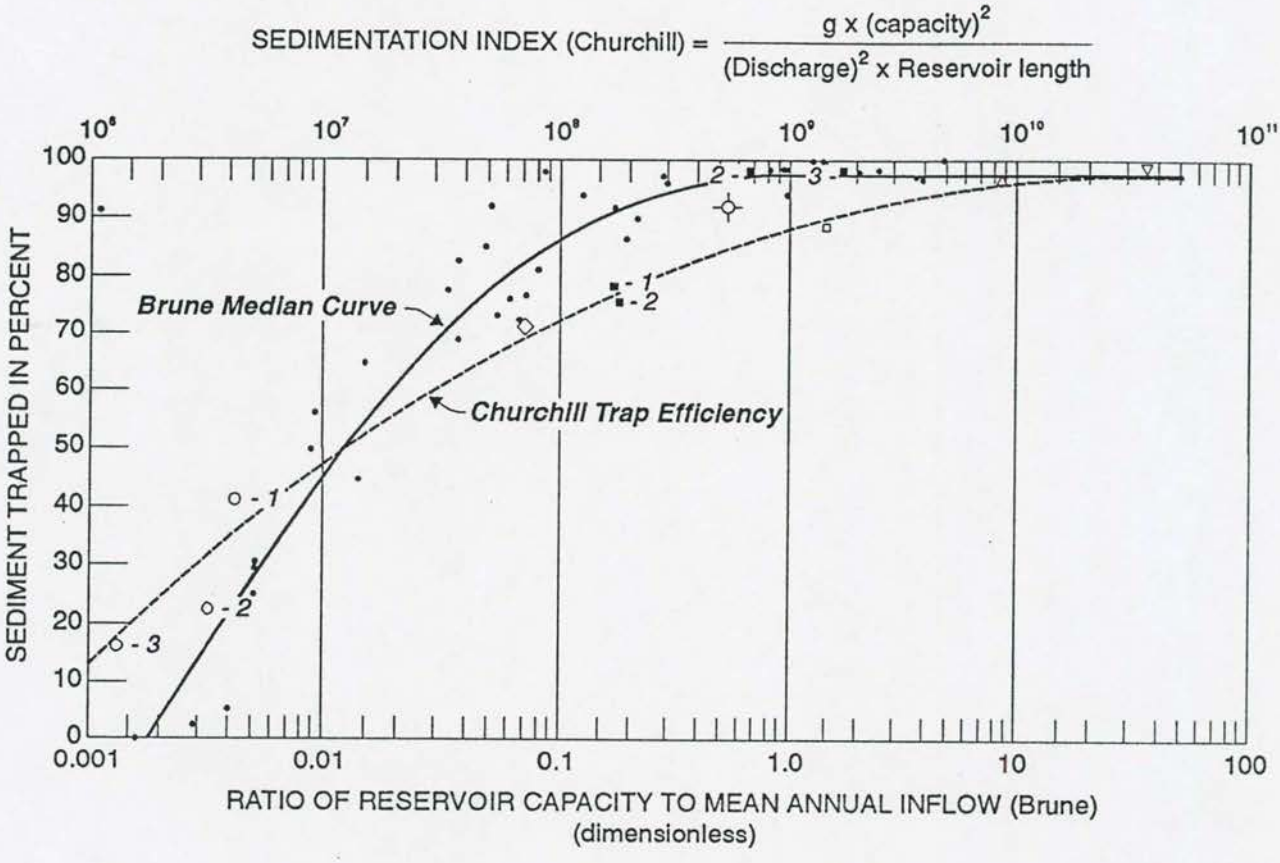

Figure 2.8 - 2 Reservoir trap efficiency

Table 2.8-1: Reservoir operation and sediment trapping in Sanmenxia Reservoir

Period	Operation *	Water level at dam site		Sediment outflow as % inflow
		Maximum	Average	
9/60 - 3/62	A	332,58	324,04	6,8
4/62 - 7/66	B	325,90	312,81	58,0
7/66 - 6/70	C	320,13	310,00	82,5
7/70 - 10/73	D	313,31	298,03	105,0
11/73 - 10/78	D	317,18	305,60	100,0

Note: * A - Storing water

B - Flood detention and sluicing through 12 outlets at 300 m

C - Flushing by opening 2 tunnels and 4 penstocks

D - Flushing : 2 tunnels, 4 penstocks, 8 diversion outlets

Two empirical indices can be used in preliminary judgement to decide on the mode of operation for sedimentation control, namely the capacity-inflow ratio (K_w) and the capacity-sediment inflow ratio (K_T). The importance of these indices is illustrated by reservoir data in **Figure 2.8-3**, and all the modes of reservoir operation are represented in this figure.

Most reservoirs have been designed to be large enough to accommodate 50 to 100 years' sediment accumulation and are located in the upper right hand quadrant of **Figure 2.8-3**. Since $K_w > 0.2$ for these reservoirs, not enough excess water is available for flushing/sluicing operation and reservoir drawdown. Therefore density current venting is practised and only in some cases.

Reservoirs designed and operated for sedimentation control should fall in the bottom left hand quadrant of **Figure 2.8-3**, with $K_T < 100$, and $K_w < 0.2$. The reservoirs where sediment sluicing/flushing are in fact practised are indicated on the graph. Relatively small reservoirs in high sediment yield areas should be designed and operated to limit sedimentation, or risk high sedimentation rates.

The zone $K_T < 100$, $K_w < 0.2$ contains reservoirs where enough excess water is available to allow hydraulic sediment control measures. In this zone, examples of successful design and operation for flushing in South Africa include First Falls, Second Falls and Phalaborwa Barrage. Examples of reservoirs with non-ideal design/boundary conditions but operated for flushing/sluicing operation are Mbashe Weir, Windsor, Welbedacht and Elandsdrift dams. Henley and Shongweni reservoirs both have bypass tunnels. Recommended values of K_w for successful flood flushing is $K_w < 0{,}03$.

It is interesting to note that many of the non-South African reservoirs which are successfully flushed, such as the Low Aswan, Sanmenxia and Tarbela have storage capacities larger than 4 % of the mean annual run-off. The reason why these reservoirs can be operated for flushing with relatively high storage capacity run-off ratio conditions is that enough excess water is available because water demands and high flows are out of phase. In the more arid conditions of South Africa high water demands and high sediment loads, especially at the beginning of the rainy season, coincide with hydrologically critical periods.

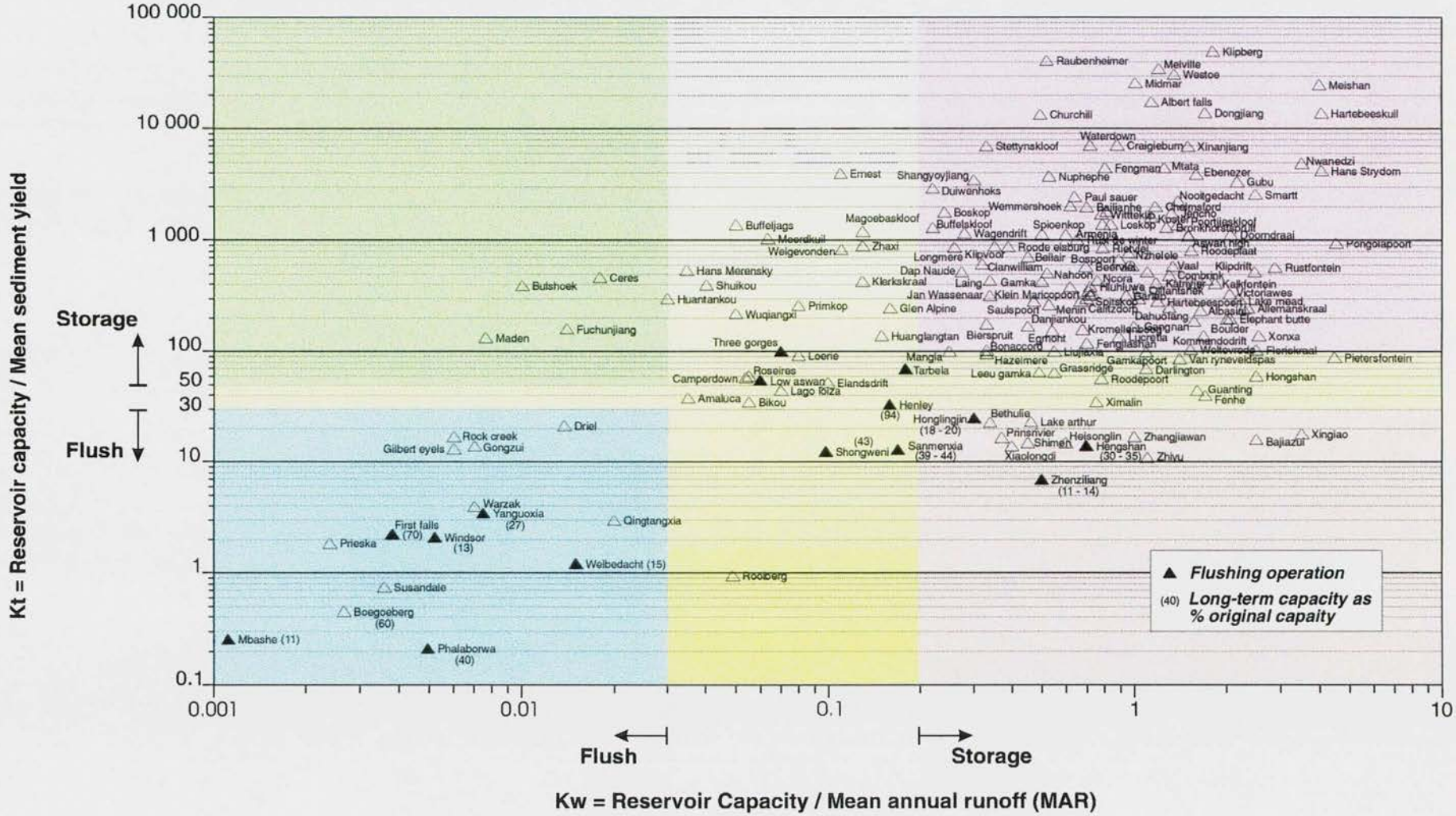

Figure 2.8 - 3 Reservoir operation and sedimentation

In the bottom right-hand rectangle of **Figure 2.8-3**, $K_w > 0.2$, $K_T < 100$, some reservoirs with a high risk of losing their capacities within a relatively short period are to be found. No excess water is, however, available for flushing/sluicing of these reservoirs. Prinsrivier Dam and Lake Arthur, constructed in 1916 and 1925 respectively, are two typical cases of reservoirs which have nearly reached the end of their lives. In the case of Lake Arthur, its users are fortunate to have the Orange-Fish transfer scheme to support them. At Prinsrivier Dam, however, the dam has been raised twice already with no possibility of future raises. In this case it seems likely that the farming community which has been established downstream of the dam for nearly 70 years may have to change to non-irrigation practices under the harsh Karoo conditions of less than 200 mm annual rainfall. Dredging (or syphon dredging) seems to be the only solution under these conditions.

The operating rules for a reservoir need not be inflexible, but can change with different stages of storage loss. Storage operation may be continued in reservoirs with large capacities relative to sediment loads, while sluicing/flushing operation can be introduced once the loss of storage capacity reaches a certain stage. These transition zones can be found between the zones represented in **Figure 2.8-3**.

In order to establish deposition and flushing patterns, it is necessary to understand the phenomena of delta formation, density current movement and sediment transport mechanisms by analysing the movement of sediment through reservoirs. The hydraulics of sediment transport through reservoirs forms the basis to which all other processes, such as sediment deposition and re-entrainment of non-cohesive and cohesive sediments, can be related.

3. TURBULENT SEDIMENT TRANSPORT

3.1 Introduction

South African experience indicates that in most rivers, the sediment transport capacity is often not limited by the hydraulic conditions, but rather by the sediment availability from the catchment. Within a reservoir this changes, however, and it is possible to quantify sediment transport in terms of hydraulic conditions.

A large number of sediment transport equations have been derived during this century. In most cases the theory has been "calibrated" by means of coefficients in the formula with laboratory (and in some cases) field data. There are basically two groups of equation formats: those that predict bed load and suspended load transport separately, and those that predict a total sediment load without the distinction between bed load and suspended load. Most equations have been tested and calibrated for sand transport only, and the so-called "wash load" (fine sediment) is not included.

For practical application, specific transport equations are favoured in certain parts of the world. A number of recent studies have compared the accuracy of these equations to predict sediment transport. Quite often, though, these comparisons are biased towards those equations which incorporate some of the verification data in their calibration. Nevertheless, what is important to note (as is shown in **Table 3.1-1**), is the rather inaccurate prediction of sediment transport, even under controlled laboratory conditions.

The reason for this is that the understanding of sediment transport processes has not been developed well enough, even after many years of research in this field. To name just a few of the complications, neither the interrelationship between bedforms, associated roughness, hydraulic and sediment transport capacities, nor the change in velocity profile when sediment is being transported have been adequately described.

Due to the abovementioned, the approach in a number of countries is to calibrate sediment transport equations for site-specific conditions. When "bed load" is the main component or under other conditions where the sediment transport capacity is the limiting factor, such an approach can be used successfully. One set of such relationships is shown in **Figure 3.1-1**.

Table 3.1-1: Accuracy ranges of commonly used sediment transport equations

White et al. (1975) compared eight formulae using 1 000 flume and 260 field measurements. The discrepancy ratio X_{calc}/X_{obs} was plotted against the dimensionless grain size $(\rho_s q_s / \rho q)$ and the percentages within the 0,5 to 2 range were as follows:

Formula	% in $0{,}5 \leq X_{calc}/X_{obs} \leq 2$ ranges
Ackers and White	68
Engelund and Hansen	63
Rottner (1959)	56
Einstein (total load)	46
Bishop et al. (1965)	39
Toffaletti (1968)	37
Bagnold (total load)	22
Meyer-Peter and Müller	10

The laboratory data include particle sizes from 0,04 to 4,94 mm and field data from 0,095 to 68 mm.

The comparison of formulae by *Yang and Molinas (1982)* also used laboratory and river data encompassing mean grain sizes from 0,15 to 1,71 mm, channel widths 0,134 to 532 m, flow depths 0,01 to 15,2 m, temperature 0° to 34,3°C, average velocity 0,23 to 1,97 m/s and slopes from $4{,}3 \times 10^{-5}$ to $2{,}79 \times 10^{-2}$. The range of data is the same as given by *Yang (1973)* for the data from which the formula was derived. The discrepancy ratio, defined as the ratio between computed and measured values, is given as follows:

Formula	Data		
	Lab.	River	All data
Colby (1964)	0,31	0,61	0,34
Yang (1973)	1,01	1,31	1,03
Yang (1979)	1,02	1,12	1,03
Shen and Hung (1971)	0,91	1,18	0,95
Engelund and Hansen	0,88	1,51	0,96
Ackers and White	1,28	1,50	1,31
Maddock (1976)	0,99	0,49	0,92

A different picture is painted by the comparative study carried out by *Van Rijn (1984)*, also using field and laboratory data. The discrepancy ratio, r, defined as the ratio of predicted to observed transport rates in per cent were as follows:

Data	$0{,}75 \leq r \leq 1{,}5$				$0{,}5 \leq r \leq 2$				$0{,}33 \leq r \leq 3$			
	1	2	3	4	1	2	3	4	1	2	3	4
US Rivers Corps Engrs	53	39	32	6	79	67	61	24	94	87	78	44
Middle Loop River	39	13	37	63	78	37	74	94	96	80	98	100
Indian Canals	30	15	27	3	60	45	48	6	90	73	70	24
Pakistan Canals	23	37	34	13	56	71	71	29	91	94	91	48
Niobrara River	55	13	29	86	95	67	58	98	98	95	98	98
Average of field data	45	32	32	22	76	64	63	39	94	88	84	55
Flumes												
Guy et al.	40	67	56	68	70	89	85	90	91	98	99	98
Oxford	37	20	31	45	84	38	59	89	96	70	81	96
Stein	54	73	81	56	70	95	97	97	97	97	100	100
Southampton A	64	49	46	49	85	73	79	82	97	91	94	94
Southampton B	18	12	82	91	81	82	96	97	94	97	100	100
Barton-Lin	35	60	30	40	65	100	50	65	100	100	100	100
Average of laboratory data	41	46	52	59	77	74	77	89	95	89	94	98
Average of all data	43	37	40	36	76	68	68	58	94	88	88	71

In the above table, column 1 lists values obtained by the method of Van Rijn; 2 by the Engelund-Hansen formula; 3 by the Ackers-White formula and 4 by the Yang formula. The result is poor accuracy by the Yang formula for canals in India and Pakistan, which have the deepest flows of the above data. Since the other formulae produce reasonable results Van Rijn concludes that "the method of Yang must have serious systematic errors at large flow depth. On the average the predicted values are much too small".

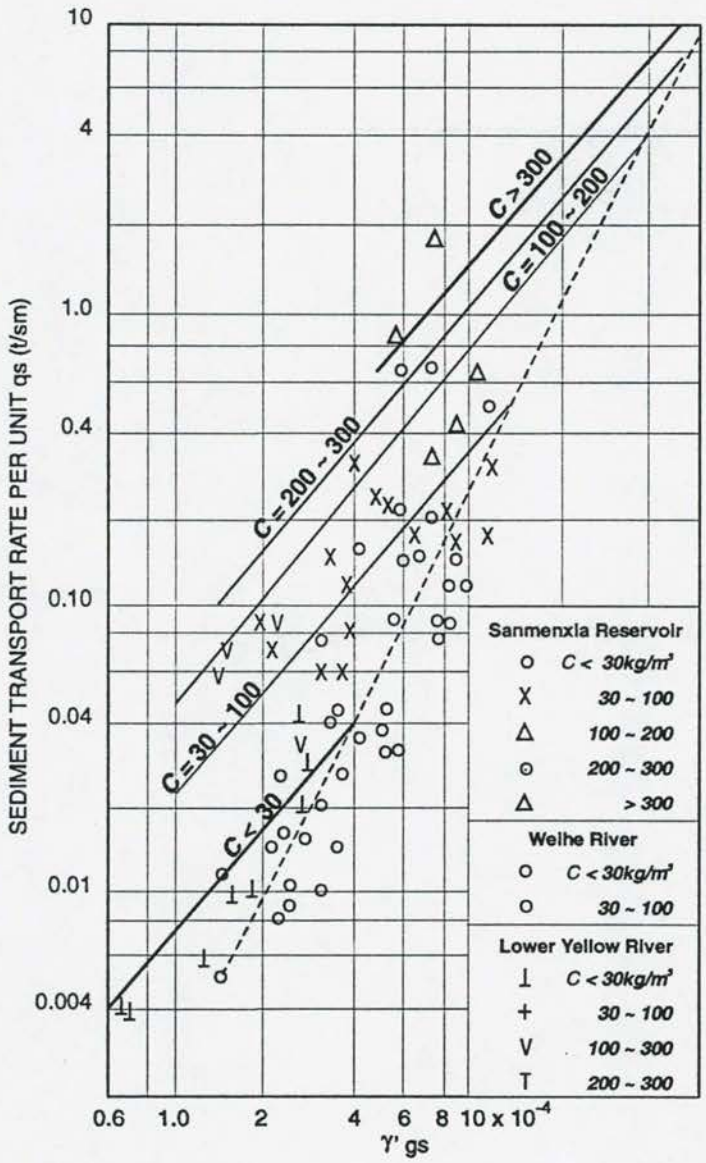

Figure 3.1 - 1 Sediment transport relationships for various Chinese Rivers

Most sediment transport equations incorporate only parameters which describe the basic hydraulics and reflect how they are influenced by bedforms and transported sediment in an indirect way. This is often done by determination of the bed roughness independently from the sediment transport equation. Some equations, like those of *Yang (1973)*, do not contain rules for calculating the velocity.

Instead of comparing the prediction accuracy of sediment transport equations based on observed data, a more appropriate comparison would be to calculate the main hydraulic variables from raw data, as was recommended by *Van Rijn (1984)*. A new approach based on the interrelationship between hydraulic variables will be followed here. For reservoir conditions, it is also important to be able to forecast the transport of fine sediments (silt and clay), since in most South African impoundments they form the main sediment body. The accurate prediction of sediment transport is important since deposit shape, resuspension, flushing channel deformation, cohesion, flocculation, etc., are all dependent on the sediment transport capacity and particle size sorting process.

In practice, the prediction of the transport of fine sediments within reservoirs is based on different approaches:

a) Use of the diffusion equation.

b) Use of sediment transport equations which were calibrated originally for sand fractions adopted to include fine sediments by recalibration with fine sediment transport data.

c) Combinations of sediment transport equations for sand fractions and diffusion equations for fine sediments.

Two further complicating matters in sediment transport are:

a) Non-uniform sediment particles. "Real" sediments are not nearly as homogeneous in size as the sediments used in laboratories. The normal approach is to assume a representative sediment particle size or to model different size groups, each with its

own sediment transport. Non-uniformity further leads to hiding/shielding and armouring phenomena involved in the re-entrainment of sediment.

b) Non-equilibrium sediment transport. Sediment transport equations as derived from theory and laboratory conditions are valid under steady, uniform flow, equilibrium conditions only. With fine sediments being transported, however, due to the slow settling velocities, reaction to changing hydraulic conditions is not immediate.

Before investigating the theory of reservoir sediment transport in detail, the validity of some of the most popular sediment transport equations used worldwide, mostly for river applications, needs to be considered.

3.2 Review of generally used equilibrium sediment transport equations

These selected equations are (in no particular order) those of:

a) *Engelund and Hansen (1967)*

By using dimensional analysis, *Engelund and Hansen (1967)* related input power per unit area of channel boundary to sediment discharge and proposed the following relationship:

$$\frac{2gDs}{v^2}\phi = 0{,}1\theta^{\frac{5}{2}} \tag{3.2-1}$$

where

$$\phi = \frac{Q_s}{\sqrt{\left(\frac{\gamma_s - \gamma}{\gamma}\right)gd^3}}\ ; \tag{3.2-2}$$

$$\theta = \frac{\rho gDs}{(\gamma_s - \gamma)d}\ ; \quad \text{and} \tag{3.2-3}$$

D = flow depth

g = gravitational acceleration

v = flow velocity

s = slope

Q_s = total sediment discharge

γ = specific weight of water

γ_s = specific weight of sediment

d = sediment particle size

The total sediment discharge can therefore be calculated directly by writing **Equation (3.2-1)** as

$$Q_s = \frac{v^2}{20gDs}\sqrt{\left(\frac{\gamma_s - \gamma}{\gamma}\right)gd^3}\left(\frac{\rho gDs}{(\gamma_s - \gamma)d}\right)^{\frac{5}{2}} \qquad (3.2\text{-}4)$$

b) ***Ackers and White (1972)***

Ackers and White (1972) used dimensional analysis to derive an equation representing total sediment discharge in terms of three dimensionless numbers, viz. a sediment transport function G_{gr}, a mobility number F_{gr} and dimensionless sediment particle size d_{gr}. The parameters are expressed as

$$G_{gr} = c'\left(\frac{F_{gr}}{A} - 1\right)^m = \frac{c'D}{\gamma_s d/\gamma}\left(\frac{\sqrt{gDs}}{v}\right)^n \qquad (3.2\text{-}5)$$

$$F_{gr} = \frac{(\sqrt{gDs})^n}{\sqrt{gd\,(\gamma_s/\gamma - 1)}}\left(\frac{v}{\sqrt{32}\log 10D/d}\right)^{1-n} \qquad (3.2\text{-}6)$$

$$d_{gr} = d\left(\frac{g(\gamma_s/\gamma - 1)}{v^2}\right)^{\frac{1}{3}} \qquad (3.2\text{-}7)$$

where v = kinematic viscosity.

The coefficients c', A, m and n are functions of sediment particle size and have the following values:

For coarse sediment ($d_{gr} > 60$): $n = 0{,}0$; $A = 0{,}170$; $m = 1{,}50$; $c' = 0{,}025$

whereas for smaller sizes ($60 \geq d_{gr} > 1$) their values are given by:

$$n = 1 - 0{,}56 \log d_{gr} \tag{3.2-8}$$

$$A = \frac{0{,}23}{\sqrt{d_{gr}}} + 0{,}14 \tag{3.2-9}$$

$$m = \frac{9{,}66}{d_{gr}} + 1{,}34 \tag{3.2-10}$$

$$\log c' = 2{,}86 \log d_{gr} - (\log d_{gr})^2 - 3{,}53 \tag{3.2-11}$$

c) **Unit (input) stream power** ***(Yang, 1973, Rooseboom, 1975)***

The basic principles of this approach were proven in South Africa in 1974 and subsequently with field data from Gariep and Welbedacht Reservoirs and with data obtained in this study. The unit stream power principle has been used extensively in the country over the last 20 years in the planning and design of reservoir sedimentation studies with success.

The suspension theory *(Rouse, 1937)* can be used to describe both bed load and suspended load (the case of suspended transport with a relatively large z-value (the suspension theory coefficient) is equivalent to the bed load condition) and the incipient motion criteria, and is therefore well suited for analysis of total carrying capacity *(Rooseboom, 1975)*.

Sediment transporting capacity per unit width in terms of flow parameters can be calculated if it is assumed that sediment particles are transported at the same velocity as the fluid:

$$q_s = \int_{y_o}^{D} Cv \, dy \quad \text{with } C \propto \left(\tau \frac{dv}{dy}\right)^z \text{ and } \tau \frac{dv}{dy} \text{ the applied power,} \tag{3.2-12}$$

with C = sediment concentration

τ = bed shear stress

z = suspension theory coefficient, $= \dfrac{w}{\kappa\sqrt{gDs}}$

w = settling velocity

χ = Von Kármán coefficient

and y_o the distance from the bed where $v = 0$ mathematically, which after integration leads to an equation of the form *(Rooseboom, 1975)*:

$$\log \frac{q_s}{q} = \alpha_1 \log \bar{v}s + \log \left[\frac{\alpha_1 \alpha_2 C_0}{\frac{(sD\sqrt{2\pi g D s})^{z_1}}{y_0}} \right] \qquad (3.2\text{-}13)$$

with α_1; α_2 = coefficients

z_1 = suspension theory coefficient as derived by *Rooseboom (1975)*

C_o = sediment concentration at the bed where $v = o$ at $y = y_o$

$\bar{v}$ = average flow velocity

Yang (1972) found through statistical analysis of available data that **Equation 3.2-13** describes sediment transporting capacity particularly well. He used a slightly different approach by including a critical stream power value for incipient motion in the equation (1972):

$$\log \frac{q_s}{q} = \alpha_3 + \alpha_4 \log (\bar{v}s - vs_{cr}) \qquad (3.2\text{-}14)$$

with α_3; α_4 = constant and coefficient,

vs_{cr} = critical input stream power for incipient motion

and later *(Yang, 1973)*

$$\log \frac{q_s}{q} = \alpha_5 + \alpha_6 \log \left(\frac{\bar{v}s - vs_{cr}}{w} \right) \qquad (3.2\text{-}15)$$

with α_3; α_4 = constant and coefficient

w = settling velocity

The last term in **Equation 3.2-13** was found *(Rooseboom, 1975)* not to vary considerably and can be equated to the α_5 coefficient of Yang.

Yang produced two dimensionless unit stream power equations for sand transport *(1973, 1979)*, with and without incipient motion. In *1984*, Yang proposed a gravel transport equation with an incipient motion term.

The maximum sediment transport capacity of a stream can therefore be determined by an equation of the type:

$$\log \frac{q_s}{q} = \propto \log \bar{v}s + \beta \qquad (3.2\text{-}16)$$

where $\bar{v}s$ represents the average input unit stream power at a cross-section in a reservoir or river, and $\propto$ = coefficient and β = constant.

d) **Stream power theory** ***(Bagnold, 1966)***

Bagnold used the stream power per unit bed area, based on general concepts in physics, to relate the rate of energy dissipation used in transporting materials to the sediment transport:

$$\left(\frac{\gamma_s - \gamma}{\gamma}\right) q_{bw} \tan \propto = \tau v e_b \qquad (3.2\text{-}17)$$

with

q_{bw}	=	bed load transport rate
$\tan\propto$	=	ratio of tangential shear to normal force
v	=	average flow velocity
e_b	=	efficiency coefficient
τv	=	stream power

and for suspended load:

$$\left(\frac{\gamma_s - \gamma}{\gamma}\right) q_{st} = 0{,}01\left(\frac{\tau v^2}{w}\right) \qquad (3.2\text{-}18)$$

with the total load (q_t)

$$= q_{bw} + q_{st} = \frac{(\gamma_s - \gamma)}{\gamma} \tau v \left(\frac{e_b}{\tan\propto} + 0{,}01\frac{v}{w}\right) \qquad (3.2\text{-}19)$$

Based on field data (rivers and reservoirs in China), the sediment carrying capacity = $e_b(\tau v) = f(\gamma_s qs)$ has been indicated in **Figure 3.2-1** for conditions of deposition and erosion.

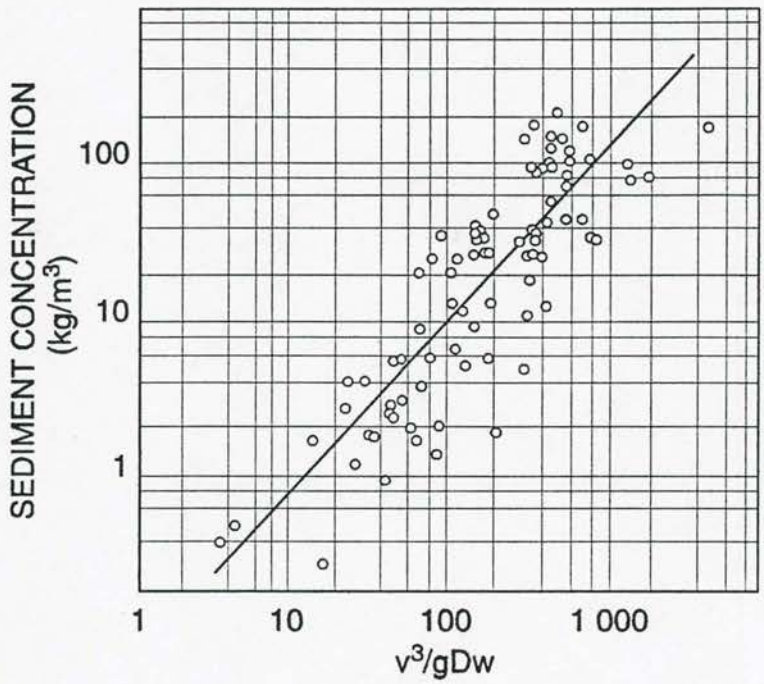

Figure 3.2 - 1 Stream power sediment transport relationship at Fenhe Reservoir, China

e) **Gravitational power theory** ***(Velikanov, 1954; Dou, 1974; Zhang, 1959)***

Velikanov (1954) divided the rate of energy dissipation for sediment transport into two parts - the power required to overcome flow resistance and the power required to keep sediment particles in suspension against the gravitational force:

$$\underset{(i)}{\rho g(1 - C_{vy})\, v_y s} = \underset{(ii)}{\rho v_y \frac{d[(1 - C_{vy})\overline{U_x U_y}]}{dy}} + \underset{(iii)}{g(\rho_s - \rho)\, C_{vy}\, (1 - C_{vy})\, w} \qquad (3.2\text{-}20)$$

with C_{vy} = time-averaged sediment concentration at a distance y above the bed in percent by volume

v_y = time-averaged flow velocity at distance y above bed

U_x, U_y = fluctuating part of velocities in the x and y directions

Integration over depth of flow yields

$$gvSD = \frac{f_o v^3}{8} + \frac{\rho_s - \rho}{\rho}(gDwC_v) \tag{3.2-21}$$

The Darcy Weisbach resistance coefficients are given by:

$$f = \frac{8gDs}{v^2}, \ (C_v \neq o) \tag{3.2-22}$$

and $$f_o = \frac{8gDs_0}{v^2}, \ (C_v = o) \tag{3.2-23}$$

with s, s_o = energy slope with and without sediment.

Assuming that f/f_k = a constant, (with f_k = resistance coefficient with saturated sediment concentration), it follows that

$$\frac{(\rho_s - \rho)}{\rho}\frac{wC_v}{vs} = \text{a constant.} \tag{3.2-24}$$

From the above, Velikanov's equation can be expressed in the form:

$$C_v = K\left(\frac{v^3}{gDw}\right) \tag{3.2-25}$$

with K = a coefficient to be determined from measured data. Sediment transport equations of this format have been used extensively by Chinese engineers. *Dou (1974)* proposed that the rate of energy dissipation to keep sediment particles suspended should be equal to that used by sediment particles in suspension:

$$C_t = K_1\left(\frac{\gamma_s}{\gamma_s - \gamma}\right)\frac{vs}{w} \tag{3.2-26}$$

with C_t = sediment concentration by weight

K_1 = coefficient

and from Chezy : $s = \frac{v^2}{C^2 D}$ (3.2-27)

gives : $C_t = K_2\left(\frac{v^3}{gDw}\right)$ (3.2-28)

with K_2 = coefficient

Zhang (1959) assumed that the energy being dissipated in keeping sediment particles suspended should come from turbulence instead of from the effective power available from the flow:

Total rate of energy dissipation of clear water - rate of energy dissipation due to sediment laden flow = total rate of energy reduction due to the damping effect (reduction in turbulence due to suspended sediment)

$$\gamma A v s_1 - [\gamma(1 - C_v) A v s_2 + \gamma_s C_v A v s_2] = k_1(\gamma_s - \gamma) A w C_v^{\alpha} \quad (3.2\text{-}29)$$

with s_2, s_1 = energy slope of sediment-laden water and clear water

α = dimensionless exponent

A = channel cross-sectional area

k_1 = dimensionless coefficient

When C_v is small:

$$C_v^{\alpha} = \left[\frac{\gamma}{k_1(\gamma_s - \gamma)}\right]\left[\frac{v}{w}(s_1 - s_2)\right] \quad (3.2\text{-}30)$$

which can be further reduced to:

$$C_t = K_3\left(\frac{v^3}{gRw}\right)^m \quad (3.2\text{-}31)$$

with K_3, m = parameters related to sediment concentration, and

$R \approx D$ = hydraulic radius

Field data plotted according to this relationship are shown in **Figure 3.2-2.**

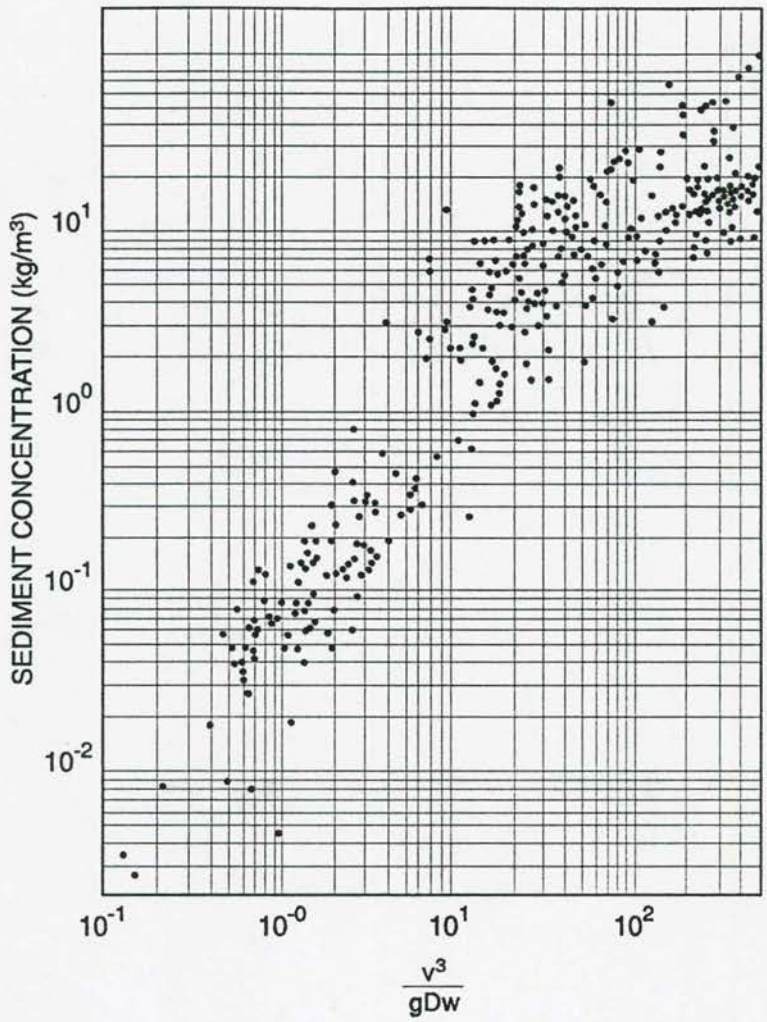

Figure 3.2 - 2 Gravitational power theory calibrated with Chinese data

The use of the stream power theory has been well researched and verified with field data. Three different approaches in the study of sediment transport, based on the concept that the rate of energy dissipation of flowing water should be related to the rate of sediment transport, are generally used.

Yang et al. (1991) carried out an analysis and comparison of the three stream power parameters:

$\frac{vs}{w}$; τv ; and $\frac{v^3}{gDw}$

The dimensionless unit stream power correlated best with concentration data by *Stein (1965)*, indicated in **Figure 3.2-3**. Velikanov's equation fitted with a S-curve instead of a straight line on a log-log plot as is required by **Equation 3.2-25**. Bagnold's equation is based on general concepts in physics without using much theory in fluid mechanics and it is not generally used, and was not reviewed further by *Yang et al. (1991)*.

Yang and Molinas (1982) showed that bed load, suspended load and total bed-sediment concentrations can all be expressed by the general form of **Equation 3.2-15**. *Yang et al. (1991)* illustrated that the three equations based on the gravitational theory can all be converted to or derived from the basic form of the unit stream power equation, with differences in coefficients and assumptions to derive coefficients. The assumptions of Dou, Velikanov and Zhang to obtain v^3/gRw cannot be supported by laboratory or field data used by *Yang et al. (1991)*. The unit stream power theory is therefore best to use and based on a sound theoretical basis *(Yang et al., 1991)*.

f) ***Van Rijn (1984)***

In the van Rijn transport model the sediment load is divided between bed load and suspended load according to the relative magnitudes of the bed shear velocity, and the particle fall velocity. When the bed shear velocity exceeds the fall velocity then sediment is transported as both suspended and bed load. Bed load is considered to be transported by rolling and saltation and the rate is described as a function of saltation height. The suspended load is determined from the depth-integration of the product of the local concentration and flow velocity. The reference concentration is determined from the bed load transport.

Bed load transport rate is computed from the product of particle velocity, u_{bs}, saltation height, δ_b, and the bed load concentration, C_b:

$$q_b = u_{bs}.\delta_b.C_b \qquad (3.2\text{-}32)$$

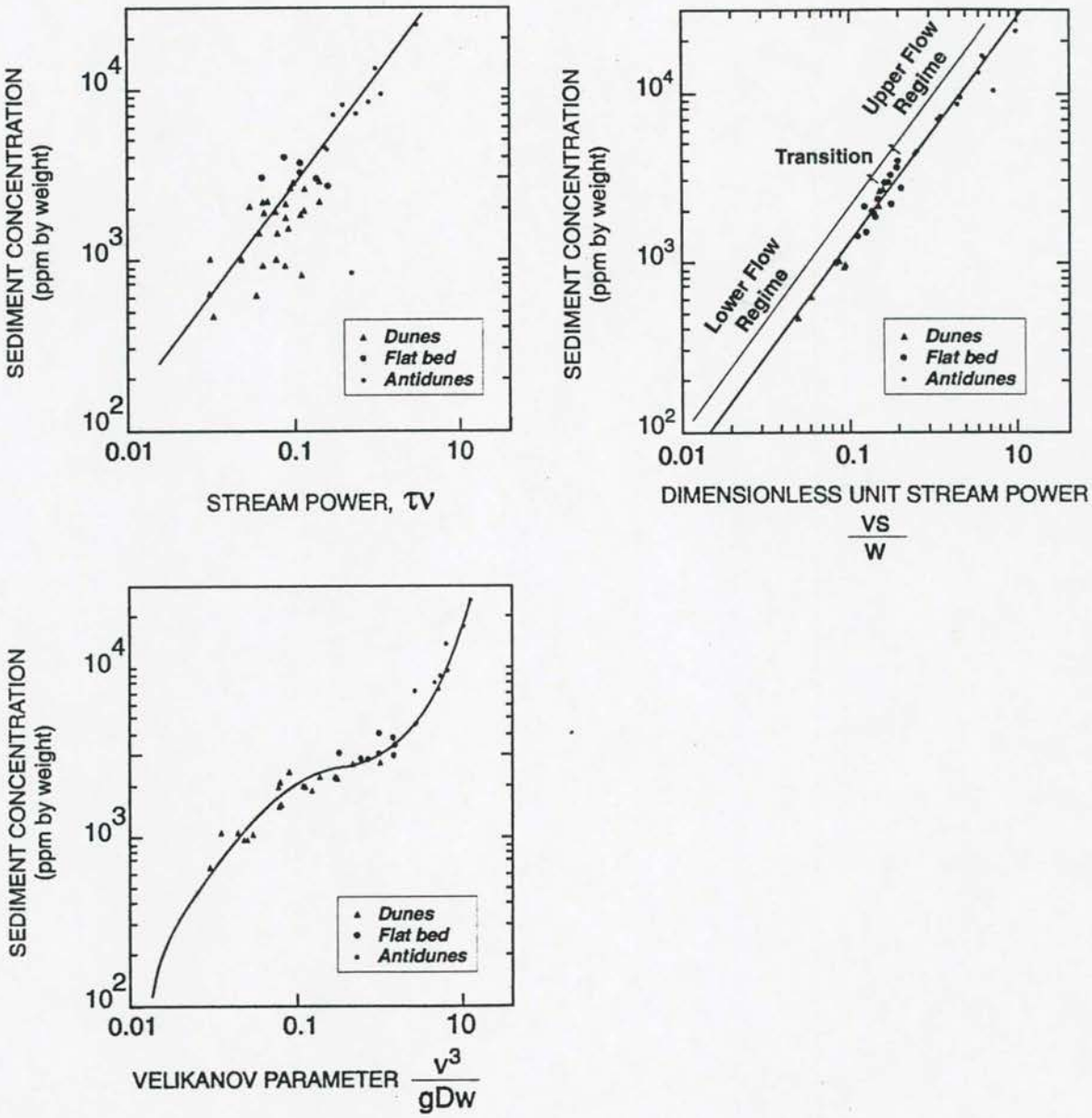

Figure 3.2 - 3 Comparison between stream power equations

Expressions for the particle velocity and saltation height were obtained by numerically solving the equations of motion applied to a solitary particle. These expressions are given in terms of two dimensionless parameters which are considered to adequately describe bed load

transport; a dimensionless particle diameter, D_*, and a transport stage parameter, T as defined below:

$$D_* = d_{50}\left[\frac{(s-1)}{\nu^2}g\right]^{1/3} \tag{3.2-33}$$

$$T = \frac{(u_g')^2 - (u_{f,cr}')^2}{(u_{f,cr}')^2} \tag{3.2-34}$$

in which u'_g is the bed shear velocity, related to grains, u is the mean flow velocity and $u'_{f,cr}$ is Shields critical bed shear velocity. u'_g is the effective bed shear and is so defined in order to eliminate the influence of bed forms since form drag was not considered to contribute to bed load transport.

Extensive analysis of flume measurements of bed load transport yielded the following expression for the bed load concentration:

$$\frac{C_b}{C_o} = 0.18\,\frac{T}{D_*} \tag{3.2-35}$$

in which C_o is the maximum bed concentration.

Combining equations for particle mobility, saltation height and **Equation 3.2-35** gives the following expression for bed load transport, valid for particles in the range 0.2 to 2.0 mm:

$$\frac{q_b}{\sqrt{(s-1)gd_{50}^3}} = \frac{0.053T^{2.1}}{D_*^{0.3}} \tag{3.2-36}$$

The Van Rijn suspended sediment load method is based on the computation of a reference concentration determined from the bed load transport. Thus the reference concentration, C_a, is described as a function of the dimensionless particle diameter, D_*, and transport stage parameter, T.

$$C_a = 0.015\frac{d_{50}\,T^{1.5}}{a\,D_*^{0.3}} \tag{3.2-37}$$

The representative particle size of suspended load is generally finer than that of bed load. Van Rijn relates this particle size, d_s to the d_{50} and geometric standard deviation, σ_s, of the bed

material:

$$\frac{d_s}{d_{50}} = 1 + 0.011\ (\sigma_s - 1)(T-25)\ \textit{for}\ T<25 \qquad (3.2\text{-}38)$$

Many factors affect the suspension parameter z, e.g. volume occupied by particles, reduction of fall velocity and damping of turbulence. These effects are grouped into a single correction factor, ψ, which is used to define a modified suspension number, Z:

$$Z' = z + \psi \qquad (3.2\text{-}39)$$

ψ was found to be a function of the main hydraulic parameters:

$$\psi = 2.5\left[\frac{w}{u_f}\right]^{0.8}\left[\frac{C_a}{C_o}\right]^{0.4}\ \textit{for}\ 0.1 \le 1 \qquad (3.2\text{-}40)$$

where C_o is the maximum bed concentration.

By combining the expression describing the velocity and concentration profiles with the expressions for z and ψ, van Rijn derived the following expression:

$$q_s = FuDC_a \qquad (3.2\text{-}41)$$

in which F is given by:

$$F = \frac{\left[\frac{a}{D}\right]^{z'} - \left[\frac{a}{D}\right]^{1.2}}{\left[1-\frac{a}{D}\right]^{z'}[1.2-z']} \qquad (3.2\text{-}42)$$

The above sediment transport equations show that:

- the stream power concept is powerful in describing the sediment transport process. Most equations are, however, based on dimensional analysis and not derived from sound theoretical principles.

- the unit input stream power equation *(Yang, 1973)*, is the only stream power

relationship which can be derived theoretically *Rooseboom, (1975)*, although some averaging assumptions had to be made.

- The Van Rijn equations are based on several empirical relationships and has the division between bed load and suspended transport which cannot be justified from fundamental theory. The equations do, however, include the change in bed roughness and energy dissipation for different flow regimes and sediment transport.

- The prediction accuracy of most sediment transport equations seems to depend on calibration with as extensive a sediment transport data base as possible (including laboratory and river data).

Sediment transport through reservoirs has traditionally only been described under conditions of deposition. When management options such as flushing are incorporated, flow through the reservoir reverts back to river conditions, but with high sediment transport. **(Photograph 3.2-1)**. A very wide range of sediment transport, hydraulic, bed roughness and other conditions are therefore encountered. To improve understanding of the processes of sediment transport, it is necessary to first understand the resistance to flow and velocity distribution in turbulent movable boundary conditions.

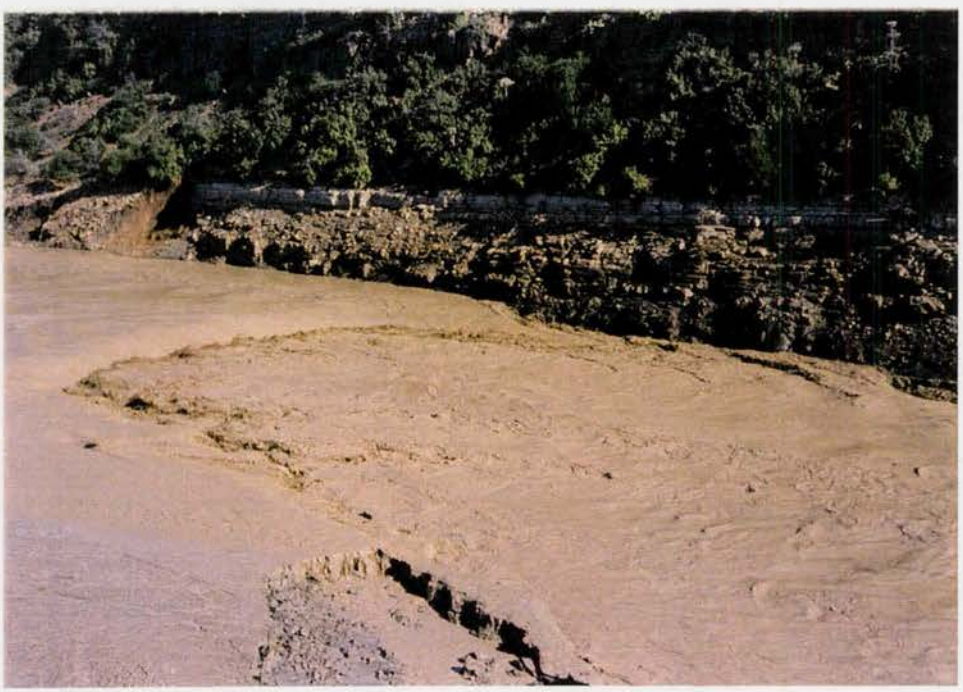

Photograph 3.2-1 Elandsdrift Reservoir flood flushing, 1985 (900 m^3/s)

3.3 Velocity distribution for a rigid bed boundary and homogeneous fluid *(Rooseboom, 1975)*

When uniform steady flow in a wide canal with small longitudinal slope (s_o) and depth of flow (D) is considered, the forces acting on a small element with height (D-y), length Δx and unit width, are in equilibrium. The resistance to flow can be described by a shear force (τ) acting on the bed which is opposing the driving force due to gravity.

Resistance force	=	Driving force	
$\tau.\Delta x$	=	$\rho g\ (D-y)\ s_o \Delta x$	
or τ	=	$\rho g\ (D-y)\ s_o$	(3.3-1)

The shear stress therefore increases linearly from zero at the surface to a maximum value of ρgsD at the bed, as indicated in **Figure 3.3-1**.

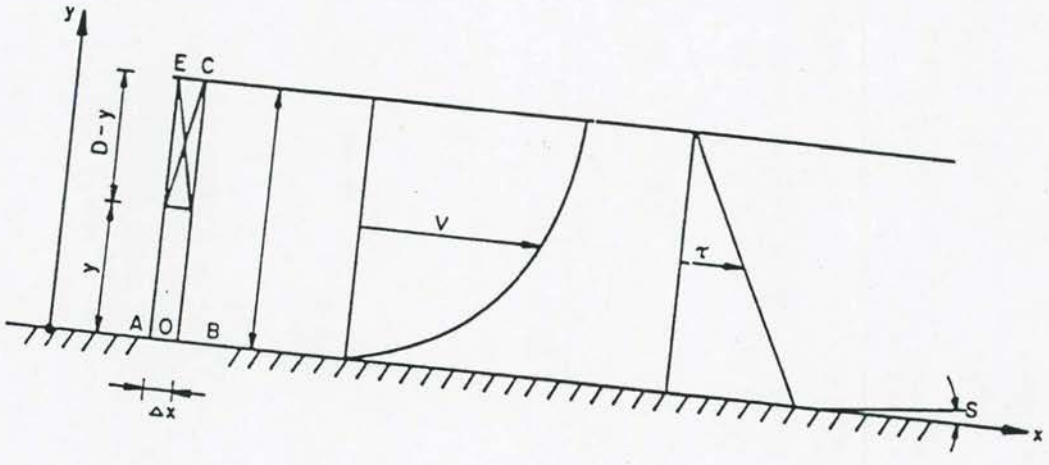

Figure 3.3 - 1 Velocity and shear stress distribution (Rooseboom, 1975)

Near the bed the velocity has to be zero, otherwise it would mean that the point of attachment of the shear force at the bed is moved, which will only be possible if bed material is moved.

In laminar flow, where shear stresses are formed through liquid interchange on a molecular scale, the relationship between shear stress and velocity distribution is given by:

$$\tau = \mu \frac{dv}{dy} \qquad (3.3\text{-}2)$$

with μ = dynamic viscosity

Equating **Equations 3.3-1** and **3.3-2** and integration give the velocity at distance y above the bed:

$$v = \frac{\rho g s}{2\mu}(2Dy - y^2) \tag{3.3-3}$$

Further integration gives an equation for average velocity $(\bar{v})$:

$$\bar{v} = \frac{\rho g s D^2}{3\mu} \tag{3.3-4}$$

In fully developed turbulent flow, shear stresses develop on a macro scale through eddies. Water particles move temporarily as units in the form of spherical eddies. *Rooseboom (1975)* stated that based on continuity principles, the angle velocity of rotation of an eddy should equal the local velocity distribution. According to Newton's second law, the force in the x direction should be equivalent to the rate of x momentum change. The shear force acting on a surface element with size ΔA and orientation parallel with the x axis will be equal to the rate of x momentum exchange across the surface **(Figure 3.3-2)**:

$$\tau.\Delta A = \frac{d}{dt}(mv)_x$$

$$= \rho\left(r\frac{dv}{dy}\cos\propto\right)\Delta A\left(r\frac{dv}{dy}\sin\propto\right)$$

$$\therefore \tau = \rho r^2\left(\frac{dv}{dy}\right)^2 \sin\propto\cos\propto \tag{3.3-5}$$

The average shear stress $(\bar{\tau})$ over the cylindrical element is:

$$\bar{\tau} = \frac{4\int_o^R\int_o^{\frac{\pi}{2}} \rho\left(\frac{dv}{dy}\right)^2 r^3 \cos\propto \sin\propto \, dr d\alpha}{\pi R^2}$$

$$= \frac{\rho}{2\pi} R^2\left(\frac{dv}{dy}\right)^2 \tag{3.3-6}$$

$$\approx 0{,}4^2\,\rho R^2\left(\frac{dv}{dy}\right)^2 \tag{3.3-7}$$

for clear water and a rigid bed.

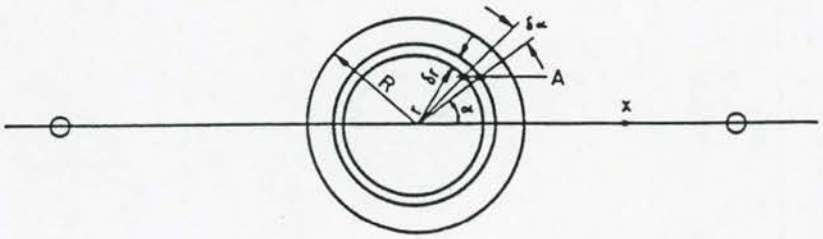

Figure 3.3 - 2 Section through eddy

Prandtl (1925) presented a hypothesis to determine the velocity of a turbulent flow assuming that the turbulent fluctuations are confined within a certain limit defined by a length (ℓ) called Prandtl's mixing length. Prandtl considered a parallel flow in which velocity only varied along the stream lines (along the x axis)

$$\tau = -\rho\overline{u'v'} \tag{3.3-8}$$

with u' and v' denoting fluctuating components of velocity, with u in the x direction and v in the transverse direction.

The turbulence is generated at the bed and groups of fluid particles travel together with other bodies of fluid, exchanging particles of fluid with each other. Consider a particle coming from a body of fluid at layer $(y_1 - \ell)$, **Figure 3.3-3.**

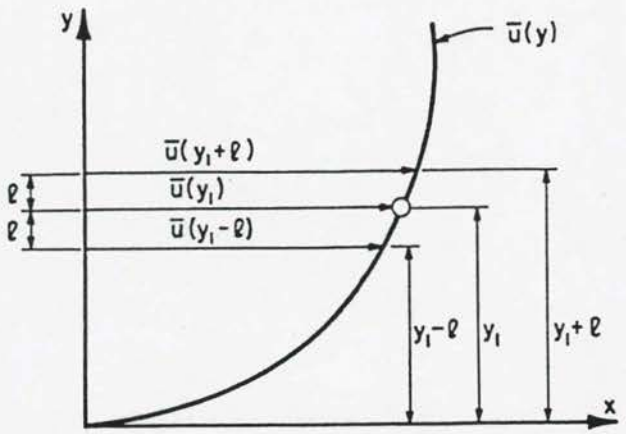

Figure 3.3 - 3 Vertical velocity distribution in a channel with turbulent flow

The velocity prevailing at that level is $\bar{u}\,(y_1 - \ell)$, while the particle arrives at layer y_1 with velocity $\bar{u}\,(y_1) > \bar{u}\,(y_1 - \ell)$. The difference in velocities is:

$$\Delta u_1 = \bar{u}\,(y_1) - \bar{u}\,(y_1 - \ell) = \ell \left(\frac{d\bar{u}}{dy}\right)_1 \qquad (3.3\text{-}9)$$

obtained through expanding $u\,(y_1 - \ell)$ and retaining the first term. The same can be done with a particle arriving from layer $(y_1 + \ell)$ to layer (y_1) with a velocity difference:

$$\Delta u_2 = \bar{u}\,(y_1 + \ell) - u\,(y_1) = \ell \left(\frac{d\bar{u}}{dy}\right)_1 \qquad (3.3\text{-}10$$

The particle with velocity $\bar{u}\,(y_1 - \ell)$ may create in layer (y_1) a fluctuation $(-u')$ in such a way that the velocity in layer (y_1) is always $(\bar{v})$. Conversely a particle with velocity $\bar{u}\,(y_1 + \ell)$ may create in the same layer a fluctuation $(+u')$. If the two particles arrive at layer (y_1) simultaneously, then the time average of the absolute value of this fluctuation is:

$$|\bar{u}'| = \frac{1}{2}\,(|\Delta u_1| + |\Delta u_2|) \approx \ell \left|\left(\frac{d\bar{u}}{dy}\right)\right|_1 \qquad (3.3\text{-}11)$$

It is possible *(Simons et al, 1977)* to show that v' and u' are of the same order and

$$\overline{u'v'} = -c\,|\bar{u}'|.|\bar{v}'| \qquad (3.3\text{-}12)$$

where $o < c < 1$

and $\overline{u'v'} = -c\ell^2 \left(\frac{d\bar{u}}{dy}\right)^2$ (3.3-13)

Combining the constant c and ℓ yields:

$$\overline{u'v'} = \ell^2 \left(\frac{d\bar{u}}{dy}\right)^2 \quad (3.3\text{-}14)$$

and the shear stress becomes:

$$\tau = \rho\ell^2 \left(\frac{du}{dy}\right)^2 \quad (3.3\text{-}15)$$

Prandtl interpreted the mixing length as the "diameter of balls of fluids which move as a whole and also as the path traversed by these balls relative to the rest of the fluid before they lose their individuality again by mixed with the surrounding turbulent fluid."

Prandtl's interpretation and **Equation 3.3-15** agree with the Rooseboom **Equation 3.3-6**.

The factor $1/2\pi$ in **Equation 3.3-6** equals $(0,4)^2 = \kappa^2$ with κ the Von Kármán coefficient. In turbulent flow of homogeneous fluids κ has been found equal to 0,4 empirically, confirming the theoretical derivation by Rooseboom.

The velocity distribution for turbulent flow can now be determined. Again the approaches followed by *Rooseboom (1975)* and *Prandtl (1925)* will be given:

Rooseboom (1975) equated **Equations 3.3-1** and **3.3-6**:

$$\rho gs\,(D - y) = \frac{\rho}{2\pi} \cdot R^2 \cdot \left(\frac{dv}{dy}\right)^2 \quad (3.3\text{-}16)$$

First it is necessary to determine how R varies with y. In turbulent flow it is not possible for fluid layers to slide over one another (as is the case with laminar flow). A thin element of fluid ABCE **(Figure 3.3-1)** therefore temporarily has to move as a unit. Since the velocity

at 0 near the bed equals zero, the only possible means of movement as unit ABCE is through rotation around 0. But since the fluid movement is translation in a canal, such movement is only possible if the rotation centre point also translates. A small fluid particle at distance y from the bed rotates at angular velocity $\frac{dv}{dy}$ and therefore the translation velocity relative to the fixed rotation centre point is $y\frac{dv}{dy}$. Translatory flow is therefore only possible if the rotation centre point moves at a speed of $y\frac{dv}{dy}$.

Since the rotation centre point is common to all particles in the vertical,

$$y\frac{dv}{dy} = constant = v_o \tag{3.3-17}$$

with v_o = speed of the centre point of rotation.

From **Equation (3.3-16)**

$$\frac{dv}{dy} = \frac{\sqrt{2\pi gs\ (D - y)}}{R}$$

and

$$v_o = y\frac{dv}{dy} = \frac{y\sqrt{2\pi gs\ (D - y)}}{R} \tag{3.3-18}$$

Near the bed $(D - y) \approx D$ and $y \approx R_o$ = radius of eddies near bed.

$$\therefore v_o = y\frac{dv}{dy} = \sqrt{2\pi gDs} \tag{3.3-19}$$

From **Equations 3.3-16** and **3.3-19**:

$$\therefore R = y\sqrt{\frac{(D - y)}{D}} \tag{3.3-20}$$

and **Equation 3.3-18**:

$$\frac{dv}{dy} = \frac{\sqrt{2\pi gDs}}{y} \tag{3.3-21}$$

Integration of **Equation 3.3-21** gives:

$$v = \sqrt{2\pi gDs}\ \ln\left(\frac{y}{y_o}\right) \tag{3.3-22}$$

with y_o = distance from bed, where velocity is mathematically zero.

Equation (3.3-16) was derived for a cylindrical element with unit width and radius R. If eddies can be described by spheres forming between roughness elements at the bed, the radius R_w at distance w from the centre point of a sphere is *(Rooseboom, 1975)*:

$$R_w^2 = R^2 - w^2 \tag{3.3-23}$$

The effective radius of a sphere is:

$$Reff^2 = \frac{\int_o^R (R^2 - w^2)\, dw}{R} = \frac{2}{3} R^2 \tag{3.3-24}$$

$$\therefore Reff = 0{,}8165R$$

The effective rotation centre point is therefore at $0{,}1835R_o$

$$\therefore v = v_o = \sqrt{2\pi gDs} = \sqrt{2\pi gDs}\ \ln\left(\frac{y}{y_o}\right)$$

$$\therefore y_o = \frac{R_o}{14{,}81} \tag{3.3-25}$$

Average velocity $(\bar{v})$ can be obtained by integration of **Equation (3.3-22)** and substitution of **Equation 3.3-25**:

$$\bar{v} = \sqrt{2\pi gDs}\ \ln\frac{5{,}45D}{R_o} \tag{3.3-26}$$

or

$$\bar{v} = 5{,}77\ \sqrt{gDs}\ \log\frac{5{,}45D}{R_o} \tag{3.3-27}$$

These equations have the basic form of the *Chezy (1775)* equation:

$$\bar{v} = C_H \sqrt{DS} \tag{3.3-28}$$

with C_H the Chezy coefficient, and agrees well with the semi-empirical relationships such as that proposed by *Keulegan (1938)*:

$$\bar{v} = 5{,}75 \sqrt{gDs} \log \frac{5{,}55D}{R_o} \tag{3.3-29}$$

The radius of spherical eddies forming near the bed (R_o) is normally described by a roughness coefficient (also known as roughness height) k_s $(= 2R_o)$ equalling the diameter of turbulent eddies. In a smooth bed k_s is a function of sediment particle size on the bed, while as the bed is deformed k_s represents the size of eddies that can form in between the ripples or dunes.

Prandtl's (1925) **Equation 3.3-15** can be rewritten

$$\sqrt{\frac{\tau}{\rho}} = \ell \left(\frac{du}{dy}\right) = u_* \tag{3.3-30}$$

where u_* is the shear velocity at a point in the vertical and the variation of shear stress τ with depth is given by:

$$\tau = \tau_o \frac{y}{D} \tag{3.3-31}$$

with τ_o the shear stress at the bed.

Prandtl substituted $\tau = \tau_o$ (assuming small friction velocity variation), which allows substitution of U_*, the mean value of the friction velocity for u_*. Combining **Equation 3.3-30** with **Equation 3.3-31**:

$$U_*^2 = \ell^2 \left(\frac{du}{dy}\right)^2 \tag{3.3-32}$$

Introducing an empirical dimensionless constant κ , *Von Kármán (1948)* assumed that the mixing length satisfies the equation:

$$\ell = -\kappa \frac{u'}{u''} \tag{3.3-33}$$

where u' and u'' are the first and second derivations of the velocity relation. Prandtl's assumption for the mixing length can be expressed as:

$$\ell = \kappa y \tag{3.3-34}$$

Substitution in **Equation 3.3-32** yields:

$$\tau = \rho \kappa^2 y^2 \left(\frac{du}{dy}\right)^2$$

$$\text{or} \qquad \frac{dv}{dy} = \frac{\sqrt{gDs}}{\kappa y} \tag{3.3-35}$$

Integration yields the Prandtl - Von Kármán velocity equation:

$$v = \frac{\sqrt{gDs}}{\kappa} \ln y + c \tag{3.3-36}$$

with c an integration constant to be determined from conditions at the bed where $y = y_o$:

$$\therefore v = \frac{1}{\kappa} \ln \left(\frac{y}{y_o}\right) \sqrt{gDs} \tag{3.3-37}$$

which equals **Equation (3.3-22)**.

Furthermore, the value of y_o in **Equation 3.3-37** was found theoretically *(Simons et al, 1977)* equal to $y_o = \frac{k_s}{30,1}$ (by assuming shear velocity at boundary layer between laminar and turbulent flow equal), almost the same as **Equation 3.3-25**

$$\text{with} \quad y_o = \frac{R_o}{14,81} = \frac{k_s}{29,62} \tag{3.3-38}$$

3.4 Power balance in open channel flow

Rooseboom (1975) and *Streeter (1971)* derived the power balance relationship, which will be shown later to be of importance in describing the interrelationship between sediment transport and bed roughness.

For a small translating fluid element with dimensions Δx, Δy and unit width, the average velocity and shear stress change over the element is shown in **Figure 3.4-1**.

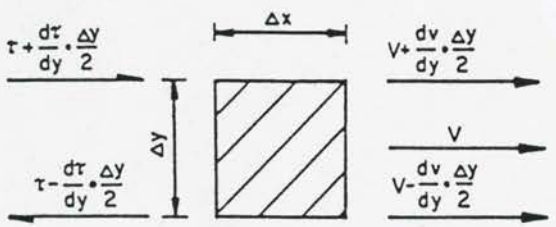

Figure 3.4 - 1 Velocity and shear stress on a fluid element

When the element translates at average velocity v at a small slope s, the power that is released due to gradual decrease in potential energy equals:

$$\rho g s \Delta x \Delta y . v \tag{3.4-1}$$

The power shortage of the element equals the work per unit time on the upper surface minus the work per unit time on the lower surface of the element:

$$\left(\tau + \frac{d\tau}{dy} \cdot \frac{\Delta y}{2}\right)\left(v + \frac{dv}{dy} \cdot \frac{\Delta y}{2}\right)\Delta x - \left(\tau - \frac{d\tau}{dy} \cdot \frac{\Delta y}{2}\right)\left(v - \frac{dv}{dy} \cdot \frac{\Delta y}{2}\right)\Delta x = \left(\tau \frac{dv}{dy} + v \frac{d\tau}{dy}\right)\Delta x . \Delta y \tag{3.4-2}$$

$\therefore$ Power deficit per unit volume

$$= \tau\frac{dv}{dy} + v\frac{d\tau}{dy} \tag{3.4-3}$$

but $\tau = \rho g\,(D - y)\,s$ (3.3-1)

$\therefore$ Power deficit per unit volume

$$= \tau\frac{dv}{dy} - \rho gsv \tag{3.4-4}$$

The term $\tau\frac{dv}{dy}$ represents the applied stream power needed to maintain flow, while ρgsv is the amount of input power made available as the element translates.

The stream power distribution is indicated in **Figure 3.4-2**, and it is especially the shape of the applied stream power distribution which will be shown later to be very important in predicting equilibrium sediment transport and bedform changes.

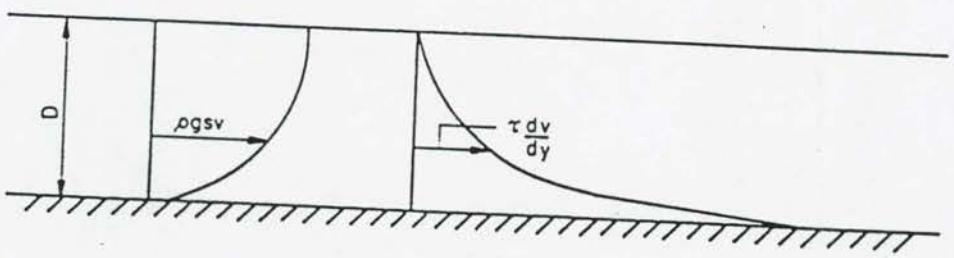

Figure 3.4 - 2 Stream power variation with depth

According to the principle of conservation of power, the total input power = total applied power *(Rooseboom, 1975)*:

$$\int_{y_o}^{D} \rho g s v.dy = \int_{y_o}^{D} \tau \frac{dv}{dy} \cdot dy \qquad (3.4\text{-}5)$$

which is applicable to laminar and turbulent flows.

3.5 Transition from laminar to turbulent flow

According to *Rooseboom (1975)*, the flow against the bed will be either laminar or turbulent based on the principle of least resistance, or in other words the least power expenditure per unit volume. This power can be represented by the applied power function $\left(\tau \frac{dv}{dy}\right)_o$ which has a maximum value near the bed.

Near a smooth bed, the radius of eddies fitting in between roughness elements on the bed will be extremely small and $\left(\frac{dv}{dy}\right)_o = \frac{\sqrt{2\pi}\ \sqrt{gDs}}{yo}$ will therefore be large.

Furthermore, the molecular structure of the fluid will limit the minimum dimension of eddies.

For a given value τ_o near a smooth bed, assuming

$$\left(\tau \frac{dv}{dy}\right)_o \textit{ laminar} = \left(\tau \frac{dv}{dy}\right) \textit{ turbulent} \qquad (3.5\text{-}1)$$

$$\therefore \frac{\rho g s (D - y_1)}{\mu} \approx \frac{\rho g s D}{\mu} = \frac{\sqrt{2\pi}\sqrt{gDs}}{y_1}$$

$$\therefore y_1 = \frac{\sqrt{2\pi}\ \nu}{\sqrt{gDs}} \qquad (3.5\text{-}2)$$

At elevation y_1, **(Figure 3.5-1)** the laminar velocity equals $\approx \frac{\rho g s}{\mu} .D.y_1$

$= \sqrt{2\pi g D s}$

= translatory velocity of the centre of rotation for turbulent flow.

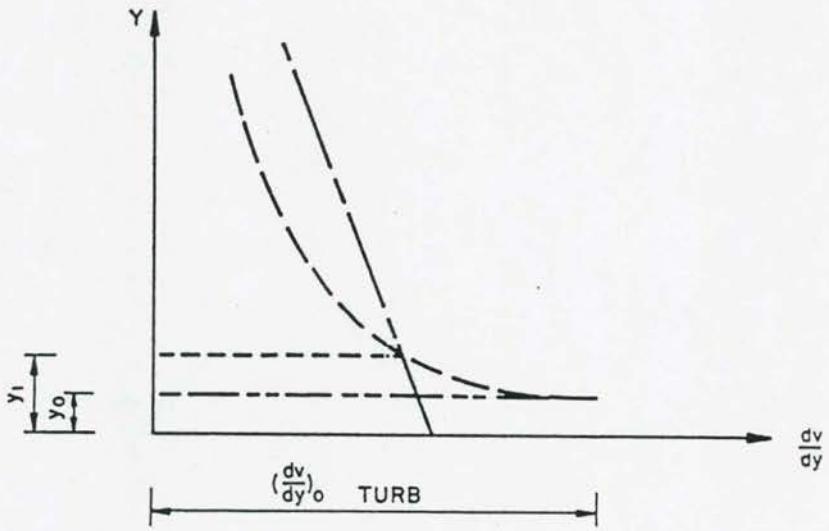

Figure 3.5 - 1 Laminar and turbulent velocity distributions ***(Rooseboom, 1975)***

A laminar layer therefore provides the necessary platform for turbulent flow so that $y\frac{dv}{dy}$ = constant, as described in **Section 3.3**.

The value of y_o (theoretical distance from bed, where v = o) should be related to the size of eddies in the transitional zone between laminar and fully developed turbulent flow.

The "effective rotational radius" R for laminar flow can be found by equating shear stresses *(Rooseboom, 1975)*:

$$\tau = \frac{\rho}{2\pi} \cdot R^2 \left(\frac{dv}{dy}\right)^2 = \mu \left(\frac{dv}{dy}\right) \qquad (3.5\text{-}3)$$

$$\therefore R = \sqrt{\frac{2\pi v^2}{gDs}}$$

$$\text{or } y_o \propto \frac{\sqrt{2\pi v^2}}{gDs} \qquad (3.5\text{-}4)$$

Nikuradse (1932) found $y_o = \frac{11{,}6\ \upsilon}{104\sqrt{gDs}}$ for pipe flow.

In the case of a laminar sublayer over a rough bed, y_o is determined by the combined effect of the laminar sublayer and the bed roughness. When y_1 is small in relation to bed roughness, the size of eddies near the bed will be determined by the dimensions of these roughness elements.

3.6 Turbulent velocity distribution for uniform flow over a movable bed in alluvial channels

In alluvial sand-bed channels, the flow is generally hydraulically rough. Because the bed configuration is a function of the interaction of fluid, flow and bed material, the resistance to flow is not independent of viscosity as for rigid boundary flow in the hydraulically rough region *(Simons et al, 1977)*.

Experimental evidence presented by *Vanoni (1960)* showed that for the same discharge, the average velocity for sediment-laden flow is larger and the velocity distribution is less uniform than that for clear water flow **(Figure 3.6-1)**. In this case, κ is substantially reduced by the suspended sediment and the turbulent intensity is damped.

Einstein et al (1954) stated that the energy dissipation per unit time and unit weight in supporting sediment suspension must come from the vertical components of turbulent fluctuations and must result in damping of turbulence.

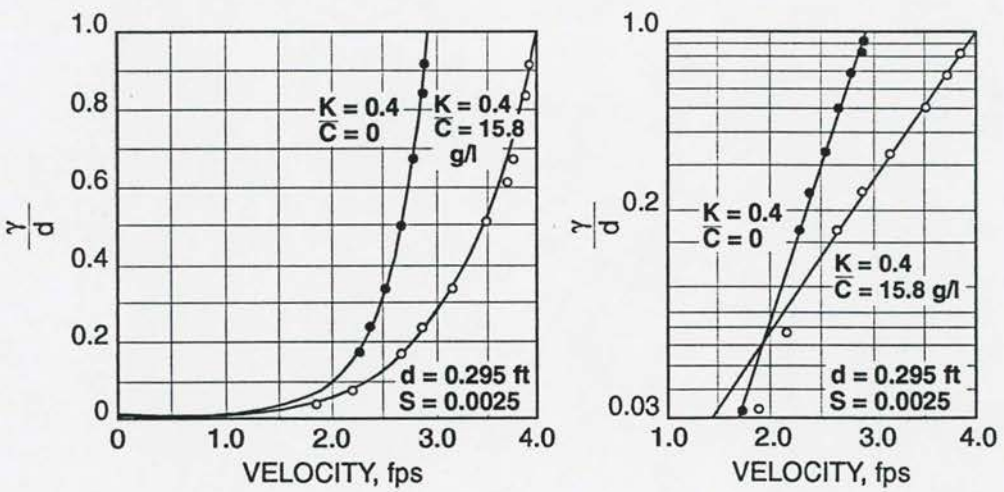

Figure 3.6 - 1 Velocity profiles for clear-water sediment laden flow (Vanoni, 1960)

Input power = $\rho gvs = (\rho_s - \rho)\, gw.C$ = power required for suspension

$$\therefore \Sigma \frac{Cw}{vs} \frac{(\rho_s - \rho)}{\rho} \propto \frac{1}{\kappa} \qquad (3.6\text{-}1)$$

with C = average suspended sediment concentration per weight

w = settling velocity

v = mean flow velocity

Σ = summation over all particle sizes in suspension

An empirical form of this relationship **(Equation 3.6-1)** is shown in **Figure 3.6-2.**

Chien (1954) suggested that the logarithmic velocity distribution equation originally derived for clear water flow is no longer adequate for sediment laden flow. A new equation for alluvial beds was developed by *Einstein et al (1955)*. By including the sediment particles in the exchange mechanism,

$$\tau = \rho_m \epsilon \frac{dv}{dy} \qquad (3.6\text{-}2)$$

where ρ_m = density of sediment-laden water

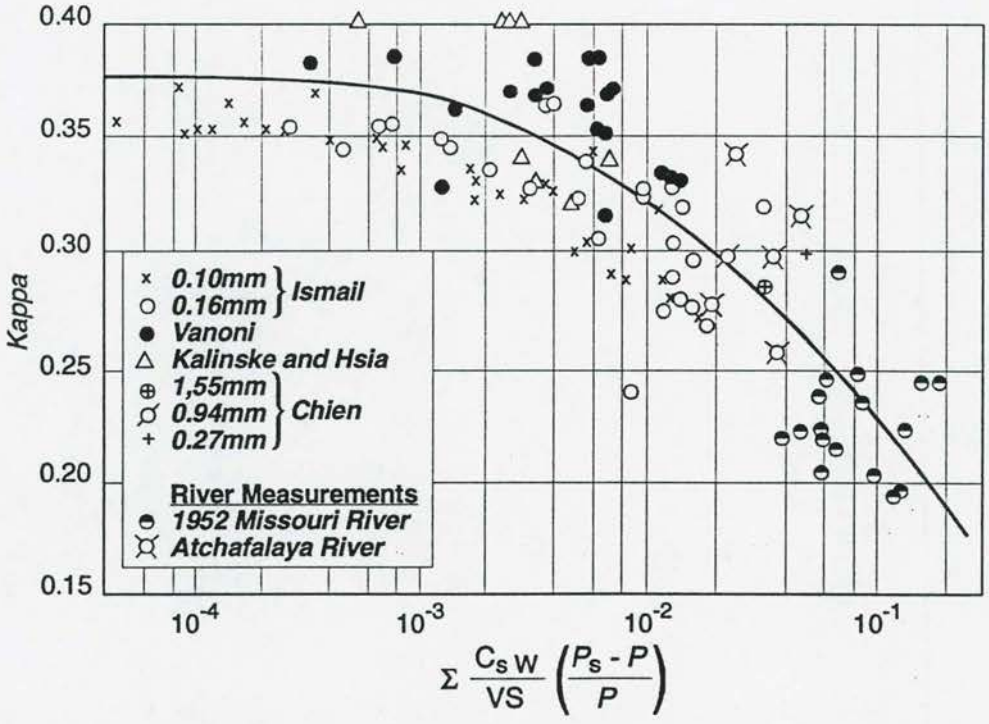

Figure 3.6 - 2 Effect of suspended load on Von Kármán coefficient (Einstein et al., 1954)

Combining **Equation 3.6-2** with **3.3-37** gives an experimental approximation of the velocity distribution:

$$\frac{v}{\sqrt{gDs}} = 17{,}66 + \frac{2{,}3}{\kappa} \log \frac{y}{35{,}45k_s} \qquad (3.6\text{-}3)$$

with κ from **Figure 3.6-2**. This relationship is shown in **Figure 3.6-3** and is valid when $\frac{y}{D} > 0{,}012$.

In *1972, Einstein and Abdel-Aal* established a diagram for determining κ which takes the effects of suspended sediment into account (**Figure 3.6-4**):

$$\kappa \propto \frac{(w_{35}d_{65})}{(q.s.\nu)^{0,5}} \qquad (3.6\text{-}4)$$

with w_{35} = fall velocity of d_{35} size sediment,

q = flow discharge per unit width, and

s = energy gradient

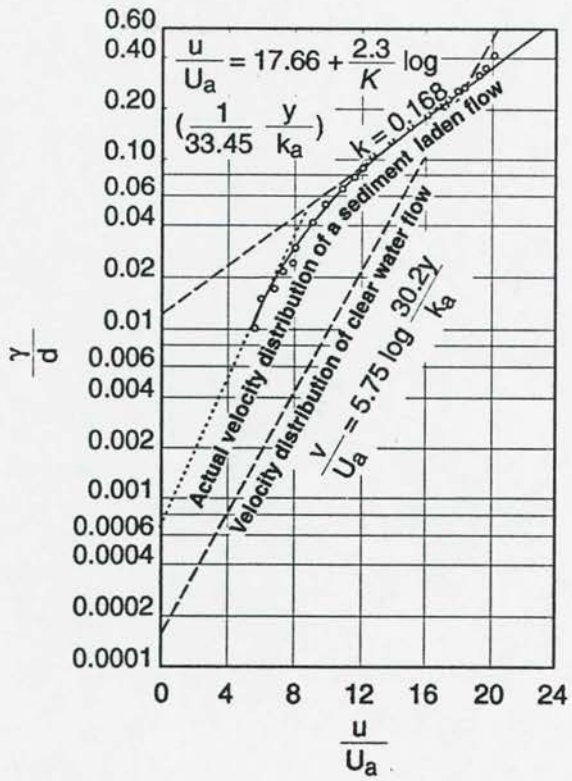

Figure 3.6 - 3 Velocity distribution of clear-water and sediment laden flow (Einstein, 1955)

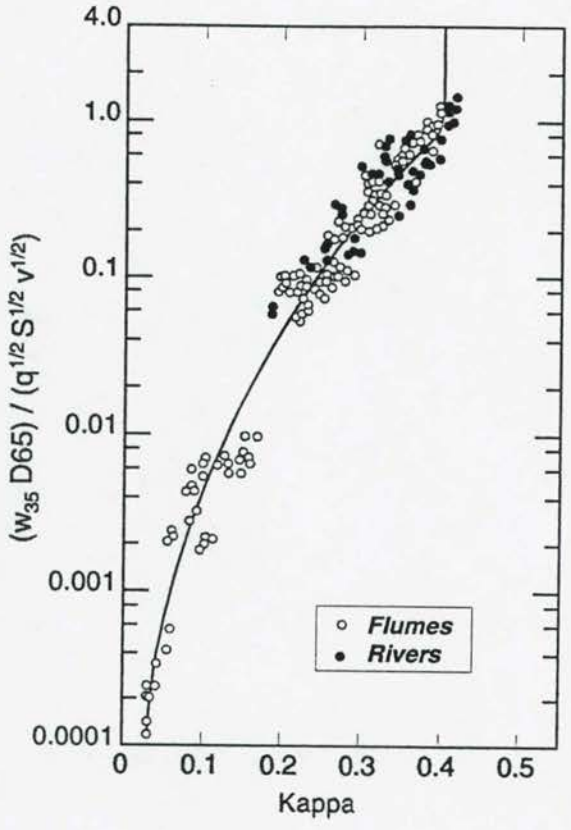

Figure 3.6 - 4 Von Kármán coefficient prediction (Einstein and Abdel Aal, 1972)

What makes this relationship so useful is that the same velocity distribution as with a rigid boundary applies:

$$\frac{v}{\sqrt{gDs}} = \frac{2{,}30}{\kappa} \log \frac{(30{,}2yx)}{k_s} \qquad (3.6\text{-}5)$$

with x = a correction coefficient

and $$\frac{\bar{v}}{\sqrt{gDs}} = \frac{2{,}30}{\kappa} \log \frac{(30{,}2\ D\ x)}{k_s} \qquad (3.6\text{-}6)$$

The change in velocity distribution with a movable bed can be described in terms of the principle of minimum stream resistance, which means that sediment will only be transported if resistance is lowered (or stream power is reduced).

In homogeneous flow, the velocity distribution is given by

$$v = \frac{\sqrt{gDs}}{\kappa} \ln \frac{y}{y_o} \qquad (3.6\text{-}7)$$

with $\kappa = \frac{1}{\sqrt{2\pi}} \approx 0{,}4$ in fully developed turbulent flow without sediment transport.

Since $y\frac{dv}{dy} = constant = \frac{\sqrt{gDs}}{\kappa} = v_o$ is the basic relationship for turbulent flow, a reduction of κ results in a decrease in resistance. **Figure 3.6-3** shows that in the case of sediment transport, only the upper part of the flow velocity distribution is logarithmic. In the lower part, a layer with pseudo-laminar flow is found with a lower value of $\left(\tau \frac{dv}{dy}\right)_o$ than if the flow were also turbulent.

The formation of ripples and dunes with sediment transport can of course also increase the rotation radius of eddies near the bed, with resultant decrease in $\left(\tau \frac{dv}{dy}\right)_o$.

An interrelationship between sediment transport, bed roughness and "damping" of turbulence (or energy dissipation) seems to exist:

Considering the general logarithmic velocity equation for turbulent flow:

$$\bar{v} = \frac{\sqrt{gDs}}{\kappa} \ln \frac{5{,}45D}{R_o} \qquad (3.3\text{-}26)$$

sediment transport leads to *(Rooseboom, 1975)*:

a) an increase in velocity of the rotation centre point for turbulent flow, giving an increased flow velocity;

b) a decrease in applied power per unit volume near the bed by
   - formation of a pseudo - laminar boundary layer,
   - deformation of the bed,

resulting in a decrease in average flow velocity.

3.7 Vertical distribution of suspended sediment concentrations

Rouse (1937) derived the variation of sediment concentration in the vertical from diffusion theory:

$$\frac{dC}{C} = \frac{w}{\kappa v*} = \frac{D}{y}\left(\frac{dy}{D-y}\right) \qquad (3.7\text{-}1)$$

with C = concentration at distance y above the bed
w = settling velocity of particles
κ = Von Kármán constant
$v*$ = $\sqrt{gDs}$ = shear velocity
D = depth of flow

Rooseboom (1975) derived the same relationship above from stream power principles. Consider a cylindrical eddy element with radius R and rotating with an angular velocity distribution of $\frac{dv}{dy}$. An element in the cylinder with area $\Delta A = \Delta r.r.\Delta\alpha$ rotates at constant velocity $\frac{dv}{dy}$ and constant radius r . As the element moves down, C increases, and if it moves up, the sediment concentration decreases **(Figure 3.7-1)**.

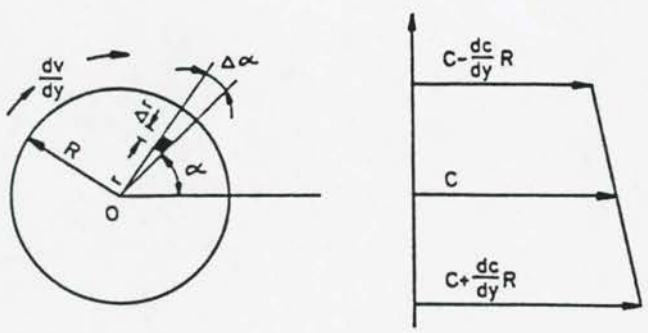

Figure 3.7 - 1 Eddy Element

The applied power required to change the sediment concentration at any moment equals the rate of change of kinetic energy of the element:

$$P = \frac{d}{dt}\left(\frac{1}{2} I \left(\frac{dv}{dy}\right)^2\right) \qquad (3.7\text{-}2)$$

with I = Moment of inertia of element around axis O

= Mr^2 and M = mass of element

$$\therefore P = \left(\frac{dv}{dy}\right)^2 \frac{r^2}{2} \cdot \frac{dM}{dt} \tag{3.7-3}$$

$$\therefore M = \rho dA + (\rho_s - \rho) C \triangle A \tag{3.7-4}$$

$$\therefore \frac{dM}{dt} = (\rho_s - \rho) \frac{dC}{dt} \cdot \triangle A = (\rho_s - \rho) \frac{dC}{dy} \cdot \frac{dy}{dt} \cdot \triangle A \tag{3.7-5}$$

but $\frac{dy}{dt} = \frac{d}{dt}(r \sin \propto)$

$= r(\cos \propto) \frac{d\propto}{dt}$

$= r(\cos \propto) \frac{dv}{dy}$

but $\frac{d\propto}{dt} = \frac{dv}{dy}$

$$\therefore P = \left(\frac{dv}{dy}\right)^2 \cdot \frac{r^2}{2} \cdot (\rho_s - \rho) \frac{dC}{dy} \cdot r(\cos \propto) \frac{dv}{dy} \cdot r dr d\propto$$

$$\therefore \overline{P} = \frac{4 \cdot \frac{1}{2} \int_o^{\pi/2} \int_o^R \left(\frac{dv}{dy}\right)^3 r^4 (\rho_s - \rho) \cos \propto \, dr \, d\propto}{\pi R^2}$$

$$= \frac{\left(\frac{dv}{dy}\right)^3 (\rho_s - \rho) 4R^5 \frac{dC}{dy}}{10 \pi R^2} \tag{3.7-6}$$

If it is assumed that $\tau = \frac{\rho}{2\pi} R^2 \left(\frac{dv}{dy}\right)^2$ is also applicable here, then

$$\overline{P} = \frac{4}{5} \tau \frac{dv}{dy} \frac{(\rho_s - \rho)}{\rho} \frac{dC}{dy} \cdot R \tag{3.7-7}$$

The power required for suspension.

An element with area ΔA takes time $2\pi/(dv/dy)$ for one revolution, and the settling distance at settling velocity w therefore equals $2\pi/(dv/dy) \cdot w$ if no work was done for suspension.

Therefore at average concentration C, the power required is:

$$\overline{P} = \int^{A} \frac{(\rho_s-\rho)\ Cr \left(\frac{dv}{dy}\right)^2 w.dA}{\pi R^2}$$

$$= \frac{2}{3}(\rho_s-\rho)\ w \left(\frac{dv}{dy}\right)^2 .\ C.R \qquad (3.7\text{-}8)$$

Equating **Equations 3.7-7 and 3.7-8**:

$$\frac{4}{5}\tau \frac{dv}{dy} \frac{(\rho_s-\rho)}{\rho} \cdot \frac{dC}{dy} \cdot R = \frac{2}{3}(\rho_s-\rho)\ w \left(\frac{dv}{dy}\right)^2 C.R$$

$$\therefore \frac{dC}{C} = \left(\frac{10}{12}\right) \frac{\sqrt{2\pi}\ w}{\sqrt{gDs}} \cdot \frac{D.dy}{y(D-y)} \qquad (3.7\text{-}9)$$

This equation is identical to the *Ippen (1969)* equation except for the factor $\left(\frac{10}{12}\right)$.

Substituting the term $\frac{\sqrt{2\pi} \cdot w}{\sqrt{gDs}}$ with z, the velocity at any depth in relation to a reference concentration C_a at distance a from the bed can be determined:

$$\frac{C}{C_a} = \left(\frac{D-y}{y} \cdot \frac{a}{D-a}\right)^{z_1} \qquad (3.7\text{-}10)$$

with $z_1 = \left(\frac{10}{12}\right) z$, which gives a better fit of data compared with the diffusion theory as indicated in **Figure 3.7-2**.

With low values of z the vertical concentration variation is small, while at high values of z, the variation in concentration with depth is large. **(Figures 3.7-3)**. Large z values are often related to so-called bed load transport, although it is now believed that the separation of suspended load and bed load in predicting sediment transport is not necessary, since the

principle of conservation of stream power can describe the whole spectrum of sediment transport conditions.

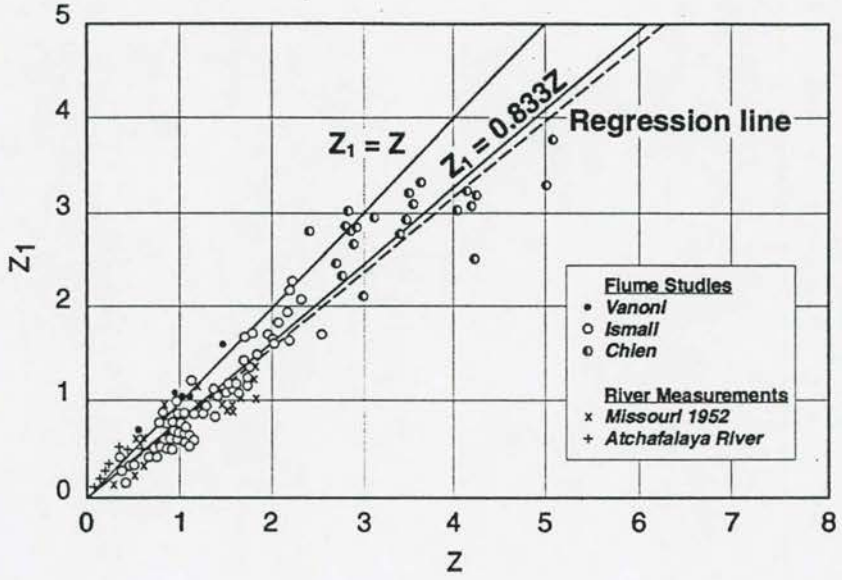

Figure 3.7 - 2 Theoretical versus measured z values

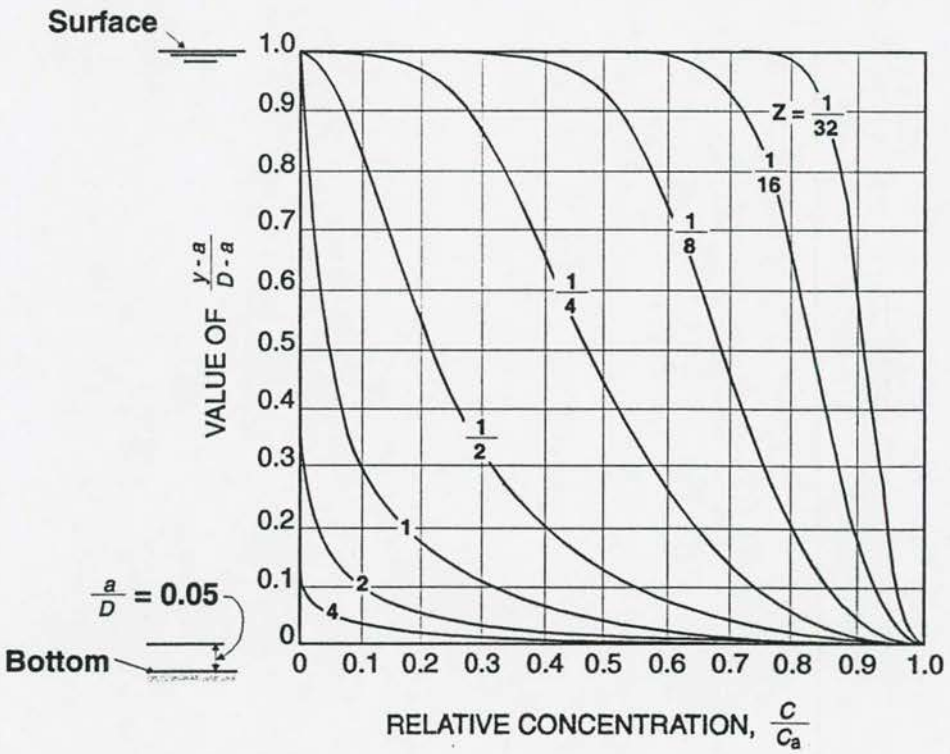

Figure 3.7 - 3 Variation of z values with suspended load distribution

3.8 Sediment transport theory: total load

Several total load sediment transport equations have been developed in the past, of which quite a number are based on principles of stream power.

Rooseboom, (1975) proposed a relationship based on the vertical velocity concentration distribution and an assumption regarding input stream power.

From **Equation 3.7-10**, taking the reference concentration at distance y_o from the bed, where the velocity mathematically equals zero:

$$\frac{C}{C_o} = \left(\frac{D-y}{y} \cdot \frac{y_o}{D-y_o}\right)^{z_1}$$

$$= \frac{\left(\tau\frac{dv}{dy}\right)^{z_1}}{\left(\tau\frac{dv}{dy}\right)^{z_1}_o} \qquad (3.8\text{-}1)$$

The suspended sediment concentration at any level is therefore proportional to the stream power to the power z_1: $\left(\left(\tau\frac{dv}{dy}\right)^{z_1}\right)$. If suspended sediment moves at the same velocity as surrounding fluid, the sediment load per unit width q_s, is given by:

$$q_s = \int_{yo}^{D} C.v.dy$$

$$= \frac{C_o}{\left(\tau\frac{dv}{dy}\right)^{z_1}_o} \int_{yo}^{D} v\left(\tau\frac{dv}{dy}\right)^{z_1} dy \qquad (3.8\text{-}2)$$

No direct solution exists for **Equation 3.8-2**, although solutions have been proposed such as by *Einstein (1950)*. With a number of assumptions, a reasonable solution is possible, however.

Assuming velocity constant across the section $(\bar{v})$ and incorporating a correction factor α_1:

$$q_s = \frac{\alpha_1 C_o \bar{v}}{\left(\tau \frac{dv}{dy}\right)_o^{z_1}} \int_{yo}^{D} \left(\tau \frac{dv}{dy}\right)^{z_1} dy \qquad (3.8\text{-}3)$$

A next assumption: $$\int_{yo}^{D} \left(\tau \frac{dv}{dy}\right)^{z_1} dy = D \overline{\left(\tau \frac{dv}{dy}\right)^{z_1}} \qquad (3.8\text{-}4)$$

and $\overline{\left(\tau \frac{dv}{dy}\right)} = \rho g s \bar{v}$. *With* $q = \bar{v}D$,

$$\frac{q_s}{q} = \frac{(\alpha_1 \alpha_2 C_o)(\rho g s \bar{v})^{z_1}}{\left(\tau \frac{dv}{dy}\right)_o^{z_1}}$$

or $$\log \frac{q_s}{q} = z_1 \log \bar{v}s + \log \frac{\alpha_1 \alpha_2 C_o}{\left(sD \frac{\sqrt{2\pi g D s}}{yo}\right)^{z_1}} \qquad (3.8\text{-}5)$$

which has the same form as the equation proposed by *Yang (1972)*:

$$\log \frac{q_s}{q} = \alpha_3 + \alpha_4 \log \bar{v}s \qquad (3.8\text{-}6)$$

Since C_o is proportional to $\left(\tau \frac{dv}{dy}\right)_o^{z_1}$ and α_1 and α_2 should not vary too much in practice, the last term in **Equation 3.8-5** was found not to vary much *(Yang, 1973)* and can therefore by taken as a constant in practical applications. Non-uniform sediment transport

can be predicted by **Equation 3.8-6** when α_3 and α_4 contain functions with settling velocity and/or particle size.

3.9 Interrelationship between sediment transport, bed roughness and energy dissipation

In this chapter the principle of applied stream power will be used to describe the sediment transport process under movable bed conditions, as well as its interrelationship with bed roughness and energy dissipation.

For equilibrium sediment transport conditions under steady, uniform flow conditions, when the power applied to maintain suspension near the bed is equated with the power required to suspend sediment particles as well as for fluid transport, the following relationship is found:

$$\left(\tau \frac{dv}{dy}\right)_o = \left(\tau \frac{dv}{dy}\right)_{o(clear\ water)} + (\rho_s - \rho) gw.C_o \qquad (3.9\text{-}1)$$

$$\therefore \frac{30\rho gsD\sqrt{gDs}}{\kappa.k_s} = \frac{30\rho gsD\sqrt{gDs}}{0{,}4.k_s} + (\rho_s - \rho) gw.C_o$$

with C_o = sediment concentration near the bed, where the velocity is mathematically = 0.

The two terms on the right of **Equation 3.9-1** represent the stream power required for movement of fluid and the power required for suspension of sediment respectively. To verify **Equation 3.9-1** with laboratory data, it can be rewritten as:

$$\frac{30\rho gsD\sqrt{gDs}}{k_s}\left(\frac{1}{\kappa} - \frac{1}{0{,}4}\right) = (\rho_s - \rho) gw.C_o \qquad (3.9\text{-}2)$$

No laboratory data exist for C_o , since it is impossible to measure concentrations at the height y_o above the bed, which is very small (in the order of 10^{-7} mm). Concentration data of suspended sediment taken close to the bed were, however, used as a first check on the validity of **Equation 3.9-2**. (see **Figure 3.9-1**).

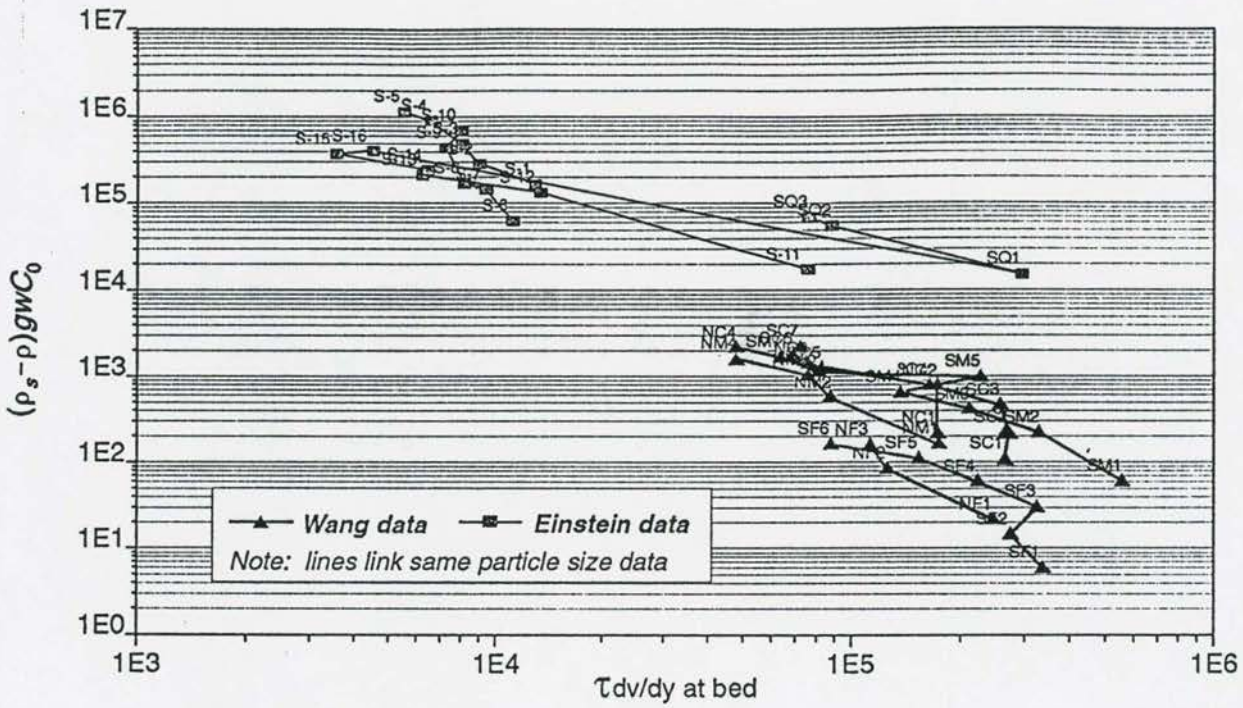

Figure 3.9 - 1 Applied power versus suspended power relationship

As C_o values increase, κ values decrease while k_s values increase in the data used in **Figure 3.9-2**. The effect of the k_s increase is, however more pronounced than that of the κ decrease and therefore the applied power (horizontal axis in **Figure 3.9-1**) decreases with increase in $(\rho_s-\rho)gwC_o$ **(Figure 3.9-1)**. The data used are those that of *Wang et al (1992)* (plastic pellets) and *Einstein et al (1953)*. Unfortunately the tests were only carried out with high Froude numbers (Fr), all greater than 1 and mostly in the order of Fr = 2 and shallow depths (± 10 cm) in order to get high suspended sediment concentrations. Although it does not provide a good enough basis for establishing the above relationship over a wide range of hydraulic conditions, the general picture is clear.

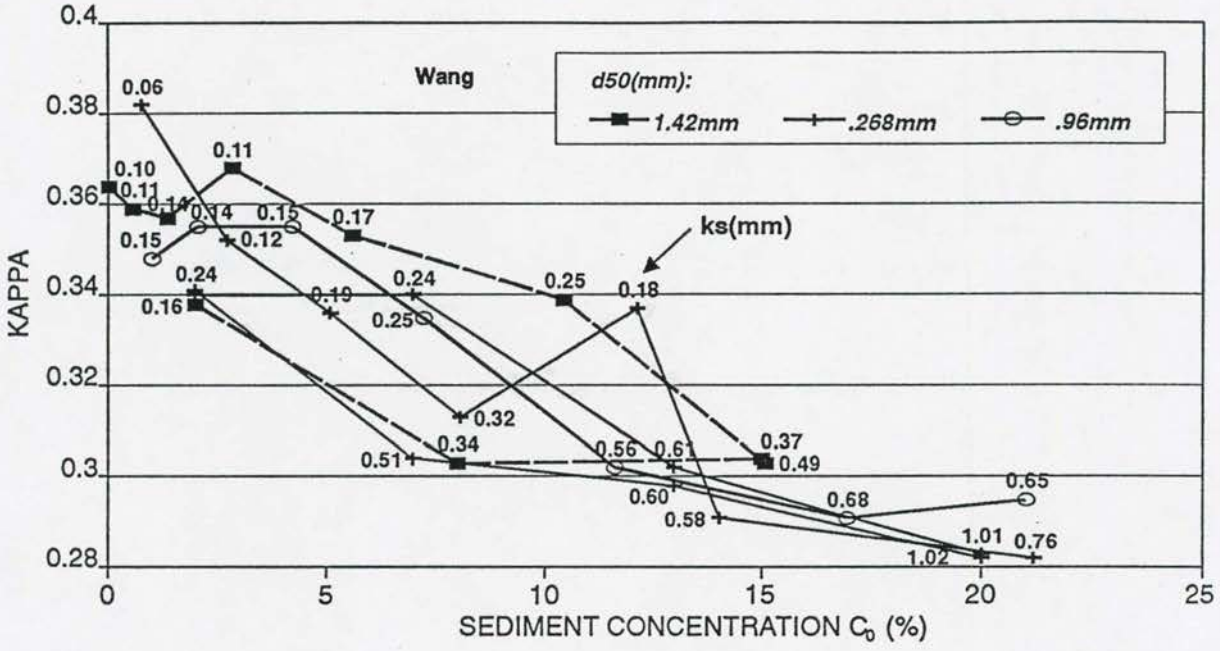

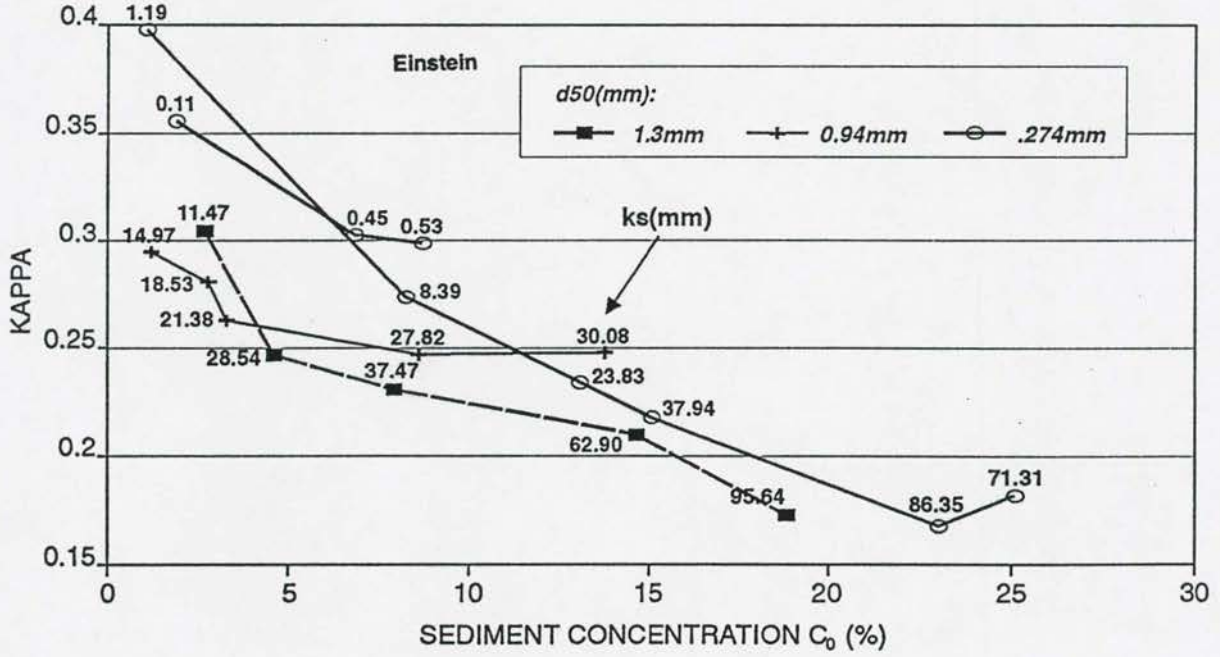

Figure 3.9 - 2 Interrelationship between C_o, k_s and κ

The use of applied stream power in **Equation 3.9-1** is valid since the vertical distribution of applied power is such that the maximum power is applied along the bed and is also representative of the total power (see **Figure 3.4-2**).

From **Figure 3.9-1** it is also clear that applied power is minimized as sediment transport increases, which proves the statement in **Chapter 3.6** that a stream will only transport sediment if applied stream power is lowered.

Itakura et al (1980) proposed a similar expression as **Equation 3.9-1**.

$$\tau\frac{dv}{dy} = g\rho\,'v' + \frac{B\rho v_*^3}{\kappa L} + \frac{\rho v_*^3}{\kappa y} \qquad (3.9\text{-}3)$$

with $g\rho\,'v'$ = the applied power due to pressure fluctuations
= applied power to suspend sediment
= $(\rho_s-\rho)gwC$, at distance y above the bed;

$B\frac{\rho v_*^3}{\kappa L}$ = rate of energy dissipation through motions of suspended sediment such as rotation, rectilinear motion relative to the fluid, collision, reduction of effective space to dissipate energy into heat;

$\frac{\rho v_*^3}{\kappa y}$ = rate of energy dissipation by turbulent motion of the fluid,

B = constant,

$\frac{1}{L}$ = $\frac{\kappa g(\gamma_s-1)wC}{v_*^3}$

v_* = shear velocity

and γ_s = specific weight of sediment

The first and second terms on the right hand side of **Equation 3.9-3** were considered proportional to each other, and combined as in **Equation 3.9-4**:

$$\tau\frac{dv}{dy} = \propto(\rho_s-\rho)gwC + \frac{\rho(gsD)^{1,5}}{\kappa y} \qquad (3.9\text{-}4)$$

with $\propto$ = "Monin-Obukhov coefficient" in meteorology *(Monin-Obukhov, 1973; Turner, 1973)*.

In clear water flow, the second term of **Equation 3.9-4** should be zero.

From **Equations 3.9-3** and **3.9-4**, *Itakura et al (1980)* showed that:

$$\frac{dy}{dy} = \frac{v_*}{\kappa y}\left(1 + \propto\frac{y}{L}\right) \tag{3.9-5}$$

Webb (1970) found from observations of data of wind velocity over the ground that $\propto = 5$. Itakura used average suspended sediment concentrations (as opposed to the data of Webb who used near bed concentrations), to calibrate $\propto = 7$.

The vertical suspended sediment concentration distribution can be derived from **Equation 3.9-5** and the diffusion theory:

The kinematic eddy viscosity, ϵ_m, is described by:

$$\tau = \rho\epsilon_m\frac{dv}{dy} \text{ and } \epsilon_m = v_*^2\frac{\left(1-\frac{y}{D}\right)}{\frac{dv}{dy}} \tag{3.9-6}$$

Assuming the dispersion coefficient of suspended sediment, ϵ_s, equal to the kinematic eddy viscosity, then from **Equation 3.9-5** and **3.9-6**, it follows that:

$$\epsilon_s = \kappa v_* y\left(1-\frac{y}{D}\right)\left(1+\propto\frac{D}{L}\cdot\frac{y}{D}\right)^{-1} \tag{3.9-7}$$

Substituting **Equation 3.9-7** into **Equation 3.9-8** which gives the equilibrium for suspended sediment, the suspended sediment distribution (**Equation 3.9-9**) can be derived:

$$\epsilon_s\frac{dC}{dy} + wC = 0 \tag{3.9-8}$$

$$\frac{dC}{C} = \frac{-w}{\kappa v_* y}\left(1+\propto\frac{y}{L}\right)\left(1-\frac{y}{D}\right)^{-1}dy \tag{3.9-9}$$

Equation 3.9-9 has the same form as the expressions derived by *Ippen (1969)* and *Rooseboom (1975)*:

Ippen: $$\frac{dC}{C} = \frac{w}{\kappa v_*}\cdot\frac{D}{y(D-y)}\cdot dy$$

Rooseboom: $$\frac{dC}{C} = \frac{w}{\kappa v_*}\cdot\frac{10}{12}\cdot\frac{D}{y(D-y)}\cdot dy \tag{3.7-9}$$

Integration of **Equation 3.9-9** yields:

$$\frac{C}{C_a} = \left[\left(\frac{D-y}{D-a}\right)^{1+\phi_2}\left(\frac{a}{y}\right)\right]^z \qquad (3.9\text{-}10)$$

with C_a the concentration at y=a,

$z = w/\kappa v_*$

and $\phi_2 = \frac{\propto D}{L}$

The classical concentration distribution **Equation 3.7-10** is a particular form of **Equation 3.9-10** when $\phi_2 = 0$

Equation 3.9-10 can also be written as:

$$\frac{C}{C_a} = \left(\left(\frac{(D-y)}{(D-a)}\right)^{\phi_2}\right)^z \cdot \frac{\left(\tau\frac{dv}{dy}\right)^z}{\left(\tau\frac{dv}{dy}\right)_a^z} \qquad (3.9\text{-}11)$$

which is similar to **Equation 3.8-1**.

Equation 3.9-10 has been successfully calibrated with data *(Itakura et al, 1980)*.

Now that it has been established that the stream power balance **Equation 3.9-4** can describe the suspended sediment distribution, is it possible to derive an expression to describe the energy dissipation (Kappa).

The energy dissipation rate for sediment transport versus clear water flow, is obtained from **Equation 3.9-4**:

$$\frac{\left(\tau\frac{dv}{dy}\right)_{sediment}}{\left(\tau\frac{dv}{dy}\right)_{clear}} = \frac{(\rho_s-\rho)gwC}{\left(\tau\frac{dv}{dy}\right)_{clear}} + 1 \qquad (3.9\text{-}12)$$

Assuming average stream power and suspended sediment concentration, and using data for sediment transport:

$$\left(\overline{\tau\frac{dv}{dy}}\right)_{clear} = \overline{(\rho gvs)}_{sediment} \qquad (3.9\text{-}13)$$

$$\therefore \frac{0,4}{\kappa} \propto \frac{(\rho_s-\rho)gwC}{\rho g\bar{v}s} + 1 \qquad (3.9\text{-}14)$$

$$\text{or} \quad \frac{1}{\kappa} = \frac{(\rho_s-\rho)wC}{0,4\ \rho\bar{v}s} + 2,5 \qquad (3.9\text{-}15)$$

which is similar to the expression 3.6-1, derived by *Einstein et al (1954)*, and derived from a sound theoretical basis.

Vanoni and Nomicos (1960) argued that most of the "damping" effect of sediment on the turbulence occurs near the bed and related Kappa to the ratio of power required to suspend the sediment in a thin layer near the bed, to the power required to overcome frictional resistance:

$$\left(\frac{\rho_s-\rho}{\rho_s}\right)\left(\frac{Cy_2y_1w}{\rho gvs}\right)\left(\frac{y_2-y_1}{D}\right) \qquad (3.9\text{-}16)$$

with Cy_2y_1 = average sediment concentration between y_z and y_1.

Equation 3.9-16 was calibrated successfully with data and indicates that the use of applied stream power, which is a maximum near the bed, could be a successful predictor of the relationship between energy dissipation and bed roughness as given in **Equation 3.9-12**. At the bed, **Equation 3.9-17** can be derived from **Equation 3.9-12**.

$$\frac{1}{\kappa} = \frac{(\rho_s-\rho)gw\bar{C}.k_s}{30\rho(gsD)^{1,5}} + 2,5 \qquad (3.9\text{-}17)$$

with $\overline{C}$ = mean suspended sediment concentration

Equation 3.9-17 is shown graphically in **Figure 3.9-3** with data with observed Kappa values. The data of *Wang et al, (1992), Einstein et al. (1953), Abdel-Aal, Barton and Lin 1955)*, and *Vanoni (1959)* have been used. The k_s-values are calculated from:

$$v = \frac{1}{\kappa} \ell n \left(\frac{12D}{k_s} \right) \sqrt{gDs_f} .$$

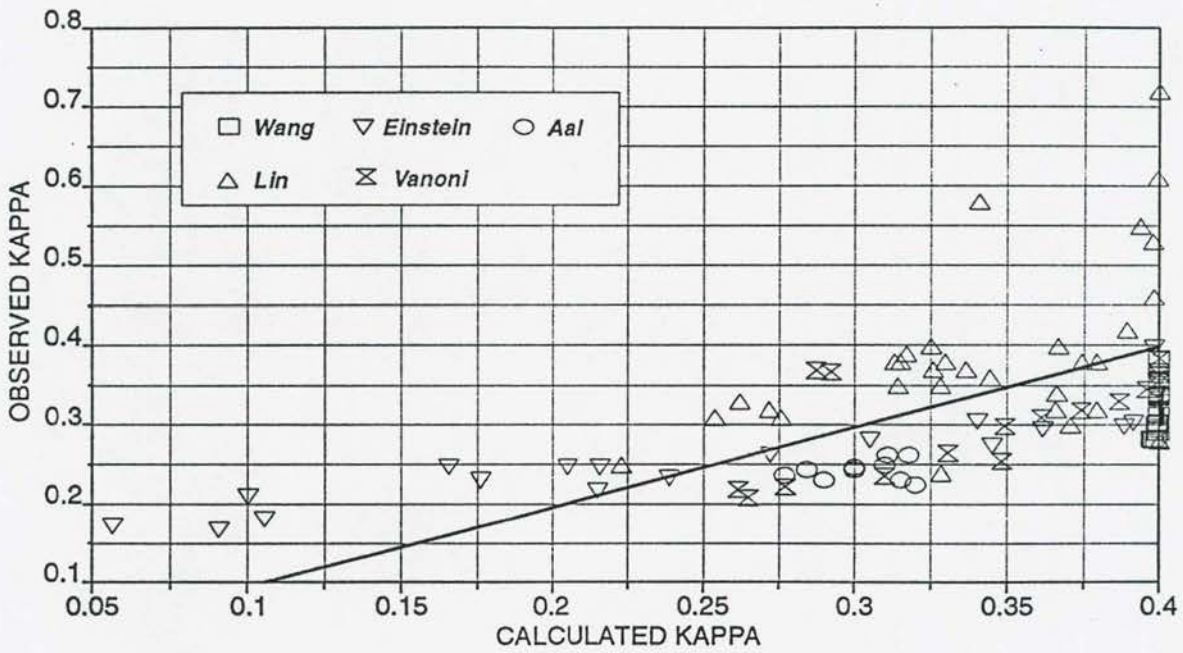

Figure 3.9 - 3 Interrelationship between κ and k_s described by applied stream power

Figure 3.9-3 indicates that **Equation 3.9-17** can be used to predict energy dissipation (Kappa), without calibration since it is based on fundamental theory. The assumption of using average sediment concentration rather than near bed concentration data in **Equation 3.9-17**, can be one reason for the data scatter in **Figure 3.9-3**. Kappa values exceeding 0,4, have been observed in clear water flow, while the assumption here was to use

the theoretically derived $\kappa = 0{,}4$ for clear water flow. With sediment transport, the κ-data of Einstein are much higher than the predicted values and it seems as if a certain physical minimum $\kappa > 0$ is approached. The use of near bed concentrations might increase the prediction accuracy of **Equation 3.9-17**.

The change in bedforms and associated bed roughness, energy dissipation at the bed, and sediment transport will be discussed next. When sediment motion starts, the bedforms rapidly develop from a plane bed to ripples to dunes with increasing k_s as $\bar{C}$ increases. κ-*values* also decrease to some extent, but the change in k_s is dominant in minimizing the applied power function. It is assumed that the flow conditions vary from laminar to turbulent with a laminar boundary layer in this so-called lower regime. The lower regime is associated with subcritical flow conditions with bedforms ranging from a smooth bed to ripples to dunes as the flow increases. At higher discharges the bedforms are washed away in the transition regime, followed by the formation of antidunes in the upper regime. The latter regime is associated with supercritical flow conditions.

As the thickness of the boundary layer decreases with increasing turbulence, in the lower regime sediment particles at the bed are more and more susceptible to suspension since settling velocities in the turbulent layer are much lower than in the laminar layer. A certain stage is therefore reached when the laminar layer is probably washed away completely, causing a rapid suspension of sediment in what is known as the transition phase. All bedforms are washed away and a smooth bed appears in this transition phase with $0{,}8 < Fr < 1{,}0$ (approximately).

Once through the transition phase at $Fr > 1{,}0$ (approximately), antidunes develop in the upper regime causing an increase in bed roughness, and it seems as if the whole process is repeated again, starting from plane bed to dunes, as in the lower regime. (See **Figure 3.9-4**). *Le Grange (1995)* in fact postulated that a laminar layer also develops at the bed during antidune development as reason why similar bedform patterns as with the lower regime are found and why the bed sediment is not washed away. The importance of the *Von Kármán* κ coefficient was, however, not considered in his evaluation.

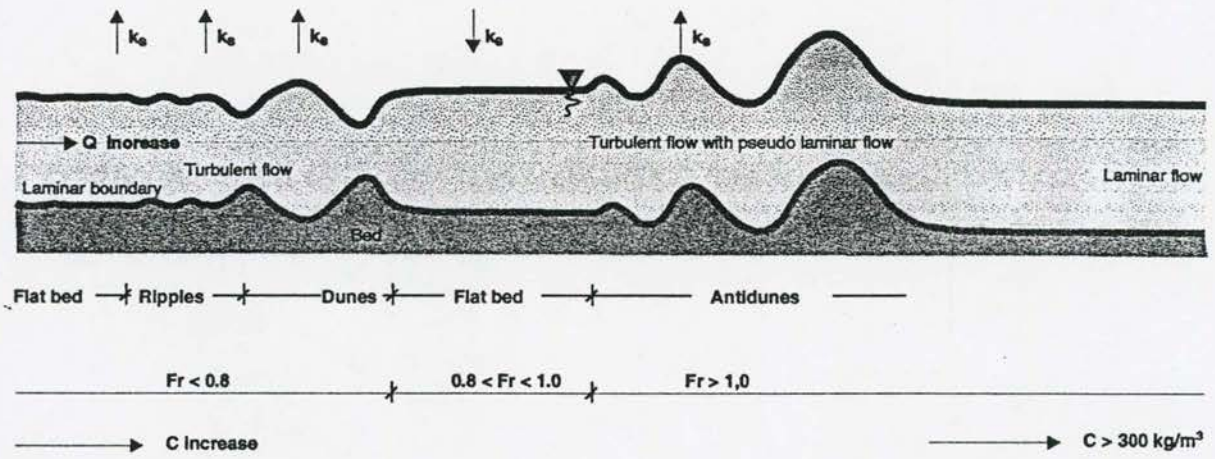

Figure 3.9 - 4 Sediment transport, bed form regimes and energy dissipation

At the onset of the transition regime, bed sediment is suddenly suspended and the κ coefficient rapidly decreases at the same time from say 0,35 (dunes) in the lower regime to say 0,2 (or even less) in the transitional regime. This almost doubles the applied stream power and therefore the sediment can be maintained in suspension. At the same time, excessive sediment transport and scour are limited by increased bed roughness (k_s), thereby reducing the applied power.

Upper regime flow conditions are highly turbulent, with antidunes moving in phase with the water surface. During reservoir flushing antidune formation has been observed at a number of reservoirs during retrogressive drawdown erosion conditions. A good example is shown in **Photograph 3.9-1** of Phalaborwa Barrage, during flood flushing with a throughflow of 900 m³/s, February 1996.

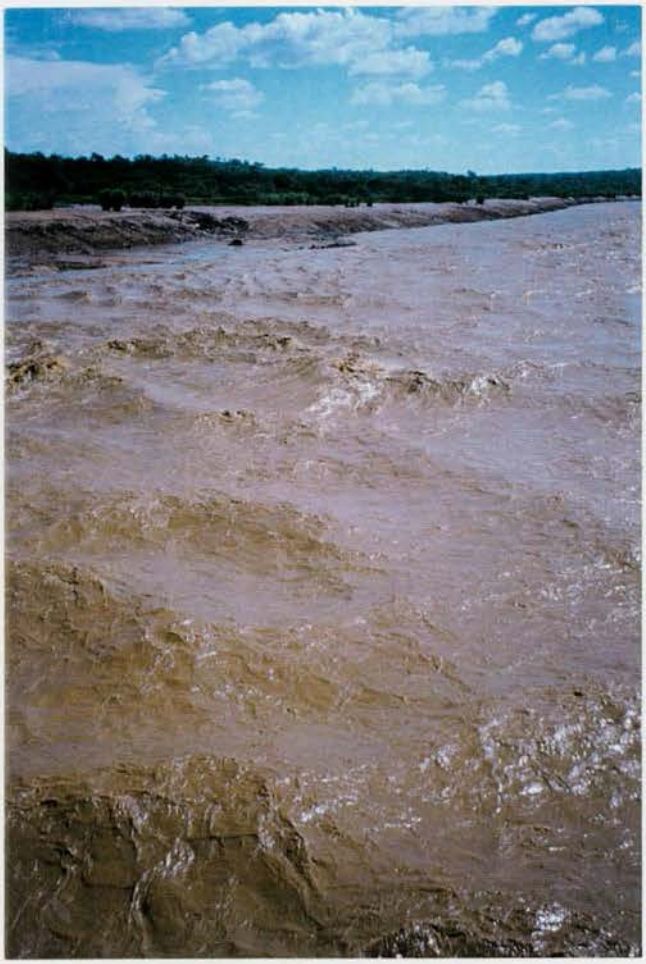

Photograph 3.9 - 1 Phalaborwa Barrage flood flushing and antidune formation (1996)

In rivers where sediment availability is not limited, such as in the Yellow River, China, hyperconcentration sediment transport is experienced with sediment concentrations mostly higher than 300 kg/m^3, but concentrations exceeding 1 000 kg/m^3 have also been experienced *(Wu, 1994)*. A further interesting phenomenon of hyperconcentration flow is that within the same channel, under turbulent flow conditions and with sediment concentration $<$ 30 kg/m^3, sediment is deposited while at hyperconcentration of 800 kg/m^3, no deposition occurs! *(Wu, 1994)*. With hyperconcentration flow, the flow structure changes to laminar conditions and the viscosity effects dominate. In **Figure 3.9-4** it was shown that hyperconcentration flow

could follow from the upper regime. In reality, with high, fine sediment availability, hyperconcentration flow probably starts immediately after the transition regime. Although it is possible that hyperconcentration flow can occur in reservoirs during flushing operation, South African reservoir data indicate sediment concentrations mostly less than 300 kg/m^3 and it would therefore seem that critical conditions for mass erosion of cohesive sediments limit sediment availability.

With rapid pool drawdown, hydraulic overpressures leading to mass failure with resulting hyperconcentrations have been experienced at the Mbashe weir, South Africa, with relatively low flow conditions. See **Photograph 3.9-2**.

Photograph 3.9 - 2 Mbashe Reservoir hydraulic overpressure low flow flushing

One may argue that according to the modified Liu diagram **(Figures 3.15-1 and 6.2-1)**, sand particles less that 2 mm diameter will be suspended once outside laminar conditions and that in the antidune regime there should therefore exist a laminar (or perhaps pseudo-laminar) layer near the bed to facilitate the formation of dunes. In fact, the κ value approaches a

minimum value and the concentration a maximum value (for specific boundary conditions), and the latter therefore limits further increase in suspension at the bed (by creating equilibrium suspension and deposition).

This is illustrated in **Figure 3.9-5** in which bed roughness (k_s) , κ and Fr are plotted. κ decreases as Fr approaches the transition regime at Fr>0,8 while k_s increases when Fr>1 or Fr<0,8 (out of the transition zone). (Unfortunately the bedform regimes have not been reported in all of the flume data and therefore the Froude number had to be used here as indicator of bedform regimes).

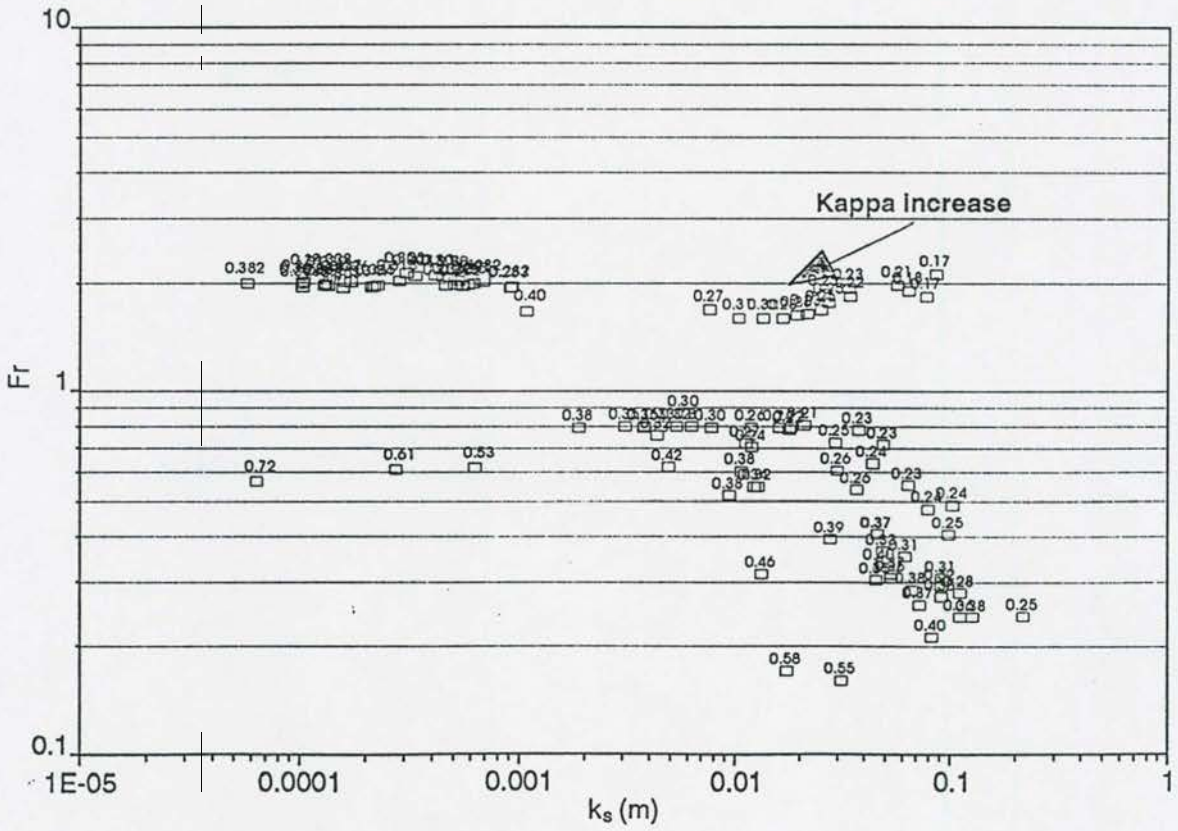

Figure 3.9 - 5 Interrelationship between k_s, κ and F_r

3.10 Derivation of a new sediment transport equation

In this section the aim is to derive a new sediment transport relationship from basic principles. The proposed relationship is based on integration of the suspended sediment relationship **(Equation 3.8-1)** and the description of the reference concentration by using the applied power function (**Equation 3.9-1**) evaluated in **Section 3.9**.

Average sediment concentration is obtained by integration of **Equation 3.8-1** with the assumption that the total applied power equals the applied power at the bed:

$$\bar{C} \propto C_o \int_{yo}^{D} \frac{\left(\tau \frac{dv}{dy}\right)^z}{\left(\tau \frac{dv}{dy}\right)_o^z} dy$$

$$\propto \frac{C_o \int_{yo}^{D} \frac{\left(\rho g s (D-y)\sqrt{gDs}\right)^z}{\kappa y} dy}{\left(\frac{30 \rho g s D \sqrt{gDs}}{\kappa k_s}\right)^z}$$

$$\propto C_o \left(\frac{k_s}{30D}\right)^z \int_{yo}^{D} \left(\frac{D-y}{y}\right)^z dy \qquad (3.10\text{-}1)$$

In order to solve this equation, the integral and C_o still need to be solved. The integral term is, however, only numerically soluble and several researchers, of which *Einstein* was probably the first, have adopted this approach.

The basic form of the solution of the integral is a function:

$$\int_{yo}^{D} \frac{(D-y)^z}{y} dy = f\left(z; \frac{k_s}{30D}\right) \qquad (3.10\text{-}2)$$

and since the final sediment transport equation is to be calibrated with data, it was decided not to use numerical integration, but rather the two terms on the right-hand side of **Equation 3.10-2** with calibration coefficients obtained from data regression. **Equation 3.10-1** therefore becomes:

$$\bar{C} \propto C_o\left(\frac{k_s}{30D}\right)^z \cdot f\left(z;\ \frac{k_s}{30D}\right) \tag{3.10-3}$$

3.11 Reference concentration

The reference concentration (C_o) at a distance y_o from the bed, where the mathematical velocity equals zero, can be described by applied stream power as given previously in **Equation 3.8-1**. By taking the second term of **Equation 3.8-1** as constant (stream power required for clear water flow), the following is obtained:

$$\left(\tau\frac{dv}{dy}\right)_o \propto (\rho_s-\rho)g.w.C_o$$

$$\therefore \frac{30\rho gsD\sqrt{gDs}}{\kappa k_s} \propto (\rho_s-\rho)g.w.C_o$$

$$\therefore C_o \propto \frac{30\rho(gsD)^{1,5}}{\kappa k_s(\rho_s-\rho)gw} \tag{3.11-1}$$

Substitution of C_o into **Equation 3.10-3** produces the final equation for total sediment transport.

$$\bar{C} \propto \left(\frac{\rho}{\rho_s-\rho}\right)\frac{(gsD)^{1,5}}{\kappa.k_s.w}\left(\frac{k_s}{30D}\right)^z f\left(z;\ \frac{k_s}{30D}\right) \tag{3.11-2}$$

with w = settling velocity describing the viscosity of the fluid as well as particle diameter.

Before proceeding to a description of the calibration of this new sediment transport equation, it is of interest to take note of previous researchers who have derived (sometimes from rather crude assumptions without any sound theoretical basis) equations for sediment transport with structures similar to the one proposed here.

3.12 Comparison between the new applied stream power sediment transport equation and work by other researchers

a) Laursen's method

Laursen (1958) considered the following parameters important in total load transport: $\frac{\sqrt{gDs}}{w}$; $\frac{d}{D}$; $\overline{C}$ in per cent by weight; and the ratio of grain shear stress τ_o' to critical shear stress τ_{oc} :

$$\frac{\overline{C}}{\left(\frac{d}{D}\right)^{7/6}\left(\frac{\tau_o'}{\tau_{oc}} - 1\right)} = f\left(\frac{\sqrt{gDs}}{w}\right) \qquad (3.12\text{-}1)$$

with $\tau_o' = \frac{v^2 d^{1/3}}{30 D^{1/3}}$ and τ_{oc} from the Shields curve (*Shields, 1936*),

and d = sediment particle size

This relationship is indicated in **Figure 3.12-1** based on experimental data

Studies of the application of Laursens equation to field data showed good agreement in some cases *(Laursen, 1958)*, while *Bondurant (1958)* and *Garde et al (1963)* reported differences with observed concentrations exceeding a factor of 4.

Comparison with **Equation 3.11-2** shows that Laursen also used the $\frac{v^*}{w}$ relationship, which from detailed evaluation of **Equation 3.11-2** proves to be quite an important parameter. Secondly, *Laursen* proposed the use of $\left(\frac{d}{D}\right)$, compared to $\left(\frac{k_s}{D}\right)$ in **Equation 3.11-2**. In flume experiments $k_s \sim d$ for a range of experiments, but definitely not for dune regimes and field conditions. By bringing in the velocity v, *Laursen* compensated to some extent for the roughness parameter.

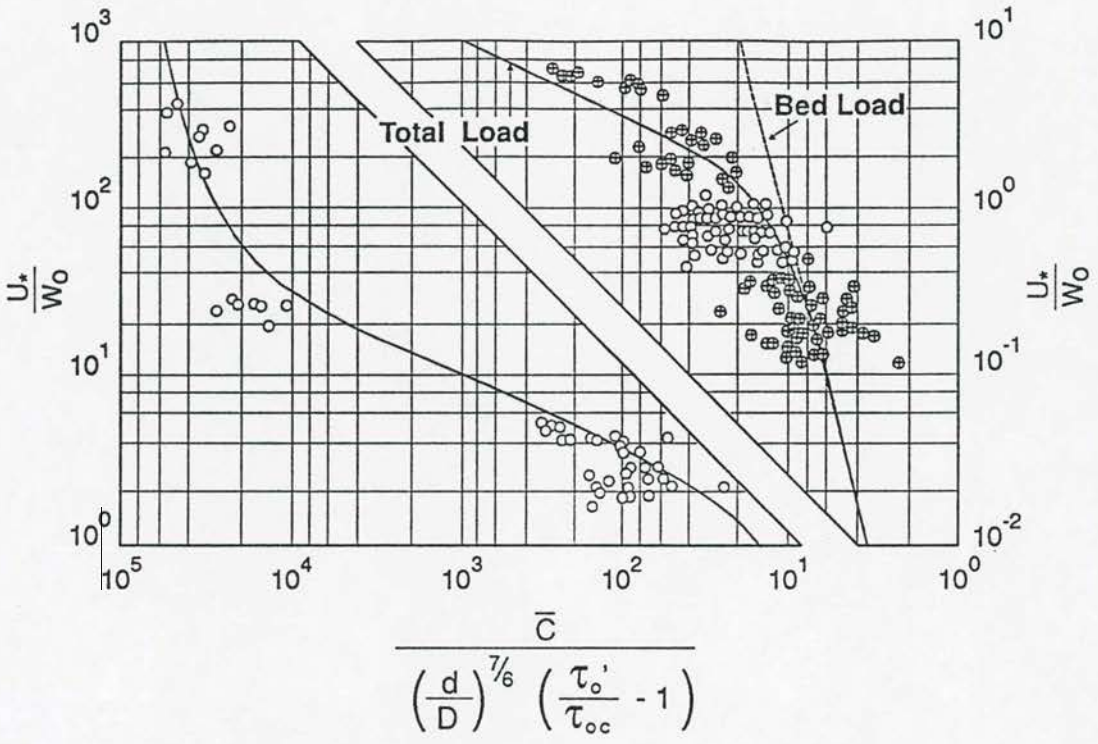

Figure 3.12 - 1 **Laursen's total load relationship**

b) *Garde and Albertson (1958)*

In their discussion of *Laursen's* paper, *Garde and Albertson* proposed a total load equation:

$$\overline{C} = f\left(\frac{v_* D}{\nu}; \frac{d}{D}; \eta\right) \tag{3.12-2}$$

with η a function of sediment size $= f\left(\frac{wd}{\nu}\right)$ *(Garde and Dattatri, 1963)*

$$\frac{v_* D}{\nu}\frac{1}{\overline{C}^{1/8}} = f\left(\frac{D}{d}; \frac{1}{\eta}\right)^{1.5} \tag{3.12-3}$$

All these terms are present in **Equation 3.11-2**, but again no account is taken of bed roughness or the change in κ values.

c) *Garde et al, (1963)*

When considering the functional form of some bed load equations, it is possible to predict total load (q_T) . See **Figure 3.12-2**.

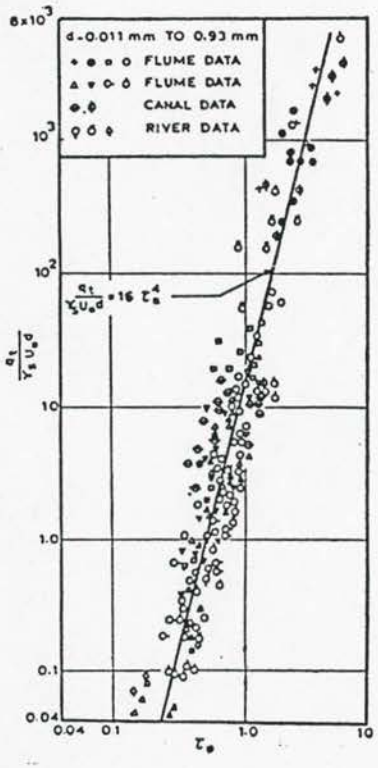

Figure 3.12 - 2 **Garde's total load relationship**

$$\text{with} \quad \frac{q_T}{\gamma_s v_* d} = f(\tau_*) \tag{3.12-4}$$

$$\text{and} \quad \tau_* = \left(\frac{\sqrt{gDs}}{w}\right)^2$$

This relationship, together with flume data compiled for this research, shows that the correlation is not as good as indicated by the original authors, probably since only a part of the applied power expression in **Equation 3.11-2** is used (v_*/w) .

d) ***Iwagaki***

Iwagaki, using Einstein's method, showed that the following functional relationship can be used for the total load:

$$\frac{q_T}{\gamma_s v_* d} = \left(\tau_*; \frac{d}{D}; \frac{k_s}{d}; \frac{wd}{\nu}\right) \tag{3.12-5}$$

This is almost the same expression as proposed in **Equation 3.11-2**; the applied power term with roughness k_s is present, the roughness to total depth relationship and settling velocity can be found. It is only κ and z that are not addressed directly, but they could of course be taken into account indirectly in the k_s , v* and w parameters. Iwagaki indicated

that the above relationship assuming $\frac{k_s}{d} = 1$ (plane bed) and $\frac{wd}{\nu} = 10$, yields a good relationship for sediment transport when calibrated with data.

3.13 Evaluation and calibration of the new sediment transport equation

The new sediment transport relationship provides all the necessary parameters to investigate the change of bed conditions (k_s), the dissipation of energy (κ), and the vertical distribution of suspended sediment (z) with sediment transport. Calibration and evaluation of **Equation 3.11-2** was first of all required to check its validity against laboratory (flume) data and to understand the interrelationship between sediment concentration, setting velocity, bed roughness, *Von Kármán* coefficient and the importance of other terms in the equation. The following steps were followed in calibration:

- Calibration with laboratory (flume) data with separate particle sizes (κ unknown* $= 0,4$).
- Calibration with all laboratory data together with κ unknown and taken as 0,4.
- Calibration with field (river) data (κ unknown).
- Comparison between field (river) and laboratory data calibrations.
- Calibration with RSA reservoir data and comparison with river/flume calibration.
- Calibration of dimensionless new sediment transport equation with laboratory data.

The slope s_f is usually given and was measured, or else assumed equal to the bed slope since most flume studies are carried out under uniform flow conditions with equilibrium sediment transport and bed deformation. All other parameters are measured data obtained from flume experiments.

For calibration and evaluation purposes, the terms in **Equation 3.11-2** were grouped into five groups, in order to evaluate their relative importance in the equation.

$$\bar{C} = f\left(\frac{\rho(gsD)^{1,5}}{(\rho_s-\rho)}; \frac{1}{\kappa k_s}; \frac{1}{w}; \frac{k_s}{30D}; \frac{w}{\kappa\sqrt{gDs_f}}\right) \qquad (3.13\text{-}1)$$

---

*Note: Unfortunately sediment-related data with observed κ-values are limited. For the main calibration therefore of **Equation 3.11-2**, k_s values had to be calculated assuming $\kappa = 0,4$. The value of k_s calculated in this way will, however, include the effect of the actual κ value, and as long as $\kappa = 0,4$ is used in applying the equation, no problems should be experienced.

with k_s calculated from: $$v = \frac{1}{\kappa}\ln\left(\frac{12D}{k_s}\right)\sqrt{gDs_f} \qquad (3.13\text{-}2)$$

$$w = \frac{1}{18}\frac{(\rho_s-\rho)gd^2}{\nu} \quad \textit{for } d < 0{,}1 \textit{ mm (Stokes range)} \qquad (3.13\text{-}3)$$

$$w = 10\frac{\nu}{D_s}\left\{\left[1 + \frac{0{,}01(s-1)gd^3}{\nu^2}\right]^{0,5} - 1\right\} \quad \text{for } 0{,}1 < d < 1 \textit{ mm (Zanke, 1977)} \qquad (3.13\text{-}4)$$

In flume experiments (except in special cases), wash load is absent and the total load would be the bed material load. On the other hand, in natural streams and especially in reservoirs the so-called wash load is often present and the total load is the summation of the bed material load and the wash load. Therefore the above-mentioned difference in the nature of laboratory and field data makes it difficult to unify the total load data collected in the laboratory and in the field. However, the majority of total load relationships are based mainly on flume data and hence can be expected to yield the bed material load. At this stage it is expected that the new sediment transport equation (or most sediment transport relationships) would underestimate river sediment transport data when calibrated only with laboratory data.

3.13.1 Calibration with laboratory (flume) data

Several laboratory data sets are available in the literature. One of the data sets that is perhaps the most well-known was compiled by *Guy et al (1966)*. Their data with other data were used to verify and evaluate the new sediment transport equation. A number of assumptions were made:

a) Flume data with width/depth ratios larger than three were used to ensure that side-wall effects are excluded from the data.

b) Only sediment data for d_{50}<1 *mm* were used in the analysis. Although the new transport equation is applicable to all sediment sizes, smaller sediments are mostly of concern in reservoir sedimentation processes.

c) d_{50}-values of sediment particles were used as a representative reference size. This is the normal approach used by most researchers since the median diameter closely represents the "effective" diameter of sediment calculated from the summation of

proportional representation (p) of sediment setting velocities Σpw in a sediment grading curve, because the particles used are more or less uniform in size.

d) The roughness coefficient (k_s) is calculated from:

$$\bar{v} = \frac{1}{\kappa}\ln\left(\frac{12D}{k_s}\right)\sqrt{gDs} \qquad (3.13\text{-}2)$$

and $\kappa = 0{,}4$

(Unfortunately most data do not indicate the actual k values, and therefore the calculated k_s value with $\kappa = 0{,}4$ represents the combined effect of the roughness and energy dissipation effect).

(e) The proposed sediment transport equation is first split into three terms as in **Equation 3.11-2**:

$$\bar{C} = \left(\frac{\rho\ (gsD)^{1,5}}{(\rho_s-\rho)\ 0{,}4k_s\ w}\right)\cdot f\left(\frac{k_s}{D};\ \frac{w}{0{,}4\sqrt{gDs}}\right) \qquad (3.13\text{-}5)$$

This empression resulted in excellent correlations with uniform particle size sediment transport data, but poor fits of the data were obtained when non-uniform (more than one particle size) sediments were calibrated. The solution seemed to be that the settling velocity should be separated as term from the other terms in the equation.

The proposed sediment transport equation is therefore split into five terms:

$$\bar{C} = f\left(\frac{\rho(gsD)^{1,5}}{(\rho_s-\rho)};\frac{1}{0{,}4k_s};\frac{1}{w};\frac{D}{k_s};\frac{w}{0{,}4\sqrt{gsD}}\right) \qquad (3.13\text{-}6)$$

$$= f(b_1,\ b_2,\ b_3,\ b_4,\ b_5)$$

with regression format:

$$\log\bar{C} = (K_o + K_1\log b_1 + K_2\log b_2 + K_3\log b_3 + K_4\log b_4 + K_5\log b_5) \qquad (3.13\text{-}7)$$

and $K_{o....5}$ = regression constant and coefficients.

The data were analysed separately first to check for any inconsistencies for a specific sediment size set of data. The result of this analysis is indicated in **Table 3.13-1**.

Table 3.13-1: New sediment transport equation calibration with laboratory data of Guy

Data source	$d_{50}(mm)$	No data	Correlation Coefficient r^2
Guy	0,19	34	0,95
Guy	0,27	18	0,98
Guy	0,28	35	0,96
Guy	0,45	43	0,93
Guy	0,93	36	0,92
Guy	0,32	29	0,98
Guy	0,33	13	0,94
Guy	0,33 (graded)	15	0,97
Guy	0,47	54	0,92
Guy	0,54	36	0,83
Guy	All	315	0,813
Guy	All (C>0,01 %) : 0,19 mm (graded) to 0,33	171	0,920

From **Table 3.13-1**, it is clear that the correlation is good (r^2 minimum = 0,83 and in most data sets close to 1). However, when plotting the observed sediment concentration versus regressed concentration, it is evident that for each sediment diameter data set the lower and upper concentration data follow different slopes. At approximately C observed = 0,01 % (100 mg/ℓ) the change in slope occurs. This has also been found with data of *Gilbert (1914)* and where κ values were known, and in the *Yang (1973)* equation, using input stream power as independent variable. The regression can therefore be improved by using two lines for lower and upper concentrations. More important, however, is to understand why this occurs. The best explanation is the change in hydraulic conditions from laminar to turbulent with laminar sublayer to fully turbulent in the transition and upper flow regimes. In laminar conditions (and low sediment transport), settling velocities are much higher than in turbulent conditions. In the regression equation used here settling velocity is only a function of viscosity, for a specific sediment diameter, whether flow is in the laminar or turbulent phases. The proposed regression therefore cannot be applied to all data unless different w values are used for laminar and turbulent flow conditions, or, on the practical side, two regression

lines need to be used. From **Figures 3.13-1** to **3.13-5** it would seem that $C \approx 0{,}01$ % (100 mg/ℓ) can be used as a minimum value for the upper concentrations, which is a relatively low concentration for South African field conditions. In all further data analyses C> 0,01 % values were used in calibrating the new sediment transport equation. Even if a lower C<0,01 % regression was attempted, it would not be very reliable, owing to the amount of scatter indicated by the new equation which could possibly be attributed to limited data and less accurate C observed values at such low concentrations.

Combining the Guy data for C>0,01 % yields a correlation coefficient = 0,92. As a next step data of *Gilbert (1914)* was analysed. The same assumptions as with the data of Guy were followed, but the viscosity was not observed in the original tests and is taken as 10^{-6} in the analysis **(Table 3.13-2)**.

Table 3.13-2: New sediment transport equation calibration with laboratory data of Gilbert

Data source	d_{50} (mm)	No observations	Correlation coefficient r^2
Gilbert	0,3048	63	0,97
Gilbert	0,375	201	0,93
Gilbert	0,506	227	0,95
Gilbert	0,786	110	0,98
Gilbert	All	617	0,94

As seen in **Table 3.13-2**, the regression analysis for Gilbert's data agrees well with that for Guy's data and correlation of the parameters in the new sediment transport equation is good. The data of Gilbert and Guy can now be combined into one regression analysis of laboratory data (with C>0,01 %). **(Table 3.13-3)**

Table 3.13-3: New sediment transport equation calibration with data of Guy and Gilbert

Data source	No observations	Correlation coefficient r^2
Gilbert and Guy: all data	932	0,92
Gilbert and Guy: C>0,01%	787	0,94

The correlated function is shown in **Figure 3.13-5**, and no inconsistencies between the two sources of data seem to exist.

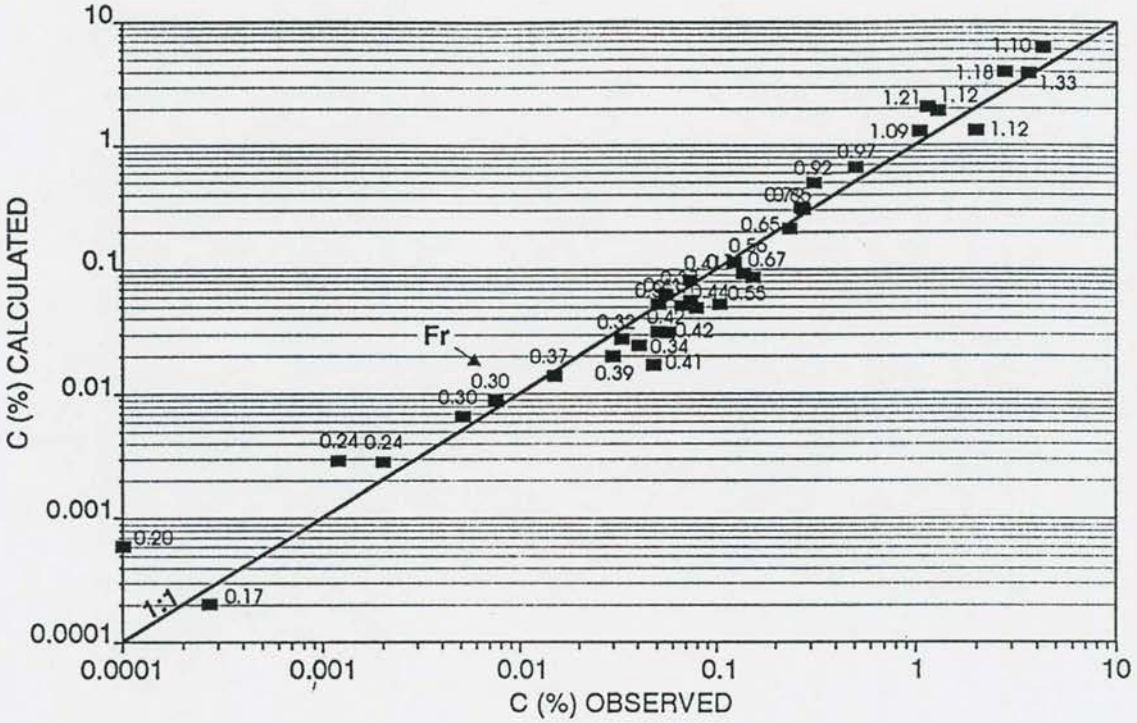

Figure 3.13 - 1 **Calibration of new sediment transport equation with data of Guy (d = 0,28 mm)**

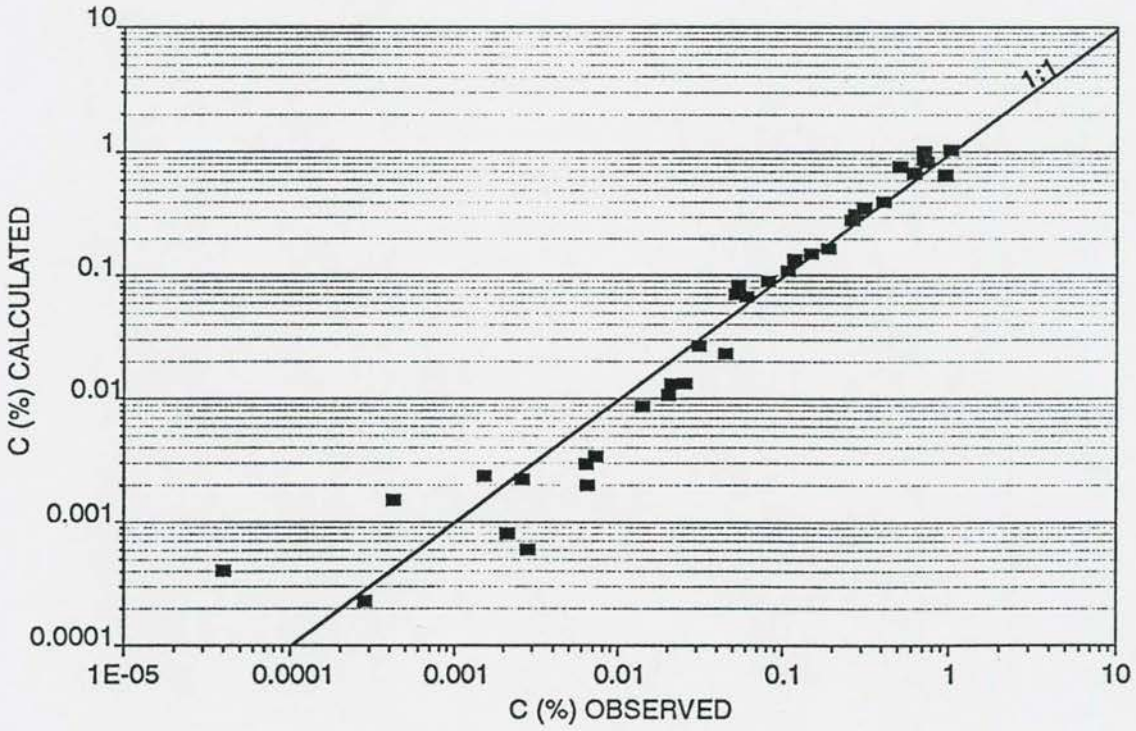

Figure 3.13 - 2 **Calibration of new sediment transport equation with data of Guy (d = 0,93 mm)**

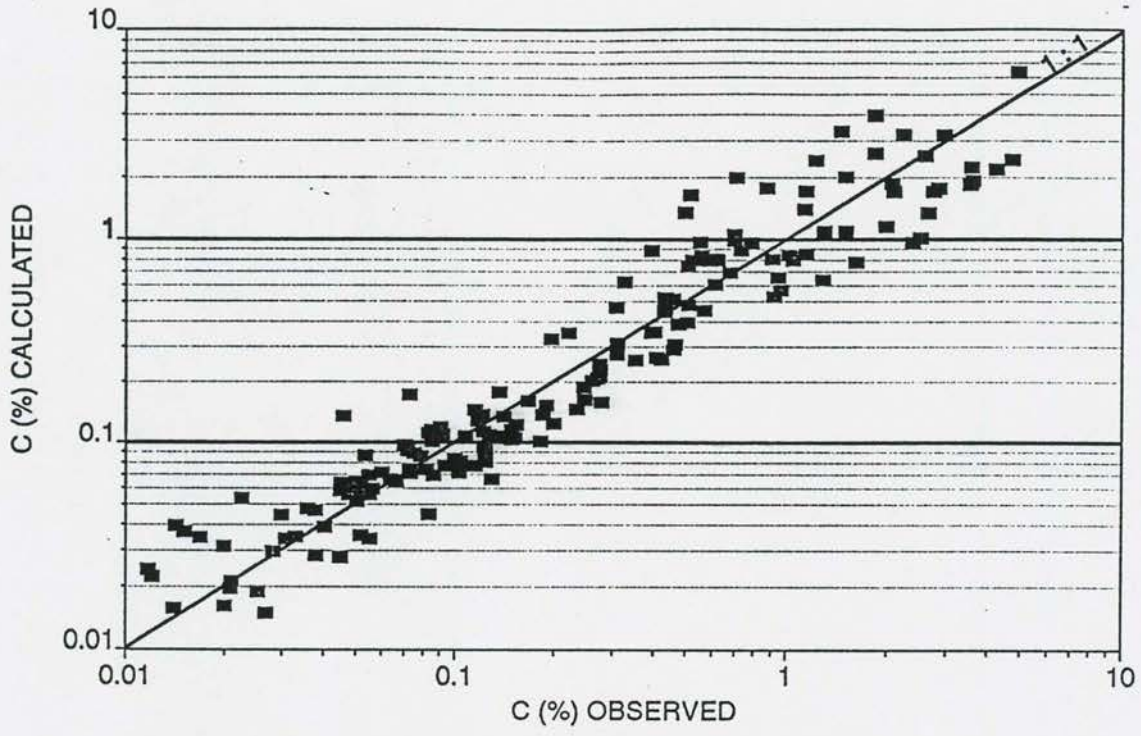

Figure 3.13 - 3 **Calibration of new sediment transport equation with data of Guy (d < 1 mm)**

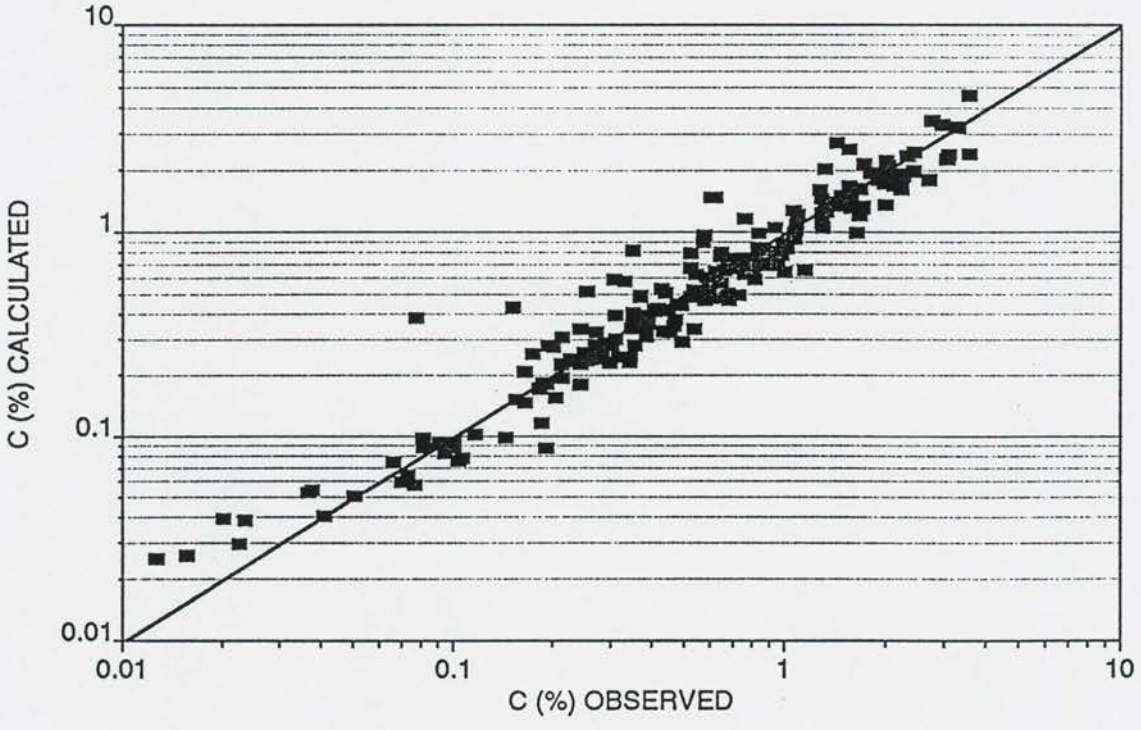

Figure 3.13 - 4 **Calibration of new sediment transport equation with data of Gilbert (d = 0,375 mm)**

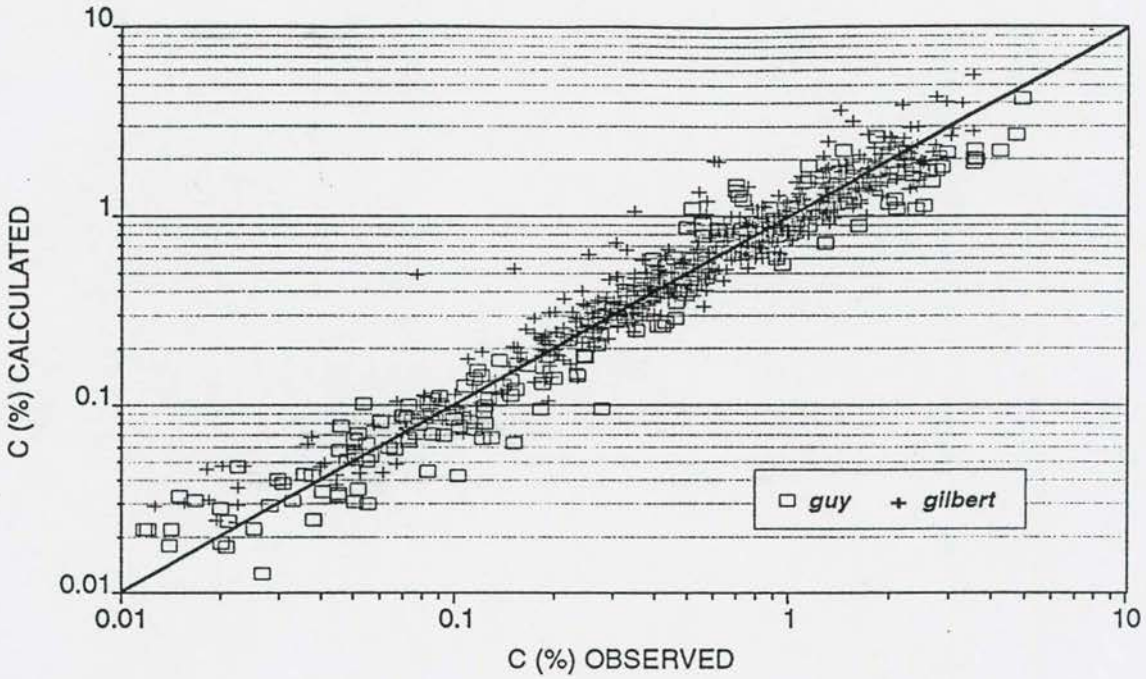

Figure 3.13 - 5 **Calibration of new sediment transport equation with data of Guy and Gilbert (d < 1 mm)**

The separation of the settling velocity (w) from the originally derived new sediment transport equation **(Equation 3.11-2)**, has proven to be very important in the calibration process to describe non-uniform sediment transport. With w part of the applied stream power function as in **Equation 3.11-2**, accurate calibration for only a single sediment particle size can be carried out. *Yang (1973)* experienced the same problem when calibrating his input stream power sediment transport equation and had to incorporate settling velocity in a term $\left(\frac{wd}{\upsilon}\right)$.

Flume data from other sources still need to be added, but at this stage it will be advisable to evaluate the new sediment transport equation with field data.

3.13.2 Calibration with river data

For calibrating the new equation with field (river) sediment transport data, reliable data (which are difficult to find) had to be obtained. The data published by *Bagnold (1966)* for United States rivers were selected for this purpose, since this data were also selected as accurate data by *Leopold (1966)*. For the field data, the settling velocity was calculated by Bagnold as Σpw of different sediment size fractions, and not the d_{50} settling velocity.

Table 3.13-4: New sediment transport equation calibration with river data

Data Source	No of Observation	Correlation coefficient r^2
Bagnold (all data)	127	0,82

The correlation coefficient for the *Bagnold* data is 0,82 **(Table 3.13-4)**, while that found with *Guy* and *Gilbert* flume data was 0,94 (C>0,01 %). The correlation is shown in **Figure 3.13-6**. No obvious inconsistencies exist and considering the many uncertainties regarding field data, the correlation is good.

The questions are now whether field sediment transport should be determined from the more reliable laboratory data base alone, as is done by using the *Yang (1973)* equation, or whether the field and laboratory data should be combined to obtain a single relationship. This can be checked by applying the flume calibrated relationship to river data as is indicated in **Figure 3.13-7**. The scatter in field data seems slightly more when the flume relationship is verified with field data, but in general it seems that reliable prediction of river sediment transport is possible by using a relationship calibrated with laboratory data only.

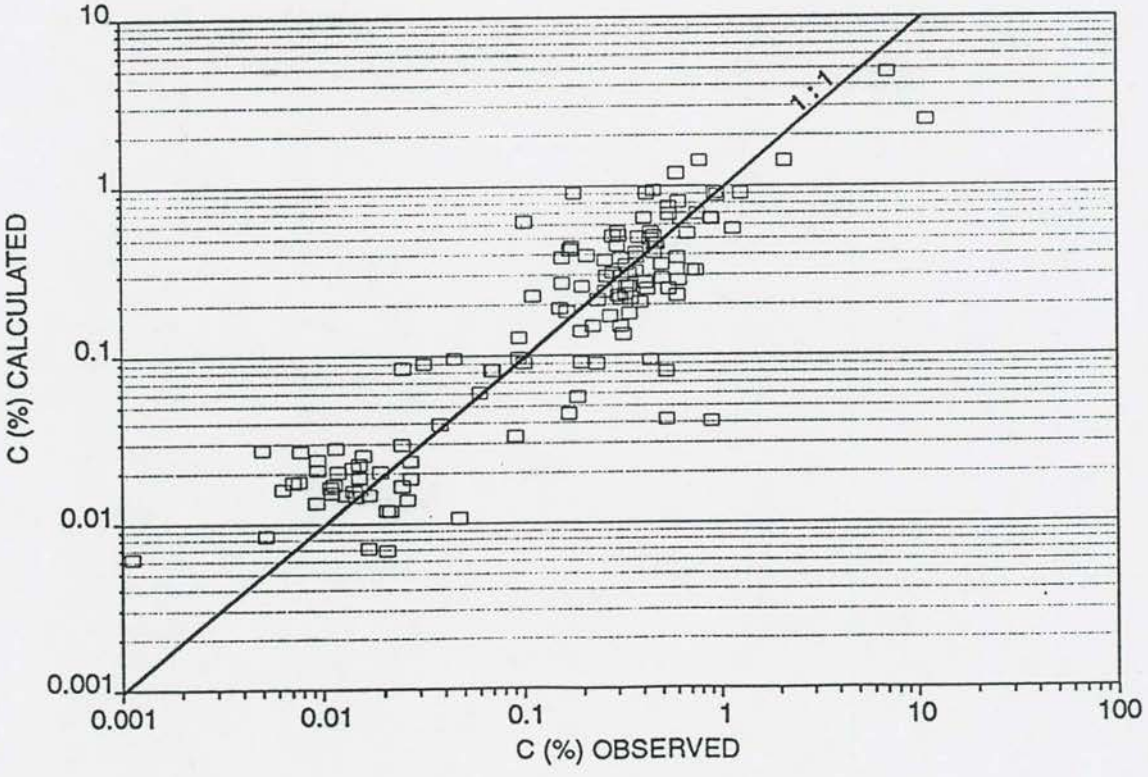

Figure 3.13 - 6 **Calibration of new sediment transport equation with river data of Bagnold**

In the next step, the flume and field data of *Guy, Gilbert* and *Bagnold* can be combined and a combined calibration can be carried out. A good correlation is obtained as is indicated in **Table 3.13-5** and **Figure 3.13-8**.

Table 3.13-5: New sediment transport equation calibration with laboratory and river data

Data Source	No of Observations	Correlation coefficient r^2
Guy, Gilbert, Bagnold	909	0,89

Quite often the accuracy of a specific sediment transport relationship is expressed in terms of its prediction of data within certain accuracy ranges, if possible with data not used in the calibration process. Some of the reported verification tests from different sources are indicated in **Table 3.1-1**. As can be seen, the results are often biased towards the author of a specific equation. The new sediment transport equation, as calibrated is tested in a similar way in **Table 3.13-6**. However, the same data as used in the calibration are used and no comparison with other sediment transport relationships is carried out.

Table 3.13-6: Accuracy of new sediment transport equation in prediction ranges (for C > 0,01 %)

Calibration based on	Percentage of data within accuracy range		
	$0{,}67<\frac{Ccalc}{Cobs}<1{,}5$	$0{,}5<\frac{Ccalc}{Cobs}<2{,}0$	$0{,}33<\frac{Ccalc}{Cobs}<3$
Gilbert and Guy flume data	86 %	97 %	99 %
Bagnold river data	48 %	68 %	89 %
Gilbert, Guy and Bagnold data	77 %	92 %	98 %

Although calibration data have been used in the above verification, the results compared with other sediment transport relationships are good and even river data are predicted with relatively good accuracy.

It has now been established that good correlations can be established with the new sediment transport equation using flume and river data. The question remains, however, whether this

relationship can also be applied to reservoir data. The reservoir data obtained in this study from field sampling at selected South African reservoirs, will be analysed here.

3.13.3 Calibration with reservoir data

There are a number of important differences between reservoir, laboratory and river data. The latter two sets are normally obtained under uniform and steady (or nearly steady) flow conditions, and with sediment transport and bed deformation equilibrium. In a reservoir the two extreme operational situations are full storage operation with non-uniform, but often near steady conditions in large reservoirs, and drawdown flushing, normally with highly unsteady and non-uniform flow conditions during the retrogressive erosion phase.

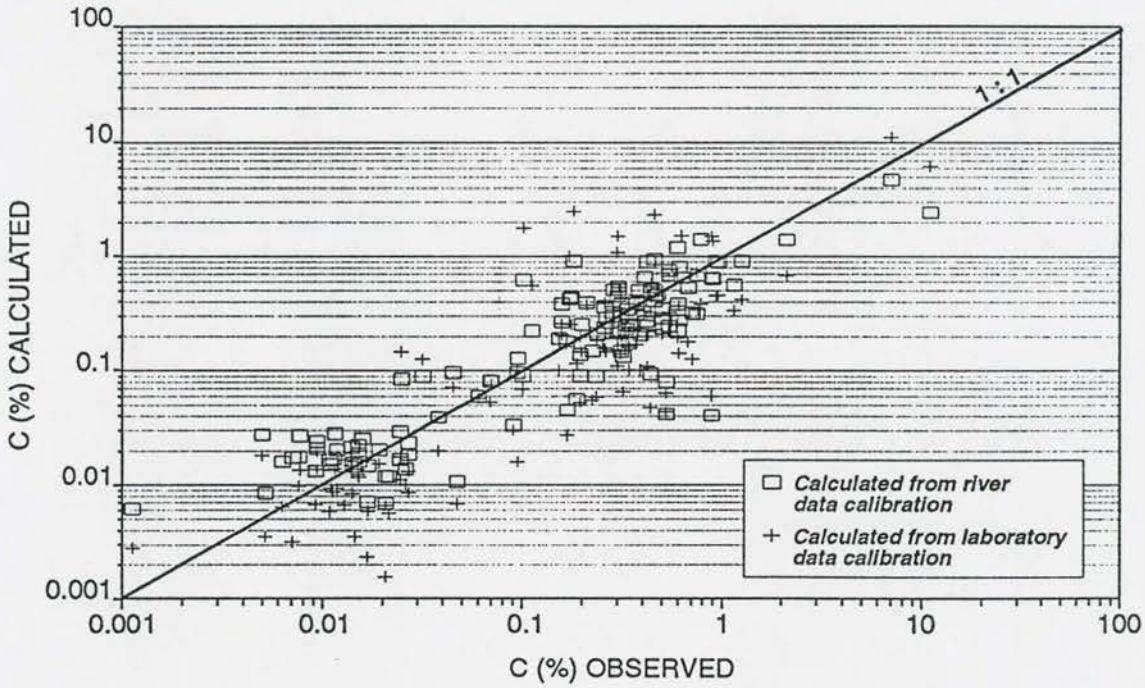

Figure 3.13 - 7 **Verification (with river data) of calibrated new sediment transport equation (based on flume data)**

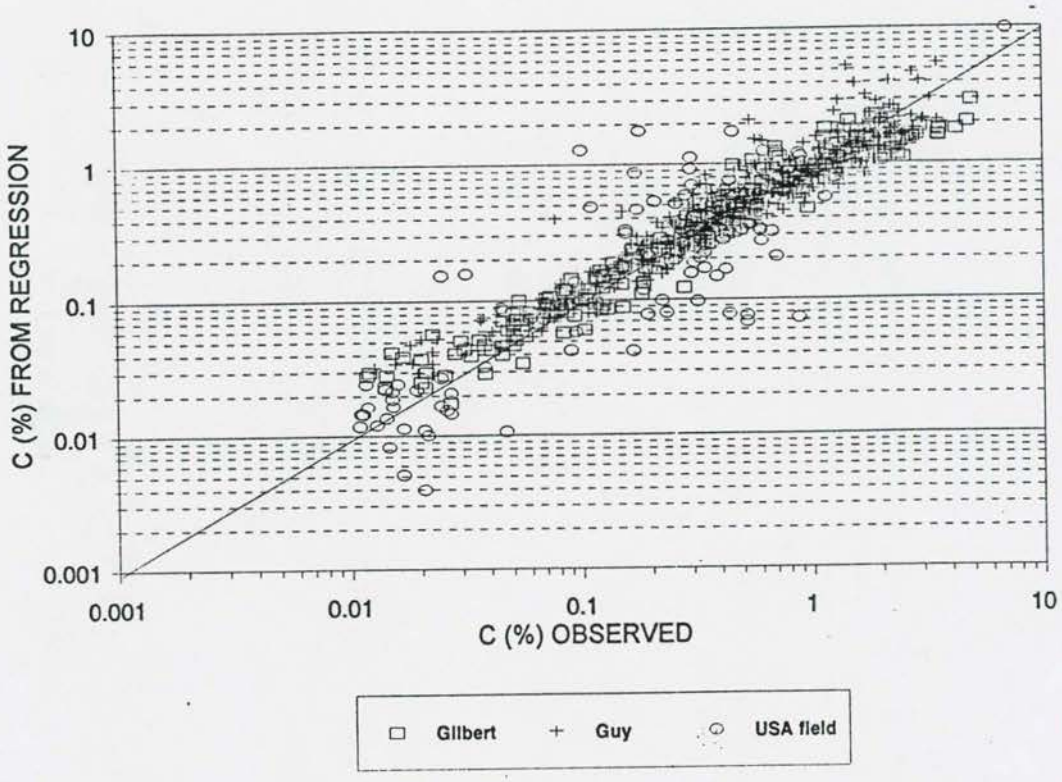

Figure 3.13 - 8 **Calibration of new sediment transport equation based on flume and river data**

The particle sizes of sediments being transported through a reservoir furthermore also differ drastically from the river and flume cases. Along the upper reaches of a reservoir, coarse sediment is still being transported, representing river conditions, but further downstream the sorting process soon causes only fine sediment to be transported. This fine sediment (under storage operation with a large reservoir) can be in the order of d_{50} = 2 micron, which is 10 times smaller than the finest sediments used or considered in flumes and rivers.

The slope to be used in the sediment transport equation should actually fall somewhere between the energy slope and bed slope for a full reservoir, while during flushing the energy slope should approach the bed slope and approach uniform flow conditions when equilibrium scour is reached.

Unsteady flow conditions during flushing can cause oversaturation, especially if erosion takes place close to the dam and suspended sediment samples are taken immediately downstream

of the dam. On the other hand, non-equilibrium sediment transport also occurs due to the time lag during which fine sediment loads adjust to changing hydraulic conditions (see discussion in **Section 3.17**).

Obtaining field data during flushing is also problematic. With complete drawdown, it is impossible and dangerous to obtain concentration samples from the flushing channel, and hydraulic variables are difficult to monitor within the reservoir.

Other processes that can play a role in reservoirs are different mechanisms of sediment transport and flocculation at high sediment concentrations, which may influence settling velocities.

All in all, reservoir data should be analysed and selected with great care. It is doubtful that a relationship which has been calibrated for coarse sediments under uniform, steady flow conditions can be used at all to predict sediment transport through a reservoir. Therefore, the approach followed here was to rather calibrate the proposed sediment transport relationship on reservoir data and to compare it with the other relationships as calibrated with river and laboratory data. Under high inflow flushing conditions it is expected that the reservoir flows will approach river conditions and that the river and reservoir sediment transport relationships should agree. A sediment transport relationship based on input stream power and storage operation for two reservoirs as shown in **Figure 3.13-9** has been used for many years in South Africa.

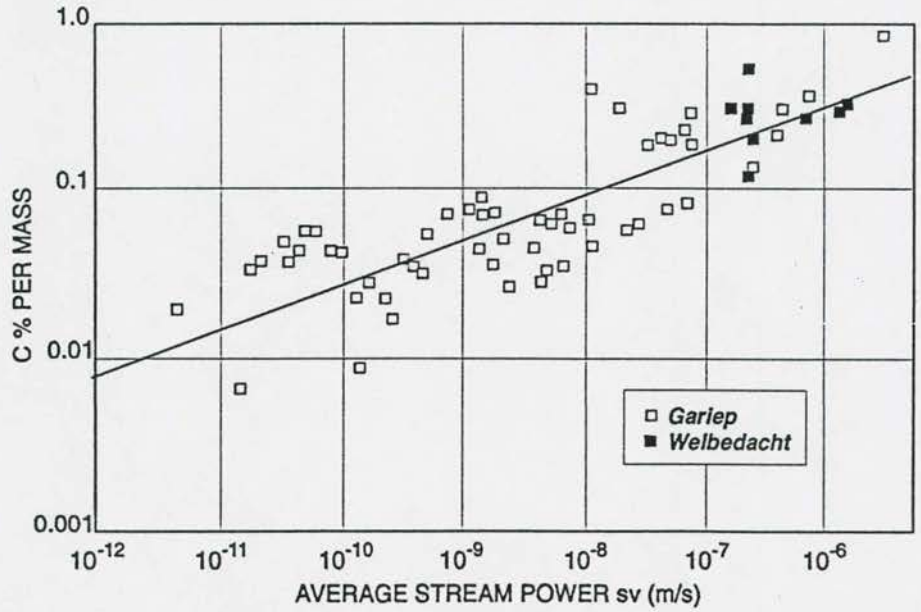

Figure 3.13 - 9 **Sediment concentration versus stream power for two South African reservoirs (Rooseboom, 1986)**

Reservoir data have been obtained at a number of reservoirs under variable operational and flood conditions, as indicated in **Table 3.13-7**.

Table 3.13-7: Reservoir data

No	Reservoir	Date	Description
1a	Welbedacht	06/02/94	Drawdown flood flushing
1b	Welbedacht	08/02/94	Drawdown flood flushing
1c	Welbedacht	19/10/95	Drawdown flood flushing
2a	Phalaborwa Barrage	10/01/91	Drawdown flood flushing
2b	Phalaborwa Barrage	08/02/85	Drawdown flood flushing
2c	Phalaborwa Barrage	21/02/96	Drawdown flood flushing
3a	Elandsdrift	04/12/93	Storage operation during minor flood
4a	De Mistkraal	04/12/93	Storage operation during minor flood
5a	Windsor	05/10//93	Drawdown flushing during low inflows
5b	Windsor	03/02/94	Storage operation during flood
6a	Mbashe	09/93	Empty reservoir with low inflows
6b	Mbashe	25/10/95	Drawdown sluicing with low inflows
6c	Mbashe	12/95-01/96	Drawdown flood flushing
7a	Nagle	24/04/93	Drawdown flushing with low inflows
8a	Gariep	1974	Storage operation during flood

To interpret the reservoir data, it was plotted as sediment concentration against input stream power (vs) in **Figures 3.13-10** and **3.13-11**. (Note that settling velocity still needs to be taken into account to form a comprehensive picture of the observed sediment transport). After each flushing and closure of the gates at Welbedacht Dam, stream power decreases rapidly, although sediment concentrations remain high for some time and only then drops back to the "normal" vs against C relationship. It was found that the sediment transported immediately after closure of the dam was much finer than with free flow. A check whether $\frac{vs}{w}$ versus C would not "correct" the relationship as indicated by vs versus C proved to be unsuccessful, and everything pointed to the fact that a density current and not turbulent sediment transport had been present. This data set was therefore removed from the data used for calibration of the new transport equation and is discussed and analysed further in **Chapter 4**.

Calibration with the remaining "accurate" selected reliable data gave a correlation coefficient (r^2) of 0,80 using the new transport equation. In a comparable test using input stream power $\left(\frac{vs}{w}\right)$, similar results were found, as indicated in **Table 3.13-8**.

Table 3.13-8: Calibration of stream power relationships

Sediment transport equation	No of data	Correlation coefficient r^2
Applied stream power (new transport equation)	180	0,80 **(Figure 3.13-12)**
Input stream power (vs/w)	180	0,72 **(Figure 3.13-13)**
Input (vs;w)	180	0,78 **(Figure 3.13-14)**

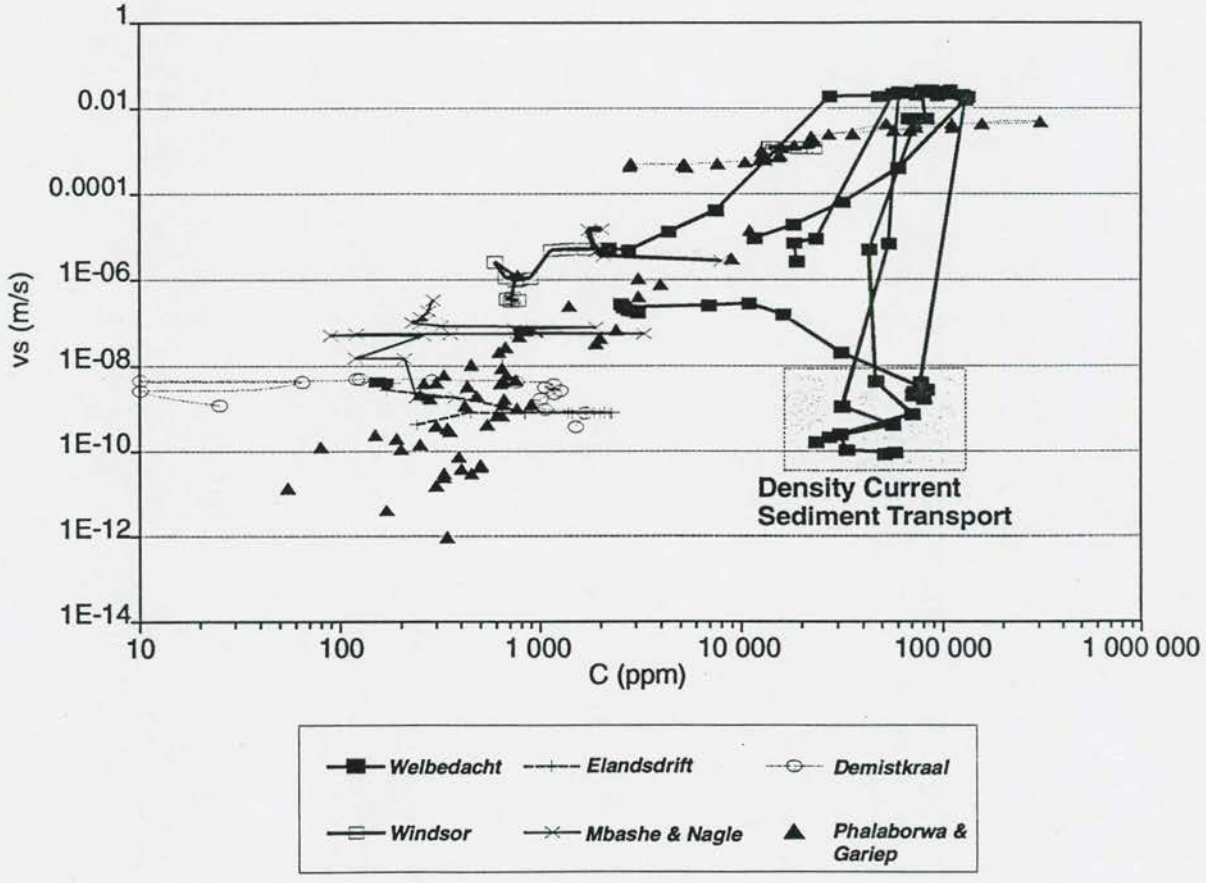

Figure 3.13 - 10 **Input stream power versus observed suspended sediment concentration for South African reservoirs**

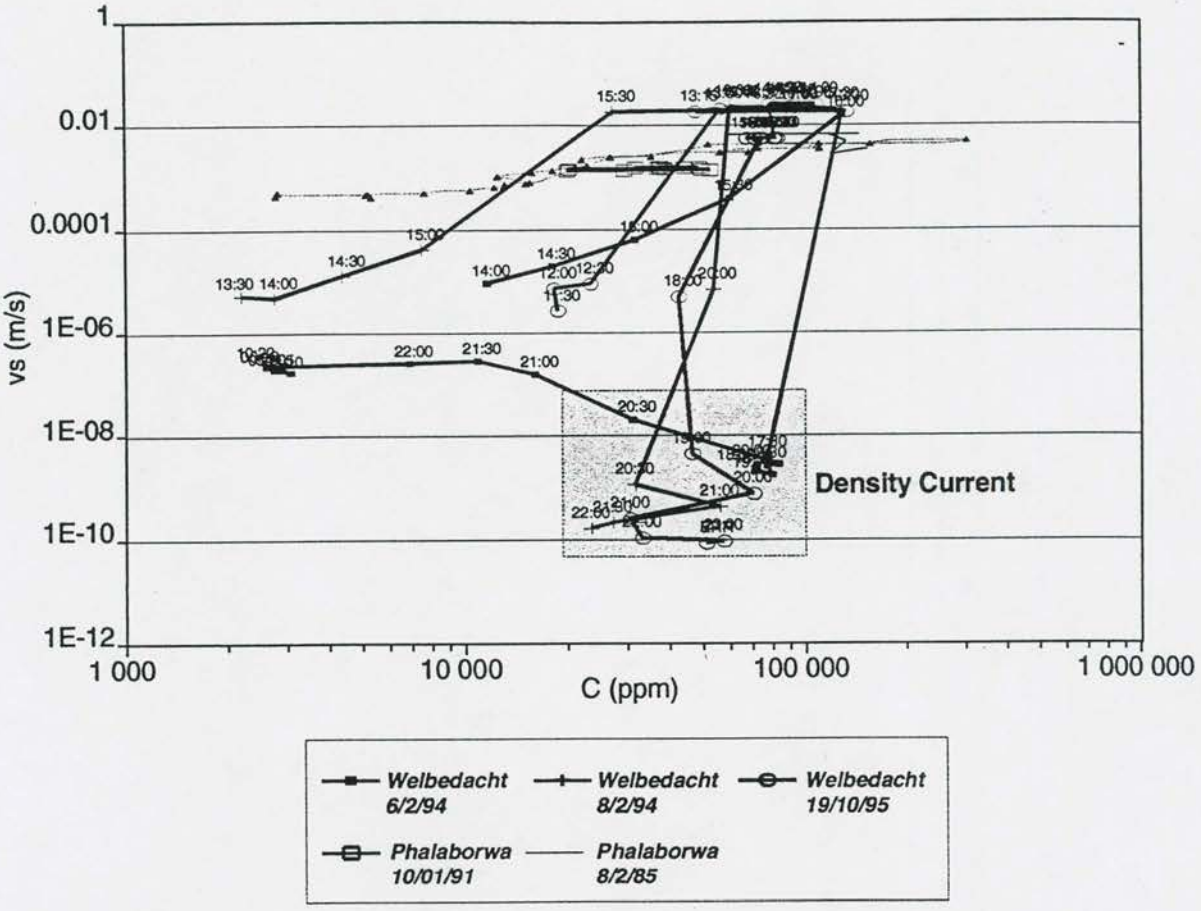

Figure 3.13 - 11 **Density current data at Welbedacht Dam**

The best correlation is obtained with the new relationship. A relationship for input stream power as a function, with the settling velocity separated, was also used, since it was found in this research and by *Yang (1973)* that w is a dominant variable. Testing of accuracy ranges is indicated in **Table 3.13-9** (using the same data used for calibration).

Table 3.13-9: Accuracy ranges of calibrated new sediment transport equation

Description	$0{,}67<\frac{Ccalc}{Cobs}<1{,}5$	$0{,}5<\frac{Ccalc}{Cobs}<2$	$0{,}33<\frac{Ccalc}{Cobs}<3$	$0{,}25<\frac{Ccalc}{Cobs}<4$
New equation	28	46	78	91
Input (vs/w)	27	41	66	76
Input = f (vs;w)	29	49	76	86
New equation calibrated with USA river data (Bagnold)	48	68	89	-

The calibration previously obtained from USA river data is also shown in **Table 3.13-9** for comparison. The variability in predictions of reservoir suspended sediment concentrations is much larger than for river or flume data. The accuracy of laboratory data normally allows a range of 0,5 to 2 of calculated/observed concentrations which includes almost all of the data, while the comparable range for South African reservoirs is at least 0,25 to 4. Nevertheless, the reservoir sediment concentration prediction is better than expected, particularly if the high non-uniformity of flows is considered.

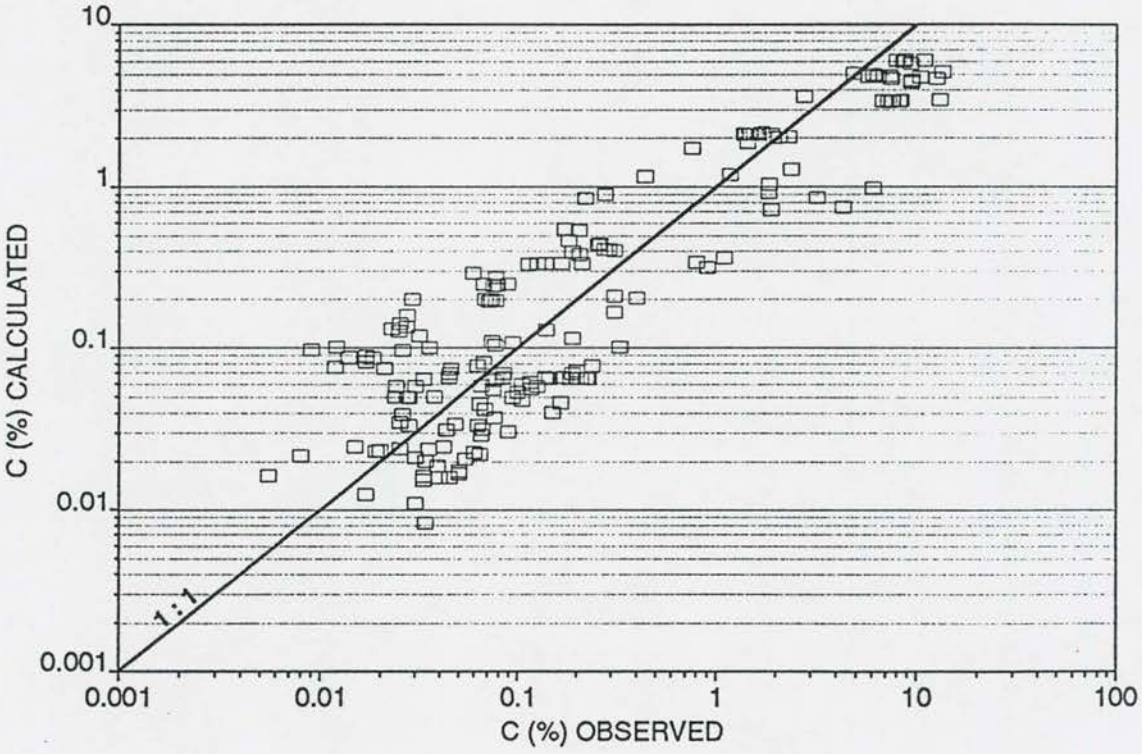

Figure 3.13 - 12 **Calibration of new sediment transport equation based on reservoir data**

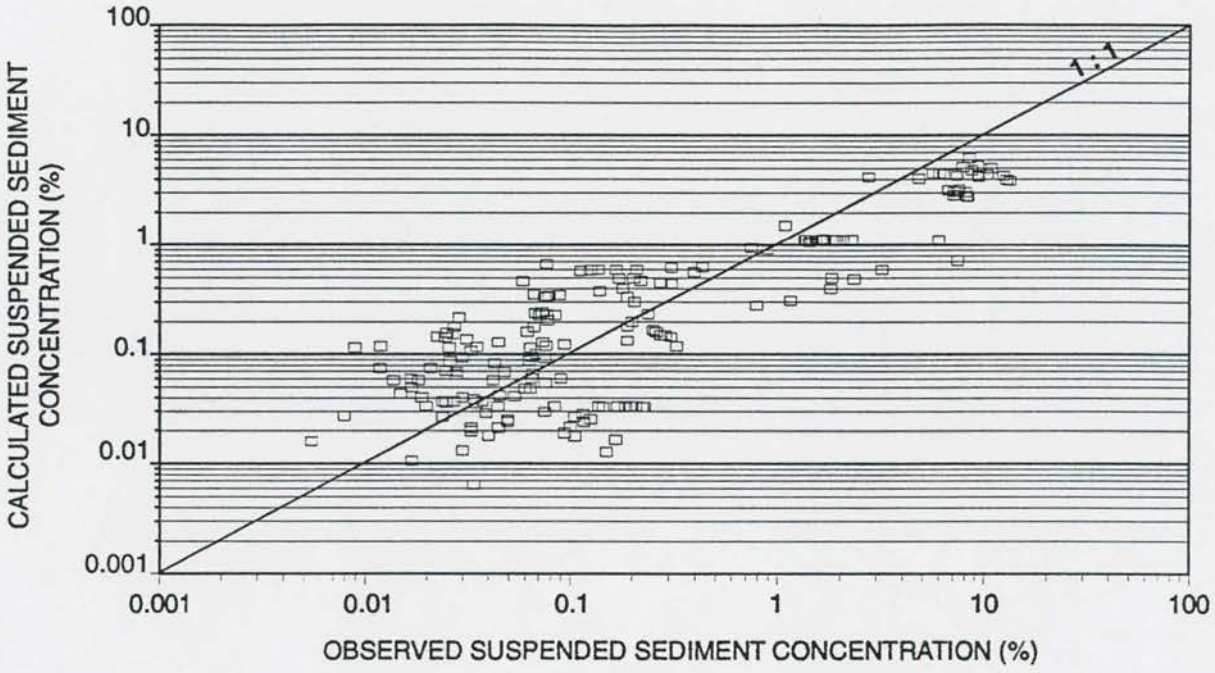

Figure 3.13 - 13 **Calibration of input stream power sediment transport equation based on reservoir data**

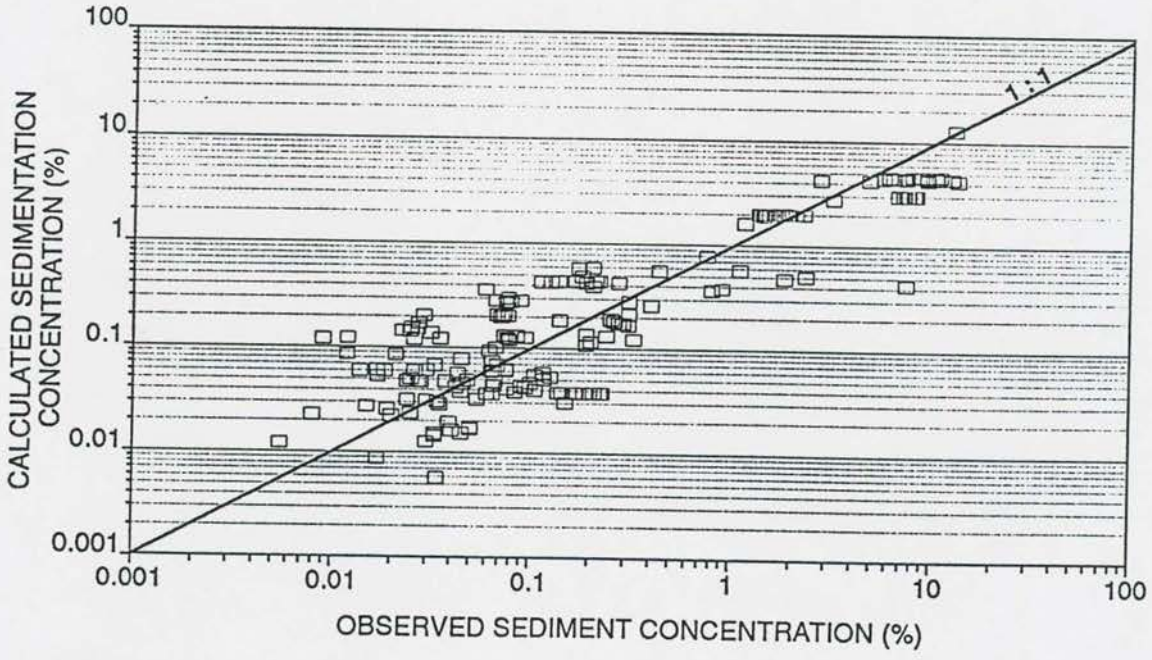

Figure 3.13 - 14 **Calibration of input stream power sediment transport equation, with settling velocity separated, based on reservoir data**

In modelling, both a sensitivity analysis and reservoir-specific data should be used as far as possible for calibration of the sediment transport relationship. It is recommended that the applied stream power relationship (new equation) be used in future modelling, preferably with local data. This relationship as calibrated here provides a relatively good estimate over a wide range of sediment concentrations and hydraulic conditions for South African reservoir data.

Mathematical modelling results of reservoir sedimentation (deposition) for the same hypothetical boundary conditions, but with two different sediment transport equations are presented in **Figures 3.13-15** and **3.13-16**, for the stream power sediment transport equation calibrated on reservoir data, and the England-Hansen equation, respectively. (The flow and sediment transport algorithms used in the modelling are described in **Chapter 7**).

3.13.4 Comparison between flume, river and reservoir data calibrated new sediment transport equation

Finally, a prediction of the reservoir data was carried out using the previously calibrated new equation based on flume and river data. This was compared with the observed and reservoir-calibrated new sediment transport equation. **Figure 3.13-17** shows that the sediment transport can be accurately predicted with formulae calibrated on river or flume data only at high concentrations ($C > 3$ %) and flow conditions approaching those of a river. At lower flow conditions and sediment concentrations (storage operation), sediment transport can be underestimated considerably. This is also the reason why modelling based on general laboratory/river data calibrations indicates such definite delta formations with almost no sediment transport downstream of the delta. Fortunately, from the point of view of reservoir sediment removal, the actual sediment transport through reservoirs is orders higher than would normally be calculated by means of equations calibrated with laboratory data.

3.14 Non-dimensional new applied stream power sediment transport equation

In the previous sections, a new sediment transport relationship was proposed as derived from the applied power at the bed and the vertical concentration distribution. Calibration with laboratory data indicated that the new equation is reliable for single particle size data, but as was found with input stream power, the settling velocity had to be separated from the rest of

the equation in order to calibrate all sediment sizes. As such the equation only provides sediment concentration, not total sediment load, since it was felt that the former format should be tested with data first. The new sediment transport equation is therefore not dimensionally homogeneous, and although no discrepancies were found with data, it is good practice to use dimensionally homogeneous sediment transport relationships. Such a new sediment transport equation will therefore be derived in this section for the calculation of total loads.

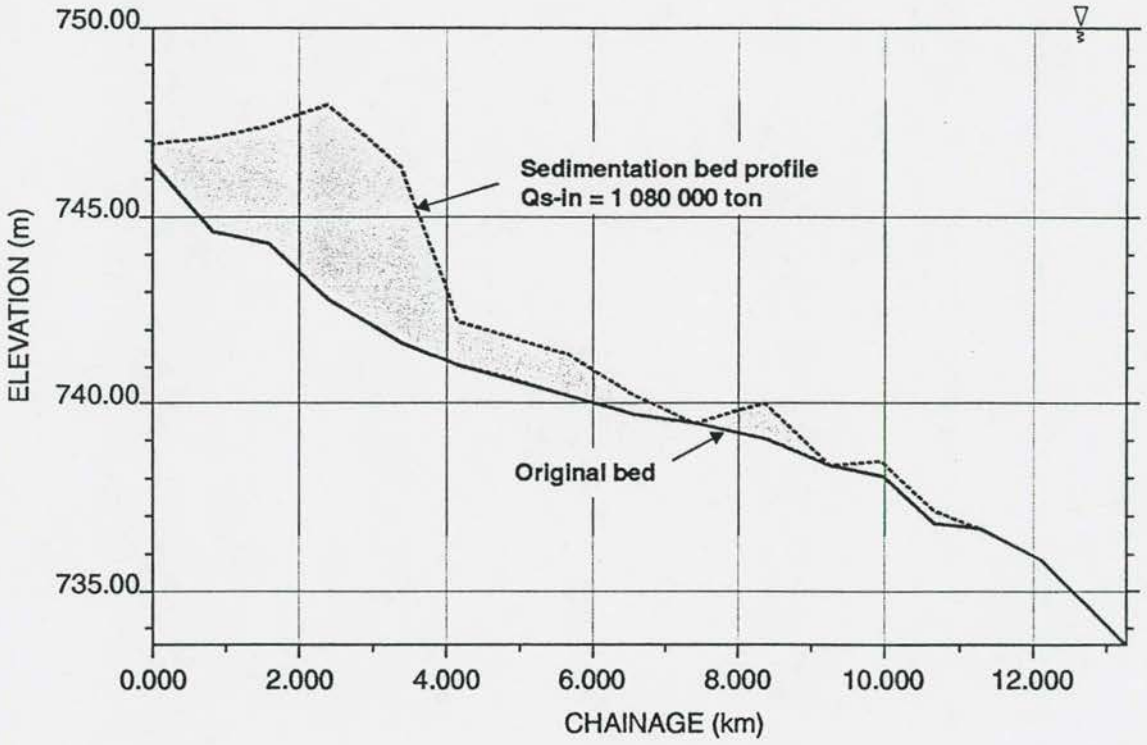

Figure 3.13 - 15 **Reservoir sedimentation based on stream power sediment transport equation calibrated on reservoir data**

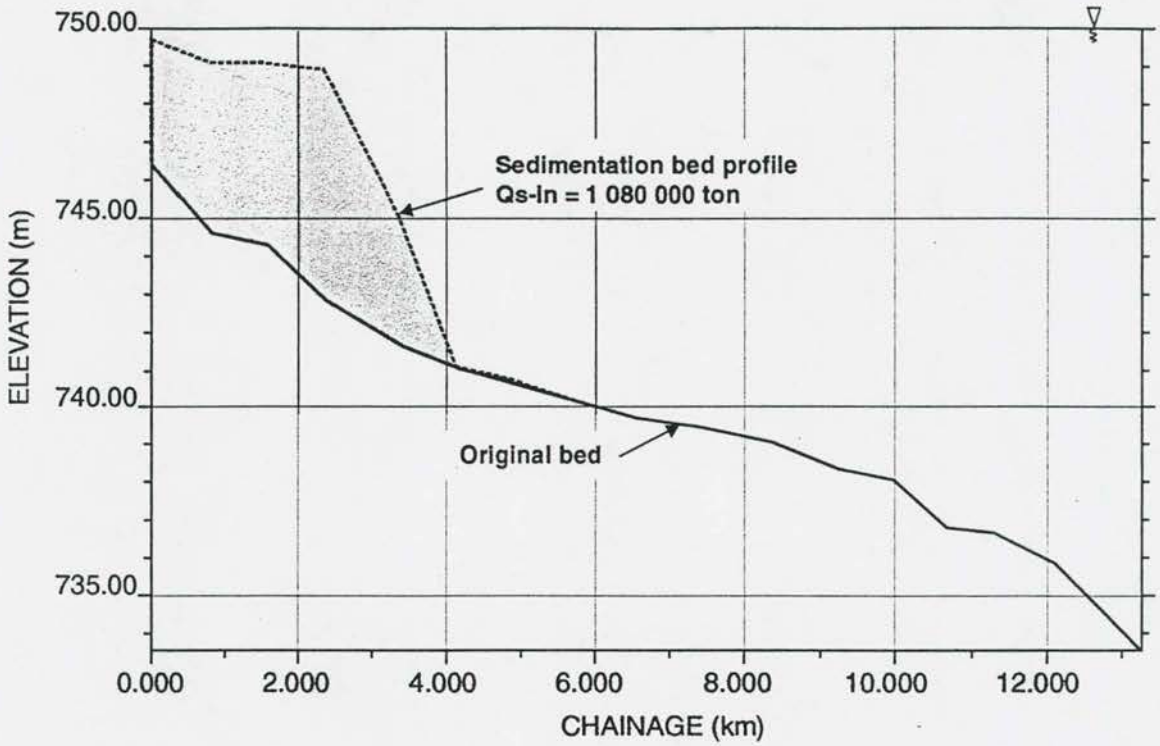

Figure 3.13 - 16 **Reservoir sedimentation based on Engelund-Hansen sediment transport equation**

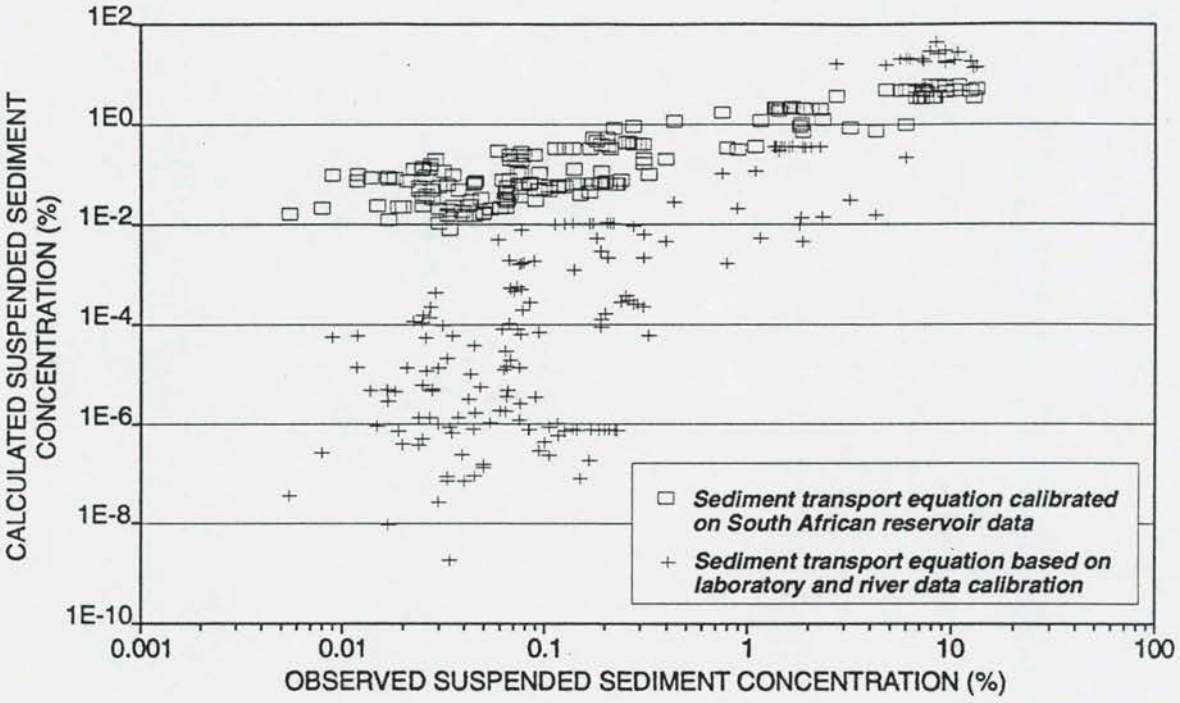

Figure 3.13 - 17 **Verification of reservoir sediment transport with new sediment transport equation based on laboratory and river data calibration**

The total sediment load (q_s) can be determined from:

$$q_s = \int_{y_0}^{D} vC\, dy$$

$$= \int_{y_o}^{D} \left(\frac{1}{\kappa} \ln\left(\frac{30y}{k_s}\right)\right) \sqrt{gDs} \cdot \frac{C_o\left(\tau \frac{dv}{dy}\right)^z}{\left(\tau \frac{dv}{dy}\right)_o^z} \cdot dy \qquad (3.14\text{-}1)$$

Substituting C_o as before yields a dimensionally homogeneous equation:

$$q_s = \frac{30\rho(gDs)^2}{(\rho_s-\rho)\kappa^2 \cdot k_s \cdot g \cdot w} \ln\left(\frac{12D}{k_s}\right)\left(\frac{k_s}{30D}\right)^z f\left(\frac{k_s}{30D}\right) \cdot \left(\frac{\kappa\sqrt{gDs}}{w}\right) \qquad (3.14\text{-}2)$$

Equation 3.14-2 can be calibrated with data in the following formats:

a) **Kappa known**

$$\log q_s = A_1 \log \frac{(30\rho(gDs)^{1,5})}{(\rho_s - \rho)\,\kappa^2 \,.\, k_s \,.\, g} \ln\left(\frac{12\,D}{k_s}\right) + A_2 \log\left(\frac{\sqrt{gDs}}{w}\right) + A_3 \,.\, z \log\left(\frac{k_s}{30D}\right)$$

$$+ A_4 \log\left(\frac{k_s}{30D}\right) + A_5 \log\left(\frac{\kappa\sqrt{gDs}}{w}\right) \qquad (3.14\text{-}3)$$

b) **Kappa unknown, assumed $\kappa = 0{,}4$**

$$\log q_s = A_1 \log \frac{30\rho(gDs)^{1,5}}{(\rho_s - \rho)\,\kappa^2 \,.\, k_s \,.\, g} \ln\left(\frac{12\,D}{k_s}\right) + A_2 \log\left(\frac{\sqrt{gDs}}{w}\right) + A_3 \,.\, z \log\left(\frac{k_s}{30D}\right) \qquad (3.14\text{-}4)$$

Calibration of **Equation 3.14-4** with the laboratory data of Guy and Gilbert as before shows the same correlation as was found with the non-homogeneous new equation for individual sediment sizes. When all sediment sizes are combined in the regression, however, the correlation is as indicated in **Figure 3.14-1** with parallel lines for different particle sizes. To rectify this the only solution would be (as before) to have the settling velocity as a separate parameter in the regression, by perhaps using a dimensionless relationship such as $\frac{wd}{\nu}$ as was used by *Yang (1973)* in calibrating the input stream power relationship.

3.15 Deformation of the bed and resistance to flow

3.15.1 Introduction

In order to be able to predict sediment load within reservoirs, the relationship between variables representing roughness (k_s) and dissipation of energy(κ), needs to be determined, as has been shown in **Section 3.9**. It has also been shown that this interrelationship is required to quantify energy dissipation (stream power). In particular, the changes of κ and k_s*-values* with sediment transport and related bedform regions need to be forecasted. Secondly, a "roughness" predictor can be utilized to forecast equilibrium depth of flow which can be incorporated in predicting flushing channel deformation (width and depth).

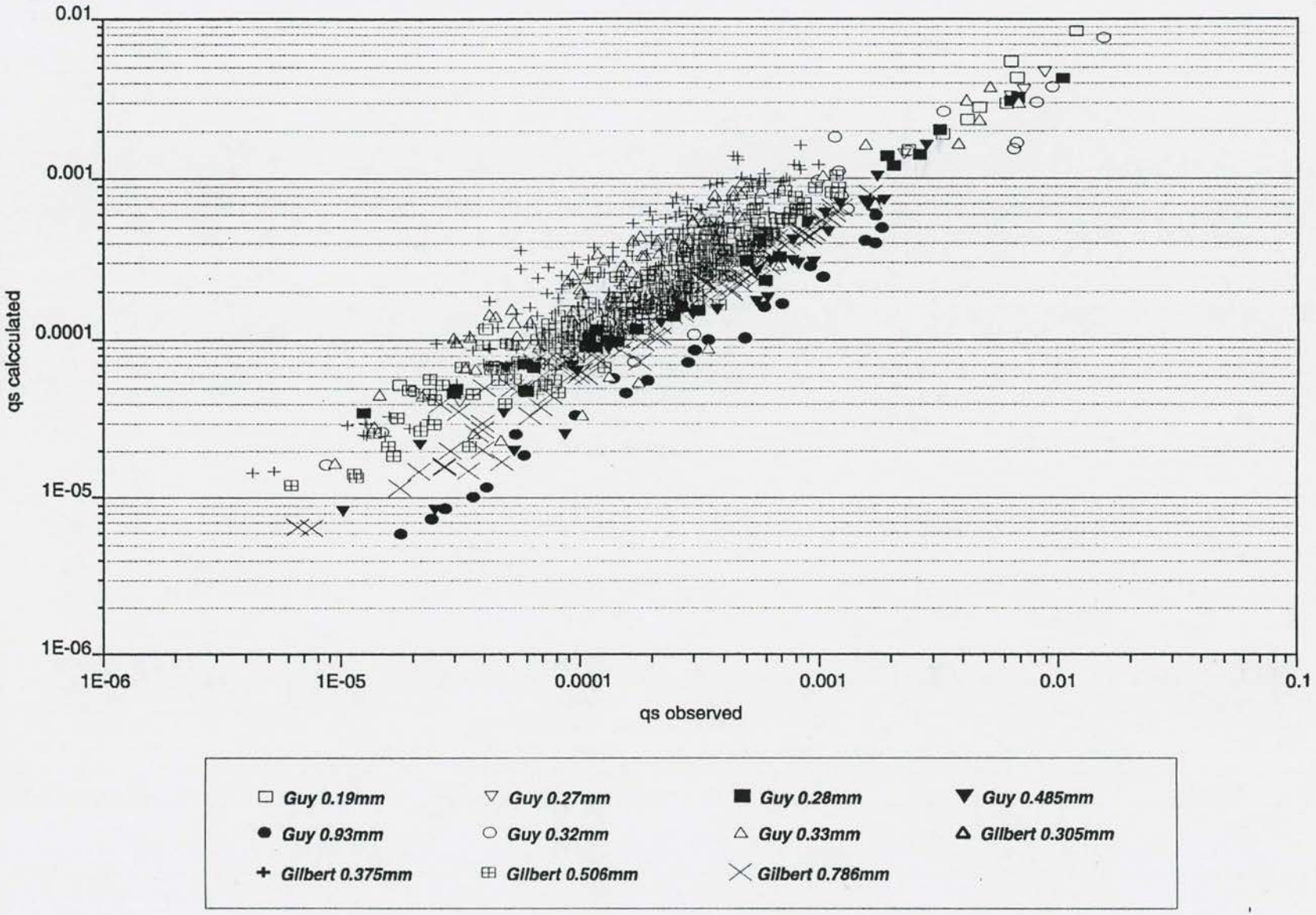

Figure 3.14 - 1 Calibration of dimensionless new sediment transport equation with flume data

Although the author believes that the changes in k_s and κ are interlinked with sediment transport, certain assumptions can be made to predict bed roughness without considering sediment transport directly.

3.15.2 Developing a new bed roughness predictor

Several researchers in the past have used separate roughness predictors for so-called friction caused by sediment particles, and form friction caused by bed irregularities such as ripples or dunes *(Meyer-Peter et al, 1948)*. It is felt that such an approach, although providing good results, is highly empirical and instead of splitting the roughness estimator, a theoretically sound k_s predictor should be sought.

Let us return to the stream power balance equation **(Chapter 3.9)** and evaluate the applied power relationship at the bed again, taking the second term (**Equation 3.9-1**) as a constant with κ = 0,4 for homogeneous fluid transport.

$$\frac{30\rho gsD\sqrt{gDs}}{\kappa k_s} \propto (\rho_s-\rho)gwC_o \qquad (3.15\text{-}1)$$

A similar equation has been used by *Rooseboom (1992)* to predict incipient motion at onset of resuspension of sediment. He assumed C_o to be a constant, which is acceptable since $\bar{C} \to o$ and the incipient relationship shown in **Chapter 6** (modified Liu diagram) were obtained for laminar and turbulent flow conditions. In a somewhat more elaborate approach *Le Grange (1995)* also used **Equation 3.15-1** as a basis for determining bed roughness in the lower and upper regimes, again assuming C_o = constant in **Equation 3.15-1**, which can therefore be neglected in further analyses (or assuming C_o is not of concern when studying the power balance on a single sediment particle). The relationship derived by *Le Grange (1995)* is indicated in a Liu diagram in **Figure 3.15-1**. The data indicated laminar trends in both the lower and upper flow regimes, with $\sqrt{gDs}/w$ constant in the transition regime. κ -values were assumed = 0,4 by *Le Grange (1995)*. This would indeed be a convenient prediction method for forecasting incipient motion under lower and upper regime equilibrium conditions at the bed. Verification of this equation with laboratory data of Gilbert with a large database for one particle size is shown in **Figure 3.15-2**. Note that κ -values were

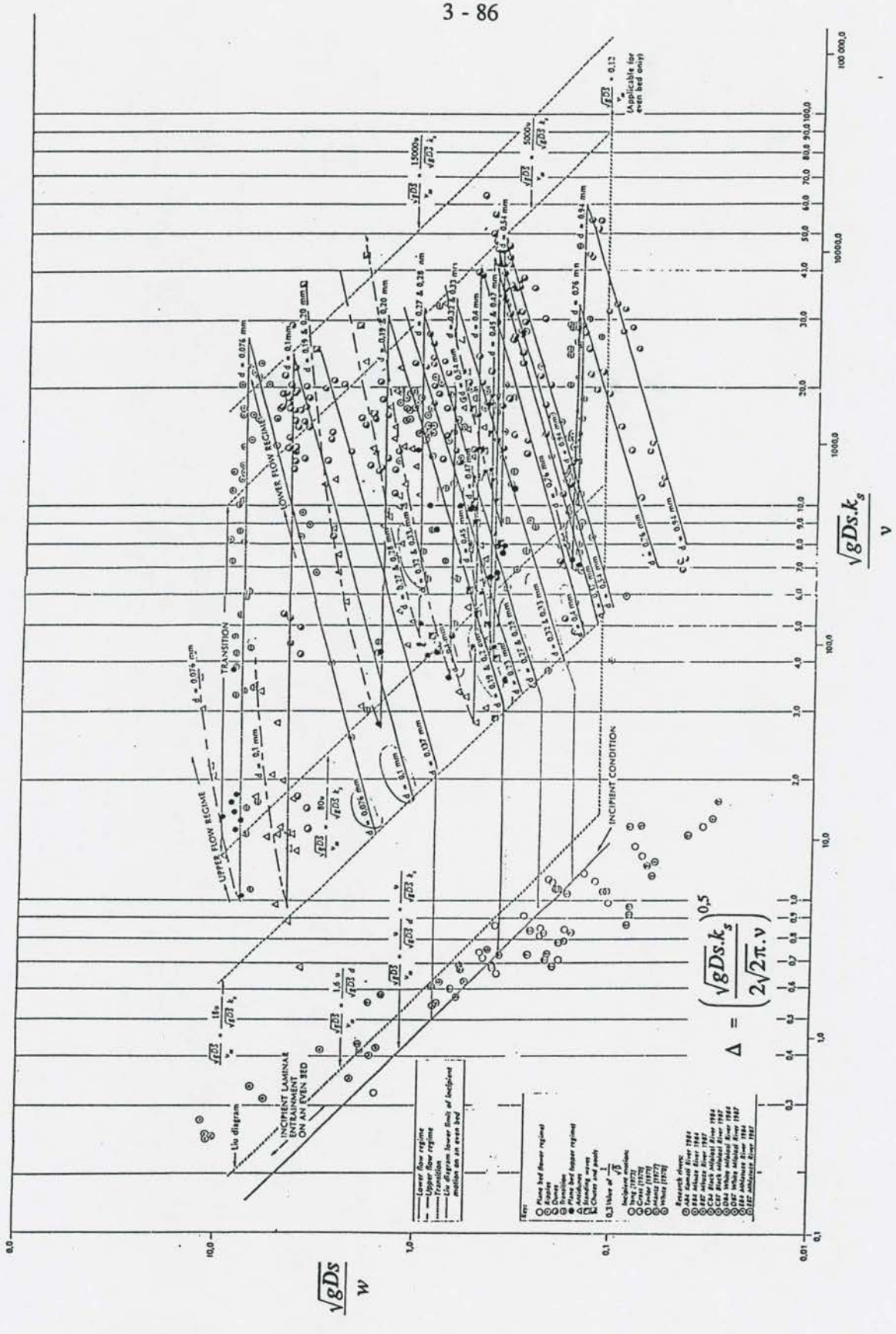

Figure 3.15 - 1 **Modified Liu diagram (Le Grange, 1995)**

not known and had to be taken as 0,4 in the calculation of k_s. The effect of changing κ is therefore incorporated in k_s. The graph follows the general trend (as found by *Le Grange (1995)* with increasing k_s in the lower and upper regime with a flat bed in the transition region. The amount of data scatter, however, makes it unsuitable for use as a prediction method. As a check on the correlation, k_s values for the lower regime and upper regime (excluding any transition data) were analysed separately, which gave regressions as indicated in **Figures 3.15-3** and **Figure 3.15-4**. It is therefore clear that the assumption of C_o = constant is not valid for lower or upper flow regime conditions, and in the transition regime the data scatter is even larger (**Figure 3.15-2**).

Some means of predicting C_o values therefore needs to be found and used in **Equation 3.15-1**. In evaluating the sediment transport **Equation 3.14-2** (in **Chapter 3.14**), it was found that the different bedform types as found in flume studies, can be closely related to the Froude number. In fact, several researchers have used the Froude number in the past as one of the predictors in estimating bed roughness or predicting different bedforms *(Athaullah, 1968)*. The approach followed here therefore assumes that the bed sediment concentration (C_o) can be linked to the Froude number and that $C_o \propto Fr$. Due to limited data on near bed sediment concentrations, average sediment concentrations are used instead. **Figure 3.15-5** shows that by using the data of *Guy* and *Gilbert*, a relationship between $\overline{C}$ and Fr can be established.

Equation 3.15-1 can therefore be rewritten as:

$$\frac{\rho(gsD)^{1,5}}{(\rho_s-\rho)} = f\,(k_s;\ w;\ Fr) \qquad (3.15\text{-}2)$$

with $Fr = \dfrac{\overline{v}}{\sqrt{gD}}$

A remarkably good correlation is found when **Equation 3.15-2** is fitted to flume data, but theoretically the incorporation of the Froude number still needs to be justified. Since the sediment transport equation includes all the necessary variables to describe the bed deformation process under equilibrium flow regime conditions, it should also be possible to derive a prediction methodology for bed roughness.

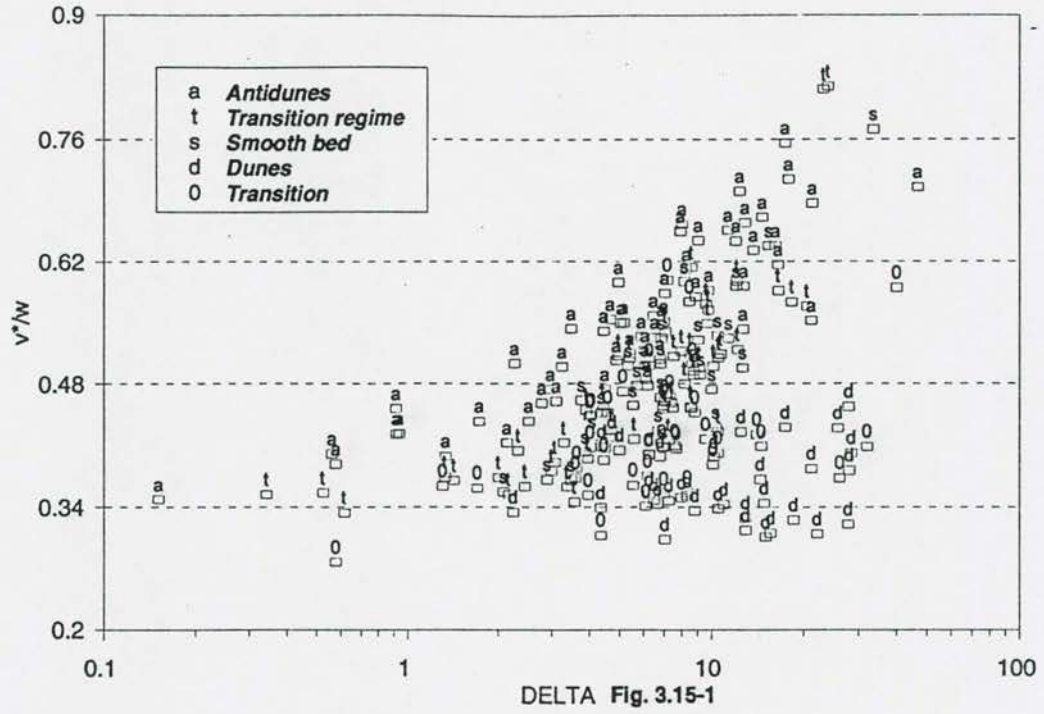

Figure 3.15 - 2 **Liu diagram calibrated on data of Gilbert (d = 0,38 mm)**

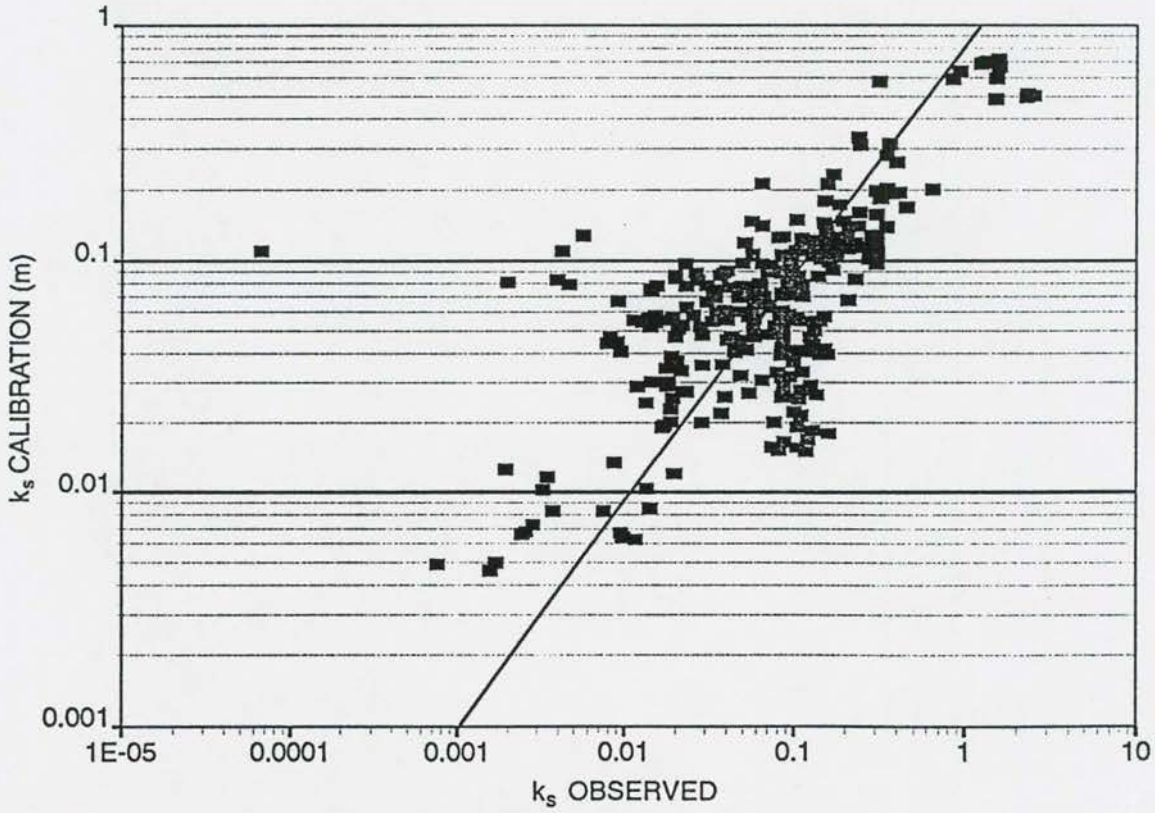

Figure 3.15 - 3 **Calibration of k_s predictor with flume data for F_r < 0,8**

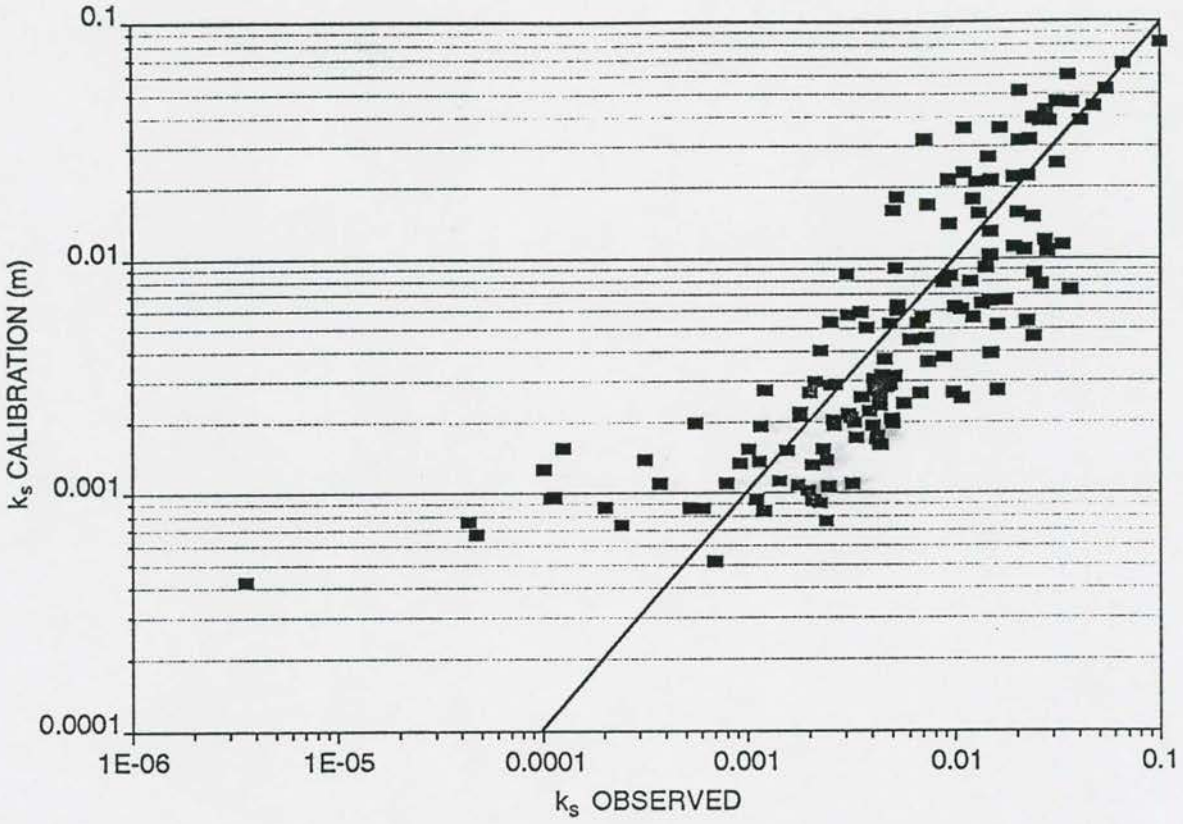

Figure 3.15 - 4 Calibration of k_s predictor with flume data for F_r > 1,0

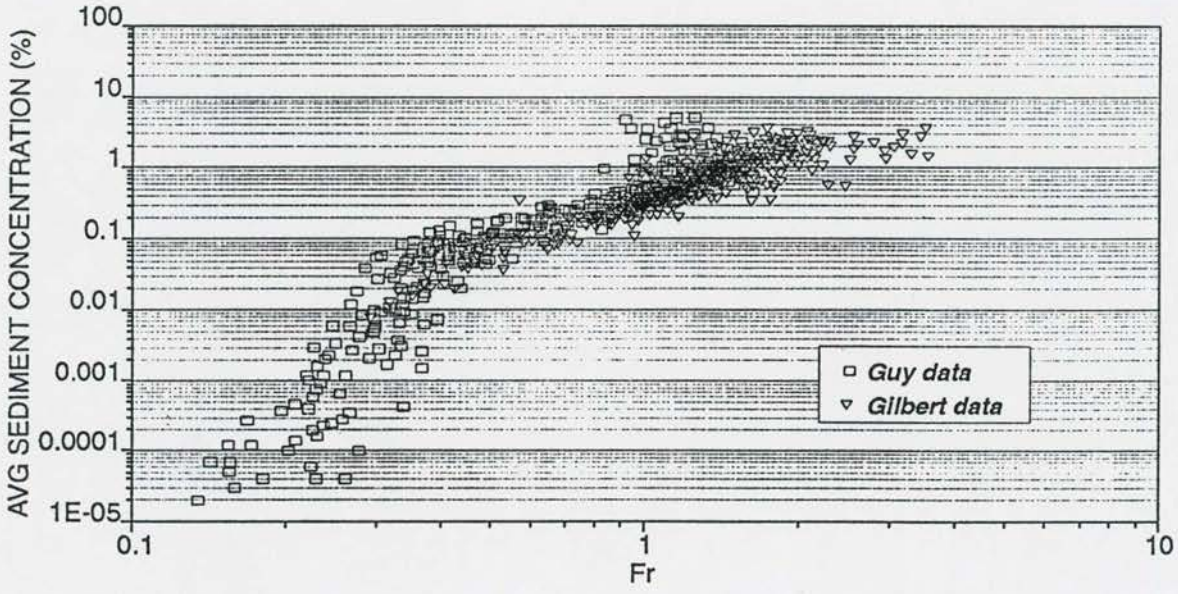

Figure 3.15 - 5 Relationship between sediment concentration $(\overline{C})$ and F_r

The new sediment transport **Equation 3.11-2** states:

$$\bar{C} \propto \left(\frac{\rho}{\rho_s - \rho}\right) \frac{(gsD)^{1,5}}{\kappa . k_s . w} \left(\frac{k_s}{30D}\right)^z . f\left(z; \frac{k_s}{30D}\right) \qquad (3.11\text{-}2)$$

but according to the sediment transport relationship based on input stream power *(Yang, 1973)*

$$\bar{C} \propto \frac{\rho g \bar{v} s}{(\rho_s - \rho) g w} \left(or \propto (\frac{\bar{v} s}{w})\right) . \qquad (3.15\text{-}3)$$

Equating **Equations 3.11-2** and **3.15-3** and simplifying yields:

$$k_s = f\left(\frac{(gDs)^{1,5}}{\kappa}; \frac{\sqrt{gD}}{\bar{v}}; w; \frac{1}{\kappa s}\right) \qquad (3.15\text{-}4)$$

with s = energy slope

As a first check on the validity of **Equation 3.15-4**, it was calibrated with laboratory data with known κ values **(Table 3.15-1)**.

Table 3.15-1: Calibration of bed roughness predictor

No	Data source	No of Observations	Correlation coefficient r^2
a	*Lin*	27	0,79
b	*Vanoni (1959)*	16	0,99
c	*Abdel-Aal*	10	0,97
d	*Einstein (1953)*	19	0,99
e	*Wang (1992)*	31	1,0
a - d	All, excluding Wang	75	0,74

Figure 3.15-6 shows the best fit curves in **Table 3.15-1** graphically. Combination of all the flume data does tend to show much larger scatter, which could probably be due to the limited data base size, or possible inconsistencies in measurement or κ calculations. The general trend is, however, consistent and k_s can be predicted in the lower, transitional and upper flow regimes. There seems to be a different trend in correlation when k_s approaches zero at incipient conditions, which can probably again be described by the effect of viscosity in the transition to laminar flow and its impact on settling velocity near the bed, as was found with the calibration of the new sediment transport equation.

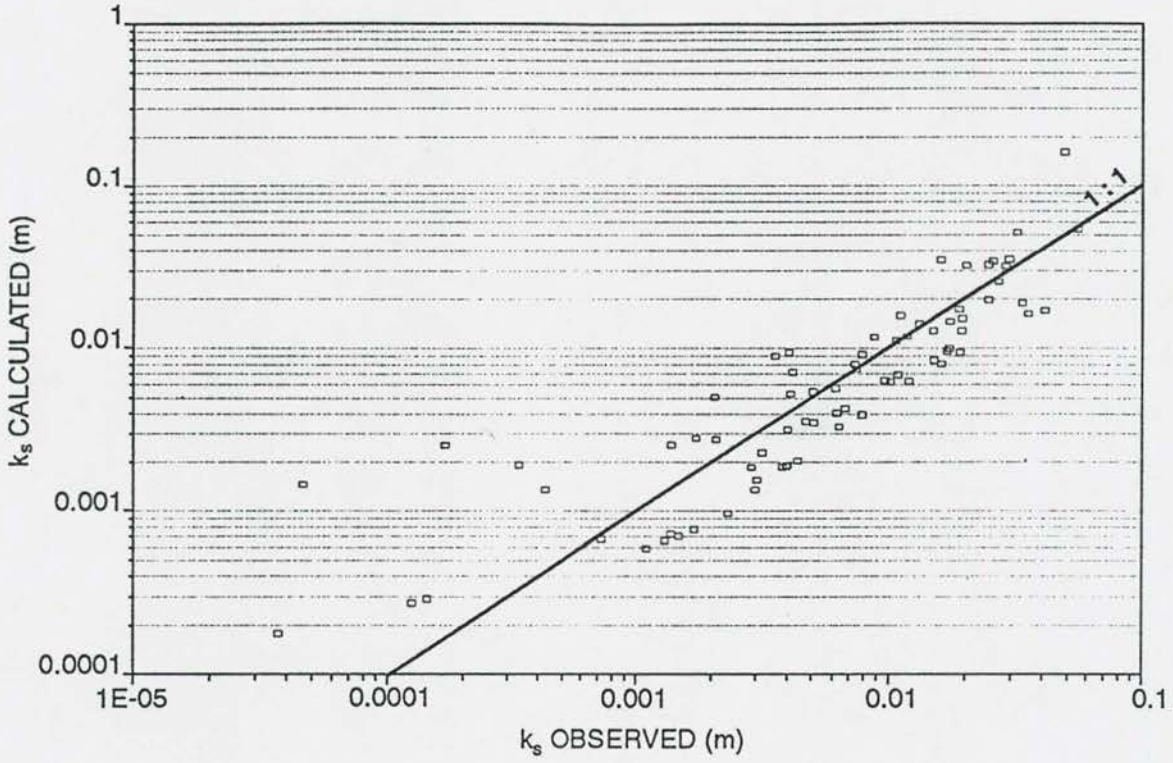

Figure 3.15 - 6 **Calibration of new k_s predictor with data with κ known**

To obtain a more comprehensive view of the prediction accuracy of the proposed new bed roughness predictor **(Equation 3.15-4)**, it also has to be calibrated on extensive, reliable laboratory data. Using the data of *Guy (1966)* and *Gilbert (1914)* with $\kappa = 0{,}4$ assumed in the calculation of k_s , a correlation coefficient (r^2) of 0,98 was found with the data of *Guy*, and $r^2 = 0{,}95$with the two sets of data combined. The best fit curves are shown graphically in **Figure 3.15-7**. Using the laboratory calibrated **Equation 3.15-4**, the k_s values for USA rivers are well predicted at high k_s values, while it is overestimated, as k_s approaches zero, as was also found with the laboratory data.

It should be remembered that an ideal correlation of the k_s relationship will be difficult to obtain because of the number of assumptions which had to be made. With the assumptions made in this section, the validity of the Froude number as additional parameter in the description of bed roughness has been proved.

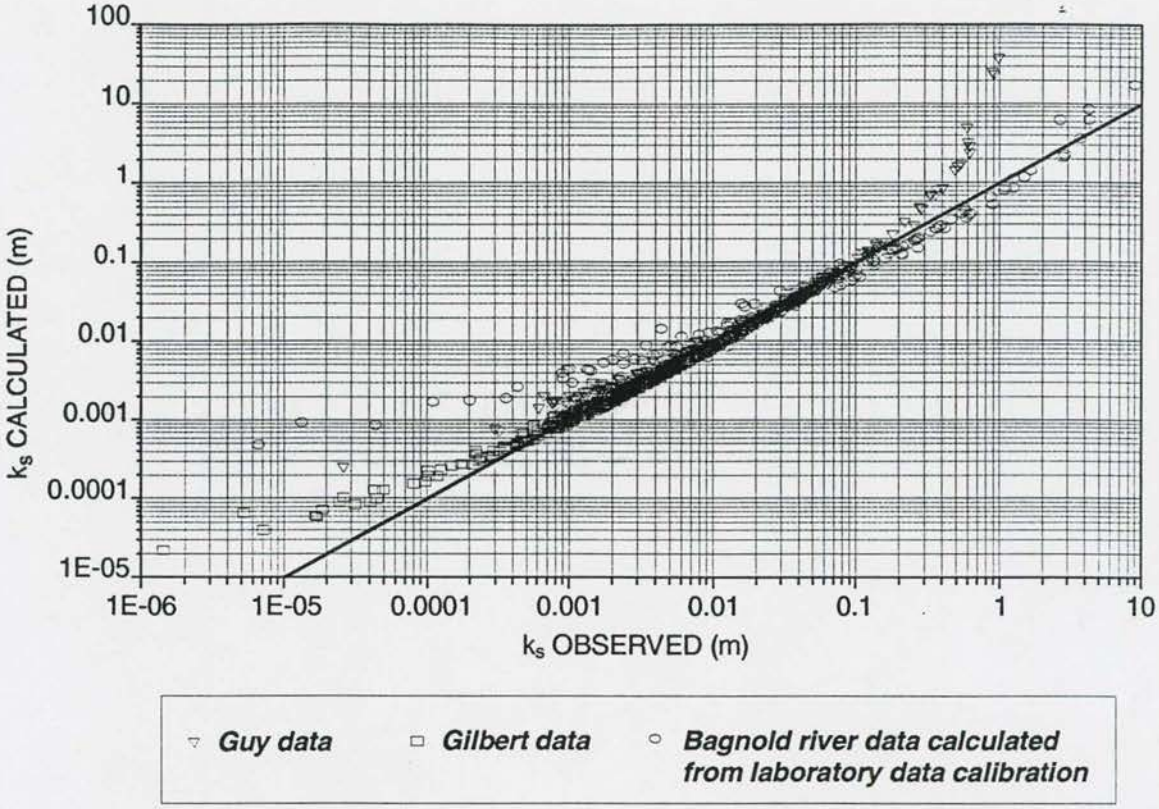

Figure 3.15 - 7 **Calibration of new k_s predictor with data with κ unknown**

Stream power theory can therefore be used to describe nature's mechanism for preventing excessive scouring of river beds and yet accommodating the necessary sediment transport. Throughout all the bed deformation processes under the equilibrium conditions, applied stream power is minimized. Bed deformation and sediment transport under equilibrium conditions can be described theoretically with this new approach and the relationships correlate well with both flume and field data.

3.16 Non-uniform sediment transport processes

Deposition and scouring processes in nature are always accompanied by changes in the size distribution of suspended load and bed material and are characterized as a self-adjustment process. *Han et al (1990)* illustrated this with a number of examples:

- In the Wotousi canal, China, it was found that for different size groups the changes in sediment concentrations are different. **Figure 3.16-1** shows that the average settling velocity changes from 1,089 mm/s to 0,0325 mm/s at the exit, decreasing by 32,5 times. The sediment-carrying capacity can be calculated with the Velikanov equation:

$$S^* = K\gamma_s\left(\frac{v^3}{gDw}\right)^m$$

$$= 0{,}927.10^{-4}\gamma_s\left(\frac{v^3}{gDw}\right)^{0{,}92} \text{ in this case} \quad . \qquad (3.16\text{-}1)$$

with S^* = sediment transport capacity
v = average velocity
D = mean depth of flow
γ_s = unit weight of sediment

From **Equation 3.16-1**, when the settling velocity decreases 32,5 times the sediment-carrying capacity will increase 25,3 times. In the case of Wotousi canal the sediment concentration was reduced by only 1,37 times, however.

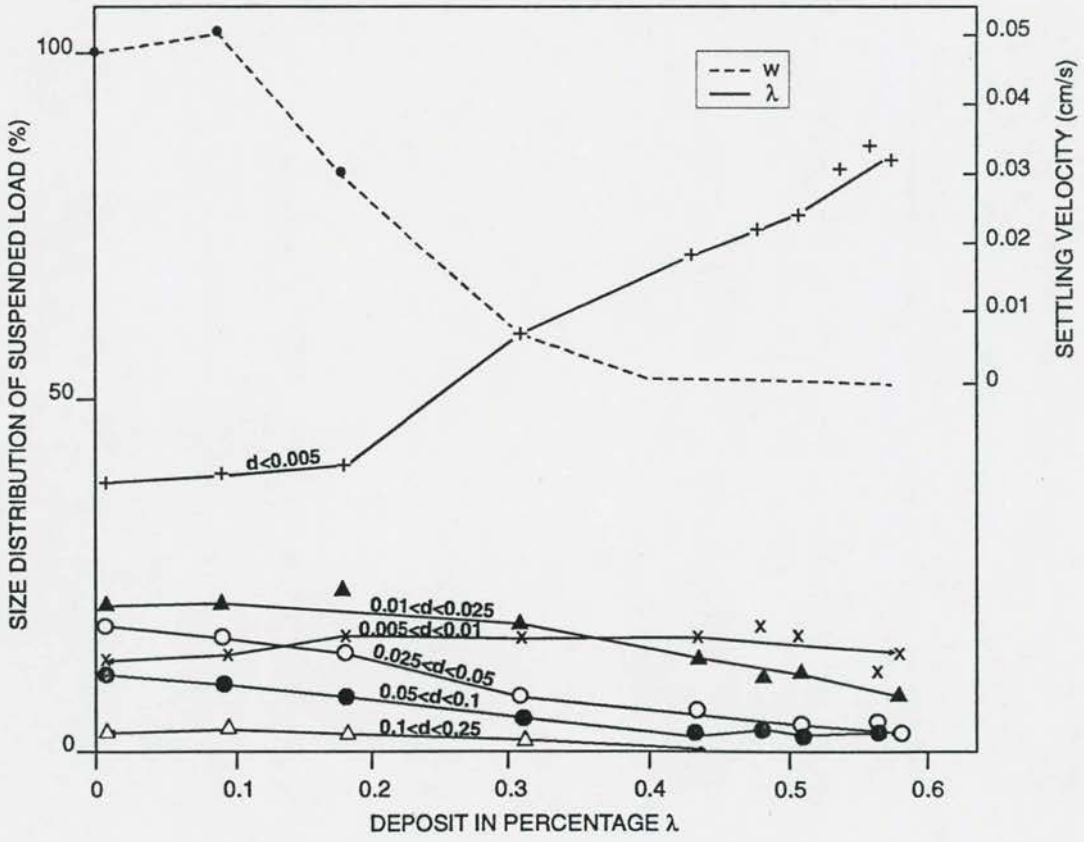

Figure 3.16 - 1 **Non uniform sediment transport in Wotousi canal, China**

- Scouring at the Sanshenggong Reservoir in China, indicated in **Figure 3.16-2**, showed that sediment concentrations of the coarsest size groups of suspended load which were picked up from the river bed increased faster than the other size groups. The average settling velocity increased and sediment-carrying capacity decreased.

  The change in size distribution of suspended load due to scouring or deposition will eventually be checked by the channel adjustment. Since coarse particles settle first in the deposition process, the suspended load gets finer, the fall velocity smaller and sediment-carrying capacity greater.

- During erosion and deposition the change in the size distribution of bed material takes place simultaneously. **Figure 3.16-2** shows coarsening of the bed sediment experienced of the Sanmenxia Reservoir, China.

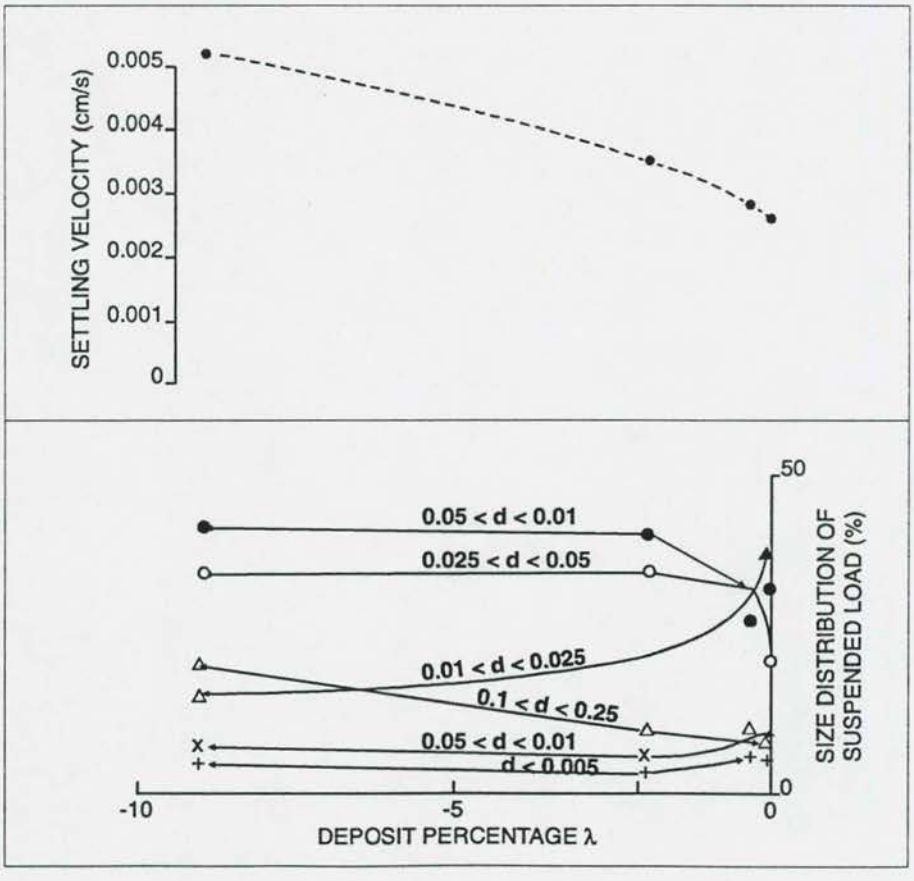

Figure 3.16 - 2 **Non-uniform sediment transport in Sanshenggong Reservoir, China**

Grading processes are observed in reservoirs due to the non-uniform characteristics of inflowing sediment grain size distribution. Three of the most important grading processes are:

- sorting when sedimentation occurs;
- hiding; and
- armouring, when erosion occurs.

These processes have been extensively researched and incorporated in models by using the hypothesis of superposition of transport rates for different grain-size fractions. The different settling velocities of the fractions (related to the grain sizes) result in a variation of the grain size distribution in transported and deposited sediments. Modelling of non-uniform sediments therefore may result in simultaneous erosion and deposition of fine and coarser sediment particles respectively.

- Sorting: Within a reservoir the coarser particles are deposited first along the upper reaches of the reservoir while finer particles are transported closer to the dam, so that the average grain size decreases towards the dam (sorting). The size distribution of bed sediment sampled in this study in some South African reservoirs is indicated in **Figure 3.16-3**.

- Hiding: Sheltering or hiding is due to the lesser mobility of coarser grains compared to finer surface grains.

- Armouring: When fine particles are eroded from the bed, only coarser sediment remains on the surface of the bed, creating a protective cover for underlying grains.

A number of river and reservoir models have been developed which incorporate modelling of non-uniform sediment:

Egiazaroff (1965) developed one of the first models for non-uniform sediment transport. The model included transport of each size fraction and the hiding of finer sizes below coarser ones.

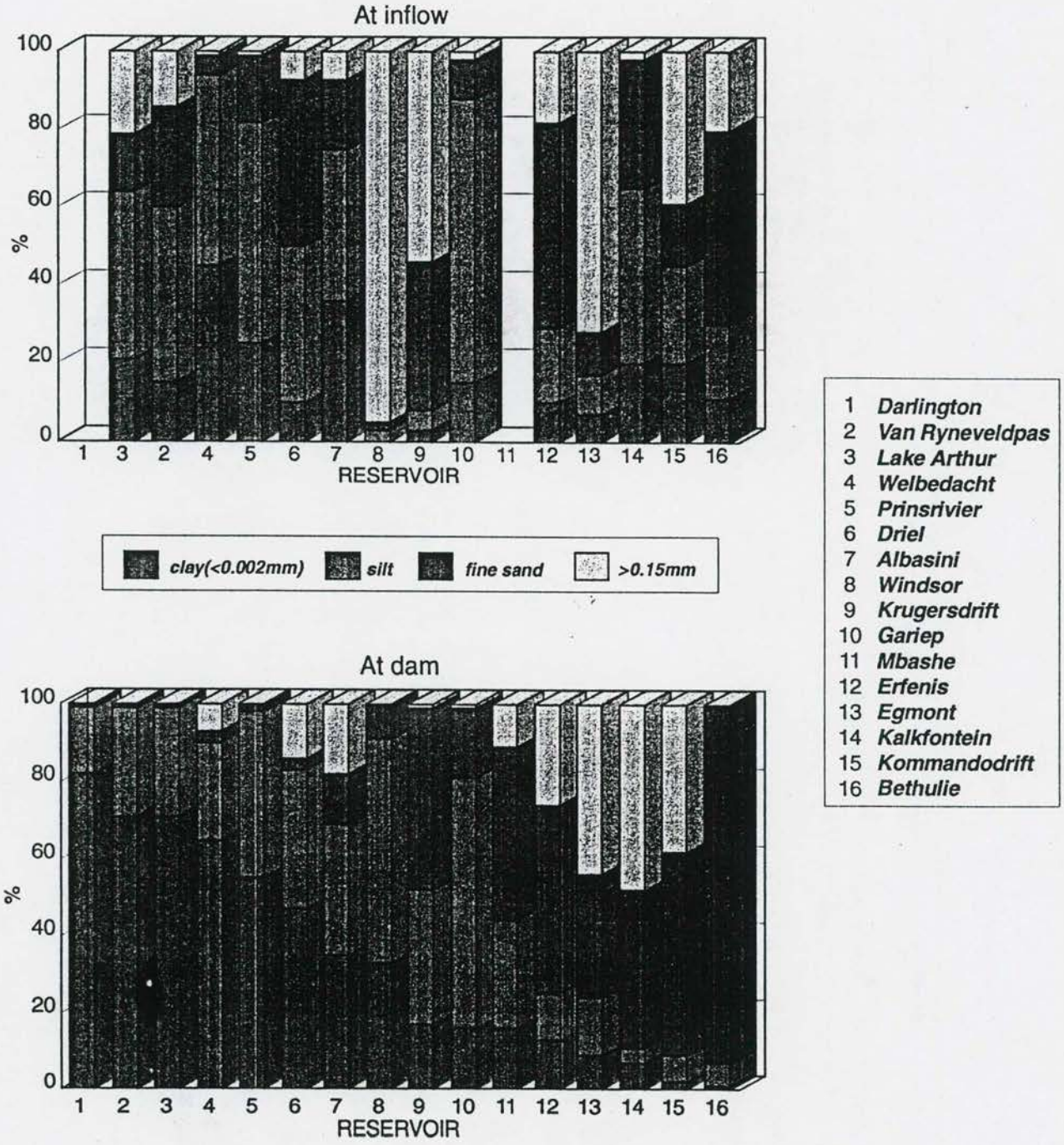

Figure 3.16 - 3 **Reservoir bed sediment size characteristics**

Gessler (1971) assumed that the probability of the shear stress distribution represents the probability of grains of diameters larger than the critical grain size just not being moved by the flow. A new grain-size distribution can be generated with this method but experimental verification is recommended *(Sloff, 1991)*.

Ribberink (1987) developed a 1D river model with non-uniform bed-load transport and a river bed consisting of a moving top-layer and a non-moving underlayer. The model was verified using laboratory data.

Little and Mayer (1976) proposed empirical methods and concentrated on the mean diameter of the armour coat.

Day (1980) and Proffitt and Sutherland (1983) adopted existing transport formulas to predict grain size distribution.

Diplas (1986, 1987) developed a bed-load relationship which allows for sediment grading effects.

Andrews and Parker (1987) developed a model for a mobile pavement assuming that all subsurface particles are of equal mobility, so that the size distribution of bed load is similar to that of the subsurface material.

He and Han (1986) concluded that bedload and washload transport are closely related and follow the same principles. Transport of non-uniform sediment is simulated in their model for reservoir sedimentation.

Belleudy and Rahuel (1987) and Holey and Rahuel (1990 a, b) developed a 1D model for non-uniform sediment transport.

James (1990) developed a river model which included particle geometry and packing and agrees well with laboratory and field data.

Parker and Sutherland (1990) describe two models for which computed armour processes agree well with data.

Wang and Zhang (1989) developed a model for non-uniform sand transport (bed load) which includes a modifying coefficient to reflect hiding and exposing effects.

Modelling of non-uniform sediment transport has been verified with laboratory and field data and is generally accepted as a modelling approach to simulate grading processes. Superposition of sediment transport for various particle sizes calibrated in flume tests for uniform sediment, may lead to inaccurate predictions when coarse and fine sediments are concerned. The fine sediment transport may change the Von Kármán coefficient to such an extent that equilibrium sediment transport of other fractions may be influenced, for example. In fact, it is believed that more flume studies should be conducted to fully understand non-uniform sediment transport where fine sediments are involved.

The new sediment transport equation as calibrated on reservoir data can be used to predict non-uniform sediment transport, but only within the calibrated particle size ranges. Reservoir sedimentation simulation based on the stream power equation (calibrated on reservoir data), has been carried out with uniform and non-uniform sediment particle size distributions (with the same boundary conditions), and results are indicated in **Figures 3.16-4** and **3.16-5**. (Details of the mathematical model flow and sediment transport algorithms are described **Chapter 7**). The differences in the sedimentation profiles as simulated in **Figures 3.16-4** and **3.16-5** emphasizes the importance of accurately predicting non-uniform sediment transport. Accurate prediction of sediment sizes is also important when considering sediment density, consolidation, critical conditions for mass erosion of cohesive sediments, non-cohesive or cohesive sediments etc.

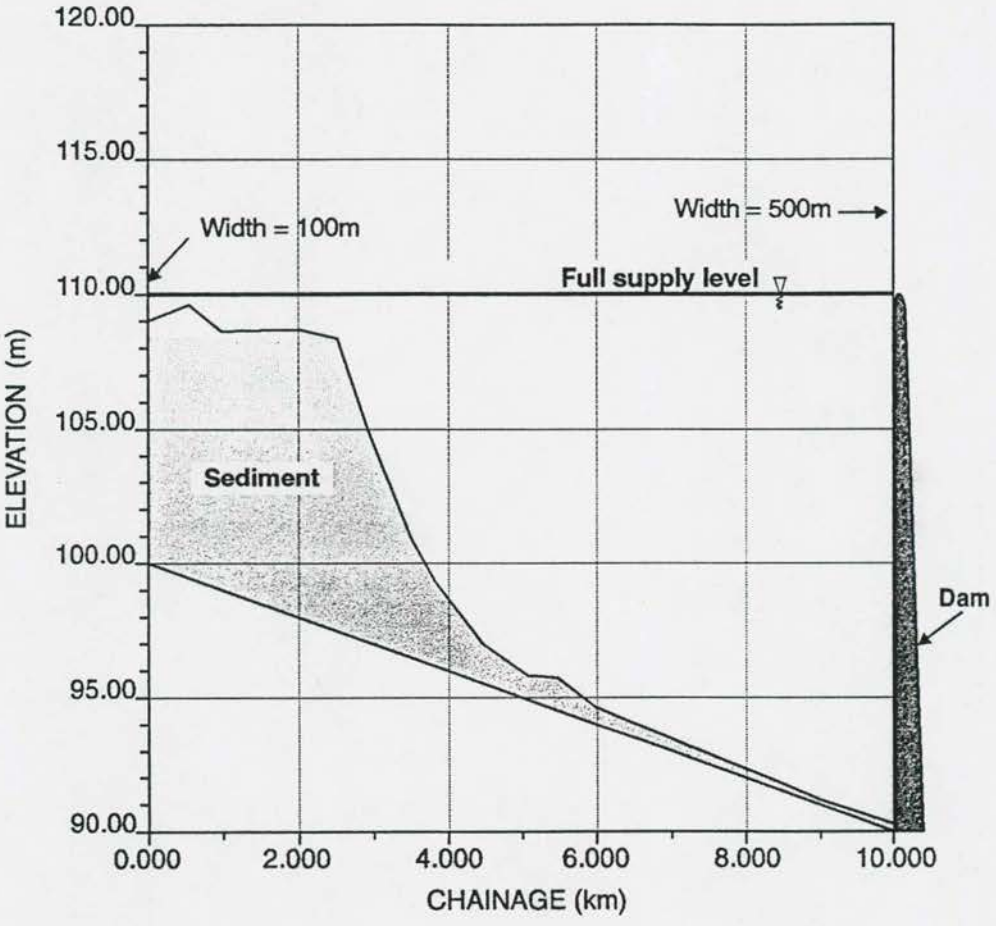

Figure 3.16 - 4 **Reservoir sedimentation with uniform sediment size**

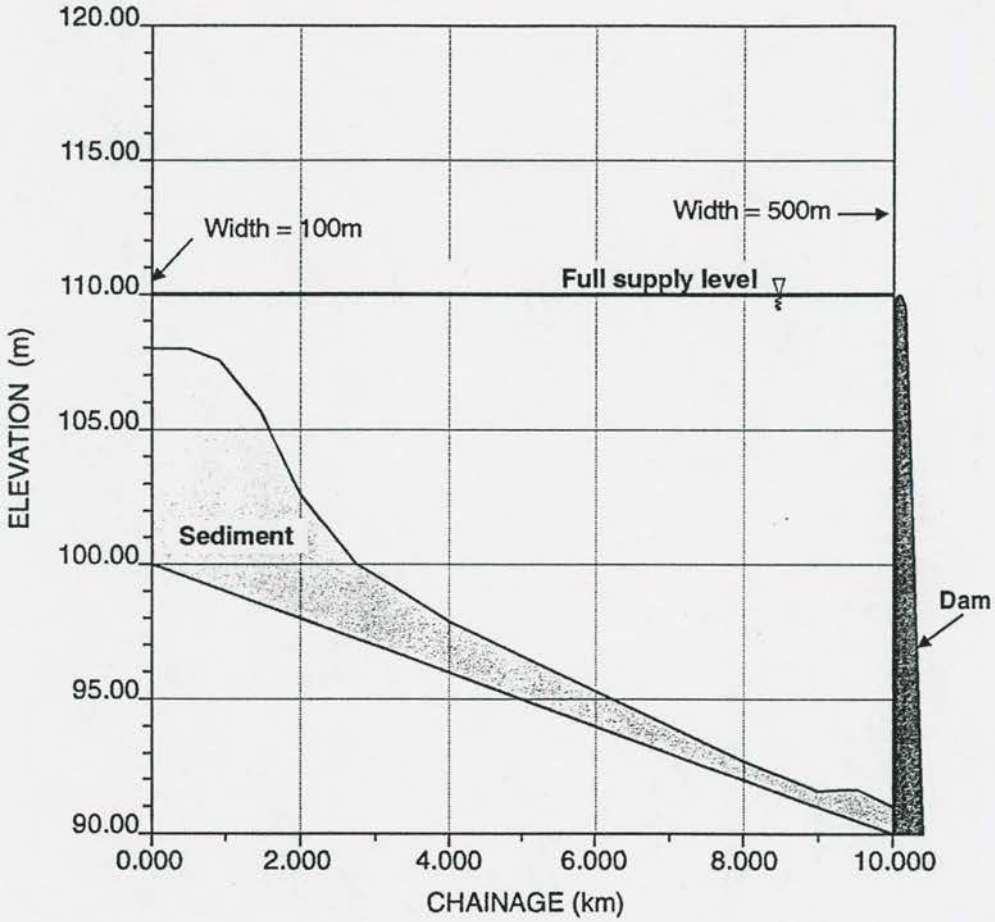

Figure 3.16 - 5 **Reservoir sedimentation with non-uniform sediment size**

3.17 Non-equilibrium sediment transport

3.17.1 Introduction

Most mathematical models are based on the assumption that the difference in the sediment transport capacities between successive cross-sections is deposited (or eroded) within that reach. A state of sediment equilibrium is therefore reached within each time step of the calculation. Equilibrium in this case refers to actual sediment transport being equal to the transport capacity at a section.

Instantaneous adaptation is a realistic assumption only when coarse sediments are transported and without any constraints on sediment availability. With fine sediments, however, the adjustment to the saturated sediment transport capacity is not instantaneous and time and distance lags are associated with the change in sediment transport, until equilibrium is reached. This lag, often called "adaptation length", is due to the small settling velocities of the fine sediments. In this adjustment process the bed roughness, the energy dissipation (Kappa) and the sediment transport changes until an equilibrium is reached, with minimized stream power.

Two types of non-equilibrium sediment transport can be identified:

- Undersaturated: sediment could be availability limited e.g. surface erosion, while mass erosion of the bed can lead to instantaneous adaptation from undersaturated to the sediment transport capacity. Some of the coarser fractions suspended during mass failure might be oversaturated and will deposit again. These processes which involves scouring will be discussed in more detail in **Chapter 6**.

- Oversaturated: Reservoir sediment deposition processes are often associated with conditions of oversaturation as the sediment transport capacity diminishes through the reservoir. With fine sediment and a deep reservoir,

adaptation lengths can be longer than the reservoir length. Different sediment particle sizes will have different adaptation characteristics.

Using a rotating annular channel-ring system, *Mehta et al (1973)* showed that suspended sediment concentration diminishes rapidly from an initial value, C_o to a constant value, C_{eq}, defined as "equilibrium concentration", although for the same flow condition various "equilibrium concentrations" were obtained as shown in **Figure 3.17-1**.

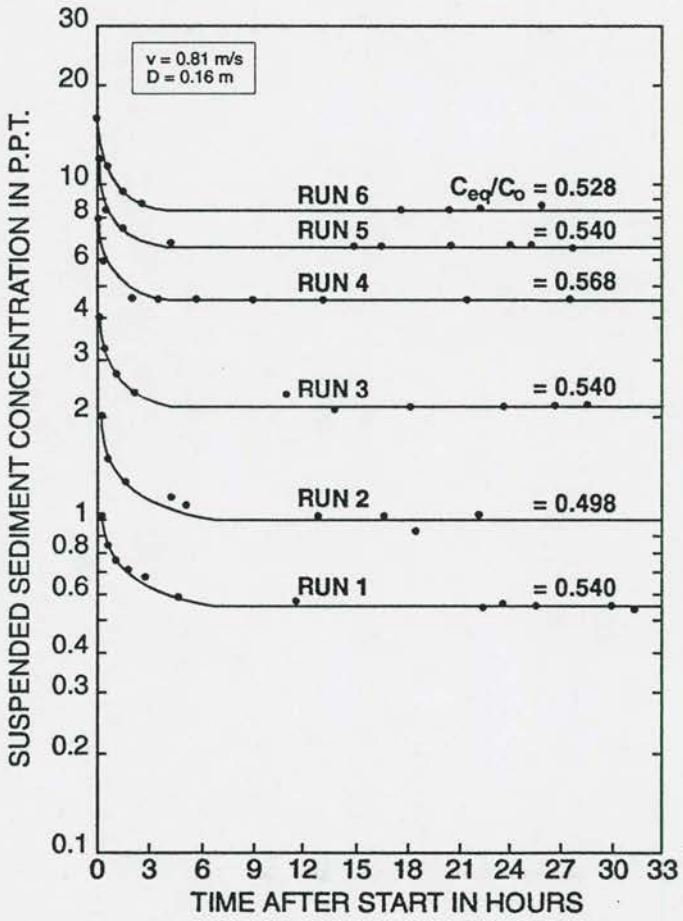

Figure 3.17-1 Variation of suspended sediment concentration with time ***(Partheniades, 1966)***

C_{eq} decreases with decreasing bed shear stress, τ_b , becoming zero for a threshold value, $\tau_{b\,min}$, of the latter. **Figure 3.17-1** shows that for a specific test, the relative equilibrium concentration, $C^*_{eq} = \frac{C_{eq}}{C_o}$, remains constant and independent of C_o *(Partheniades, 1986).* C^*_{eq} was found to depend on τ_b as shown in **Figure 3.17-2.**

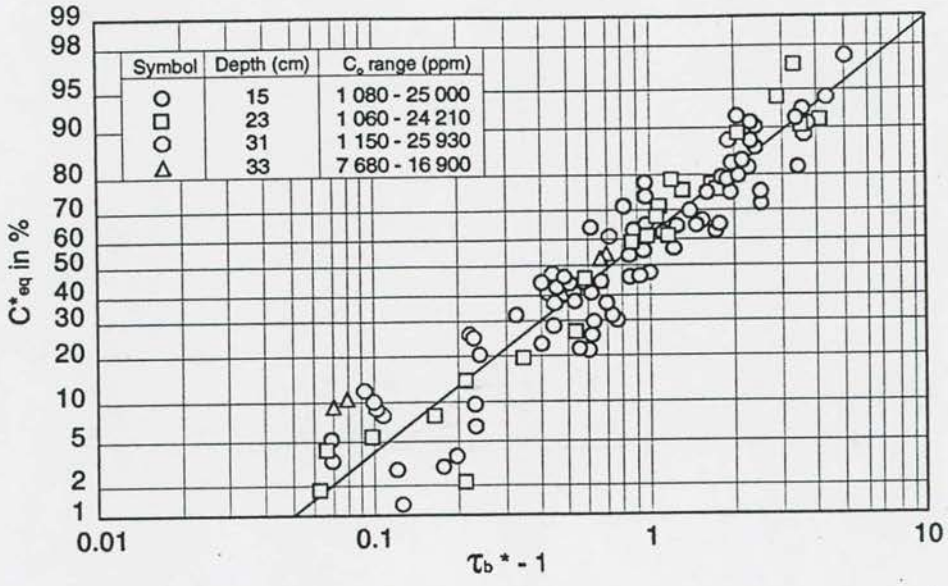

Figure 3.17-2 Relative equilibrium concentration versus bed shear stress parameter ***(Mehta, 1973)***

The time rate of deposition can be represented by $C_o - C_{eq}$, the depositable part of the sediment. The best fit was found with $C^* = (C_o - C) / (C_o - C_{eq})$ and t/t_{50} with t_{50} the time at which $C^* = 0{,}50$ on a log-normal scale. See **Figure 3.17-3**.

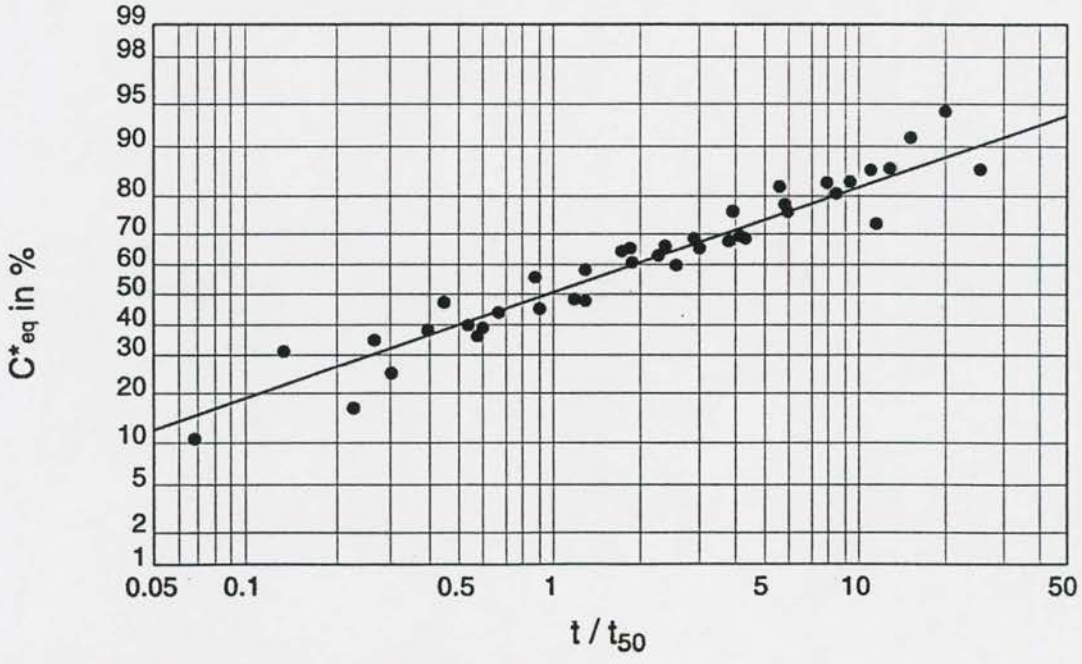

Figure 3.17-3 Deposition rates (Mehta, 1973)

Considering present knowledge of sediment transport, the adjustment to "equilibrium" sediment transport under the same flow conditions, and thereby reducing the suspended sediment as shown in **Figure 3.17-3**, must be attributed to the initial adjustment of the stream power to minimize energy dissipation. The adjustment is not immediate, due to the relatively slow settling velocities of the cohesive sediment. The "equilibrium" that is reached is not at equilibrium sediment transport (or maximum transport), but rather an equilibrium under conditions of limited sediment availability.

Mathematical descriptions of the non-equilibrium transport process have been given by *Galapatti et al (1986) and Di Silvio (1995)*, but the key variables involved in minimization of stream power were not included. Chinese researchers *(Han et al., 1990)*, have calibrated non-equilibrium equations with field data and have established criteria for non-equilibrium sediment transport calibration coefficients for rivers and reservoirs. Most of these equations have the format of the steady advection-dispersion equation.

3.17.2 Review of existing theory

The sediment transport component was until recently reduced to the selection of the "best" equilibrium transport formula among dozens of such equations in the literature. Sediment transport in real life, especially in reservoir storage operation, is often in non-equilibrium. Equilibrium formulae based on uniform flow experiments in hydraulic laboratories are no longer considered as a satisfactory component of a mobile-bed modelling system. Time and space lags between actual and equilibrium transported sediment load should therefore be considered *(Cunge, 1989)*.

The basic equation of 2D diffusion of sediment concentration can be written in the form *(Zhang, 1980)*:

$$v \frac{\delta C}{\delta x} = \epsilon \frac{\delta^2 C}{\delta z^2} + w \frac{\delta C}{\delta z} \qquad (3.17\text{-}1)$$

with
- $C\ (x, t)$ = sediment concentration
- ϵ = coefficient of turbulent exchange
- w = settling velocity of sediment particles
- v = flow velocity

An analytical solution of **Equation 3.17-1** is possible with the following boundary conditions for the case of deposition:

at the water surface : $z = D, \quad \epsilon \frac{\delta C}{\delta z} + wC = 0$

on the reservoir bed : $z = 0, \quad \frac{\delta C}{\delta z} = -\frac{w}{\epsilon} C_{K,0} = constant$

at entrance : $x = o, \quad C = C_o f(z)$

Zhang (1980) determined the analytical solution as:

$$C_{cp}(x) = C_{Kp} + (C_o - C_{kpo}) \sum_{n=1}^{\infty} \frac{2\alpha_n^2}{(\alpha_n^2/K_1 + K_1^2/4)(\alpha_n^2 + K_1^2/4 + K)} \qquad (3.17\text{-}2)$$

which, after differentiation and simplification, reads:

$$\frac{dC_{cp}(x)}{dx} = \alpha w[C_{Kp} - C_{Cp}(x)]/q \qquad (3.17\text{-}3)$$

By substituting initial conditions $x = 0, C_{cp}(x) = C_0$, the final expression of the rate of change in sediment concentration along the reservoir is given by:

$$q_s = q_{st} + e^{(-\alpha wx/q)} (q_{s0} - q_{st}) \qquad (3.17\text{-}4)$$

with q_s = sediment discharge per unit width at the exit
q_{st} = sediment carrying capacity
q_{so} = sediment inflow per unit width at the entrance

If $\zeta = e^{(-\alpha wx/q)}$ denotes sediment transport under non-equilibrium conditions ($0<\zeta<1$), when $x = 0, \zeta = 0, q_{so} = q_s$: no net deposition or scouring occurs and incoming sediment discharge equals outflowing discharge. When $x = \infty, \zeta = 0, q_{so} = q_{st}$ it means that outflowing sediment discharge equals the sediment-carrying capacity after self-adjustment along the river course.

Computation of sediment transport under equilibrium conditions is a special case of non-equilibrium conditions. Generally, the equilibrium can be re-established only after a long distance (for fine sediment) *(Zhang, 1980)*.

In the case of scouring, similar equations can be derived *(Zhang, 1980)*

The boundary conditions are:

$$Z = o,\ C_{ko} = Const.$$

$$Z = D,\ \epsilon\frac{\delta C}{\delta z} \pm wC = 0$$

$$x = o,\ C = Const.$$

and the final equation: $q_s = q_{st} - e^{(-\alpha wx/q)}\ (q_{so} - q_{st})$

In the case of deposition $\alpha_1 = 1 + K_{1/2} \approx 1$ (3.17-5)

and $\zeta_1 = e^{(-wx/q)}$

while with scouring

$$\alpha_2 = \pi^2/K_1 + K_{1/4}$$

$$\approx \pi/K_1$$

$$= Kv* \pi^2/6w$$

$$v* = \sqrt{ghs}$$

$$= K^{0,5}\ g^{0,5}\ Q^{0,3}\ s^{0,5}$$

Final expressions with the inclusion of empirical coefficients (K_3, K_4 *and* K_5) read:

Deposition : $\zeta_1 = \exp\ (-K_3\ C^{K4}\ (0{,}41\ -\ 0{,}77/gC)\ x/q)$ (3.17-6)

Erosion : $\zeta_2 = \exp\ (-K_5\ Q^{0,3}\ s^{0,5}\ x/q)$ (3.17-7)

Soares et al (1982) derived equations for non-equilibrium suspended sediment transport, similar to those of Zhang.

The mass balance of sediment of given size d_j is:

$$Q\left(\frac{\delta C^j}{\delta x}\right)\Delta x = (-q_d^j + q_e^j)T\Delta x \qquad (3.17\text{-}8)$$

with $q_d^j,\ q_e^j$ = fluxes of deposition and erosion of sediment

Q = flow rate

T = width

$\frac{\delta C}{\delta t}$ is neglected in this equation

Let CT^{*j} = average concentration of sediment transporting capacity, then:

if $C_i^j > CT_{i+1}^{j*}$ (deposition):

Rate of deposition : $q_d^j = -w_j\ (C^j\ -\ CT^{j*})$ (3.17-9)

and **Equation 3.17-8** becomes = $\frac{\delta C^j}{\delta x} = -w_j(C^j\ -\ CT^{j*})\ T/Q$ (3.17-10)

Integrating **Equation 3.17-10** between two sections:

$$C_{i+1}^j = (C_i^j\ -\ CT_{i+1}^*)\ \exp\ (-w_j\ \Delta x T/Q) \qquad (3.17\text{-}11)$$

if $C_i^j \le CT_{i+1}^{j*}$ (erosion will occur depending on the availability of sediment of the given size class at d_j on the stream bed)

Rate of erosion: $q_e^j = \lambda(C_b^j - C^j)$ (3.17-12)

Erosion is proportional to the difference between the availability on the bed and the concentration carried by the flow. Although erosion is dominant, deposition will still occur at rate $w_j C^j$ and **Equation 3.17-8** becomes:

$$\frac{\delta C^j}{\delta x} = -(C^j - \frac{\lambda_j}{\lambda_j + w_j} C_b^j) \frac{T}{Q} (\lambda_j + w_j) \quad (3.17\text{-}13)$$

Integration of **Equation 3.17-13** between sections i and $i + 1$ yields:

$$C_{i+1}^j = \left(C_i^j - \frac{\lambda j}{\lambda_j + w_j} C_b^j\right) \exp\left[-(\lambda_j + w_j) \frac{T\Delta x}{Q}\right] + \frac{\lambda_j}{\lambda_j + w_j} C_b^j \quad (3.17\text{-}14)$$

When Δx is large, flow in section $(i + 1)$ will approach its transport capacity CT_{i+1}^{j*} :

Therefore $CT_{i+1}^{j*} = \frac{\lambda_j}{\lambda_j + w_j} C_b^j$ (3.17-15)

and the final equation: $C_{i+1}^j = CT_{i+1}^{j*} + \left(C_i^j - CT_{i+1}^{j*}\right) \exp\left[-\frac{T\Delta x}{Q} (\lambda_j + w_j)\right]$ (3.17-16)

Equation 3.17-16 is similar to the equation presented by *Karanshev (1963)*:

$$C_{i+1}^j = CT_{i+1}^{j*} + \left(C_i^j - CT_{i+1}^{j*}\right) \exp\left[-\frac{T\Delta x}{Q} (1 + K_j) w_j\right] \quad (3.17\text{-}17)$$

and also similar to that of Zhang:

$$q_s = q_{st} - (q_{so} - q_{st}) \cdot \exp(-\alpha w x/q) \quad (3.17\text{-}5)$$

Sundborg (1967) developed another non-equilibrium equation which does not allow for erosion:

$$C_{i+1}^j = C_i^j \exp[-(T\Delta x/Q)\, w\phi\,(w)] \quad (3.17\text{-}18)$$

Equation 3.17-18 was used by *Hurst and Chao (1975)* in a model for the Tarbela Reservoir. The equation implies that if in section i the concentration of sediment of size d_j is zero, the same will be true for all downstream sections, which is clearly an error.

While the transport of coarse sediment depends exclusively on local hydrodynamic conditions, the transport of fine particles also depends on the conditions upstream. *Di Silvio (1995)* proposes the use of the following non-equilibrium transport equation:

$$\frac{\delta C_i}{\delta x} = \frac{1}{L_i^*} (\beta_i C_{ci}^* - C_i) \qquad (3.17\text{-}19)$$

with C_i the actual sediment transport per fraction,
β_i the % of i-th fraction in the bed composition,
L_i^* the adaption length for each fraction,
C_{ci} the transport capacity of the i-th class

The adaptation length L_i^* can be obtained either experimentally or by an asymptotic solution of the 2D suspended transport equations *(Di Silvio and Armanini, 1981; Galapatti, 1985, etc.)*. An evaluation of L^* is given by the following approximate formula:

$$\frac{L_i^* w_i}{\nu D} = \frac{k_s}{D} + (1-\frac{k_s}{D}) \exp\left(-1{,}5 \left(\frac{k_s}{D}\right)^{-1/6} \cdot \frac{w}{v_*}\right) \qquad (3.17\text{-}20)$$

For fine particles, $L_i^* \rightarrow$ particle falling distance $= \frac{\nu D}{w_i}$, which means that the adaptation length of silt and clay may be even larger than the reservoir length.

For coarse sediment, $L_i^* \rightarrow 0$, and C_i to $\beta_i C_{ci}^*$, and the erosion rate becomes $\frac{\delta \beta_i C_{ci}}{\delta x}$ as with equilibrium transport and instantaneous adaptation.

All the above non-equilibrium sediment transport equations have the same format and were derived for steady flow conditions.

3.17.3 Proposed non-equilibrium sediment transport methodology

Reservoir sedimentation processes are highly dynamic in reality and it has therefore been decided to describe the non-equilibrium sediment transport by using an unsteady advection-dispersion **Equation 3.17-21**.

$$\frac{\delta C}{\delta t} + u\,\frac{\delta C}{\delta x} - D\,\frac{\delta^2 C}{\delta x^2} = ss \qquad (3.17\text{-}21)$$

with D the dispersion coefficient,

u = flow velocity,
t = time,
x = distance in direction of flow

In case of non-cohesive sediments the source/sink term (ss) is represented by:

$$ss = \frac{(C^* - C)}{aT} \qquad (3.17\text{-}22)$$

with C* the equilibrium sediment transport calculated with a sediment transport formula,

"T" is the time scale defined as settling time (water depth divided by settling velocity),

"a" is a calibration parameter and can be interpreted as a mean (relative) settling depth. In the model implementation, the coefficient "a" is different for various given size fractions, for erosion and deposition.

The dispersion coefficient in **Equation 3.17-21** is not of importance in the non-equilibrium sediment transport prediction.

No attempt will be made here to formulate a mathematical description of the parameter "a" mainly because very little data are available to verify assumptions. Instead, the advection-dispersion equation was incorporated into a mathematical model (MIKE 11) and calibrated with data for non-equilibrium sediment transport conditions.

In order to calibrate the non-equilibrium sediment transport for different sediment size ranges, it is necessary to know the transport capacity of each size range. Although the available reservoir suspended sediment data involving fine sediments, have been used to calibrate an equilibrium stream power sediment transport equation during this research, weighted mean settling velocities have been used. There is therefore a need for more detailed flume studies on equilibrium fine sediment transport where near uniform particle sizes are used in each test, as has been done with coarser sediments (d_{50} > 0,03mm).

3.17.4 Non-equilibrium sediment transport tests

In order to calibrate and evaluate the proposed advection-dispersion methodology of modelling the non-equilibrium transport, a series of tests have been designed. Flow velocities typically found in main reservoir basins, where deposition processes dominate, of 0,1 to 0,2m/s were used. The aim was to monitor suspended sediment transport along a canal under conditions of upstream input sediment load overloading.

In order to evaluate the full sediment transport process from oversaturated to equilibrium sediment transport, a laboratory flume exceeding 100 metres in length had to be found, preferably with adjustable bed slope. No such flume could be found in South Africa, and in stead a concrete lined irrigation canal was selected. The trapezoidal canal has a top width of 2 m and approximate depth of 1 m. Flow depths of between 0,3 and 0,6 m were used with downstream control, while the inflows were regulated between 40ℓ/s and 90ℓ/s. The idea was to establish uniform flow conditions through the canal without downstream water level control for 0,3 m flow depths, while some damming was required to lower the flow velocities to 0,1 m/s, which led to slightly non-uniform flow conditions through the canal. Without a practical means of changing the bed slope, this was the only way of testing with near constant inflows. With smaller flow depths, it should be possible to decrease the adaptation length to say 50 m and carry out the tests in a laboratory flume under much more controlled conditions, but the flume boundaries might influence the sediment transport process to such an extent that it would be difficult to transfer the data and calibration for practical application.

Suspended sediment samples were taken at 10 m, 25 m, 50 m, 75 m, 100 m, 125 m, and 150 m intervals along the canal, measured from the upstream sediment input position. At each point samples were taken by pipet, at the centreline of the canal at regular intervals,

from small bridges across the canal. The pipet was used to obtain samples with least flow disturbance in order not to influence the sediment transport. Samples were obtained at various depths, and usually 2 to 3 depth samples per time point were obtained, depending on the flow depth.

Design of non-equilibrium sediment transport tests is quite difficult because of the dynamic processes involved. On the one hand the aim is to run the test as long as possible to allow bed regime equilibrium to establish, but with high sediment inputs, sediment deposition near the upstream end of the canal can be so dramatic with a long test duration, that sediment transport and bed conditions change quickly at a specific point in the canal. This does not necessarily have to be a problem if the unsteady non-equilibrium sediment transport is calibrated, but the bed slope change because of deposition adds an extra dimension which complicates the analysis. For the canal tests, therefore, test durations were kept as short as possible by limiting the sediment input duration until the sediment front has travelled 150m and the suspended sediment samples had been obtained at the most downstream point.

The tests were carried out during winter in one of the Loskop Dam irrigation scheme canals. Wind did not influence the tests. Each test was started with clear water steady flow conditions, without sediment deposits in the canal.

Two sediment types have been tested. Welbedacht Reservoir sediment deposits were excavated from opposite the Tienfontein pump station. The deposits did contain fine sediment particles, but more fine sediments is located closer to the dam. The Tienfontein deposits were, however, dry, making transport possible, while that closer to the dam were saturated and even when dried it still has to be powderized due to the high clay content.

A second sediment was obtained from a cyclone. The particle size characteristics of the sediments as obtained from pipet method, are indicated in **Table 3.17-1**.

The possible impact of the difference in water qualities between Welbedacht Reservoir and the Loskop canals (the latter has higher total dissolved solid concentrations) on sediment transport has been evaluated in terms of sediment settling velocities and negligible differences were found.

Table 3.17-1: Non-equilibrium tests sediment characteristics

Particle size range mm	Percentage of sediment in size range	
	Welbedacht	Cyclone
0,25-0,106	12,2	1
0,106-0,05	55,1	25
0,05-0,02	19,4	42
0,02-0,002	5,8	22
<0,002	7,2	10

Sediment feed was by hand, and has been calibrated with sediment concentrations to ensure the correct rate of sediment input. Sediment input concentrations varied between 1 000mg/ℓ to 100 000 mg/ℓ for different tests.

The non-equilibrium tests carried out are indicated in **Table 3.17-2**.

Table 3.17-2: Non-equilibrium sediment transport tests

Test no	Sediment type	Sediment input concentration (ppm)	Flow (ℓ/s)	Approximate flow velocity (m/s)
2	Cyclone	10 000	74	0,1
4	Cyclone	1 000	82	0,2
5	Welbedacht	1 000	82	0,2
7	Welbedacht	10 000	82	0,2
9	Cyclone	100 000	82	0,2
10	Welbedacht	100 000	67	0,2
13	Cyclone	30 000	46	0,1

3.17.5 Data analysis

The suspended sediment concentration data of each test as obtained 0,1m above the bed, 0,1m below the water surface, and at mid depth have been plotted against canal chainage as first indication of the data variability. These graphs are indicated in **Figures 3.17-4** to **3.17-10**.

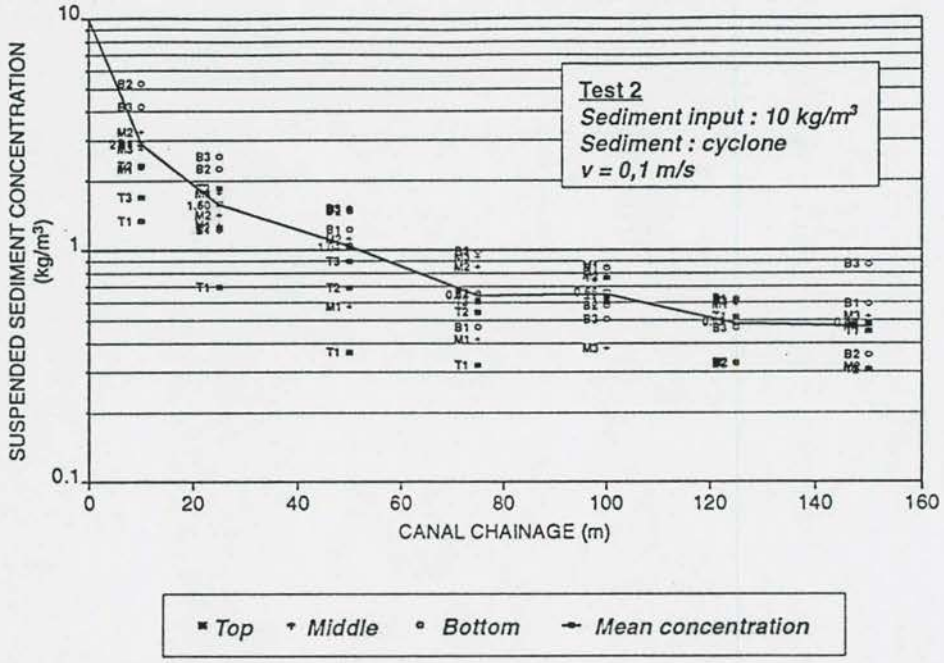

Figure 3.17-4: Non-equilibrium sediment transport test 2

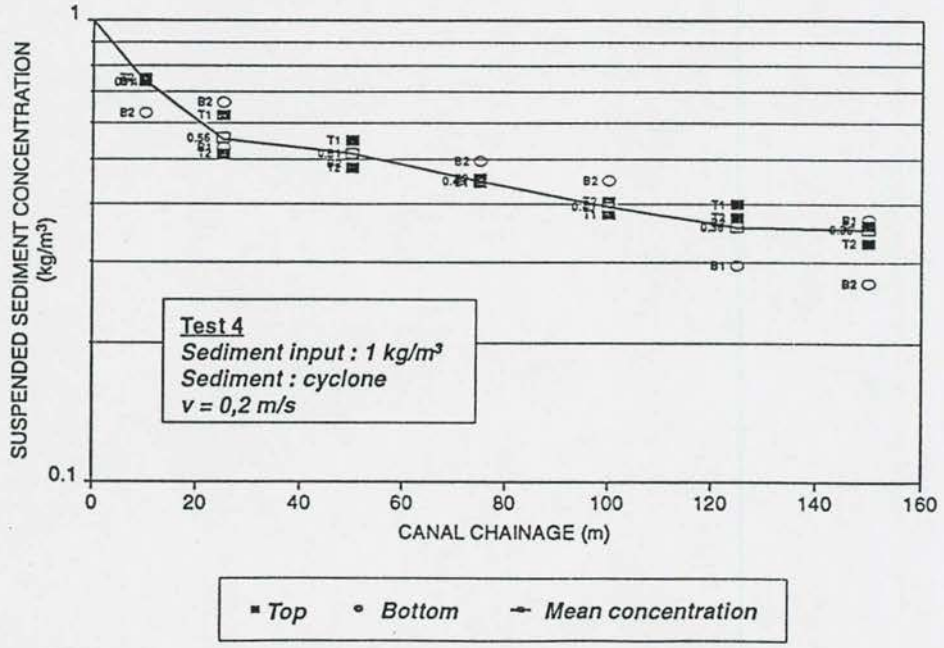

Figure 3.17-5: Non-equilibrium sediment transport test 4

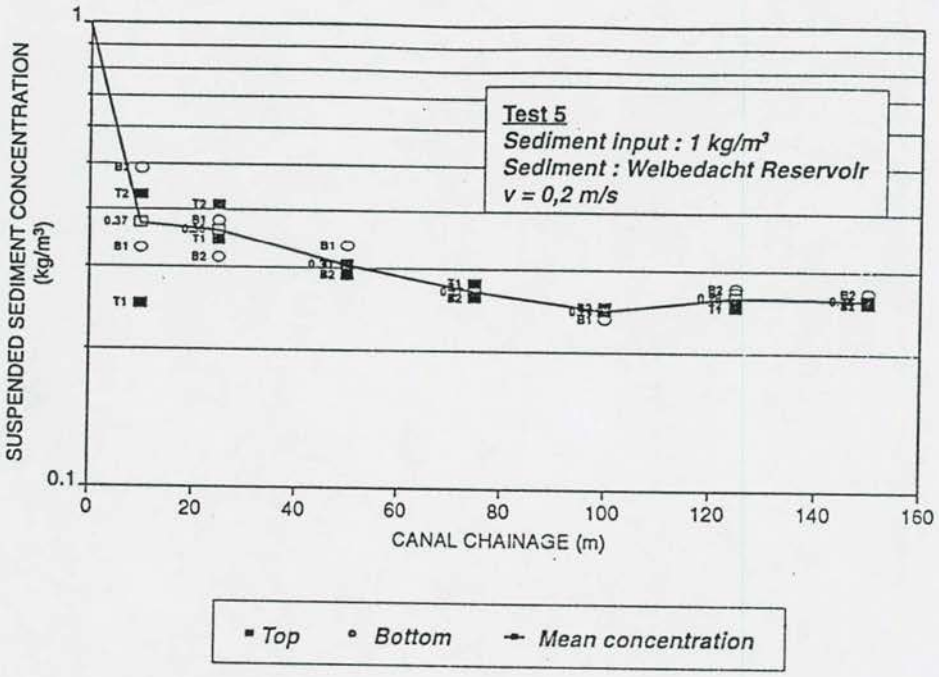

Figure 3.17-6: Non-equilibrium sediment transport test 5

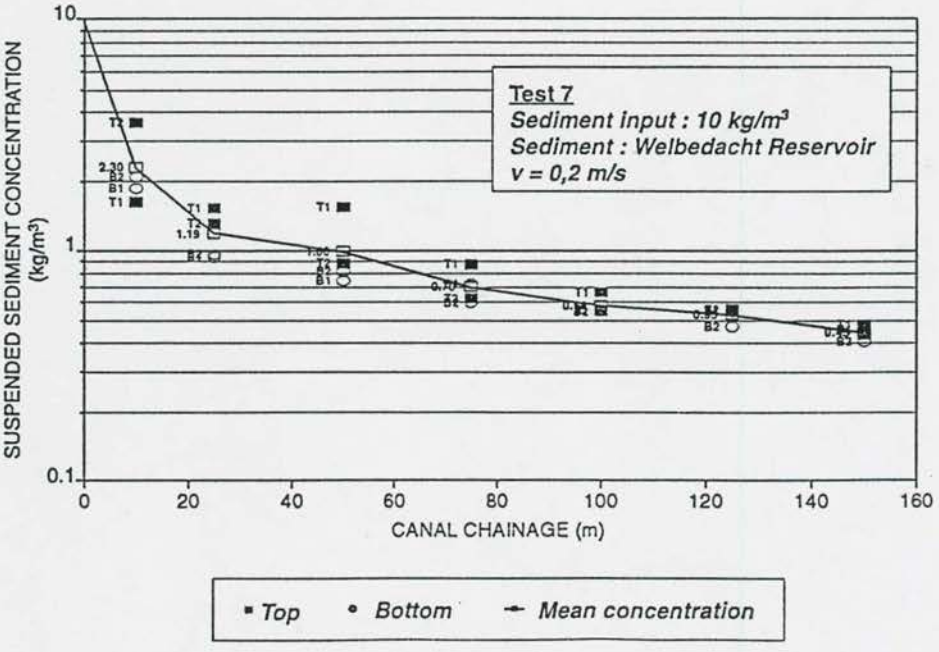

Figure 3.17-7: Non-equilibrium sediment transport test 7

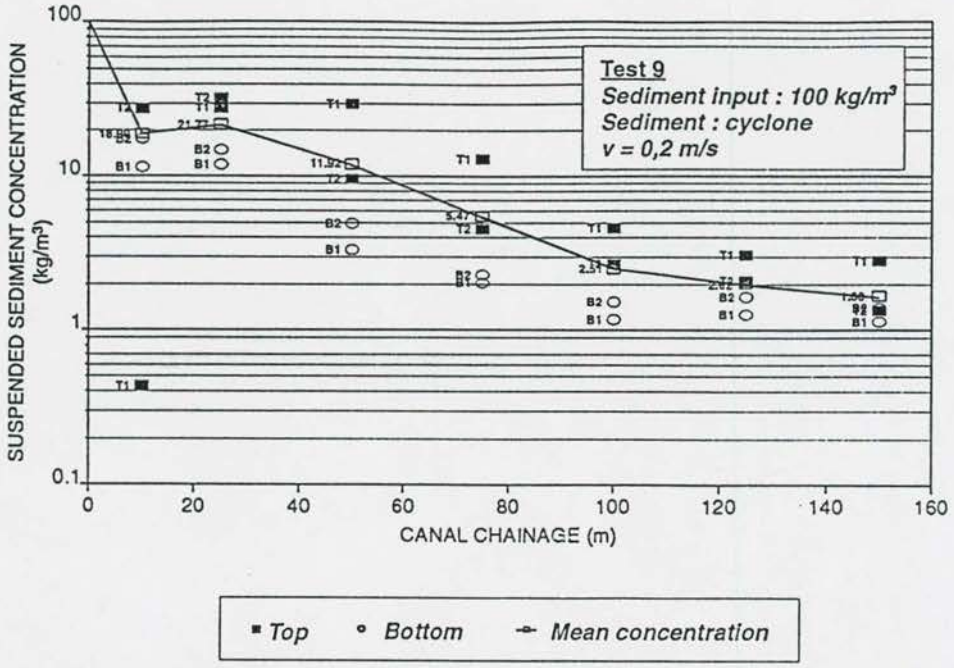

Figure 3.17-8: Non-equilibrium sediment transport test 9

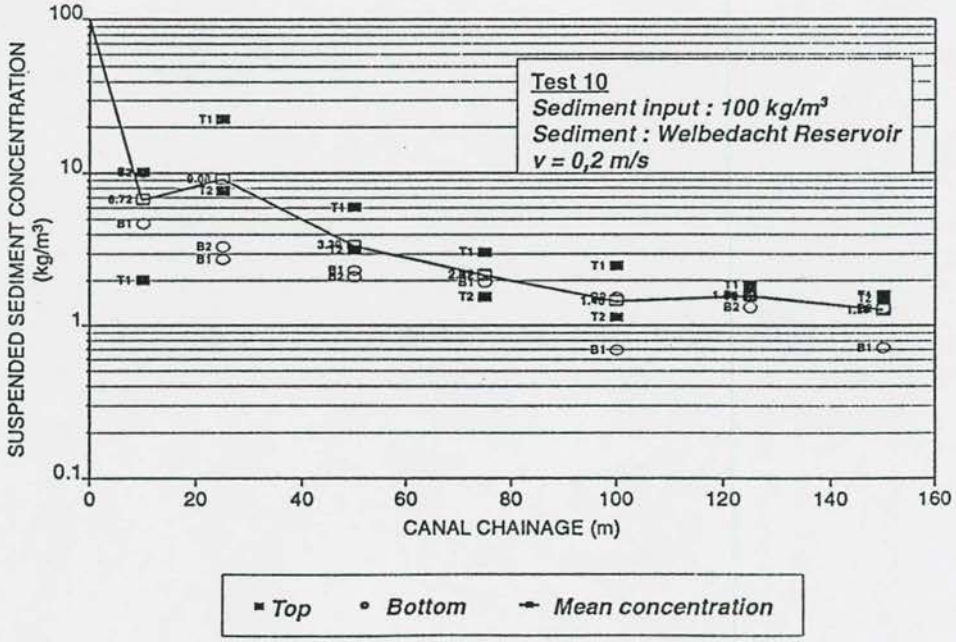

Figure 3.17-9 Non-equilibrium sediment transport test 10

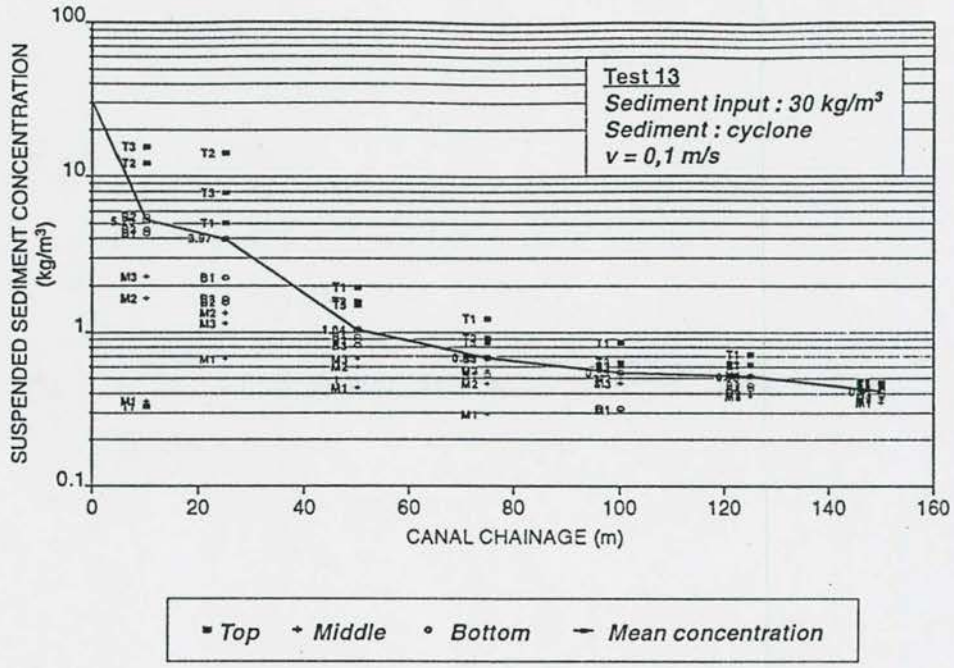

Figure 3.17-10 **Non-equilibrium sediment transport test 13**

From these figures it could be seen that:

- Similar adaption patterns are found for high and low sediment inputs.

- Low sediment inputs (1 000 ppm), which on average is below the sediment transport capacity of the canal, also illustrates the adaption, even after all of the coarse sediment have been deposited near the inflow end of the canal. This adaptation of fine sediments could be ascribed to sediment transport and bed adjustment as non-uniform transport occurs, as also found in the tests of *Mehta et al (1973)*.

- In many of the tests the suspended sediment concentrations varied little with depth, especially further downstream of the sediment feeding point. This was expected since the z-value in the suspension theory changes with fine sediment transport, resulting in near uniform vertical suspended sediment concentrations, also found in Gariep Reservoir in 1974 *(Rooseboom, 1975)*. At the 10m chainage, more scatter is found in suspended sediment data since the turbulent flow structure has not been re-established so close to the sediment feeding point.

3.17.6 Model calibration and evaluation

A one dimensional mathematical model with equilibrium modelling of one coarse sediment fraction and non-equilibrium modelling of 2 fine fractions has been calibrated with the canal data. (A comprehensive description of the model is given in **Chapter 7**).

The adaptation coefficient ("a") was calibrated for each test. The equilibrium sediment transport equation calibrated on South African Reservoir data was used in the calibration.

Although it should only be the clay and silt fractions which do not adjust instantaneously to the equilibrium sediment transport, clay as fraction could not be calibrated since the equilibrium sediment transport equation used the weighted settling velocities which include coarse fractions. Clay and silt fractions particle size range therefore had to be adjusted in the calibration to include coarser sediments, ensuring accurate calculation of sediment transport. The selected particle fraction size ranges as obtained from suspended sediment concentration data are indicated in **Table 3.17-3**.

Table 3.17-3: Non-equilibrium sediment transport fraction ranges

Fraction no	Transport type	Particle size range (mm)	Percentage in size range	
			Welbedacht	Cyclone
3	Equilibrium	0,106-0,25	12	1
2	Non-equilibrium	0,05-0,106	55	25
1	Non-equilibrium	<0,05	33	74

Average suspended sediment concentrations have been used for calibration at each sampling point.

The calibrated a-values for fraction 1 are given in **Table 3.17.4**. Fraction 2 adaptation was kept constant at "a"=2, since it was found insensitive to other values.

Table 3.17-4: Calibration of non-equilibrium sediment transport

Test no	Sediment type	Sediment input concentration (ppm)	Flow (ℓ/s)	Approximate flow velocity (m/s)	Calibrated "a" (fraction 1)
2	Cyclone	10 000	74	0,1	2,0
4	Cyclone	1 000	82	0,2	2,5
5	Welbedacht	1 000	82	0,2	2,8
7	Welbedacht	10 000	82	0,2	2,8
9	Cyclone	100 000	82	0,2	1,5
10	Welbedacht	100 000	67	0,2	2,0
13	Cyclone	30 000	46	0,1	1,8

The calibrated suspended sediment concentration profiles are indicated in **Figure 3.17-11** to **3.17-17**.

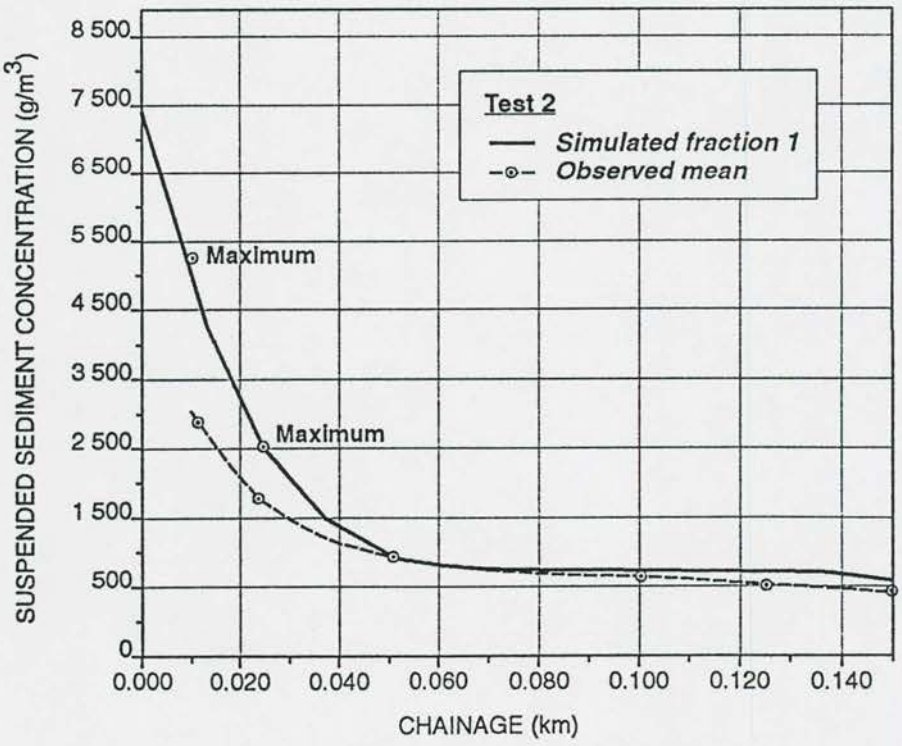

Figure 3.17-11: Non-equilibrium sediment transport calibration: test 2

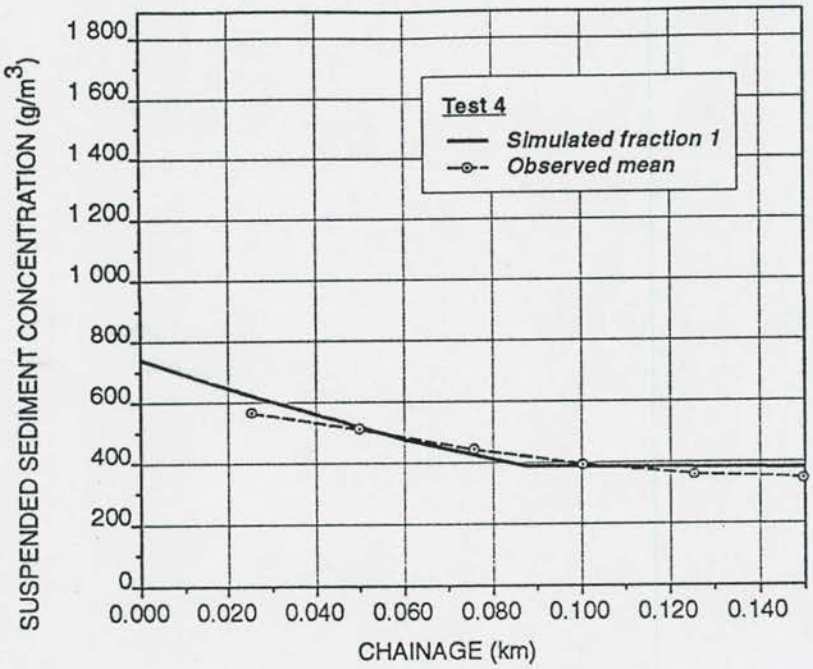

Figure 3.17-12: **Non equilibrium sediment transport calibration: test 4**

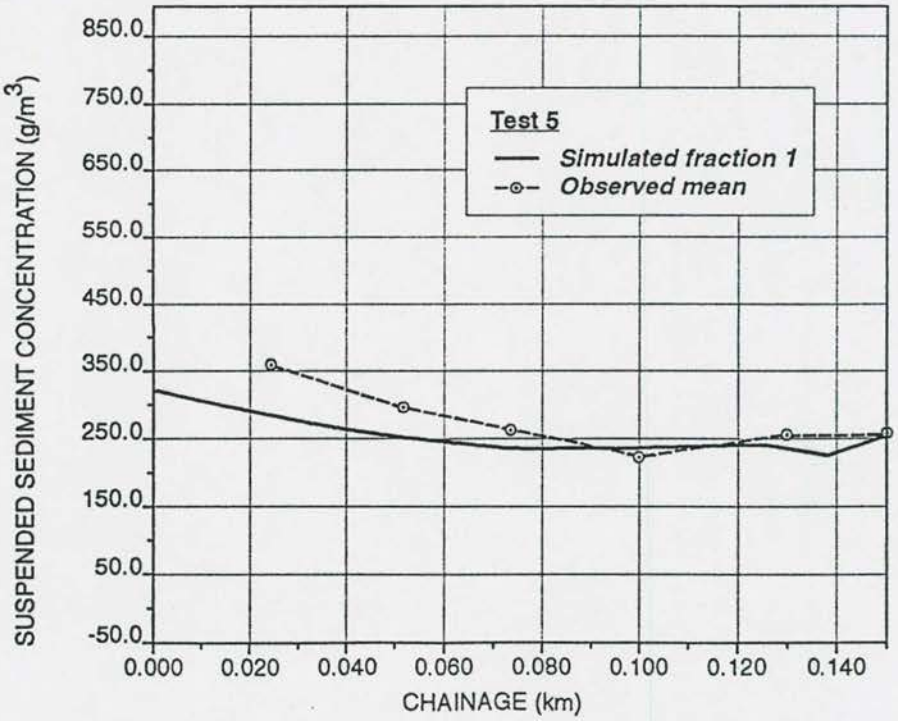

Figure 3.17-13: **Non-equilibrium sediment transport calibration: test 5**

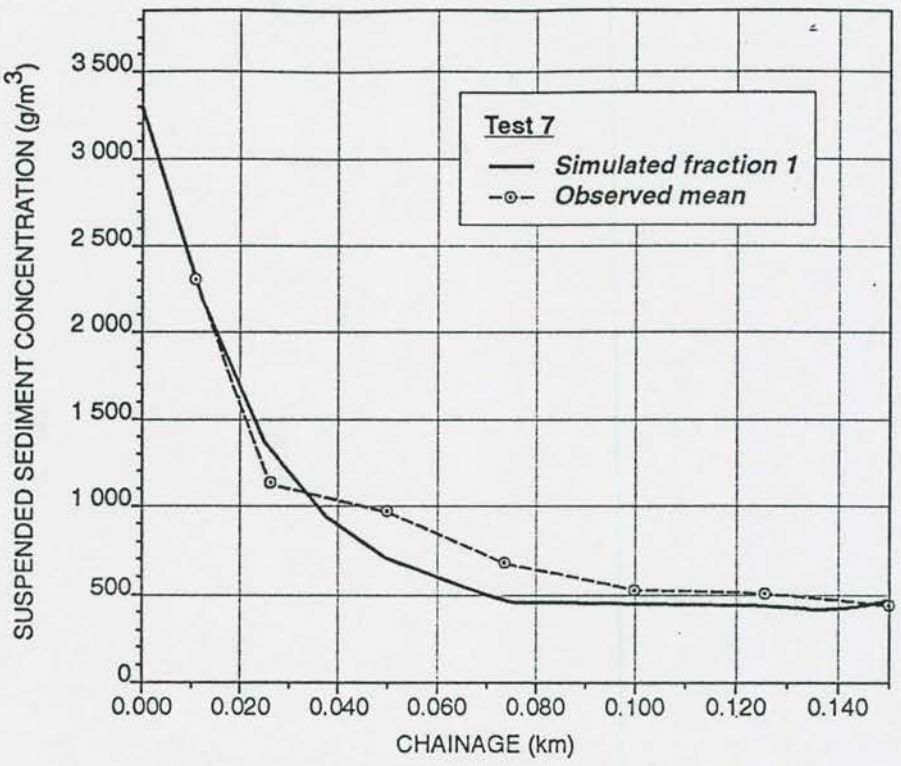

Figure 3.17-14: **Non-equilibrium sediment transport calibration: test 7**

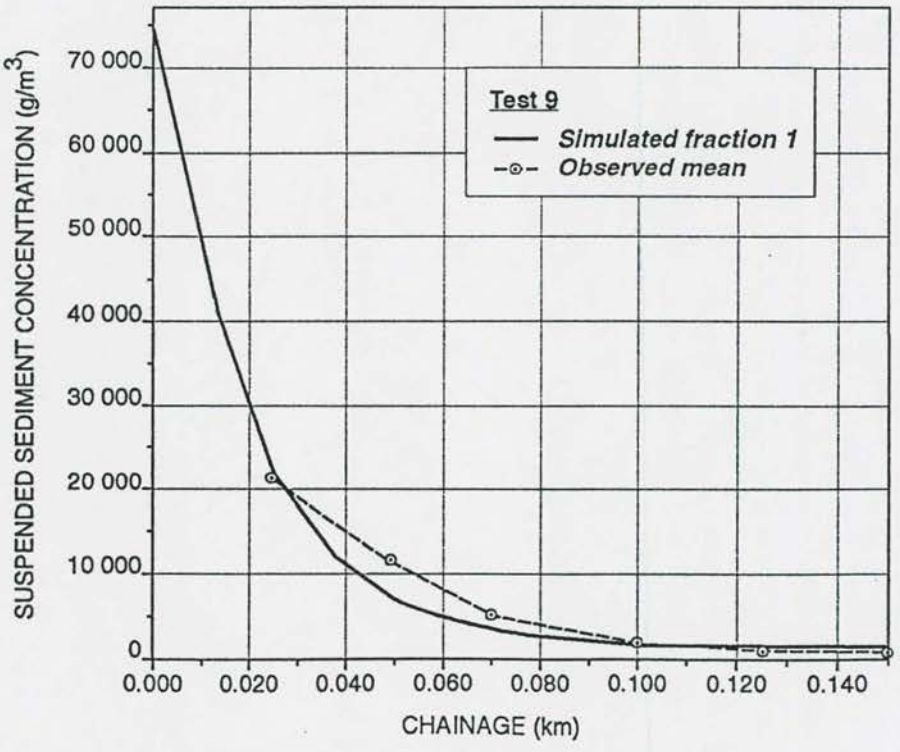

Figure 3.17-15: **Non-equilibrium sediment transport calibration: test 9**

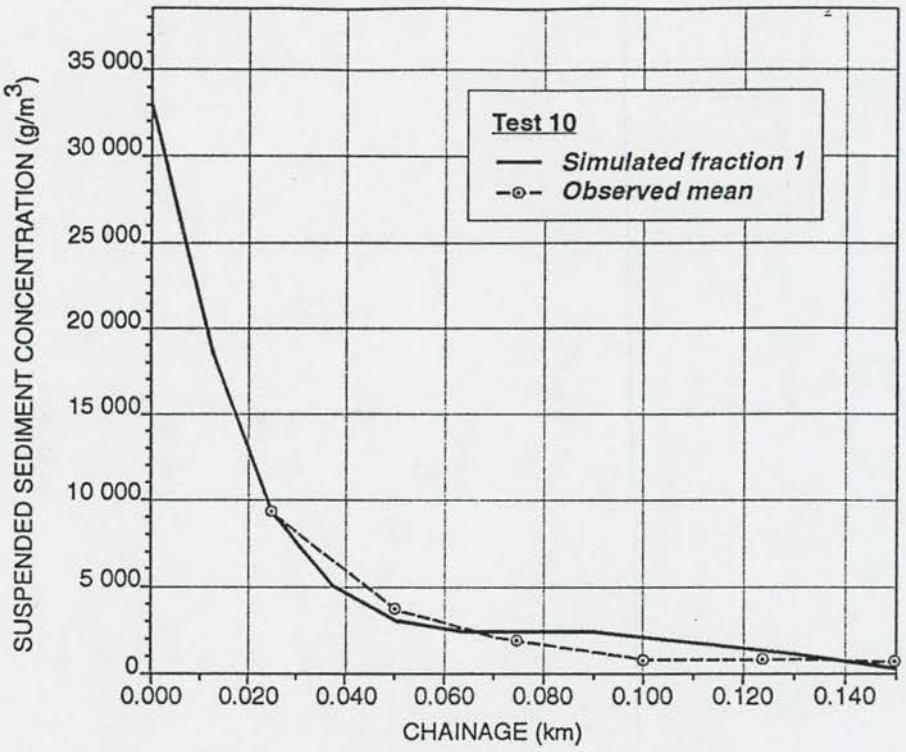

Figure 3.17-16: **Non-equilibrium sediment transport calibration: test 10**

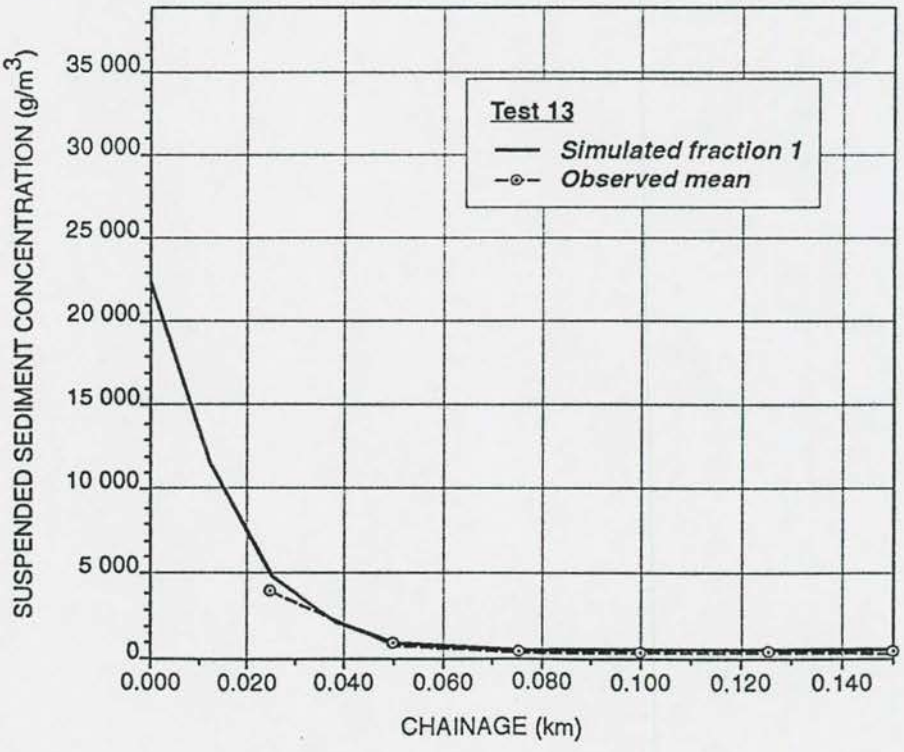

Figure 3.17-17: **Non-equilibrium sediment transport calibration: test 13**

Results from the calibrations are:

- The Welbedacht calibrated "a"-values ranged between 2,0 to 2,8, while that of the cyclone sediments ranged between 1,5 and 2,5. This is expected since the cyclone sediments are finer than the Welbedacht sediment used in the tests.

- All the calibrated tests show good agreement with the observed longitudinal suspended sediment profiles.

- The highest sediment concentrations (input), tests 9, 10 and 13, had the lowest a-values for each sediment type. This could be because of more coarse sediment transport due to the reduction of the Von Kàrman coefficient at high sediment concentrations. The coarser sediments adapt quicker to equilibrium sediment transport. The whole process is very dynamic and complex. The change in the energy dissipation along the canal as the suspended sediment concentrations reduce, will also mean that equilibrium sediment transport through the canal will vary from upstream to downstream.

- In many of the tests carried out, equilibrium sediment transport are not reached within the 150 m canal length.

- The calibrated a-values fall into relatively narrow ranges, and have been tested for extreme conditions of oversaturation, variable flows, velocities and flow depths.

3.17.7 Modelling of non-equilibrium sediment transport processes : Welbedacht Reservoir

In the previous section, oversaturated sediment transport tests carried out in a canal, under steady, uniform flow conditions, have been analysed.

In reservoirs, inflows, water levels and inflow sediment concentrations are highly variable and unsteady, non-uniform flow conditions prevail especially during floods when high sediment loads are transported into a reservoir. Testing of the proposed non-equilibrium sediment transport approach has been carried out for Welbedacht Reservoir for the period 1973 to 1976. The modelling started in August 1973 when the first fill of the reservoir commenced.

Observed instantaneous inflows and sediment concentrations, and water levels at the dam have been used as boundary conditions. The simulations continued to October 1976 when the first basin survey was carried out. During this three year period major floods occurred in the Orange River system and 36 million m^3 storage capacity was lost in Welbedacht Reservoir due to sedimentation.

Using a typical suspended sediment particle distribution as has been observed at the reservoir inflow, one equilibrium and 2 non-equilibrium fractions have been modelled as indicated in **Table 3.17-5**.

Table 3.17-5: Suspended sediment size distribution of Welbedacht Reservoir inflow

Fraction no	Particle size range (mm)	Percentage in size range
3	0,106 - 0,25	5
2	0,05 - 0,106	19
1	< 0,05	76

The simulated sedimentation profiles for Welbedacht Reservoir are indicated in **Figure 3.17-18**.

The simulated and observed sedimentation profiles as indicated in **Figure 3.17-18** show that an adaptation coefficient for the fine sediment of "a" $\geq$ 2,8 gives a reliable sedimentation profile prediction. There are, however, many uncertainties involved such as:

- unknown sediment density
- cross-sectional deformation, assumed here proportional to flow depth for erosion and deposition
- changing suspended sediment size distributions of inflows during low and high flows
- sediment cohesion and consolidation, limiting re-entrainment during floods.

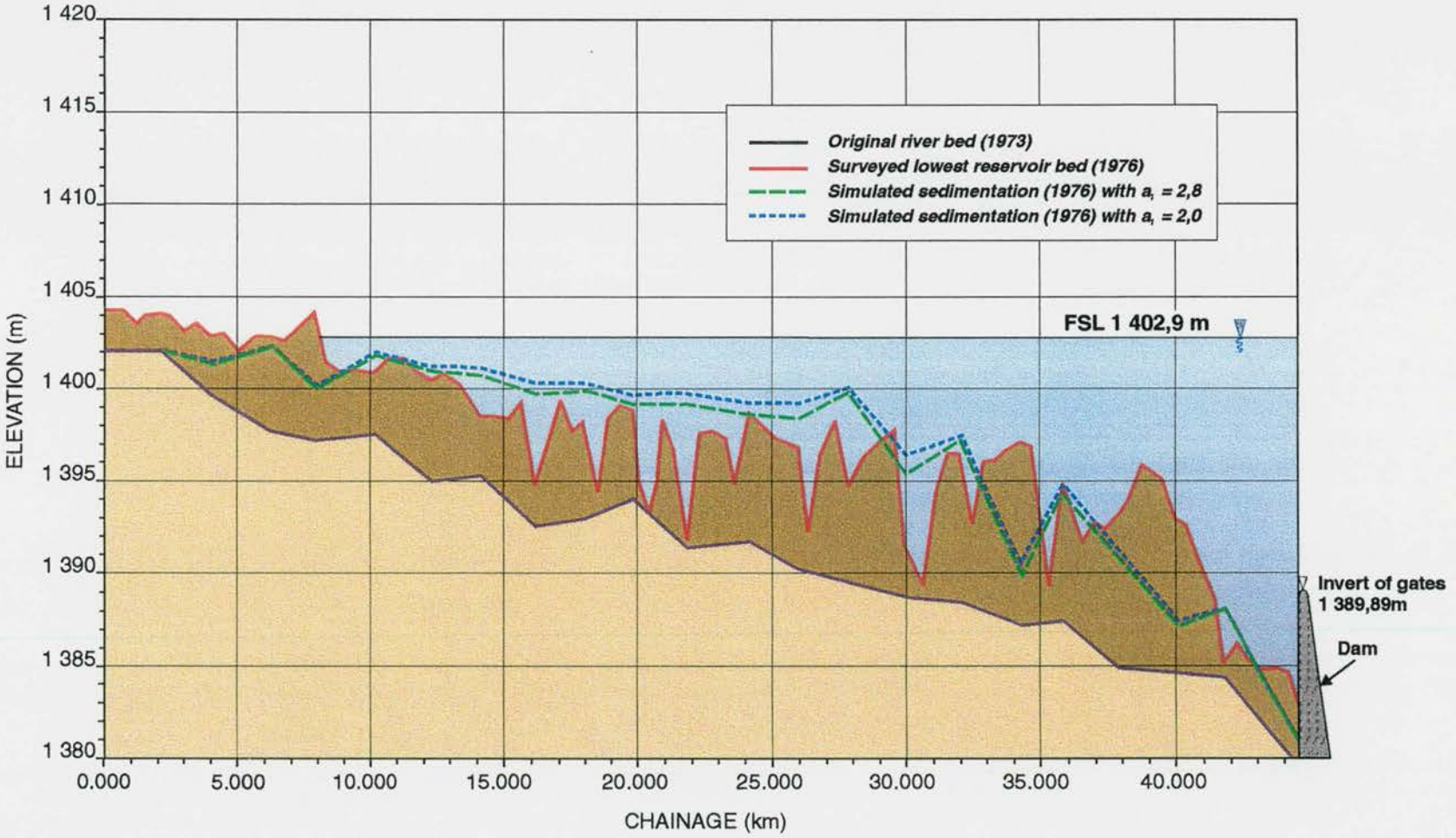

Figure 3.17-18: Non-equilibrium sediment transport calibration: Welbedacht Reservoir, 1973 to 1976

3.17.8 Comparison between calibrations

Han et. al. (1990) give typical calibrated adaptation coefficient values for Chinese field data as:

Reservoir sedimentation (deposition)	: α	= 0,25 (a = 4,0)
Reservoir flushing with fine sediments	: α	= 1,0 (a = 1,0)
Rivers with coarse, non-uniform sediments	: α	= varies for each fraction

The Chinese α -values are related to the "a"-values given in brackets above, for steady conditions. These adaptation coefficients calibrated with Chinese data agree very well with the calibrated canal adaptation coefficients which varied between 2,0 and 2,8 and 1,5 to 2,5 for Welbedacht and cyclone sediments respectively. The differences between Chinese and South African calibrated adaptation parameters can be ascribed to:

- different fraction size ranges
- different sediment characteristics
- different equilibrium sediment transport equation for fine sediments.

3.17.9 Conclusions

Non-equilibrium sediment transport processes have been analysed using the advection - dispersion equation. Calibration of an adaptation parameter with canal data (steady, uniform) and a reservoir (unsteady, non-uniform) has been carried out successfully. More controlled, detailed experimental flume studies are required, however, to address:

- equilibrium sediment transport per size fraction and its interrelationship with energy dissipation and bed roughness
- non-equilibrium sediment transport as above, with observed flow velocities and sediment concentrations in the vertical for oversaturated conditions.

4. DENSITY CURRENTS

4.1 Introduction

Apart from turbulent suspended sediment transport, which is the dominant mechanism by which sediment is transported through most reservoirs, density currents in certain reservoirs provide an alternative mechanism to transport sediment. A density current, is not that different from normal open channel flow: in the latter case air replaces the overlaying fluid body and the stream can therefore also be seen as a "density current"; only in the case of air above a water stream the density difference is so large that the inertia effects of the air compared with those of water may be neglected.

Density currents are not only found when liquids of different densities move relative to each other. The movement of moist air in the form of clouds spilling down a mountain valley or dust rolling down a slope are common examples of density currents. When one analyses the behaviour of density currents related to sediment transport through reservoirs (also known as turbidity currents), a number of questions come to mind:

- Why do density currents occur?
- Under what conditions will density currents form?
- How can the density current movement be described hydraulically?
- What is the relationship between sediment transport and the hydraulics of a density current?
- Can density currents be utilized effectively as a means of transporting sediment through a reservoir without deposition?

4.2 Description of density currents in reservoirs

The formation of density currents was first observed at the beginning of this century in some of the world's large reservoirs. Along the upper reaches of a reservoir, stable, floating debris is observed, indicating the so-called "plunge point" where the inflowing river stream changes into a density current **(Photograph 4.2-1)**. The stationary position of the debris is caused by the slow upstream movement (or near zero velocity) of the overlying water mass, just downstream of the point where the sediment-laden inflow dives below the stored water mass.

Apart from the evidence at the plunge point, nothing can be seen of the density current, except when it exits the reservoir through suitable low-level outlets provided it reaches the dam. Under unfavourable boundary conditions, the density current could either be broken up through turbulent mixing in certain parts of the reservoir or through deposition of sediment, whereby the density difference which drives the density current, decreases.

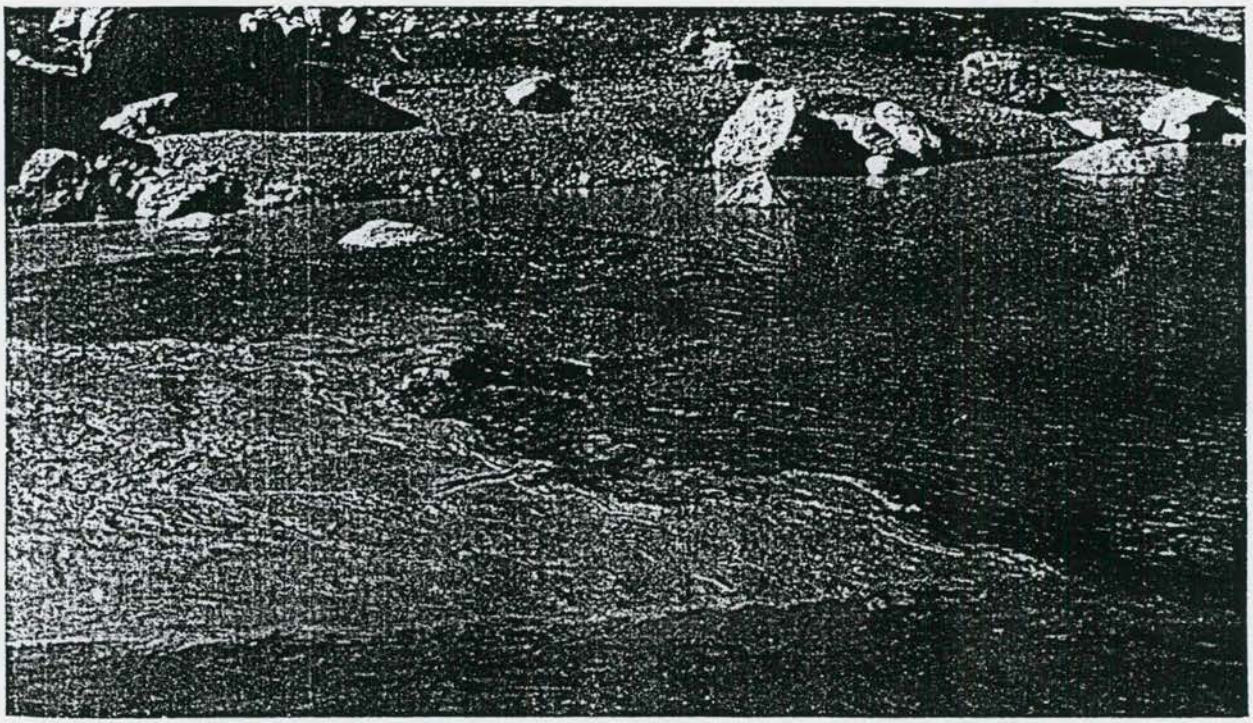

Photograph 4.2 - 1 Plunge point at Eril Emda Reservoir

Density currents do not only occur in reservoirs on heavily silt-laden rivers such as the Eril Emda Reservoir in Algeria, Lake Mead in the USA or Sanmenxia Reservoir in China, but also in reservoirs with flows containing low sediment concentrations such as the Sautet Reservoir in France.

Density currents may travel long distances through reservoirs, for example over 100 km in Lake Mead and 80 km (1961) in the Sanmenxia Reservoir.

Typical density current velocity and suspended sediment profiles are shown in **Figure 4.2-1** as observed in Gaunting Reservoir, China and **Figure 4.2-2** as observed in Sanmenxia Reservoir, China. *(Fan, 1986)*

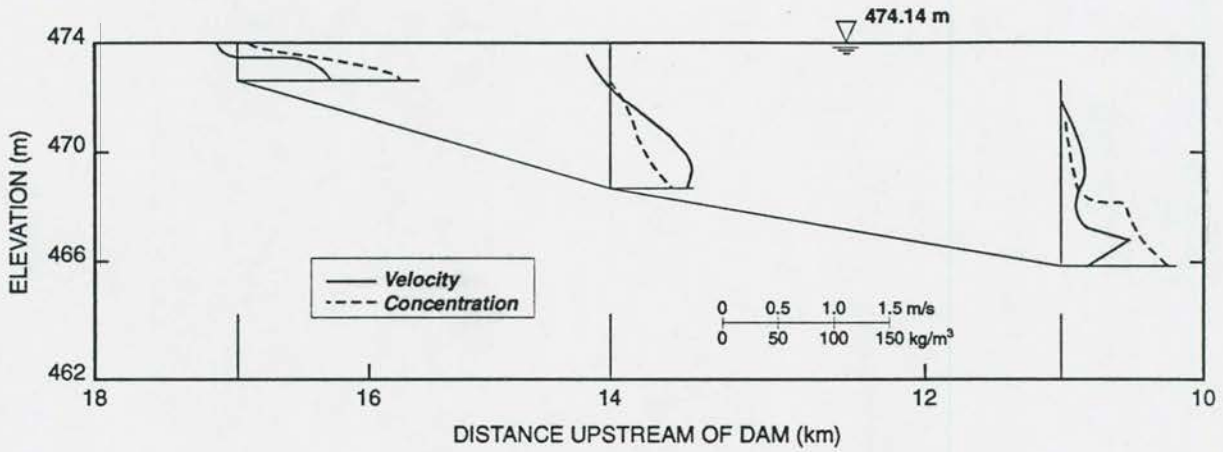

Figure 4.2 - 1 Density current in Guanting Reservoir (Fan, 1986)

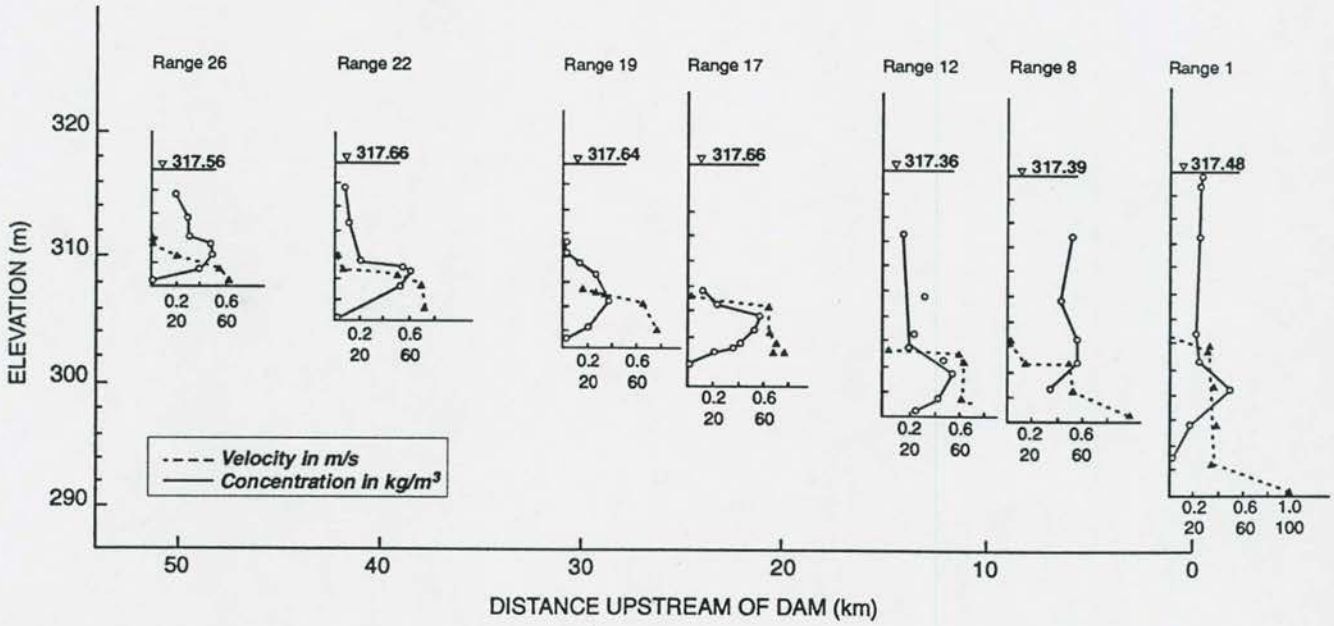

Figure 4.2 - 2 Density current in Sanmenxia Reservoir (Fan, 1986)

It was found in practice that a density current moves at a slow speed, typically of the order of 0,1 to 0,3 m/s (in some cases higher), and yet is able to transport high sediment loads for distances over 100 km through a reservoir. As will be shown later, these low velocities are related to the density difference between the lower denser fluid and upper "clear" water, which effectively reduces the effective gravitational acceleration by 100 to 1 000 times. The effect of this is that the flow of the gravity current can be described as if in "slow motion". In flume experiments it was noticed that a density current can "jump" over obstacles in its path, due to the low relative "gravity" (g). Around bends the surface level increase is often so much that fluid spills out of the main channel and at the downstream outlet the density current can flow vertically upwards provided that the outlet is correctly sized and is at a certain height.

Density currents have often been associated with delta formation in reservoirs. It was and is still believed that the delta provides the ideal boundary conditions for the density current to form. The author, however, believes that in fact a density current leads to the formation of a delta, not the other way around. As will be shown later, more favourable conditions for the formation of a density current exist without a delta.

Graf (1983) stated that density currents in reservoirs typically transport sediment particles smaller than 20 micron in diameter with a settling velocity of less than 0,03cm/s, which implies that a density current velocity of 0,03 cm/s is required for maintaining suspension of sediment. He stated that density currents will be either depositing, eroding or steady state, with equilibrium between bed erosion and bed deposition existing in the latter case.

It will be shown in this chapter that density current sediment suspension is similar to that in open channel flow. Deposition of coarse sediment normally occurs at the plunge point due to insufficient transport capacity of the density current, while the further movement of the density current can be associated with deposition of sediment (at underwater obstacles) or with steeper slopes erosion may occur depending on the critical shear stress and sediment availability.

At the plunge point, transition occurs from a normal turbulent stream to a density current, with continuity in discharge being maintained. Not all incoming sediment is however removed by the density current, as the larger particle sizes are immediately deposited, and

invariably in reservoirs all over the world it has been found that only the finest sediment fractions of silt and clay are transported by density currents through the reservoirs. This means that although the settling velocities of the particles are much reduced through the reduction in effective gravity, the transport capacity of the density current is still not sufficient for the transport of all incoming sediments.

4.3 Hydraulic description of density currents

4.3.1 General

In the previous sections, density currents and possible reasons/explanations for some of the associated phenomena were given in general terms. It is necessary to obtain a better mathematical understanding of the movement of a density current and also to review some of the theories proposed by other researchers in the past, as no generally accepted theory exists.

Consider the vertical velocity, suspended sediment concentration and shear stress distribution in density current flow, as indicated in **Figure 4.3-1**, which will form the basis of discussions in the following sections.

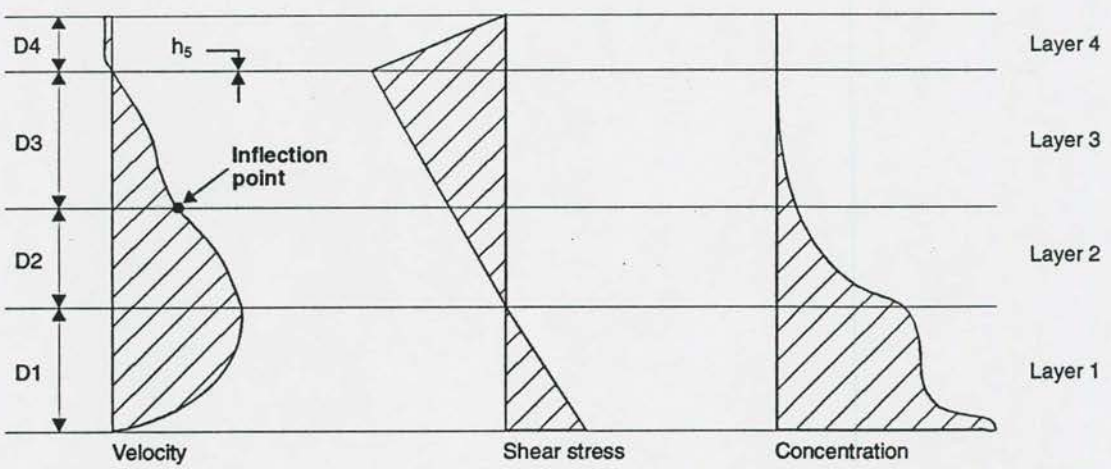

Figure 4.3 - 1 Density current velocity, suspended sediment concentration and shear stress distributions

4.3.2 Velocity distribution

In laboratory and field studies, the vertical velocity distribution has been found to be increasing logarithmic in layer 1 from the bed to the maximum velocity level (between layers 1 and 2) (**Figure 4.3-1**). *(Ashida et al, 1975; Chikita, 1989)* From this point upwards in layer 2, the profile again seems to be decreasing logarithmic until a sudden change in slope at the so-called "inflection point" between layers 2 and 3 is reached. Through layer 3 the velocity decreases upward until it reaches zero at the point of contact where the velocity becomes negative due to upstream flow in the upper reservoir layer. In layer 4 the velocity is often zero or slightly negative with a typical open channel velocity distribution.

4.3.3 Vertical suspended sediment distribution

The sediment distribution should be seen in relation with the velocity distribution. (**Figure 4.3-1**). In the lower layer 1, the sediment distribution is similar to that found under turbulent flow conditions. Normally the sediment is also uniformly distributed due to the small particle sizes. The reduction in the z value is due to the low settling velocity and related change in distribution as explained in **Chapter 3**, with

$$z = \frac{w}{\kappa\sqrt{gD_1 s}}$$

Just above the maximum velocity level, the sediment concentration decreases rapidly to almost zero near the inflection point in the velocity profile, which is also normally specified as the upper boundary of the density current. Only a small quantity of sediment is diffused into layer 3 and is transported in this layer.

In terms of our knowledge of turbulent suspended sediment transport, it is easy to explain the rapid reduction in sediment concentration in layer 2. The relative suspended concentration for turbulent open channel flow is given by:

$$\frac{C}{C_o} = \frac{\left(\tau \frac{dv}{dy}\right)^z}{\left(\tau \frac{dv}{dy}\right)^z_o} \qquad (3.8\text{-}1)$$

$$\therefore C \propto \left(\tau \frac{dv}{dy}\right)^z$$

which means that as the maximum velocity is reached at the top of layer 1, $\frac{dv}{dy} \rightarrow 0$ and $\tau \rightarrow 0$ and therefore $C \rightarrow 0$. It is thus only the turbulence along the boundary of the density current which carries any suspended sediment above layer 1. In theory the suspended sediment transport in layer 2 should be zero, caused by the "barrier" of $\tau \frac{dv}{dy} \rightarrow 0$ at $v = v_{maximum}$ between layers 1 and 2.

4.3.4 Shear stress distribution

Within the lower two layers (1 and 2), the shear stress varies linearly (**Figure 4.3-1**) (*Ashida, 1975*). In layer 3 a non-linear shear stress distribution is found, while at the top in layer 4, the distribution is linear as in open channel flow.

Although layers 1 and 2 are normally described as the density current, it is believed that at least layers 1, 2 and 3 should be considered in the mathematical description of a density current. From continuity:

$$q = \overline{v}_1 D_1 + \overline{v}_2 D_2 + \overline{v}_3 D_3 \qquad (4.3\text{-}1)$$

and $$q_c = \int_{y_o}^{D_1} v_1 C_1 \, dy + \int_{D_1}^{D_2} v_2 C_2 \, dy + \int_{D_2}^{D_3} v_3 C_3 \, dy \qquad (4.3\text{-}2)$$

$$\approx \int_{y_o}^{D_1} v_1 C_1 \, dy$$

with y measured from the bed and if it is assumed that layers 2 and 3 make insignificant contributions to the sediment load. Therefore all 3 layers form part of the density current.

4.4 Mathematical description of velocity distribution and the layer thickness of a density current

i) Within the lower layer D_1, *Ashida (1975)* found a logarithmic velocity distribution in his laboratory tests (see **Figure 4.4-1**) and he therefore adopted a velocity distribution equation of the form:

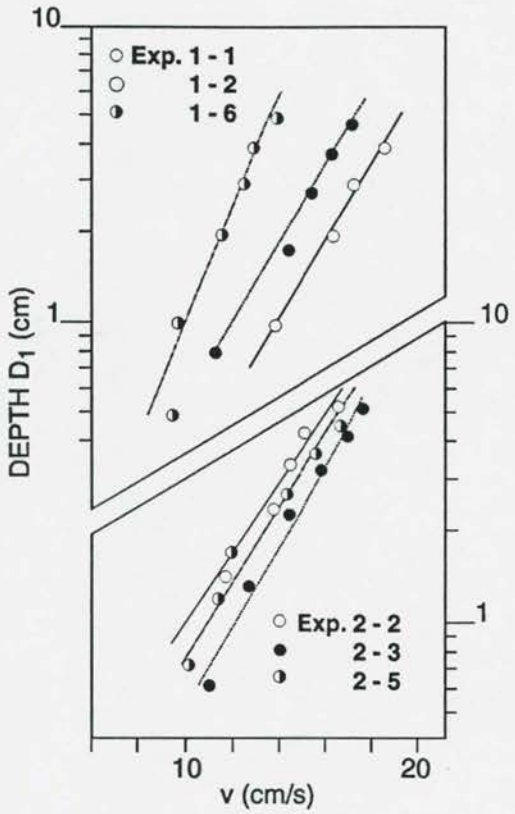

Figure 4.4 - 1 Velocity distribution from channel bed to maximum velocity (Ashida, 1975)

In layer two, at the interface, Ashida related the mixing length (ℓo) to the layer thickness (D_2) and found the relationship indicated in **Figure 4.4-2**.

With $\ell = \ell o + \kappa_2 (D_1 + D_2 - y)$ at the interface, Ashida again assumed a logarithmic velocity distribution for layer 2. By making further assumptions regarding the shear stress distribution in layer 3 (see **Figure 4.4-3**), Ashida derived a velocity distribution relationship for layer 3 and together with assumed sediment concentrations, the discharge and sediment transport continuity equations could be solved mathematically.

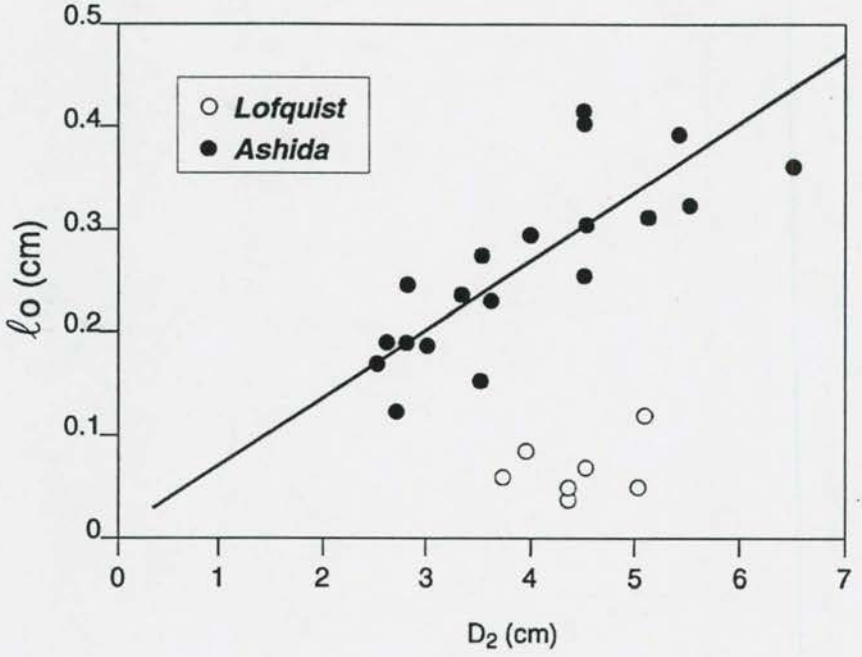

Figure 4.4 - 2 Relationship between mixing length (l_o) at interface and D_2 (Ashida, 1975)

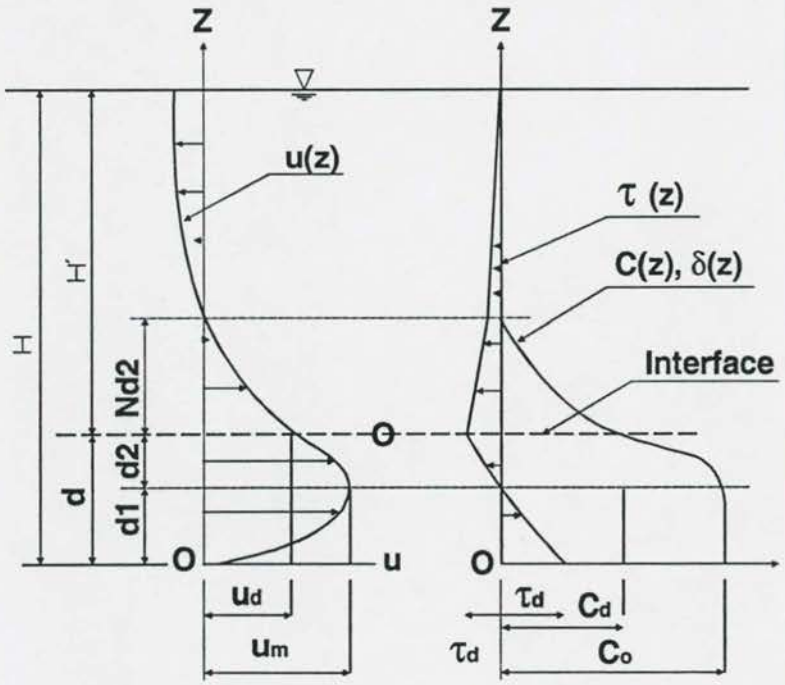

Figure 4.4 - 3 Distribution of velocity, shear stress and sediment concentration (Ashida, 1975)

Ashida was one of the first authors to describe the velocity, shear stress and suspended sediment distribution in the density current. Some of the assumptions made by Ashida can, however, be criticized. The assumed relationship between ℓo and D_2 is not based on theory and need therefore not be true for all data, as is found with different data in **Figure 4.4-2**. The mixing length (or R) at the interface should rather be calculated theoretically by using boundary layer theory as will be shown in the next section.

In density current flow, 3 boundaries can be observed: at the bed, at the top of layer 2 where the suspended sediment concentration $\rightarrow 0$, and at the level where $v \rightarrow 0$. With certain assumptions, it should be possible to describe the velocity distribution and layer thicknesses in a density current mathematically. The knowledge of laminar and turbulent boundary conditions derived in **Chapter 3** can be used effectively to describe the mathematical relationships. Unlike for turbulent homogeneous flow, the velocity distribution relationship for a density current cannot be established without considering the influence of sediment transport.

The suspended sediment transport in a density current affects the energy dissipation rate as represented by kappa (κ) as follows:

a) At the bed in layer 1, the highest sediment concentration is found with a related reduction in κ to estimated values of as low as 0,2. (Typical of that found in open channel flow). A reduction in κ leads to an increased velocity gradient $\left(\frac{dv}{dy}\right)$ in layer 1 near the bed.

b) At the top of layer 3, $v \rightarrow 0$ and the suspended sediment concentration approaches zero. Therefore $\kappa \rightarrow 0{,}4$, a typical value in turbulent open channel flow with no sediment transport.

c) As the sediment concentration rapidly decreases in layer 2, the inflection point in the velocity distribution (or the interface) is probably caused by the sudden change in the value of κ at the interface.

The velocity profile of a density current can be described by assuming the following:

i) A laminar boundary layer at the top of layer 3 where $v \to 0$.

ii) Turbulent flows, corrected for density difference, in layers 3 and 2. Laminar flow above the interface (above layer 2) would at first seem to be more probable, but such an assumption cannot explain the relatively great depth of layer 3 and the velocity distribution. A correction of the density difference is also necessary, since some sediment is diffused upward and transported in layer 3.

iii) Turbulent flow, corrected for density difference, in layer 1, derived from the same principles as those applicable to rough bed conditions.

iv) Logarithmic velocity distributions in layers 1, 2, and 3 for turbulent conditions, adjusted with correct κ values as these values change with depth in each layer.

For layers 2 and 3

At the top of layer 3, with y measured downward as in **Figure 4.3-1**, in the laminar layer, and following the same approach as with open channel flow in **Chapter 3**.

$$\tau = \mu\frac{dv}{dy} = \Delta\rho gs(D_{2+3}-y)$$

$$\therefore \frac{dv}{dy} = \frac{\Delta\rho gs(D_{2+3}-y)}{\mu} \qquad (4.4\text{-}2)$$

In the rest of layer 3, the flow is turbulent and the shear stress:

$$\tau = \frac{\rho}{2\pi}R^2\left(\frac{dv}{dy}\right)^2 = \Delta\rho gs(D_{2+3}-y) \qquad (4.4\text{-}3)$$

Following the same derivation as with turbulent open channel flow in **Chapter 3**, it is possible to show that:

$$\therefore \frac{dv}{dy} = \frac{\sqrt{2\pi\Delta\rho g D_{2+3} s}}{\rho y} \qquad (4.4\text{-}4)$$

Assuming that at the boundary between the laminar and turbulent density current flow at the top of layer 3,

$$\tau \frac{dv}{dy}\, laminar = \tau \frac{dv}{dy} turbulent$$

and $\tau_{laminar} = \tau_{turbulent}$, then

$$\frac{dv}{dy} laminar = \frac{dv}{dy} turbulent$$

$$\Delta\rho g s \frac{(D_{2+3} - y)}{\mu} = \frac{\sqrt{2\pi g' D_{2+3} s}}{y}, \text{ with } g' = \frac{\Delta\rho}{\rho} . g \qquad (4.4\text{-}5)$$

Solving **Equation (4.4-4)** now for $y = h_5$, the thickness of the boundary layer, to be used as integration constant when deriving the velocity:

$$\therefore h_5 = \frac{\sqrt{2\pi g' D_{2+3} s} . \mu}{\Delta\rho g s (D_{2+3} - h_5)}$$

$$= \frac{\sqrt{2\pi}\mu}{\sqrt{\rho\Delta\rho g (D_{(2+3)} - h_5) s}}$$

$$= \frac{\sqrt{2\pi} . \mu}{\sqrt{\rho\Delta\rho g D_{(2+3)} s}}; \text{ assuming } D_{(2+3)} - h_5 \approx D_{(2+3)} \qquad (4.4\text{-}6)$$

Integration of **Equation 4.4-4** yields:

$$v_{(2+3)} = \sqrt{2\pi g' D_{(2+3)}\, s} \ln y + A \qquad (4.4\text{-}7)$$

with A an integration constant.

At the top of layer 3 at the boundary layer:

$$v_{(2+3)} = \frac{\Delta\rho gs}{2\mu}(2Dy - y^2.h_5) = \sqrt{2\pi g'Ds}\ \ell n\ h_5 + A \tag{4.4-8}$$

$$\therefore A = \frac{\Delta\rho gsDh_5}{\mu} - \sqrt{2\pi g'Ds}\ell n h_5$$

and **Equation 4.4-7** becomes:

$$v_{(2+3)} = \sqrt{2\pi g' D_{(2+3)}}s\ell n\left(\frac{y}{h_5}\right) + \frac{\Delta\rho gsD_{2+3}h_5}{\mu}\Big|_{h5}^{D_{2+3}} . \tag{4.4-9}$$

Substituting **Equation 4.4-6** in **Equation 4.4-9** gives:

$$\begin{aligned} v_{2+3} &= \sqrt{2\pi g' D_{(2+3)}}s\ell n\left(\frac{y\sqrt{gsD}\sqrt{\rho\Delta\rho}}{\sqrt{2\pi}\mu}\right) + \frac{\Delta\rho gsD\sqrt{2\pi}.\mu}{\mu.\sqrt{gsD}\sqrt{\rho\Delta\rho}} \\ &= \sqrt{2\pi g' D_{(2+3)}}s\ell n\left(\frac{y\sqrt{gsD}\sqrt{\rho\Delta\rho}}{\sqrt{2\pi}\mu}\right) + \sqrt{\frac{\Delta\rho}{\rho}}\sqrt{2\pi}\sqrt{gsD} \end{aligned} \tag{4.4-10}$$

In layer 1, the velocity at any level can be derived as in **Chapter 3**, but with the density difference adjustment.

Therefore

$$v_1 = \sqrt{2\pi g' D_1}s\ell n\left(\frac{D_1}{y_o}\right) \tag{4.4-11}$$

Equations 4.4-10 and **4.4-11** can now be solved together by using the fact that the maximum velocities in both equations are common:

Equation 4.4-10 becomes

$$v_{(2+3)}(\max) = \sqrt{2\pi g' D_{(2+3)}s}\ \ell n\left(\frac{D\sqrt{gD_{(2+3)}s}\sqrt{\rho\Delta\rho}}{\sqrt{2\pi}\mu}\right) + \sqrt{2\pi}\sqrt{gsD_{(2+3)}}\sqrt{\frac{\Delta\rho}{\rho}} \tag{4.4-12}$$

and **Equation 4.4-11**:

$$v_{(1)}\max = \sqrt{2\pi g' D_1}s\ell n\left(\frac{D_1}{y_o}\right) \tag{4.4-13}$$

with $y_o = \frac{k_s}{30}$

Equations 4.4-12 and **4.4-13**, however, contain 3 unknowns: D_1, D_{2+3} and v_{max}. A third equation is therefore required which expresses D_1 in terms of D_{2+3}. This third equation is found when combined translation and rotation in turbulent flows are considered.

As was indicated in **Chapter 3** for turbulent open channel flow, turbulent flow translates at relative velocity $v_o = y_o \frac{dv}{dy}$. In a density current the same principle applies near the bed as well as at the top of layer 3, so that the translation velocity at the top and bottom of the density current velocity profile should be equivalent:

$$y_1 \frac{dv}{dy_{10}} = y_3 \frac{dv}{dy_{30}} = \text{constant if no acceleration} \qquad (4.4\text{-}14)$$

$$\therefore \frac{\sqrt{g' D_1 s}}{\kappa_1} = \frac{\sqrt{g' D_{(2+3)} s}}{\kappa_{2+3}} \qquad (4.4\text{-}15)$$

$$\therefore \frac{D_1}{D_{(2+3)}} = \frac{\kappa_1^2}{\kappa_{(2+3)}^2}$$

with typical expected values of κ_1 0,2 to 0,3 and $\kappa_{(2+3)}$ = 0,3 to 0,4

Equations 4.4-12, **4.4-13** and **4.4-15** can now be applied simultaneously to solve for D_1 and D_{2+3}.

4.5 Verification of theory to predict velocity profile and layer depth of a density current with laboratory and field data

Using the data of *Ashida (1975)* and *Chikita (1989)* as sources of laboratory and field data respectively, it is possible to calculate the upper layer depths D_{2+3} from observed D_1-values as a first check on the validity of **Equations 4.4-12** and **4.4-13**. Predicted $D_{(2+3)}$ values can, however, only be determined accurately if correct values of κ_1 and $\kappa_{(2+3)}$ are used. Although κ_1 values have been determined by Ashida and Chikita, no data for $\kappa_{(2+3)}$ -values are available, and realistic values had to be assumed.

Assuming $\kappa_{(2+3)} = 0,4$ (as for no sediment transport) and $\kappa_1 = 0,2$ at the bed, the predicted D_{2+3} versus observed D_{2+3} data are indicated in **Figure 4.5-1**. It is clear that the assumptions made in the derivation of **Equations 4.4-12** and **4.4-13** give consistent upper layer depths for both laboratory and field data. Predicted versus observed $D_{(2+3)}$ depths however still need to be compared using real Kappa values.

Unfortunately D_3 data were not published by Ashida, and in only 3 experiments was the ratio of $D_{(2+3)}/ D_2$ indicated as varying from 2,1 to 2,5. Using $\kappa_1 = 0,25$ and $\kappa_{2+3} = 0,32$ provides realistic observed κ_1 data as well as solutions in terms of **Equation 4.4-15** for assumed D_1 and $D_{2+3} = 2,5 \times D_2$ values for Ashida's data. With κ_1, κ_{2+3} and D_1 known, D_{2+3} can be calculated from **Equations 4.4-12** and **4.4-13** and compared with "observed" $D_{(2+3)}$ data $= 2,5 \times D_2$ as shown in **Figure 4.5-1**. Using the same approach, reservoir data of *Chikita (1989)*, are also used to verify the mathematical assumptions, as shown in **Figure 4.5-1**. In this case $D_{(2+3)} = 3 \times D_2$ had to be used, as inferred from the data of *Chikita*.

Although a number of assumptions had to be made owing to the lack of certain observed variables in the laboratory and field data, it is believed that the basis of the theory used in deriving **Equations 4.4-12, 4.4-13** and **4.4-15** is sound, as was provisionally proven in **Figure 4.5-1**. Future detailed laboratory tests will be required to establish κ_1, κ_2, κ_3, D_1, D_2 and D_3 values with different channel slopes, discharges, sediment loads and bed roughnesses.

4.6 Movement of a density current : flow resistance and velocity

It is possible to derive theoretically, from equations of sediment transport and discharge continuity, a relationship for the average velocity of a density current by integrating the velocity distribution with depth and by using the theory as derived in the previous sections. The many unknowns in such a relationship make it difficult to apply in practice and therefore most researchers have resorted to a Chezy type equation with all the unknowns incorporated into a single empirical constant C_H in the equation:

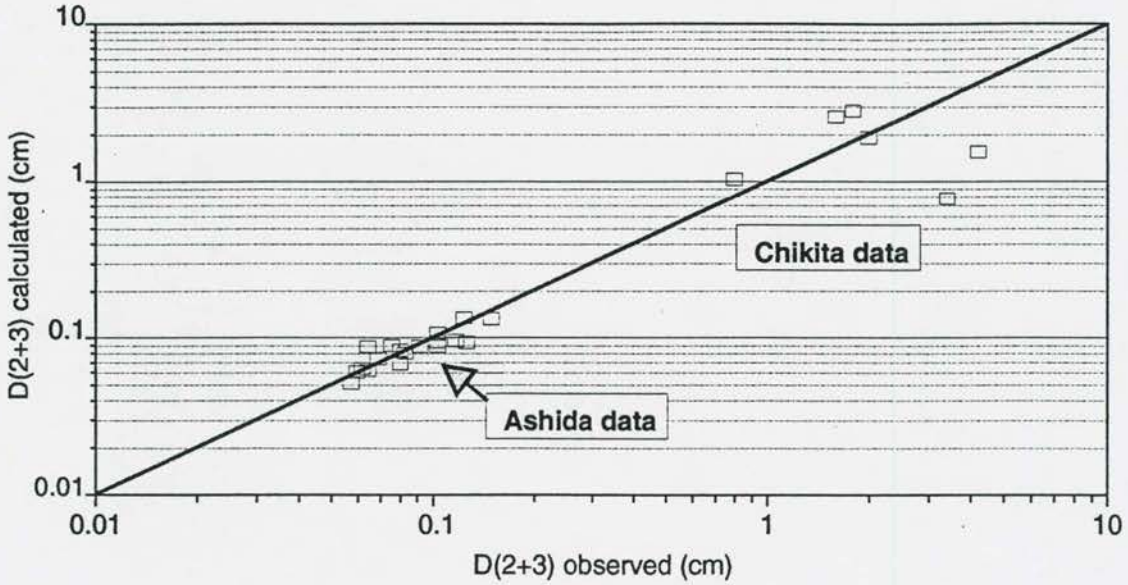

Figure 4.5 - 1 Observed versus calculated density current layer depths

$$\bar{v} = C_H \sqrt{g' D s} \qquad (4.6\text{-}1)$$

with s = s_o, the bed slope, assuming a uniform density current
and D = depth of layers 1 and 2.

Studies have been undertaken by *Raynaud (1951), Bata (1953), Blancket (1954), Michon (1955)*, and *Levy (1958)* on the value of C_H in laminar and turbulent regimes.

Fan (1960) described the movement of a density current in terms of the equation of motion. Consider a fluid element in a density current:

$$\frac{1}{\gamma'}\frac{dp}{dx} + \frac{dy}{dx} + \frac{1}{\gamma'}\frac{d\tau}{dy} + \frac{v}{g} + \frac{dv}{dx} + \frac{1}{g} + \frac{dv}{dt} = 0 \qquad (4.6\text{-}2)$$

with p = total pressure = p_1 (due to lighter fluid) + Δp (due to density difference)

γ' = specific weight of the density current

y = distance from horizontal reference line

If the depth of the density current is h´ and the depth of the overlying water h, then the total depth is $H = h + h'$ (see **Figure 4.6-1**).

Assuming homogeneous fluids, above and below the interface

$$p + \gamma' y = \gamma H + (\gamma' - \gamma) h' + \gamma y_o \tag{4.6-4}$$

and $$\frac{dp}{dx} + \gamma' \frac{dy}{dx} = \frac{dH}{dx} + \Delta\gamma \frac{dh'}{dx} + \gamma' \frac{dy_o}{dx}$$

with γ = specific weight of overlying water

Fan further assumed that τ_o, the mean bed shear stress, and τ_i, the shear resistance at the interface, are proportional to the square of the mean velocity:

$$\tau_o = \frac{\lambda_o}{4} \rho' \frac{v^2}{2} \; ; \; \tau_1 = \frac{\lambda_i}{4} \rho \frac{v^2}{2} \tag{4.6-5}$$

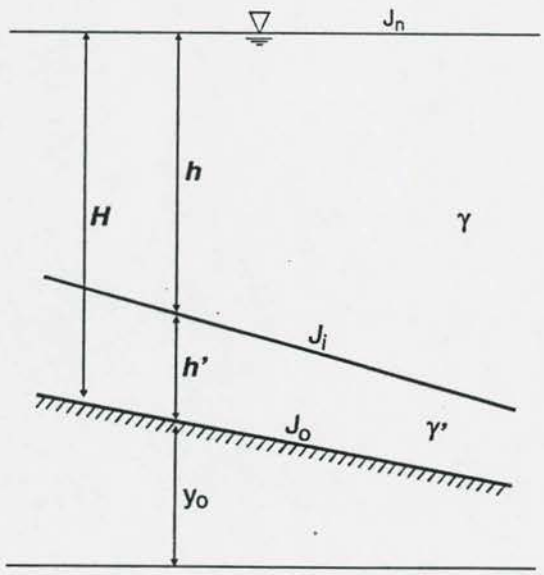

Figure 4.6 - 1 Schematic diagram of a density current

Where λ_o and λ_i are the corresponding coefficients of friction.

Considering a segment of the density current with width b, bed slope J_o and interface slope J_i, the equation of mean motion of the density current reads:

$$\frac{1}{\gamma'}\frac{dH}{dx} + \frac{\Delta\gamma}{\gamma'}\frac{dh'}{dx} + \frac{dy_o}{dx} + \left(\frac{\lambda_o v^2}{8\,gh'} + \frac{\lambda_i v^2}{8gh'}\right) + \left(\frac{v}{g}\frac{dv}{dx} + \frac{1}{g}\frac{dv}{dt}\right) = 0 \qquad (4.6\text{-}6)$$

in which

$$\frac{dH}{dx} = J_0 - J_n$$
$$\frac{dy_o}{dx} = J_0$$
$$\Delta\gamma = \gamma' - \gamma$$

and J_n = negative slope at water surface.

The frictional stress exerted along the interface is

$$\tau_i = \frac{\lambda_i}{4} p' \frac{v^2}{2} = -\gamma \frac{bh}{b + 2h} J_n$$

Substituting the above equations into **Equation 4.6-6** yields:

$$\frac{\Delta\gamma}{\gamma'}\left(J_o - \frac{dh'}{dx}\right) + \frac{v^2}{gh'}\frac{dh'}{dx} - \frac{\lambda m v^2}{8gR} - \frac{1}{g}\frac{dv}{dt} = 0 \qquad (4.6\text{-}7)$$

with λ_m = mean friction coefficient of the underflow

$$= \lambda_o + \lambda_i\left[\frac{b}{2h'+b} + \frac{h'\,(b+2h)}{h\,(b+2h')}\right] \qquad (4.6\text{-}8)$$

For <u>unsteady, non-uniform</u> density currents, *Fan* used **Equation 4.6-7** to predict depths. For steady density currents λ_m = 0,02 to 0,03, but *Fan* used λ_m = 0,05 for unsteady conditions.

For steady, non-uniform density currents:

$$\frac{dh'}{dx} = \frac{J_o - \left(\frac{\lambda_m v^2}{8 \frac{\Delta\gamma}{\gamma'} gR} \right)}{1 - \left(\frac{v^2}{\frac{\Delta\gamma}{\gamma} gh'} \right)} \qquad (4.6\text{-}9)$$

with R = hydraulic radius = $bh'/(2h'+b)$

and for uniform flow $\frac{dh'}{dx} = 0$; then

$$\bar{v} = \sqrt{\frac{8}{\lambda_m} \cdot \frac{\Delta\gamma}{\gamma'} \cdot gRJ_o} \qquad (4.6\text{-}10)$$

$$= \sqrt{\frac{8}{\lambda_m}} \cdot \sqrt{g' RJ_0}$$

which is similar to a Chezy type equation for uniform open channel flow.

Fan found the mean friction factor λ_m **(Equation 4.6-8)** from flume studies to be independent of the *Reynolds* number and to remain almost constant as shown in **Figure 4.6-2**, when the flow is turbulent.

For a bed friction of $\lambda_o = 0{,}02$, Fan found the interfacial friction factor $\lambda_i \approx 0{,}005$ as shown in **Table 4.6-1**.

Table 4.6-1: Interfacial friction factor

J_o	*Average* h' *(cm)*	*Average* λ_i
0,0005	14,4	0,0047
0,005	17,8	0,0051

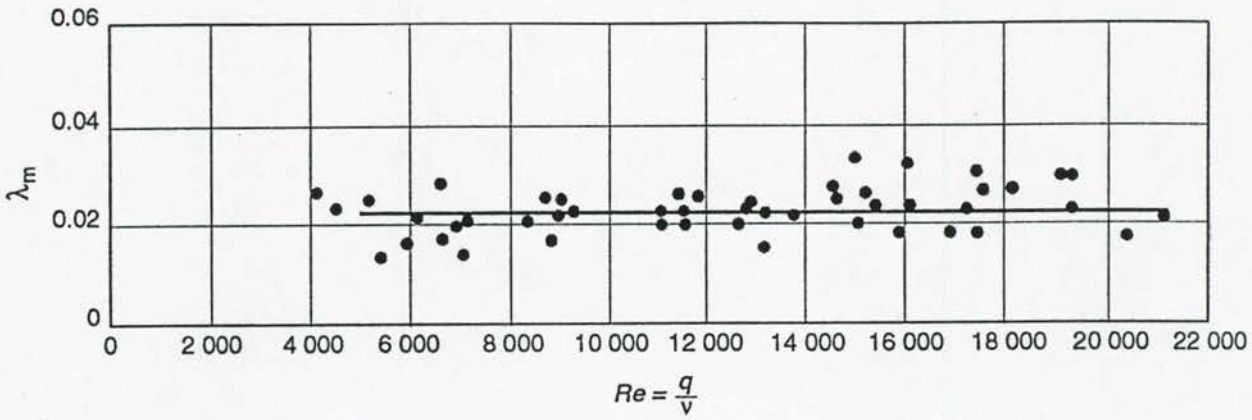

Figure 4.6 - 2 Friction factor λ_m from flume studies

In the Guanting Reservoir, China, *Fan* found the same constant mean friction factor as in the flume tests (with the same sediment), with λ_m = 0,02 to 0,03 as shown in **Figure 4.6-3**.

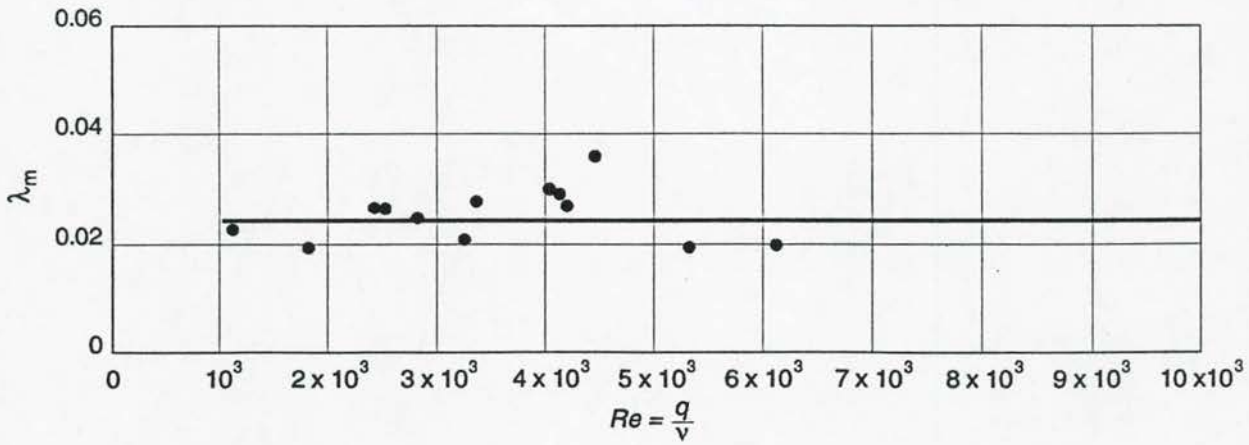

Figure 4.6 - 3 Friction factor in Guanting Reservoir

Fan (1960) also found that supercritical and subcritical conditions can prevail in the density current, and the transition from one condition to another is possible in the plunging phase, with submerged hydraulic jumps being formed.

A relationship between typical depths of flow and density current thicknesses for the Guanting Reservoir as well as flume data is shown in **Figure 4.6-4**.

Such a relationship will be site specific and will depend on a number of specific boundary conditions such as bed slopes, discharge, sediment characteristics, etc.

So far, only one-dimensional density currents have been considered. The influence of flow width on a density current is, however, also important in order to quantify total sediment transport.

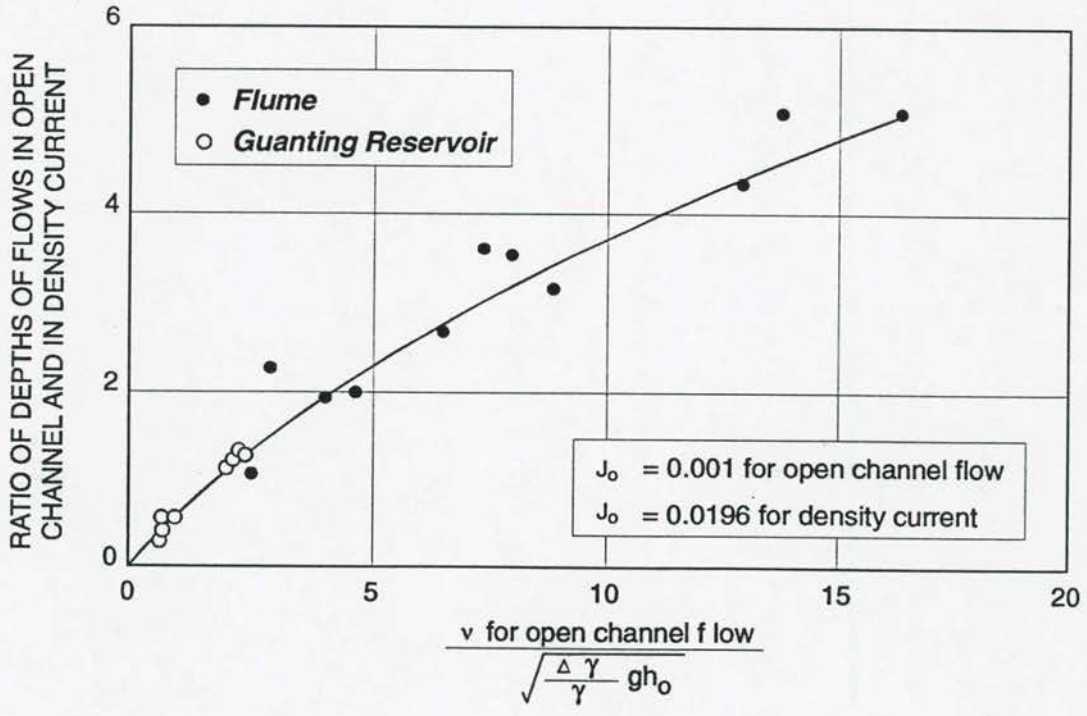

Figure 4.6 - 4 Ratio of density current depth to open channel flow depth in Gaunting Reservoir

4.7 Cross-sectional variation in velocity and sediment concentration across a density current in a reservoir

At the early stages of impoundment, a density current usually moves along the original river channel. Later, as the main channel is filled through sedimentation, the topographical width exceeds the width of the density current. Examples of observed lateral and vertical velocity and concentration distributions in the Sanmenxia Reservoir, 1961, are depicted in **Figure 4.7-1** *(Fan, 1986)*.

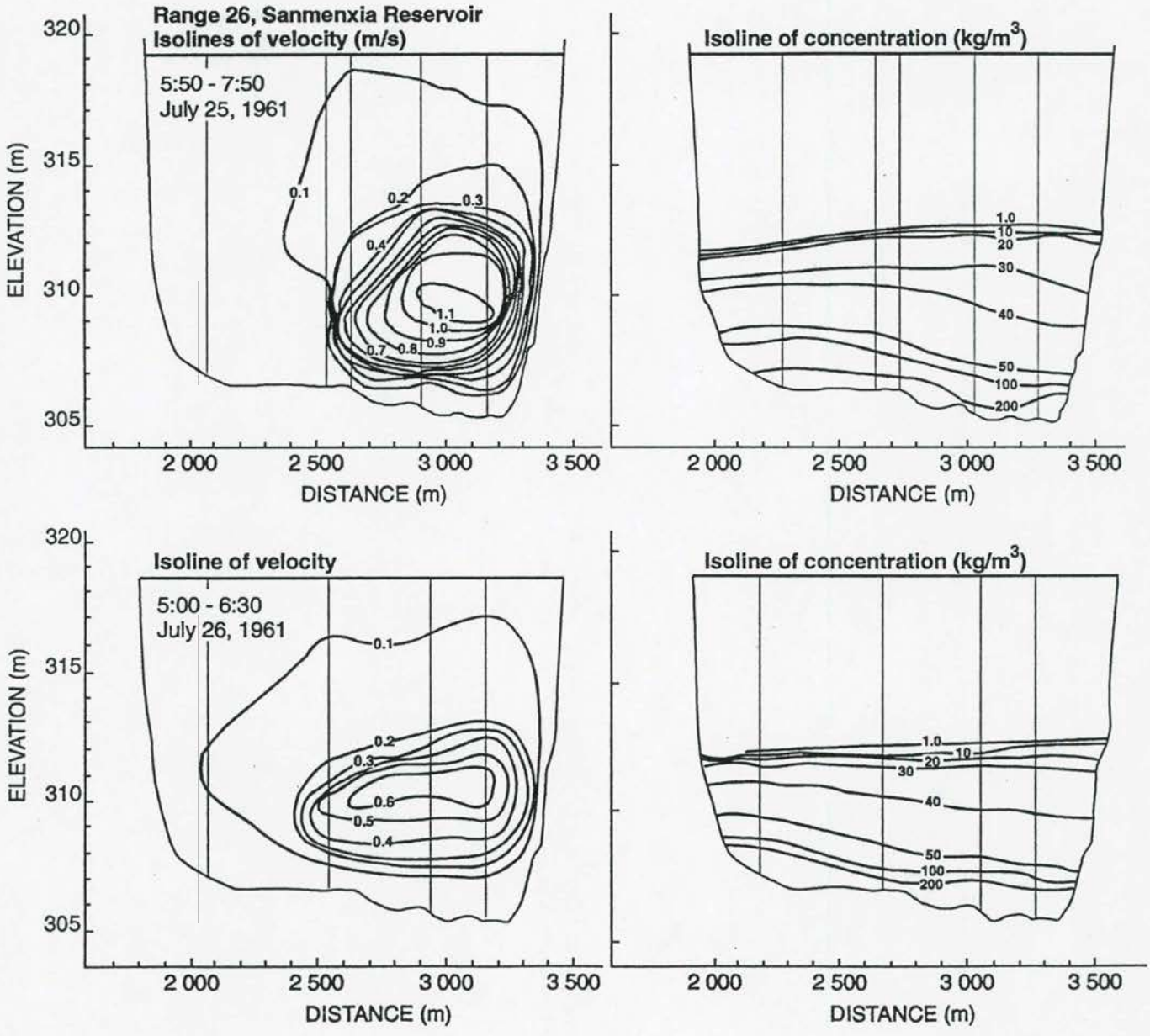

Figure 4.7-1 **Density current lateral velocity and concentration distribution in Sanmenxia Reservoir**

The general validity of a density current uniform flow velocity equation of the Chézy type has been demonstrated by experimental studies and applied successfully.

Harleman (1961) used:

$$v = \sqrt{\frac{8}{f(1 + \alpha)}}\sqrt{g'}\sqrt{hs_o} \qquad (4.7\text{-}1)$$

with f = Darcy-Weisbach friction factor

and α = factor describing shear distribution at interface as function of bed shear, with $\tau_i = \alpha\tau_o$ (4.7-2)

Harleman proposed the use of $\alpha = 0{,}43$ for turbulent density current flow and f-values from the Moody diagram for pipe flow.

For laminar flow (Re < 1000), Harleman proposed

$$v = 0{,}375\sqrt{Re}\sqrt{g'}\sqrt{hs_o} \qquad (4.7\text{-}3)$$

which was determined theoretically.

Harleman (1961) applied equation 4.7-1 to Lake Mead, USA and obtained consistent results with actual measurements. *Middleton (1966)* experimentally confirmed **Equation 4.7-1** for density currents of salt solution and clay suspensions, with $\Delta\rho<1$ and $s_o < 0{,}03$.

Keunen (1952) obtained a simple relationship from flume studies:

$$v = C''\sqrt{g''}\sqrt{h_o s_o} \qquad (4.7\text{-}4)$$

with $g'' = \dfrac{g(\rho_1-\rho_2)}{\rho_2}$

in contrast to $g' = \dfrac{\Delta\rho}{\rho_1}$

with ρ_2 = density in density current,

Keunen proposed $C'' = 280$ cm^{½}/s in reservoirs for $s_o > 20°$

Hinze (1960) showed that the empirical relationship used by *Keunen (1952)* can be derived theoretically. Using boundary layer theory, Hinze obtained **Equation 4.7-4** with $C'' = f$(suspension density distribution, friction coefficient at interface) with $280 < C'' < 560$ cm ^{½}/s.

Bagnold (1962) proposed an auto-suspension model as the criterion for the continued self-maintenance of a density current, which can be rewritten in the form:

$$v = C\sqrt{g'}\sqrt{h\sin\theta}, \tag{4.7-5}$$

but the term $\sin\theta$ is replaced by $(\sin\theta - \frac{w}{v})$, with w = settling velocity of particles.

Bagnold used an energy balance principle:

Layer integrated turbulent energy production = work done against negative buoyancy force + turbulent energy dissipation.

$$\int_o^H (\overline{u'v'})\frac{\delta u}{\delta y}.dy = \int_o^H bv\cos\theta dy + \int_o^H E dy \tag{4.7-6}$$

$$\therefore s_2 BHU(\sin\theta - v_f\cos\theta) = \int_o^H E dy$$

The energy dissipation term cannot be evaluated properly without velocity and density profiles. It is therefore difficult to verify Bagnold's concept *(Middleton, 1966)*.

4.8 Motion of the head of a density current

Every uniform flow region of a density current is preceded by an initial head also known as the nose. *Hinze (1960)* referred to it as the spreading-out phenomenon, during which the density current displaces the fluid which it enters. *Altinaker (1990)* plotted the shape of the head non-dimensionally as shown in **Figure 4.8-1**.

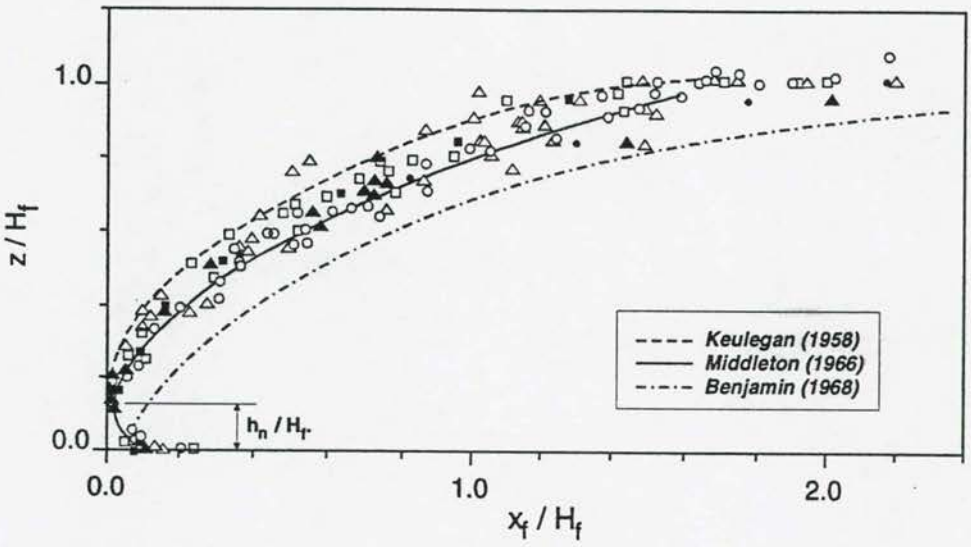

Figure 4.8-1 Non dimensional density current head shape

Middleton (1966) observed that the head had a well-defined shape, with a depth twice the uniform flow depth, while the velocity is less than that of the uniform flow. It is also a region of intensive erosion. *Middleton (1966)* found from flume studies that the motion of the head in the density current was closely described by the laws developed by *Keulegan (1958)* for saline surges. It was found that the velocity of the density current head on slopes up to 4 % is adequately expressed by *Keulegan's (1958)* formula:

$$v_n = 0{,}75\sqrt{g' h_n} \qquad (4.8\text{-}1)$$

with h_n = thickness of the head.

Turner (1973, 1979) proposed **Equation 4.8-2** for the velocity of the head:

$$v_n = \sqrt{2}\sqrt{g' h} \qquad (4.8\text{-}2)$$

with h = depth of uniform density current flow.

When considering the three-dimensional motion and slope influence, Turner proposed:

$$v_n = 0{,}75\sqrt{g' h_n} \qquad (4.8\text{-}3)$$

which is the same equation as proposed by *Keulegan (1958)*.

Density currents are characterized by a distinctive raised head, followed by a quasi-uniform flow region called the body. **(Figure 4.8-2)**

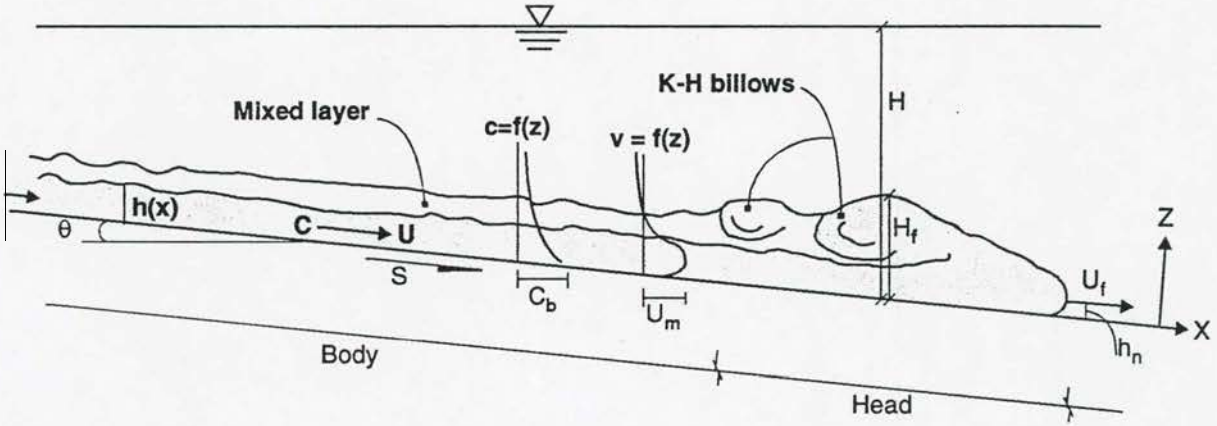

Figure 4.8-2 Density current head

The head constitutes a region of intense mixing and wave breaking, with a highly irregular front.

Altinaker (1990) compared his flume data with those of Middleton and Turner and proposed a smaller "Chezy" coefficient value of 0,63 in the equation:

$$v_n = 0{,}63\sqrt{g' h_n} \qquad (4.8\text{-}4)$$

which is shown graphically in **Figure 4.8-3**.

The data used in **Figure 4.8-3** show considerable scatter, but this is understandable since the channel slope was not considered. The data in the Altinaker experiments were derived from bed slopes < 3 %.

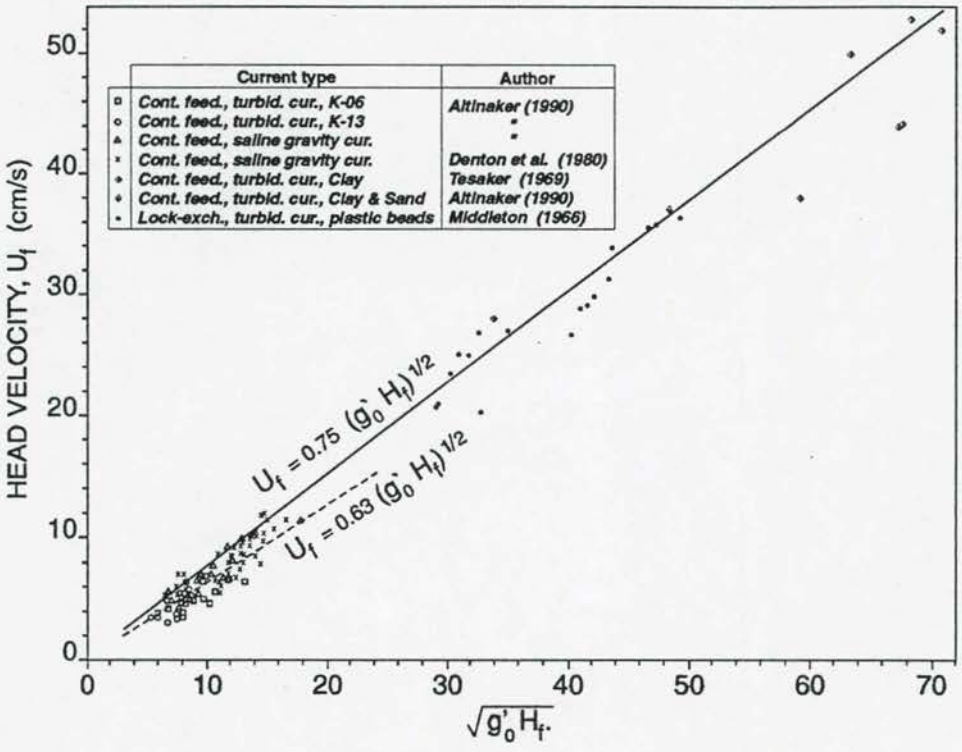

Figure 4.8-3 Density current head velocity

Altinaker further considered the head velocity as a function of initial buoyancy flux $B_o = + g_o' q_o$ and slope (s_0):

$$Uf = (g_0' q)^{1/3} f(s_0) \qquad (4.8\text{-}5)$$

as is shown graphically in **Figure 4.8-4**.

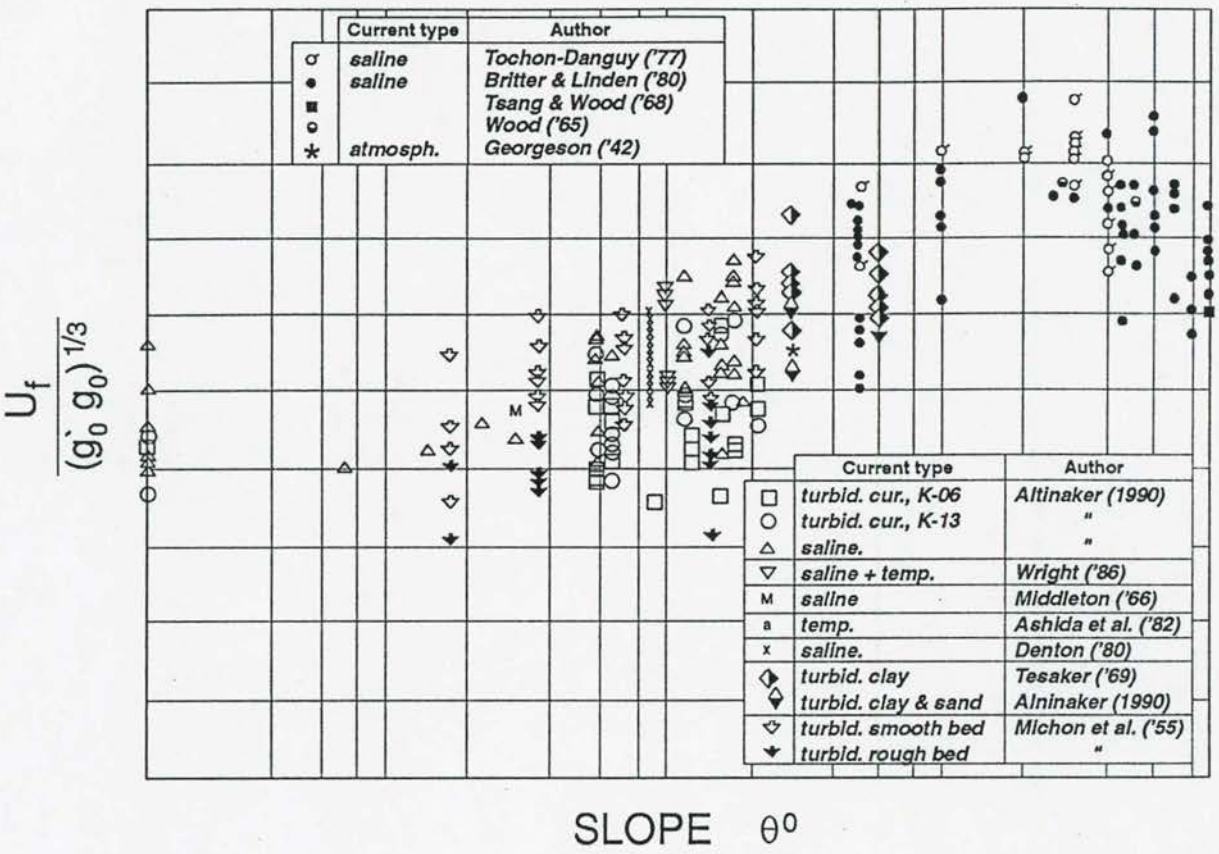

Figure 4.8-4 Dimensionless head velocity as function of bed slope

The data show considerable scatter, which *Altinaker* attributed to experimental errors and different drag coefficients.

Although the movement of the density current head differs from uniform flow owing to the displacement of stagnant water at the nose, it is proposed here that since $v_n = f(g', H_f, s_o)$, a Chezy equation as for the uniform density current with a different C coefficient may be used:

$$v_n = C_n \sqrt{g' H_f s_o} \qquad (4.8\text{-}6)$$

The data of Altinaker are shown in **Figure 4.8-5** and it is clear that **Equation 4.8-6** will indeed provide an accerate predictor of the density current head velocity.

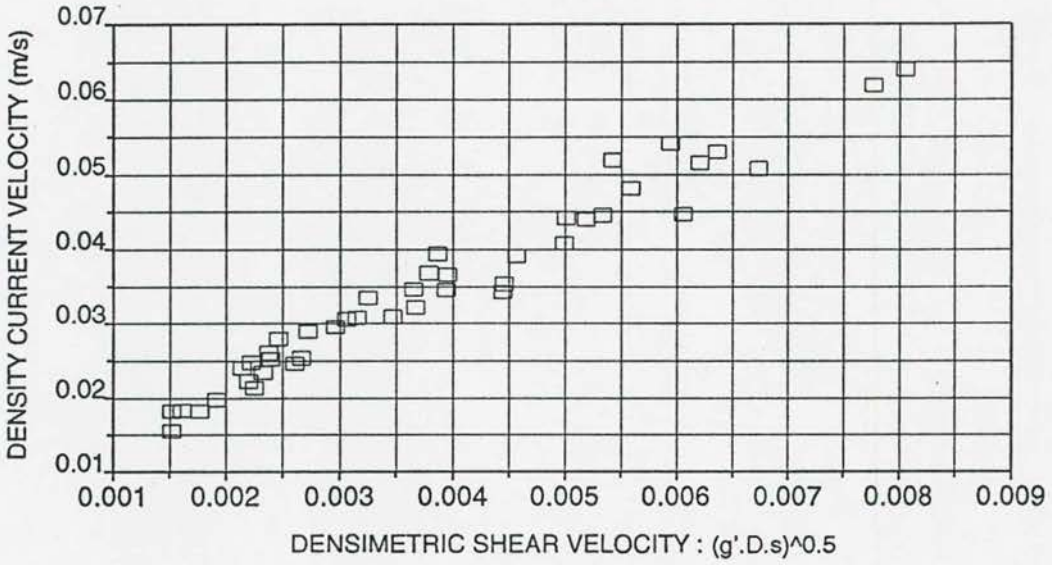

Figure 4.8-5 Velocity of density current head using Chezy type equation

4.9 Sediment transport by density currents

Bell (1940) expresses a very interesting view on density currents: "In ordinary streams, water propels suspended sediment. In turbid density currents, sediment propels water. Once the significance of this paradox has been grasped, a deal of mystery that surrounds density currents is stripped away".

From our current knowledge of hydraulics, we know that the density difference associated with sediment transport is required for density current movement. Both open channel flows and density current flows will however transport sediment (if available), since the sediment provides the mechanism through which the bed can be deformed and whereby the applied energy can be minimized. It is therefore not the water that propels the suspended sediment or vice versa in streams or density currents, but rather an intricate interrelationship between sediment and clear water transport in a process of minimization of energy.

When a density current develops from turbulent inflow into a reservoir, coarser sediment is immediately deposited (in the delta area) while the fine sediments, up to the sediment transport capacity of the density current, can be carried through the reservoir (see **Figure 4**). The physics involved in the sediment transport process is almost the same as with turbulent open channel flow.

As was illustrated by **Equation 3.8-1**, the vertical suspension of sediment is limited by the applied power $\tau\frac{dv}{dy} \rightarrow o$ at the maximum velocity level between layers 1 and 2. Although some sediment is diffused into layers 2 and 3, the amount is negligible compared with the load in layer 1.

The sediment being transported in a density current consists of the silt and clay fractions, with typical particle sizes and concentration distributions shown in **Figures 4.9-1**. It is clear that in layer 1 a constant suspended sediment concentration and density can be assumed in most cases, and therefore the sediment transport can be given by:

$$q_c = \int_{y_o}^{D_1} Cv\, dy = \overline{C}\,\overline{v} \qquad (4.9\text{-}1)$$

with

$$\overline{C} = C_o \int_{y_o}^{D_1} \frac{\left(\tau\frac{dv}{dy}\right)^z}{\left(\tau\frac{dv}{dy}\right)_o^z}\, dy$$

Density current movement is unsteady due to the nature of floods, especially in arid areas. Measurements at the Guanting Reservoir clearly illustrate the characteristic of an unsteady density current with a reduction in sediment transport and with finer sediment being transported by the density current than the by inflow **(Figure 4.9-1)**.

Fan (1960) investigated the sediment transport capacity of density currents in terms of the limiting particle size being transported. From flume tests he established that coarse sediment settles almost immediately while finer particles are transported at a constant gradation d_{90} = 0,008 to 0,018 mm and d_{50} = 0,002 to 0,003 mm, with plunge point velocities of 40-80 mm/s.

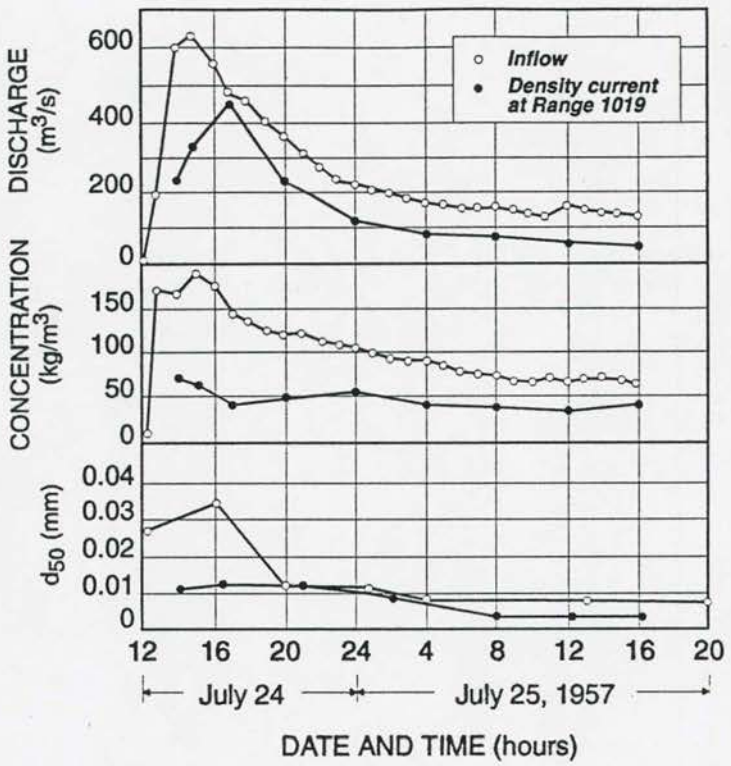

Figure 4.9-1 Unsteady density current measured in Guanting Reservoir

In the Guanting Reservoir the suspended sediment in the density current was found to be much coarser with d_{90} = 0,01 to 0,13 mm and d_{50} = 0,002 to 0,003 mm, with a plunge point velocity of 0,2 m/s resulting in greater transport capacity and the related larger particles that were transported compared to flume studies.

4.10 Sediment transport in South African reservoirs

While *Lewis (1936)* stated that density currents had been observed in Lake Arthur, no quantitative data or information was published. No other density currents (turbidity driven) have been reported in the country. Although the sediment loads in many rivers are high

enough to create density differences, and suspended sediment loads include enough fine particles, the main limiting factor must be the flat bed slopes of reservoirs, especially after some time of deposition, which prevent transport through the reservoir.

During this research density currents were observed after each flushing of Welbedacht Reservoir during filling of the reservoir. While the 5 gates in the dam were closed to cause filling of the empty reservoir, river outlets remained open which allowed venting of sediment transported towards the dam.

While suspended sediment samples taken near the surface upstream of the dam indicated low concentrations, the suspended concentrations of outflows sampled just downstream of the dam continued to be high for many hours after closure of the main gates, as shown in **Figure 4.10-1**.

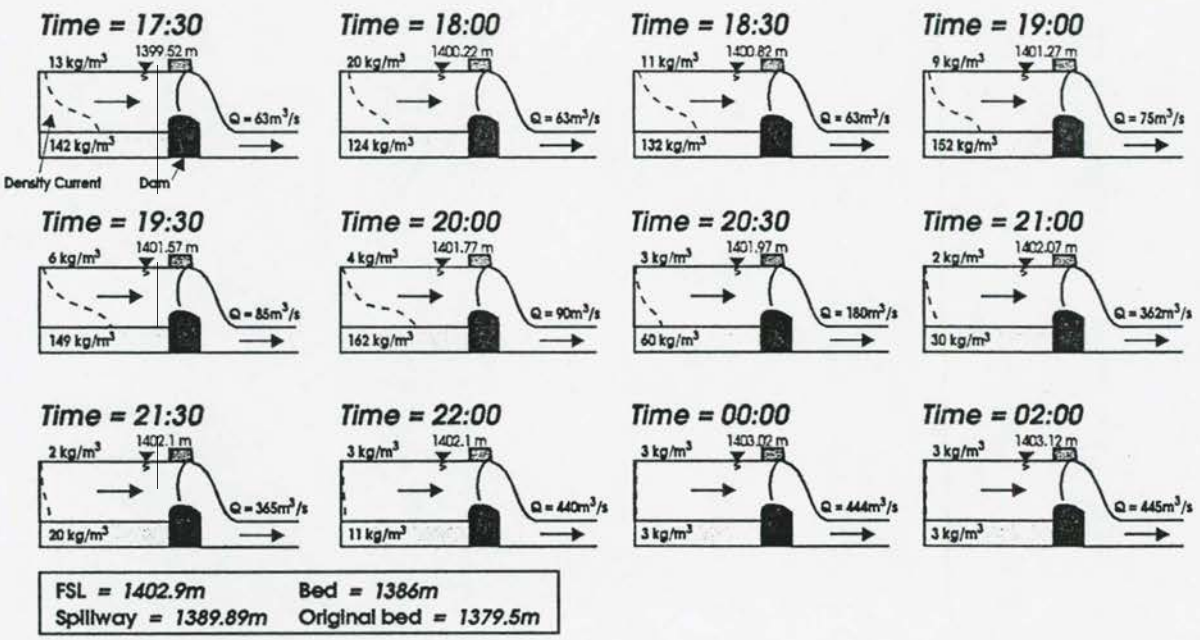

Note: Observations of suspended sediment taken at water surface and near bed, at the dam

Figure 4.10-1 Density current venting at Welbedacht Reservoir

The streampower relationship (**Chapter 3.13-3**) proved that the high observed concentrations cannot be related to turbulent suspended sediment transport in the reservoir and some other transport mechanism, which could only be density currents, had to be responsible for the high concentrations being vented from the reservoir. Flushing with water level draw-down of course provided high turbulent sediment transport capacity and related high concentrations. Once the main outlets were closed, however, the coarse sediments were immediately deposited, whereas high concentrations of fines created density differences, resulting in density currents moving along the bed as the reservoir filled. The steep front set slope within Welbedacht Reservoir provided enough streampower for the density current to move through the reservoir down to the dam (**Figure 4.10-2**). The duration of density current flow is limited, however, by the limited availability of sediment after the turbulent scouring action during the flushing process. After some time, the outflow density current concentration decreased to become equal to the inflow sediment concentration.

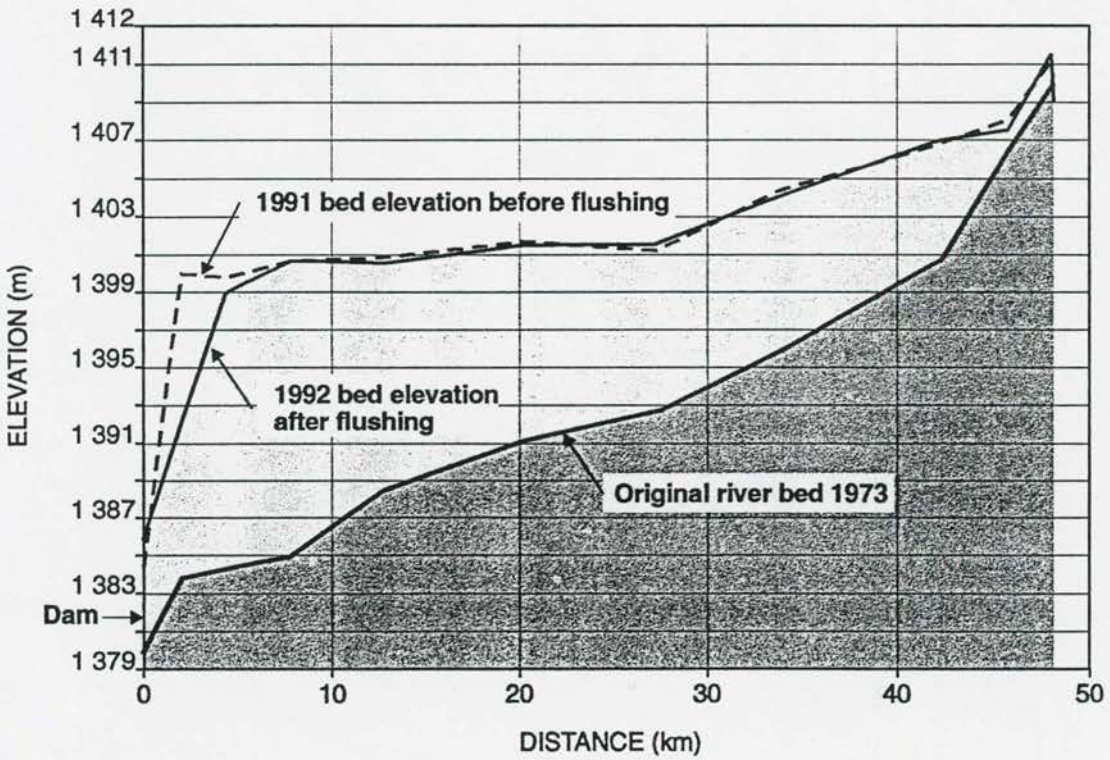

Figure 4.10-2 Longitudinal profile of Welbedacht Reservoir bed

Using the scoured profile of the main channel, it is possible to calculate the mean velocity of the density current observed in Welbedacht Reservoir. Suspended sediment concentration can then be related to the input streampower function for the density current and compared with similar reservoir data from China.

Unfortunately only the averaged suspended sediment particle size distribution was determined for the 1994 flushings at Welbedacht Dam, and information on the sediment size transported by the density current as compared to turbulent transport could not be established. During 1995, however, the reservoir was flushed again under similar flow conditions as in 1994 and this time more detailed sampling and grading analyses were carried out. **Figure 4.10-3** shows the effective settling velocity changes from the full reservoir before flushing, during flushing and during filling with density current venting.

Wu (1994) derived a sediment transport equation for a density current based on similar assumptions as those which were used to obtain the Velikanov sediment transport equation for open channel flow sediment transport:

$$\overline{C} = K_1 \frac{\overline{v^3}}{gh\, w_{50}} \qquad (4.10\text{-}1)$$

with $$\overline{v} = K_2 \sqrt{\frac{\Delta\gamma}{\gamma} gh}$$

and K_1 , K_2 = constants

h = height of density current

w_{50} = settling velocity of median particle diameter

Field data of Gaunting, Sanmenxia and Hongshan Reservoirs with sediment concentrations $< 100 kg/m^3$ were used to calibrate **Equation 4.10-1** as indicated in **Figure 4.10-4** and **Equation 4.10-2**.

$$C = 12{,}75 \left(\frac{v^3}{ghw_{50}} \right)^{0{,}285} \qquad (4.10\text{-}2)$$

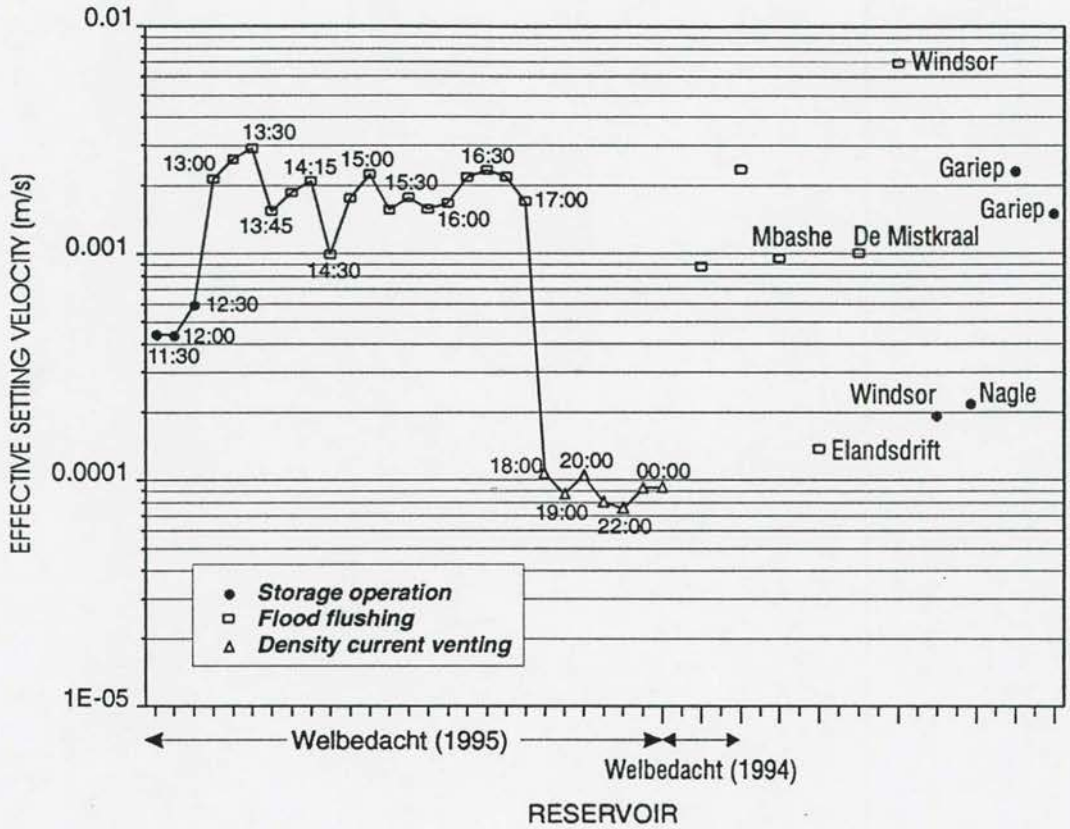

Figure 4.10-3 Reservoir operation and settling velocity based on observed sediment characteristics

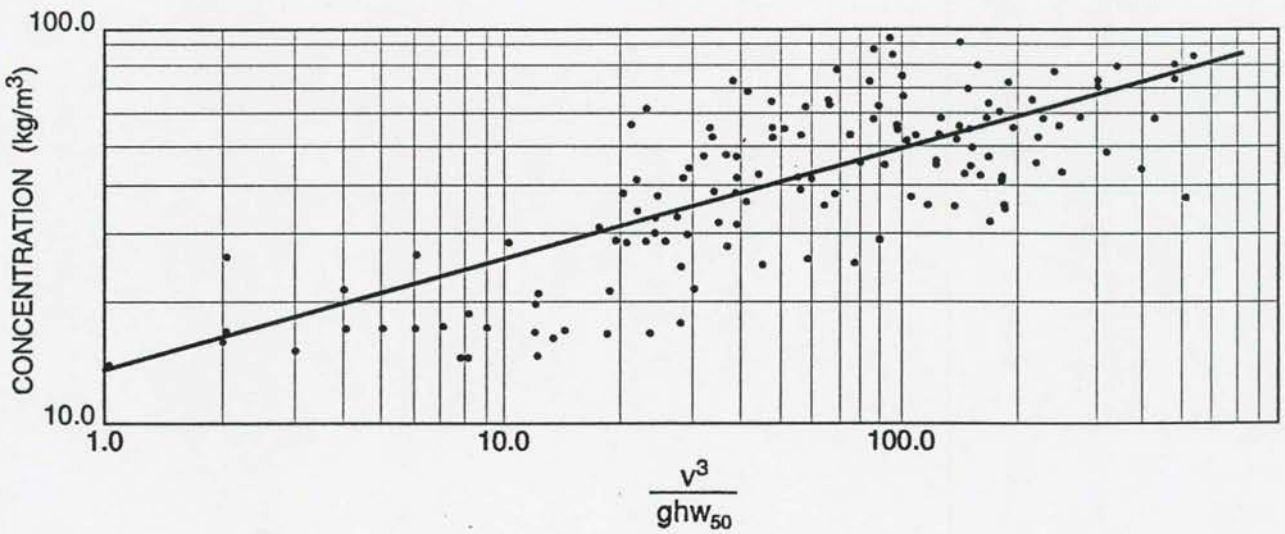

Figure 4.10-4 Chinese Reservoir density current sediment transport relationship

Calculation of the input streampower versus sediment transport of the Welbedacht Reservoir density current shows a direct relationship **(Figure 4.10-5)** and also agrees with Chinese reservoir data **(Figure 4.10-4)**.

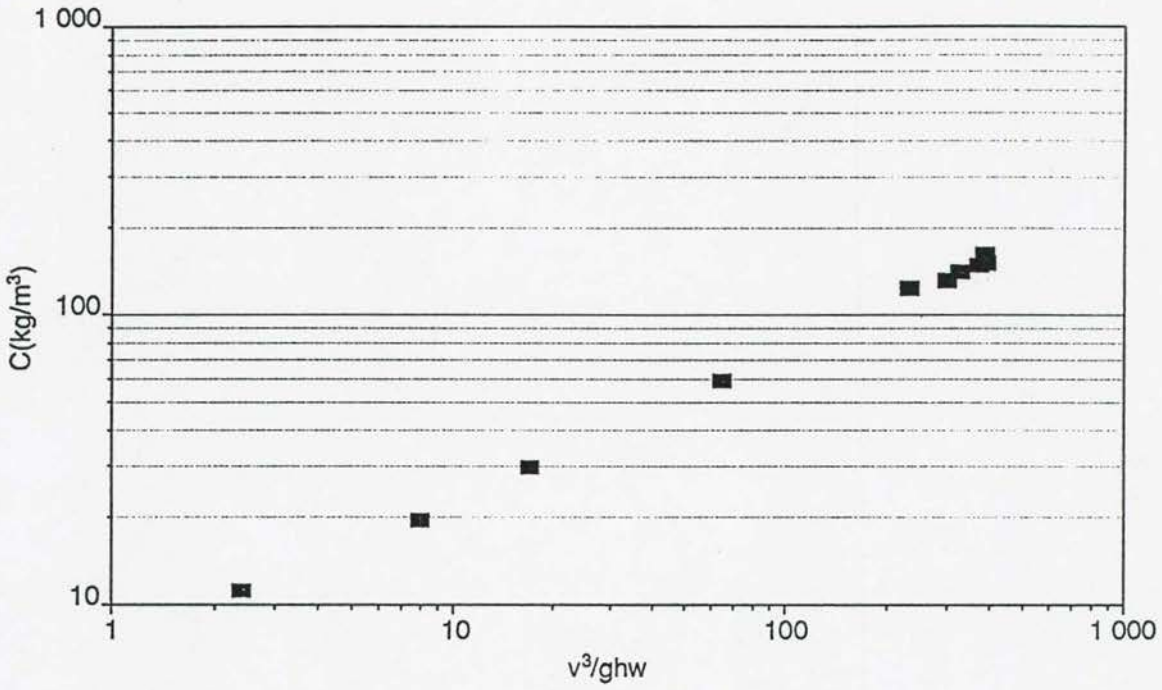

Figure 4.10-5 Welbedacht Reservoir density current sediment transport relationship

4.11 Non-equilibrium density current transport

Wu (1994) proposed the use of a non-equilibrium methodology in predicting/modelling sediment transport by density current through a reservoir, similar to the approach followed for turbulent fine sediment transport in reservoirs in China and also proposed in this dissertation:

$$\frac{dC}{dx} = \frac{-\alpha w}{vh}(C - C^*) \qquad (4.11\text{-}1)$$

with α = coefficient

C^* = equilibrium sediment concentration

v = density current velocity

h = density current depth

Equation 4.11-1 which has been calibrated for turbulent open channel flow conditions in this dissertation (**Chapter 3**), will probably also be applicable to density current sediment transport. Much more data and analyses of equilibrium sediment transport in density currents need to be carried out, however, before a good theoretical understanding of non-equilibrium sediment transport would be possible.

4.12 Graded sediment transport by density currents and the sorting process

Field data from China has been used to establish an empirical relationship between sediment size and transport:

$$\frac{C_x}{C_o}\,\% = 1{,}1 \cdot \frac{dx_{90}}{dD_{90}}\% - 12 \qquad (4.12\text{-}1)$$

with C_o = mean suspended sediment concentration at entrance (plunge point),

D_{90} = size of particles for which 90% material is finer, read from local size frequency distribution curve.

This relationship is shown graphically in **Figure 4.12-1** *(Wu, 1994)*.

Non-uniform sediment transport in a density current can be predicted as for homogeneous open channel flow when the equilibrium sediment transport equation is calibrated for various particle sizes suspended in the density current.

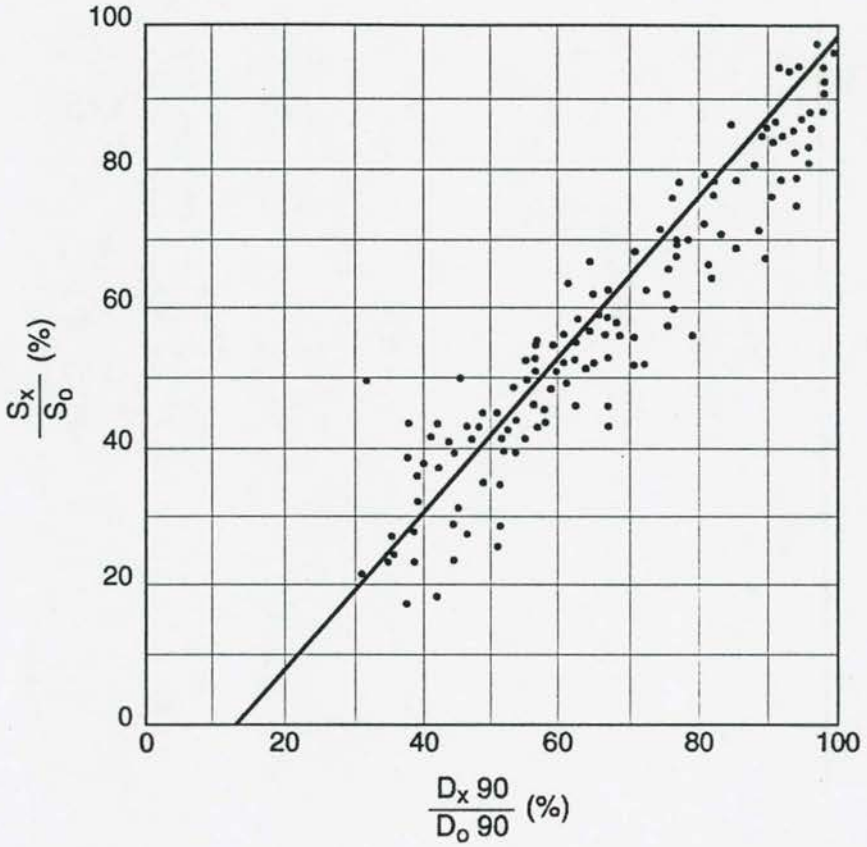

Figure 4.12-1 Graded sediment transport in a density current (Wu, 1994)

4.13 Formation of a density current

4.13.1 Review of theory

Many attempts have been made to predict the formation of a density current:

Dequennois (1956) suggested $(\gamma' - 1)q$ as a criterion for the turbulent flow to form a density current.

Levy (1958) analysed the minimum silt concentration below which a density current will not occur.

Fan (1960) concluded that in the transition from open channel flow to density current flow, $\frac{dh'}{dx}$ increases rapidly at the interface, and $\frac{dh'}{dx} \to \infty$. **Equation 4.6-9** can therefore be rewritten with

$$\frac{v^2}{\frac{\Delta\gamma}{\gamma'} gh'} = 1 \qquad (4.13\text{-}1)$$

From **Figure 4.13-1**, it is evident that the velocity decreases as the depth increases in the transition zone and that the velocity reaches a minimum and water depth a maximum value at the plunge point. Fan therefore proposed that the specific energy

$$E = h' + \frac{v^2}{2\frac{\Delta\gamma}{\gamma} gh'}$$

has a minimum value at the plunge point, or

$$\frac{dE}{dh'} = 1 - \frac{q^2}{\frac{\Delta\gamma}{\gamma} gh_o^3} = 0$$

$$\therefore \quad \frac{v_o}{\sqrt{\frac{\Delta\gamma}{\gamma'} gh_o}} = 1$$

This parameter is known as the densimetric Froude number (Fr_D) .

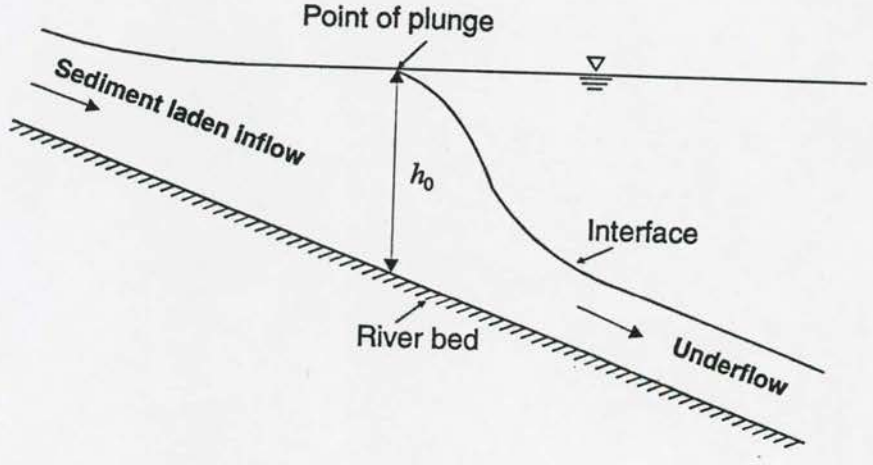

Figure 4.13-1 Schematic diagram of density current formation

By conducting flume tests, *Fan* established a relationship for the densimetric Fr_D as given in **Figure 4.13-2.**

$$\text{with} \quad \frac{v_o}{\sqrt{\frac{\Delta\gamma}{\gamma} g h_o}} = 0{,}78(<1) \qquad (4.13\text{-}2)$$

Fan gave the reason for the experimental $Fr_D < 1$ as "a point of inflection in the streamlines at the interface, which is located downstream of the plunge point, where $Fr_D = 1$. "

Fan (1986) found that the formation of density currents can be forecasted by means of **Equation (4.13-2)** for concentrations < 100kg/m³. It was, however, found that the densimetric Froude number also depends on the inflow sediment concentration and decreases with increasing concentration. This explains why different researchers have found such a wide range of densimetric Froude numbers which predict density current formation from their experiments.

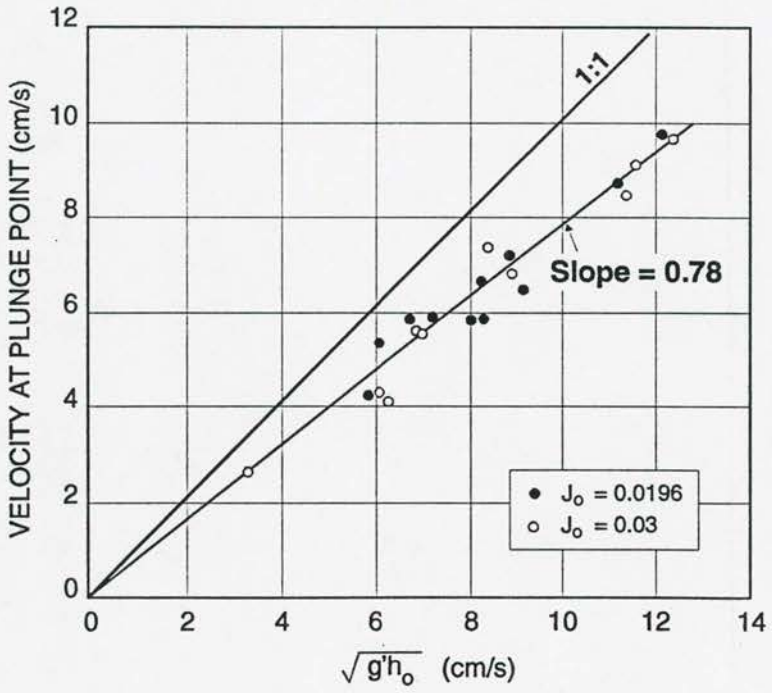

Figure 4.13-2 Densimetric Froude number and density current formation

Cao (1992) published a relationship between Fr_D and the density difference **(Figure 4.13-3)**. It appears that when sediment concentrations are $< 40 kg/m^3$, $Fr_D \approx 0{,}78$. As the sediment concentration increases the density current changes from turbulent to transitional to laminar with hyperconcentrations.

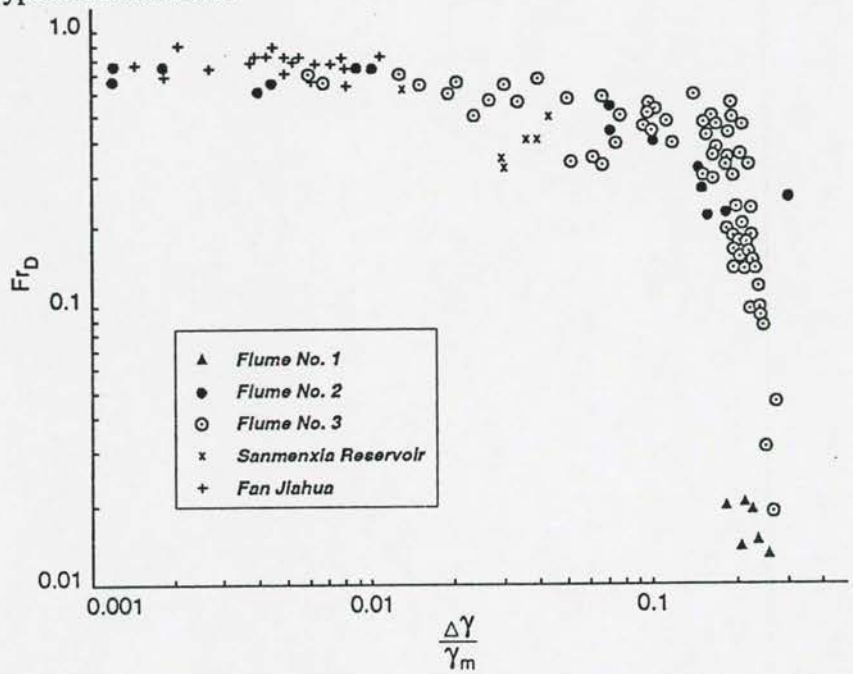

Figure 4.13-3 Densimetric Froude number and density difference ratio

Akiyama and Stefan (1987) found an approximate average densimetric Froude number of 0,68 at plunging. The Fr_D was only weakly related to the inflow densimetric Froude number (F_o) and the angle of channel divergence as shown in **Figure 4.13-4**.

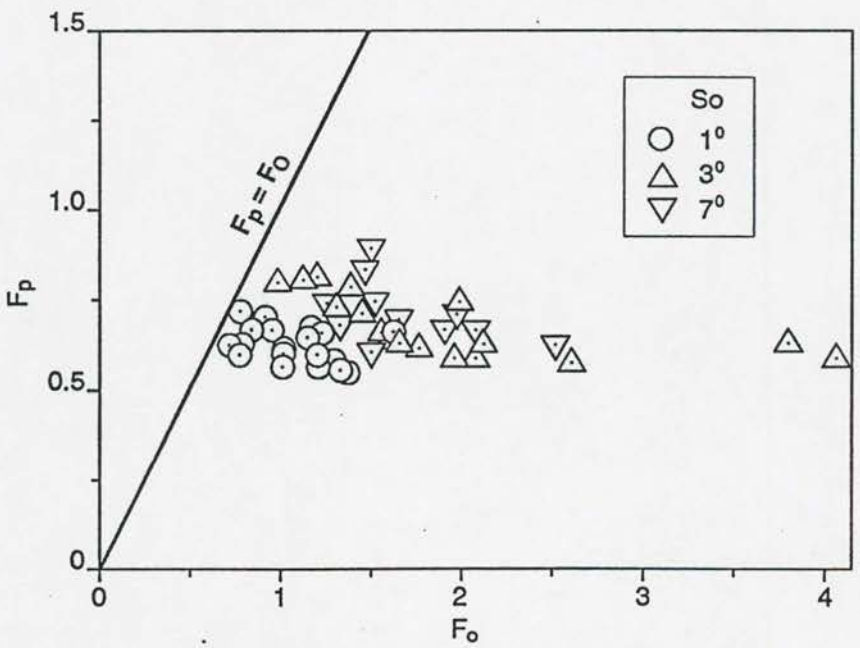

Figure 4.13-4 Densimetric Froude number (Akiyana and Stephan, 1987)

Savage and Brimberg (1975) considered the plunging phenomenon in terms of equations of motion for a gradually varying two-layer flow. The pressure distribution was considered to be hydrostatic and mixing was neglected. Different solutions for the interface profile were obtained depending on the bed slope and the relative importance of the two boundary shear stresses.

Denton et al (1981) carried out experiments on temperature-induced density currents and found that for mild bed slopes, interfacial and bed shear stresses are important, but for steep slopes $(S_o > 0{,}02)$, momentum balance conditions at the plunge point dictate a maximum densimetric Froude number criterion of 0,67.

Singh and Shah (1971) and *Philpott (1978)* also conducted flume studies and obtained $Fr_D \approx 0{,}7$ for the plunge point, although a range of $0{,}3 < Fr_D < 0{,}7$ was observed.

The criteria for plunging used by the above researchers indicate a general variation of observed values $0{,}1 < Fr_D < 0{,}7$, which shows the unreability of prediction of density current formation.

Previous studies have dealt with sloping channels, rectangular cross-sections of constant width, or triangular shapes that represent a reservoir geometry. Investigations of the formation of a density current based on the densimetric Froude number show considerable variation, as shown in **Table 4.13-1**.

Table 4.13-1: Densimetric Froude number (Fp) at plunging

Reference	Fp
Ford and Johnson (1980)	0,1 to 0,7
Itakura and Kishi (1979)	0,54 to 0,69
Singh and Shah (1971)	0,30 to 0,80
Kan and Tamai (1981)	0,45 to 0,92
Fukuoka et al (1980)	0,40 to 0,72
Farrell and Stefan (1986)	0,66 to 0,70
Akiyama and Stefan (1987)	0,56 to 0,89

Akiyama and Stefan (1987) showed that the angle of divergence also plays a role in estimating F_p, but the scatter of data is still considerable.

Rooseboom (1975) also proposed a method to predict the formation of a density current.

Consider a fluid element with density $\rho + \Delta\rho$ underneath a non-uniform fluid layer of density ρ. Under normal turbulent flow conditions, the element with length Δx is pushed forward owing to a pressure difference which exists across the element:

$$\Delta p = \rho g s_s . \Delta x \qquad (4.13\text{-}3)$$

with s_s = slope of surface line,

ρ = mass density of upper fluid.

In situations where density currents are important, the value of s_s is small and $\approx s_f$, the energy slope.

Due to the existing density difference, an additional pressure difference is generated across the element $= \Delta\rho g s_o \Delta x$ (s_o = reservoir bed slope).

The ratio

$$\frac{\text{"density" pressure}}{\text{"turbulent" pressure}} = \frac{\Delta\rho . s_o}{\rho . s_f} > 1 \qquad (4.13\text{-}4)$$

indicates the relative importance of density differences in the forward propulsion of sediments through reservoirs.

Using the Chezy equation, **Equation 4.13-4** can be rewritten to

$$\frac{\Delta\rho s_o C^2 R}{\rho v^2} \qquad (4.13\text{-}5)$$

with R = hydraulic radius, C = Chezy coefficient.

Density difference will therefore play an important role relative to turbulent suspension if the value of **Equation 4.13-5** is high, ie in cases of :

- large flow depths
- large density differences

- steep reservoir bed slopes
- low flow velocities.

Assuming $\frac{\Delta\rho}{\rho} \approx$ constant in all reservoirs, R = average water depth at full supply level, and taking the cross-sectional area as D^2,
the following dimensionless parameter was obtained:

$$\frac{s_o.C^2.D^5}{Q^2} \qquad (4.13\text{-}6)$$

with Q = discharge, with sufficient sediment transport capacity through reservoir.

The data in **Table 4.13-2** were used to calibrate **Equation 4.13-6**:

Table 4.13-2 Density current formation ***(Rooseboom, 1975)***

Reservoir	s_o	D(m)	Q(m^3/s)	C($m^{½}/s$)	$\left(\frac{So.C^2.D^5}{Q^2}\right)$
Lake Mead	0,00074	82	500	70	54 000
Sautet	0,018	50	200	63	56 000
Treska	0,004	10	9,5	55	13 000
Sengari	0,0049	16	1	59	18 000 000

With the limited data it is difficult to obtain a definite relationship. Conditions in Treska Reservoir represent a poorly developed density current and therefore a value of >10000 for the dimensionless parameter was assumed *(Rooseboom, 1975)*.

4.13.2 Prediction by means of minimum stream power principles

A flowing stream of water with a movable bed will always try to change the boundary conditions imposed on it until equilibrium conditions are reached. At equilibrium the energy dissipation per unit volume is minimized. In terms of applied stream power, this means that the flow can adjust the values of κ, k_s, D and s_f in **Equation 4.13-7**.

$$\tau = 30\ \rho g\ s_f\ D\ \frac{\sqrt{gDs_f}}{\kappa.k_s} \qquad (4.13\text{-}7)$$

Minimization of streampower will also be the reason why a turbulent stream dives to the reservoir bed to be transported as density current through the reservoir. At the plunge point (as indicated in **Figure 4.13-5**) input streampower for the density current should therefore become equal to or less than that of the turbulent inflow, assuming that the streampower in the upper layer is approximately zero as $v \to o$ in the upper layer.

At the plunge point from streampower continuity:
Streampower of turbulent inflow = streampower of density current

$$\int_{y_o}^{D} \rho g \bar{v} s_f = \int_{y_o}^{d} \Delta\rho g \bar{v} s_o \qquad (4.13\text{-}8)$$

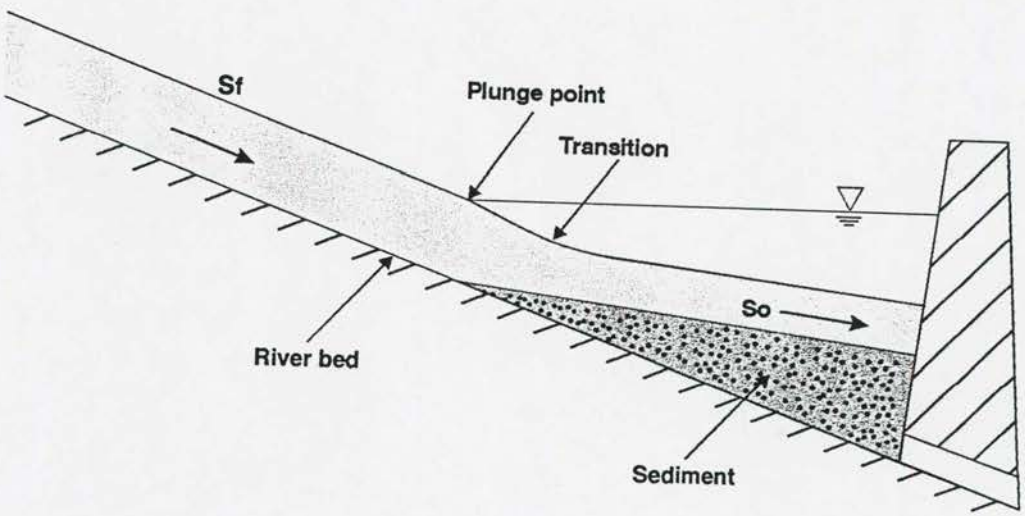

Figure 4.13-5 Plunge point characteristics

Therefore, for a density current to form it is expected that:

$$\frac{\Delta\rho g Q s_o}{\rho g Q s_f} \leq 1 \quad \text{and from continuity this simplifies to} \qquad (4.13\text{-}9)$$

$$\frac{\Delta\rho . s_o}{\rho . s_f} \leq 1 \qquad (4.13\text{-}10)$$

Laboratory data on the plunge phenomenon is rather scarce since most experiments concentrated on uniform density current movement. As a preliminary test of **Equation (4.13-10)**, laboratory data of *Akiyama et al. (1987)* in which the density difference was created by temperature differences was used **(Figure 4.13-6)**. Verification of **Equation 4.13-10** to test for density current formation does indeed show that less streampower is used by the density current than by the turbulent open channel inflow. Furthermore, **Figure 4.13-5** shows that the densimetric Froude number does not provide an accurate means of predicting density current formation due to the large scatter in values. The general trend indicates a lower density current stream power value as the densimetric Froude number increases.

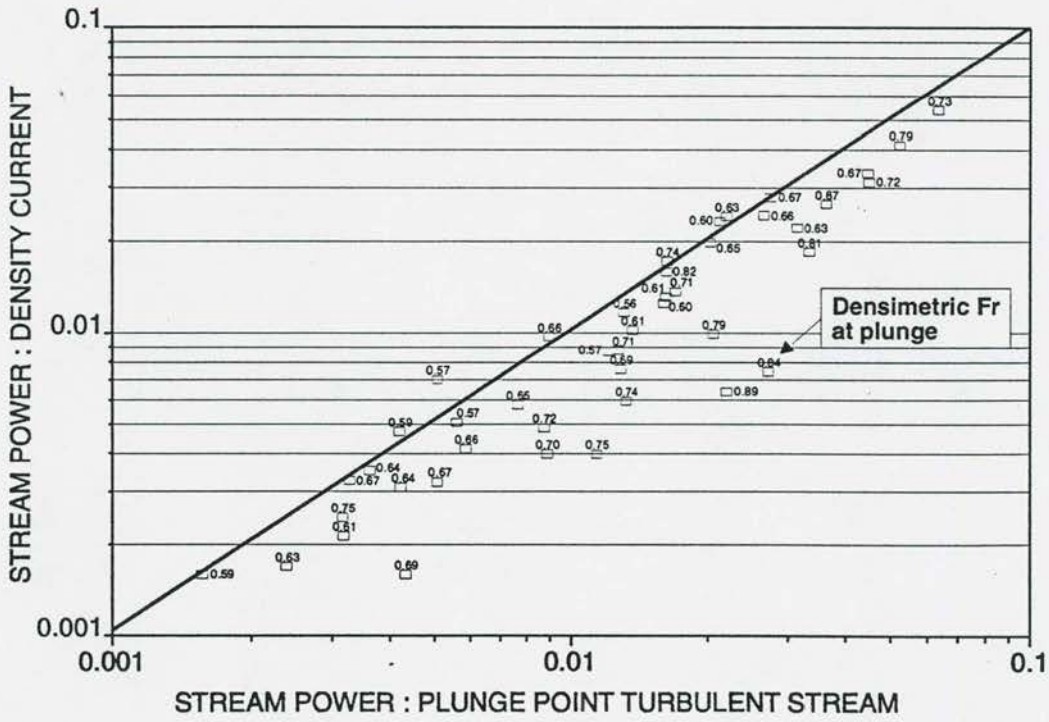

Figure 4.13-6 Density current formation and minimum stream power

Even if the stream power in the layer above the density current is added to that of the density current streampower, the difference will be negligible due to the small slope (due to the reservoir depth) and low velocity in the upper layer.

Equation 4.13-10 seemingly contradicts the **Equation 4.13-4** proposed by *Rooseboom (1975)*, who stated that larger density differences, larger slope s_o, and smaller slope s_f (of reservoir) will provide better conditions for density current formation. A steep bed slope in the reservoir and large density difference will indeed help to ensure the continuous movement of the density current through a reservoir, but what **Equation 4.13-10** in fact says is that at the plunge point a steeper approaching turbulent flow slope s_f will create favourable conditions for density current formation as the river meets the water mass in the reservoir. The high momentum of the inflowing river enables it to dive underneath the water mass, and once near the bed the density difference creates the density current flow and prevents a "hydraulic jump" of the submerged flow, with consequent turbulent suspended sediment transport through the reservoir. This is shown schematically in **Figure 4.13-5**.

Field and laboratory studies indicate that the density differences between riverflow/density current and reservoir water can be very small. The dominant variables therefore in the formation of a density current (given that there is some density difference), are the river and density current slope differences. On the other hand, the bed slope in the reservoir still needs to be steep enough for the propagation of the density current after formation.

Equation 4.13-10 also shows that for a given inflowing river slope, the reservoir bed slope at the plunge point has an upper limit at which turbulent mixing can prevent a density current from forming.

4.14 Laminar density currents associated with hyperconcentrated sediment transport

So far only the characteristics of turbulent density currents have been addressed. Laminar density currents also occur and are associated with hyperconcentrated sediment transport.

First, consider the differences between vertical velocity distribution in laminar and turbulent density currents as shown in **Figure 4.14-1** *(Cao, 1992)*.

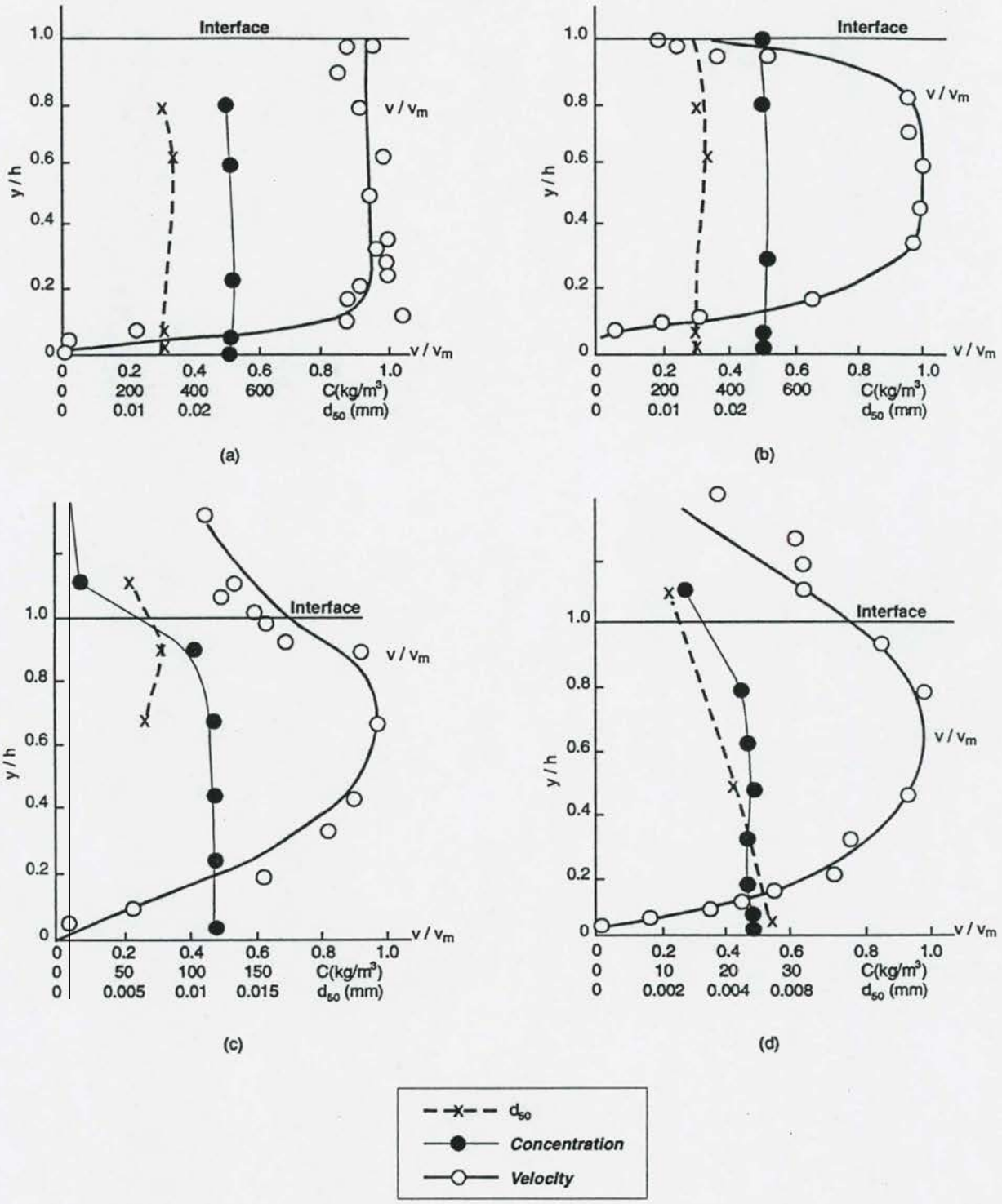

Graph	Q(l/s)	S(kg/m³)	Re_m	λ_m	K
(a)	2.5	520	11.6	9.26	107
(b)	2.5	410	70	1.71	120
(c)	2.5	124	1 250	0.15	188
(d)	2.5	24	38 300	0.041	

Figure 4.14-1 Typical density current velocity distribution (Cao, 1992)

Figures 4.14-1a and **4.14-1b** show typical laminar conditions in the density current. At Reynolds number (Re_n) < 43 (**Figure 4.14-1a**), the boundary condition at the interface is laminar, the resistance at the interface is relatively small, and the profile of velocity distribution of the density current is similar to that of open channel flow. The resistance at the interface is, however, not negligible as in homogeneous flow.

From flume studies, *Cao (1992)* established three types of plunging patterns (**Figure 4.14-2**):

Type A: Supercritical open channel flow with hydraulic jump transition at the plunge point.

Type B: Subcritical open channel flow with mild undulation transition to density current.

Type C: Hyperconcentrated homogeneous laminar open channel flow with still transition to density current. Two types C can be further observed:

$J_m = J_o$ (**Figure 4.14-2C**) and $J_m > J_o$ (**Figure 4.14-2C^1**). In the latter the plunging point is not stationary but keeps progressing until reaching the point where a non-uniform density current forms with the stable gradient $J_m = J_o$ when the plunging point becomes stationary.

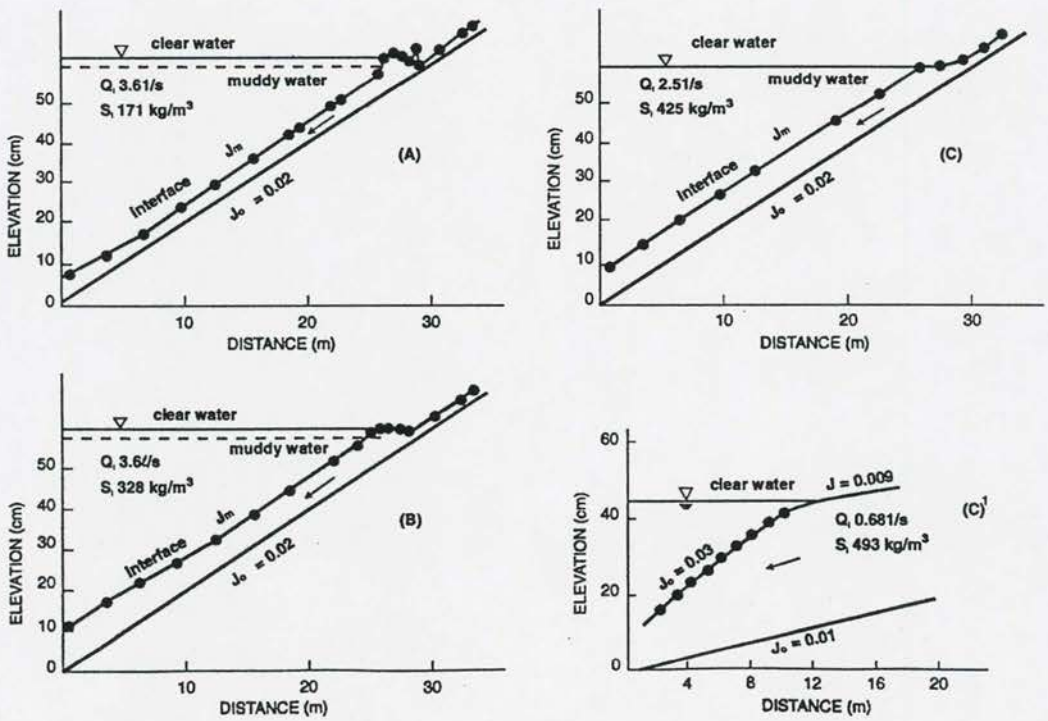

Figure 4.14 - 2 **Profile of interface of density current (Cao, 1992)**

The flow velocity, sediment transport and prediction of formation of laminar density currents can be derived following similar approaches as with turbulent density current flow in the previous sections.

4.15 Venting of density currents through reservoirs

When a density current reaches the dam, it can either be vented through bottom outlets or will "climb" up the dam wall and fall back to form a muddy pool. The climbing nature of the density current can be utilized to vent the density current at a high level. By either providing a siphon type outlet or curtain at the wall, the density current can be aided to flow out at even higher levels above the bed. This approach will especially be useful at existing reservoirs without bottom outlets and where density current flows are experienced.

Bell (1942) indicated the possibility of using a curtain near the dam in flume studies as shown in **Figure 4.15-1**.

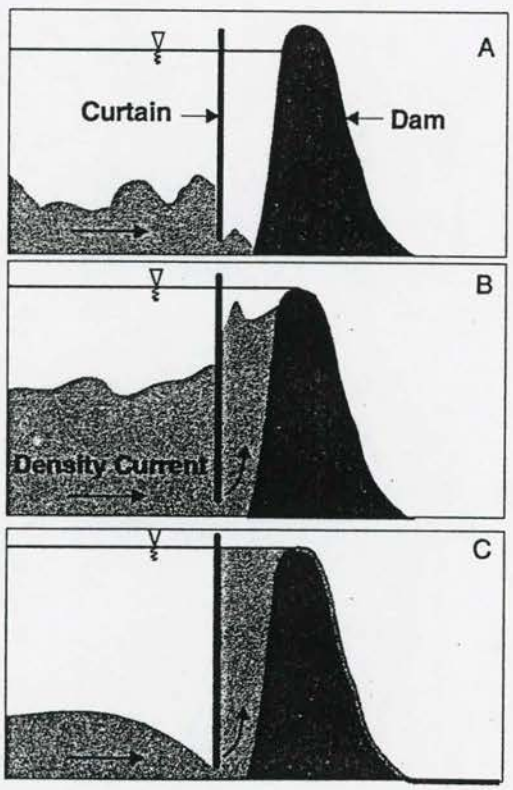

Figure 4.15-1 Density current climbing

Fan (1960) investigated the maximum height up to which a density current can "climb" to be vented and found that openings directly in the path of a density current were the most efficient.

Laboratory results indicated that the maximum height (h_L) to which a density current can climb to be vented through a circular outlet *(Wu, 1994)*:

$$h_L = \left(\frac{0{,}154\gamma Q^2}{\Delta\gamma g}\right)^{1/5} + \left(\frac{\gamma_o q^2}{2\Delta\gamma g h^2}\right) \qquad (4.15\text{-}1)$$

with
- q = unit width density current discharge (m^2/s)
- h = height of density current (m)
- Q = outlet capacity (m^3/s)
- γ = specific weight of clear water (kg/m^3)
- γ_o = specific weight of turbid water

The discharge capacity of outlets should equal the density current flow for maximum discharge of transported suspended sediments. Secondly the outlets should not be too high above the bed, but at a maximum elevation given by the potential energy of the density current, represented in the last term of **Equation 4.15-1**.

5. SEDIMENT DEPOSITION PROCESSES

5.1 General

Although delta formation has been extensively studied by many researchers and a number of empirical forecasting methods have been proposed, it is believed that delta formation is the end result of a member of complex reservoir sediment transport processes associated with non-uniform sediment and non-equilibrium transport, with the accompanying phases including deposition and re-entrainment. Prediction of delta function processes should therefore be based on the sediment transport processes within reservoirs.

Reservoir sedimentation leads to the formation of deltas which are often characterised by changes in bed slope and particle size at the transition from top-set to foreset deposits. The flood plane delta deposits are formed during significant discharge events and subsequently incised during pool drawdown to create a main channel **(Figure 5.1-1)**.

Multi-deltas may form due to seasonal drawdown of reservoirs *(Brown, 1958)*. Fine sediments are carried in suspension in most rivers in Southern Africa, and the nature of operation of reservoirs results in highly variable water levels, which makes the long-term establishment of a localised delta impossible. High sediment loads also occur at the end of dry seasons when reservoirs are generally at very low water levels. High inflows after a dry season and low water levels will initially lead to scouring (reworking) of the existing deltaic deposits, which are transported further into the reservoir into zones previously occupied mainly by clays and silts.

In some reservoirs (especially in South Africa) typical delta formation may be distorted by highly fluctuating water levels or because inflowing sediments are being deposited over a long distance along a narrow impoundment. However, there is typically an abrupt change in the particle diameter sizes at the limit of the deltaic zone as is also found in Chinese reservoirs. **(Figure 5.1-2)** *(Fan, 1992)*

5.2 Non-cohesive sediments

Deposition of non-cohesive sediments is a function of the sediment transport capacity as discussed in **Chapter 3**.

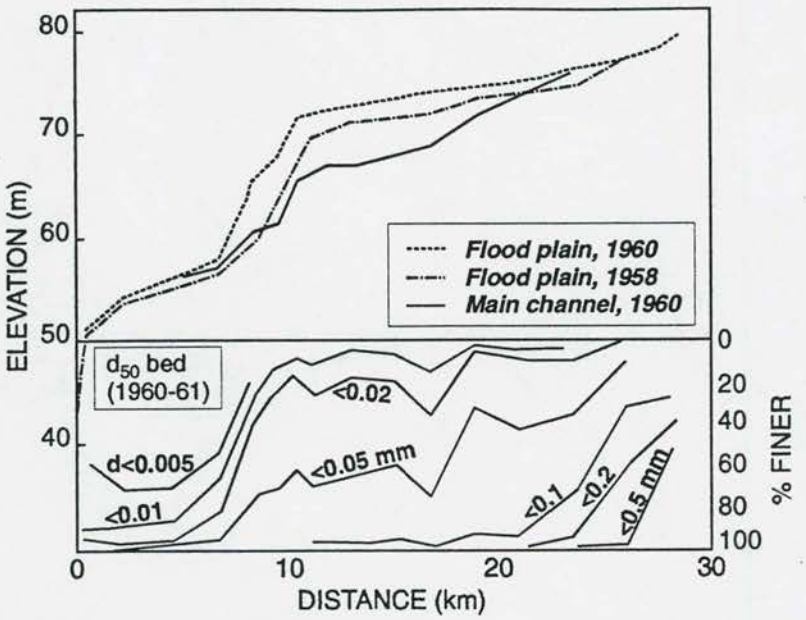

Figure 5.1-1 **Delta deposition and variation in particle size of bed sediment in Gaunting Reservoir (Fan, 1992)**

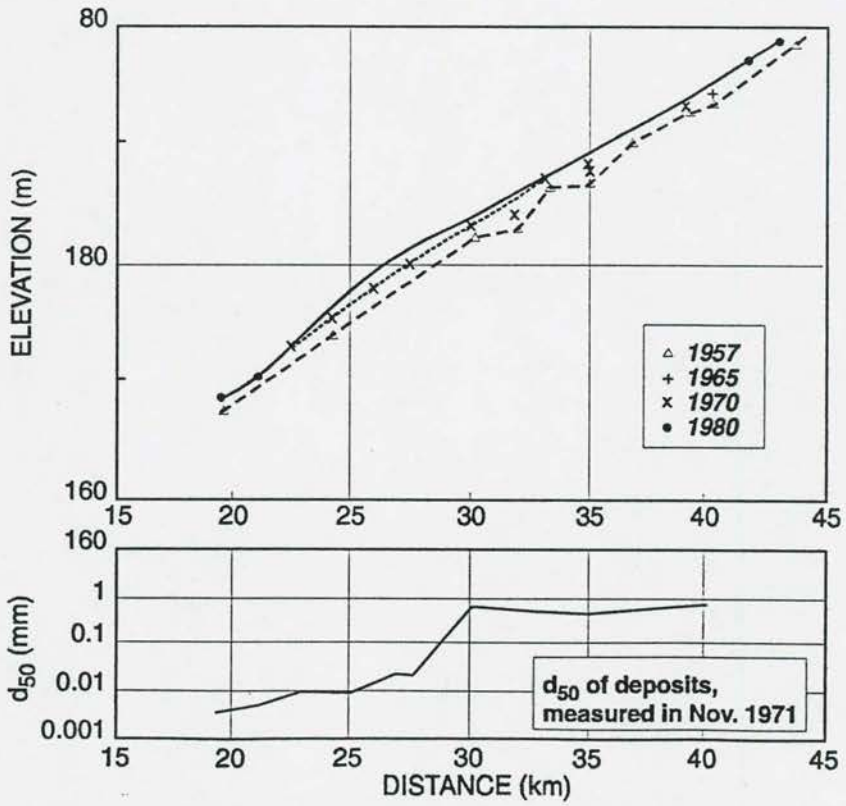

Figure 5.1-2 **Longitudinal profile of Shanyiujiang Reservoir and variation in particle size**

5.3 Cohesive sediments

5.3.1 General

Cohesive sediments are very fine ($d < 0{,}002$ mm) negatively charged clay minerals which have a certain capacity to absorb cations. When they are in colloidal suspension, the repulsive forces between these particles will dominate and they can remain in suspension for a long time. Cohesion occurs when repulsion is reduced by reduced distance, decreased temperature, or increasing salt concentration, resulting in the formation of flocs and settling.

Cohesive sediments are normally transported as suspended load. Although many models have been developed for suspended sediment transport, modelling of cohesive sediment as found in most South African reservoirs is still not well understood.

Deposits of cohesive sediment are held together by the bonding force of positive and negative ionic charges on clay minerals. The settling rate of cohesive sediments is affected by flocculation. Flocs and aggregates are formed by the bonding force of positive and negative ionic charges of the clay minerals and occurs when a river flows into a saline reservoir (salt concentrations < 400 to 600 ppm are sufficient) *(Sloff 1991)*, or at high concentrations of cohesive sediment. Collisions of the sediment particles are caused by:

- Brownian motion parakinetic flocculation

This is a slow process only significant at concentrations above 10g/ℓ, and weak aggregates are formed.

- Velocity gradients/shear motion: ortokinetic flocculation

Only particles with similar sizes aggregate, forming strong, dense aggregates.

- Settling velocity differences of particles

Such differences cause weak aggregates.

The last two collision-causing mechanisms are the most significant.

The order of processes are: clay particles form flocs, flows form floc aggregates, which form aggregate networks on the bed.

When no aggregate break-up occurs and aggregation is well advanced, the median settling velocity w is a function of the suspended solid concentration C_s.

$$w = a(C_s)^b \tag{5.3-1}$$

Values for b have been found equal to 1 for montmorillonite *(Migniot, 1968)* and $b = 4/3$ for mixed mineral mud *(Krone, 1962)*. The settling velocity increases with concentration to 10 g/ℓ. At higher concentrations hindered settling occurs *(Piece and Williams, 1966)*.

Slumping, the flow of disturbed bed material following the failure of an underwater slope, caused by flushing or deposition, occurs when the downslope component of buoyant weight of the material above the rupture plane exceeds the resisting force mobilized by the sediment *(Mitchell et al, 1972)*. This phenomenon is partially responsible for the horizontal deposition patterns found in reservoirs.

Photograph 5.3-1: Mbashe Reservoir sediment slumping

5.3.2 Basic properties of cohesive sediment

Cohesive sediments are characterised by two main properties: plasticity and cohesion, due to surface physico-chemical forces on the sediment particles smaller than 2 microns *(Partheniades, 1986)*. Under the influence of these forces and fluvial conditions, colliding fine particles stick to each other forming agglomerations known as flocs, with sizes and settling velocities exceeding by orders of magnitude those of the individual particles. The rate of floc growth is determined by the concentration, physico-chemical properties of the sediment-water system and the flow turbulence, while forces counteracting floc growth include interflow collision, drag shear stresses during deposition and high near-bed shear stresses in a river.

Settling primary flocs may collide with others to form higher-order aggregates. Three classes of particle aggregates considered are: the primary floc, floc aggregates consisting of a number of flocs, and aggregate networks consisting of a number of floc aggregates as found in recent fine sediment deposits, schematically shown in **Figure 5.3-1**.

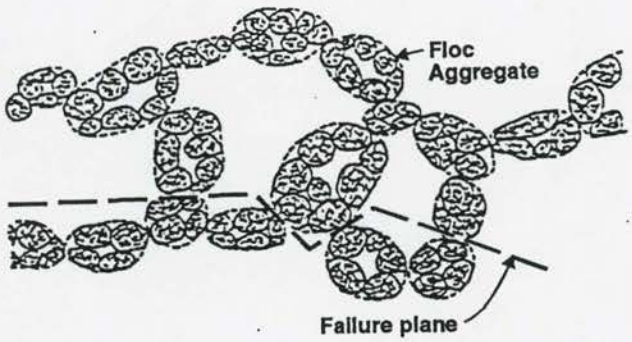

Figure 5.3-1 Schematic picture of flocculated recently deposited cohesive bed

The boundary between cohesive and cohesionless sediment is, unfortunately, not clearly defined and generally varies with the type of sediment. However, dominance of interparticle cohesion over gravitational force increases with decreasing particle size. Thus the effect of cohesion on the behaviour of clays ($d_{50} < 2\mu m$) is much more pronounced than on silts (2 to 60 μm) *(Mehta, 1989)*.

Several studies have been carried out on the effect of suspended sediment concentration on floc formation during deposition. *Quinn (1980)* found the settling velocity to be directly related to sediment concentration in quiescent water. *Partheniades (1986)*, however, concluded that "Deposition experiments, however, in quiescent water may reveal some important aspects of flocculation, ..., but they bear little resemblance to the depositional processes in flowing water. In quiescent settling all aggregates eventually deposit and a settling interface is formed marking the lower limit of the settling velocity of the flocs .... In flowing waters ... no such interface is observed; the far-bed turbulence constitutes the dominant mixing mechanism while the highest floc disruptive shear stresses are encountered in the near-bed region."

5.3.3 Flocculation and hindered settling

The effects of suspension concentration, salinity and the flow turbulence on aggregate settling velocity are found the be the most important factors. In general the settling velocity increases with concentrations up to 5 000 to 10 000mg/ℓ, above which it begins to decrease with increasing concentration as a consequence of hindered settling. Hindered settling occurs when the sediment forms a nearly continuous network through which pore water must escape slowly upwards for settling to continue. *(Mehta, 1989)*.

Settling velocities of flocculated cohesive sediments typically increase with increasing salinity up to 10 points per ton *(Krone, 1962)*. *Krone (1962)* found settling velocities from flume experiments only about 20 percent of those from quiescent settling tests.

In this dissertation sediment transport equations were calibrated assuming individual particle settling velocities as determined by Stokes' law for fine sediment. Flocculation was not considered, as it is believed that with turbulent flow conditions, flocculation will probably not

occur. This assumption was confirmed to some extent by the calibrated sediment transport equations using reservoir data obtained under a wide variety of conditions.

Although so-called sink terms for deposition in terms of settling velocity (often related to sediment concentration to include the effect of flocculation) have been established, it is believed that deposition of cohesive and non-cohesive sediment is controlled by the sediment transport capacity of specific flow conditions only. A sediment deposition function can only be related to the transition from non-equilibrium to equilibrium transport, which is not instantaneous as with non-cohesive sediment.

5.4 Reservoir cross-section deformation

From reservoir basin surveys it is evident that cross-sections change systematically under conditions of deposition and scouring. During flushing operation and complete draw-down of water levels, the retrogressive erosion scours a channel in the deposits, while no removal of overbank deposits is possible. Although the scoured channel and deposition geometry and scouring rates might be complicated due to sediment cohesion, it should be possible to describe these changes using the principles of minimization of stream power. In most mathematical models, however, the geometry of cross-sections is adjusted by empirical relationships based on data from the field or physical models.

The stream power being applied in maintaining motion reaches a very high maximum value along the bed. Whenever alternative modes of movement exist, the stream will follow that mode which requires the least applied power.

Across a section with width B the applied power along the bed is represented by:

$$\frac{\rho g s \sqrt{gDs}.B}{\kappa y_o} \qquad (5.4\text{-}1)$$

with

s	=	slope
D	=	depth of flow
κ	=	Von Kármán coefficient
$y_o \propto R_o$	=	integration constant
R_o	=	radius of turbulent eddies formed along the bed

In determining the dimensions of a channel, the laws of conservation of mass for both water and sediment as well as the equations of motion have to be satisfied. That particular combination which corresponds to minimum applied stream power will determine the actual channel shape. As the major portion of the applied power is used along the bed, the total power input (ρgsQ) may be taken to represent applied power along the bed. Equilibrium cross-sections in stable alluvial channels therefore correspond to conditions where (ρgsQ) reaches a minimum value *(Chang, 1980)*.

In unsteady channel conditions, when the discharge or slope changes, the total power input changes and the applied power changes accordingly:

$\frac{\rho gsD\sqrt{gDs}.B}{\kappa\, y_o}$ represents the power being applied across the stream per unit distance.

If the power input increases, this could be accommodated by:

- increase in slope (s) by taking a shorter route
- increase in depth (D) by scouring of stream bed
- increase in width (B)
- decrease in κ with increased sediment transport
- smoothened streambed by decreasing y_o

The relative change in each variable will depend on the relative ease with which a given stream can adjust each of the variables.

Stable bank slope (m_c)

For rivers, a number of side slope criteria are given in textbooks. Typical m_c values are listed in **Table 5.4-1**.

Table 5.4-1: Critical bank slopes for river conditions (units: 1 to values in table) ***(Deng, 1994)***

Mountain reaches	Hillside reaches	Middle reaches	Lower reaches			Wandering reaches
			Clay bank	Loam	Sand	
1,25 - 1,5	1,5 - 2,0	2 - 3	2 - 3	3 - 4	4 - 6	6 - 12

It is more difficult to determine m_c values for a reservoir, where m_c is the maximum side slope at which sediment particles on an incline attain their threshold condition of motion due to tractive force τ_c . $m_c \propto \frac{1}{\tau_s}$ and $\tau_c = f$ (specific weight (γ_d) of deposits) *(Deng, 1994)*. Deposition m_c values for several reservoirs expressed in terms of relative density $\left(\frac{\gamma_d}{\gamma_s}\right)$ are shown in **Figure 5.4-1**. (γ_s = specific weight of sediment).

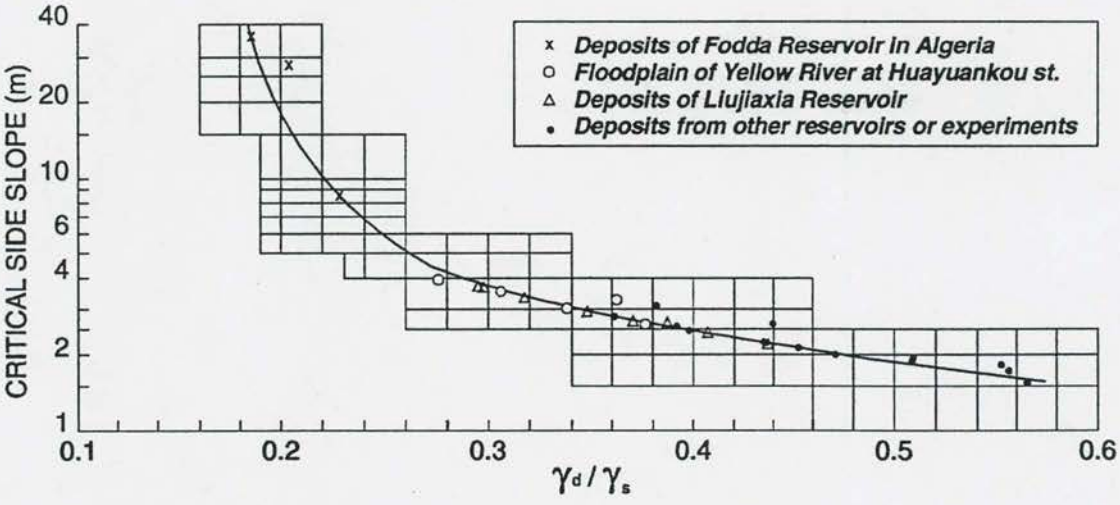

Figure 5.4-1 Critical bank slopes of deposited sediment

5.5 Sediment density

Sediment densities of as low as 200 to as high as 2 000 kg/m³ have been observed in reservoirs. Prediction of the correct sediment densities as well as changes in density with

time can be crucial in establishing reliable sediment deposition profiles in a reservoir. The hydraulics of reservoir sedimentation are not only affected by different sediment densities following from deposition processes; especially during re-entrainment of cohesive sediments, sediment densities play a dominant role in determining critical conditions for mass erosion, as will be shown in **Chapter 6**. Sediment densities are interrelated with several other hydraulic processes within a reservoir and are of such importance that an in-depth review of theory and verification with field data is included in this chapter.

Sediment deposits consolidate in time forming a dense, cohesive mass with low erodibility *(Delft, 1992)*. The density is a function of:

- the weight of overburden
- particle size and distribution
- the degree of exposure to drying/reservoir operation (most significant factor)
- permeability
- the age of deposits and consolidation rate

A widely used method to predict sediment density has been developed by *Lane* and *Koelzer* (1943) modified by *Miller (1953)*, and *Lara and Pemberton (1965)*. Sediment consolidation is described as a function of time, sediment characteristics and reservoir operation based on the analysis of more than 1300 field samples and shown in **Figure 5.5-1**.

The method is described by *Strand (1974), Zhang and Qian (1965)* and *Annandale (1987)* and was applied by *Braune (1984)* to South African reservoirs, where it was found to be reliable.

Reservoir operators were classified according to type as indicated in **Table 5.5-1**.

Table 5.5-1: Reservoir operation classification

Type	Reservoir operation
1	Sediment always submerged or nearly submerged
2	Normally moderate to considerable reservoir draw-down
3	Reservoir normally empty
4	Riverbed sediments

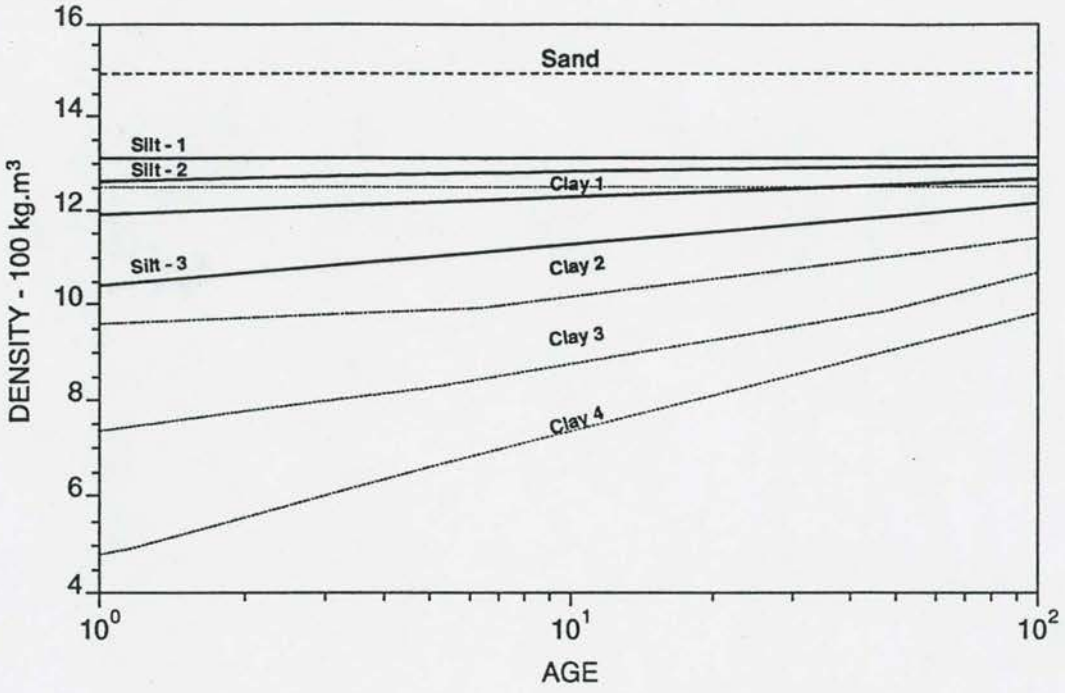

Figure 5.5-1 Sediment consolidation, sediment characteristics and submergence (Mahmood, 1987)

The initial density of sediment (kg/m³) deposits can be estimated from:

$$\rho_0 = (\rho_c p_c + \rho_m p_m + \rho_s p_s) \qquad (5.5\text{-}1)$$

with ρ_c, ρ_m, ρ_s = densities of clay, silt and sand respectively, obtained from field data

and p_c, p_m, p_s = percentages of clay, silt and sand, respectively, of the incoming sediments within each size range (American Geophysical Union) **(Table 5.5-2)**:

Table 5.5-2: Sediment type classification

Sediment type	Size range (mm)
Clay	<0,004
Silt	0,004 to 0,062
Sand	0,062 to 2,0

Initial sediment densities are given in **Table 5.5-3**.

Table 5.5-3: Initial weight of sediment deposits

Reservoir type	Initial weight (kg/m³)		
	ρ *clay*	ρ *silt*	ρ *sand*
1	416	1 120	1 550
2	561	1 140	1 550
3	641	1 150	1 550
4	961	1 170	1 550

Figure 5.5-1 reflects the importance of reservoir operation and frequent flushing in terms of flushing efficiency. Younger sediments can be remobilised more easily either by flushing, water injection or dredging *(Delft, 1992)*.

Reported observed sediment densities in reservoirs vary as follows *(Braune, 1984)*:

Submerged clay and silt:	320 to 960 kg/m³
Air-dried fine sediment:	1 200 to 2 000 kg/m³
Dry sand and mixed sediments:	1 360 to 1 600 kg/m³

Spatial density variation of sediment was reported by *Heineman (1972)*, who found a strong correlation between density and clay content and a gradual increase in density from 560 kg/m³ at the dam to 1 470 kg/m³ at the upstream end of a reservoir basin.

Generally, the densities increase with depth up to about 1,2 m to 1,5 m and remain fairly constant at greater depths *(Vanoni, 1975); (Braune, 1984)*. *McHenry (1980)* also found constant densities below 2 m depth in a reservoir. **Figure 5.5-2** shows measured density changes with depth in Lake Mead with increasing density with depth.

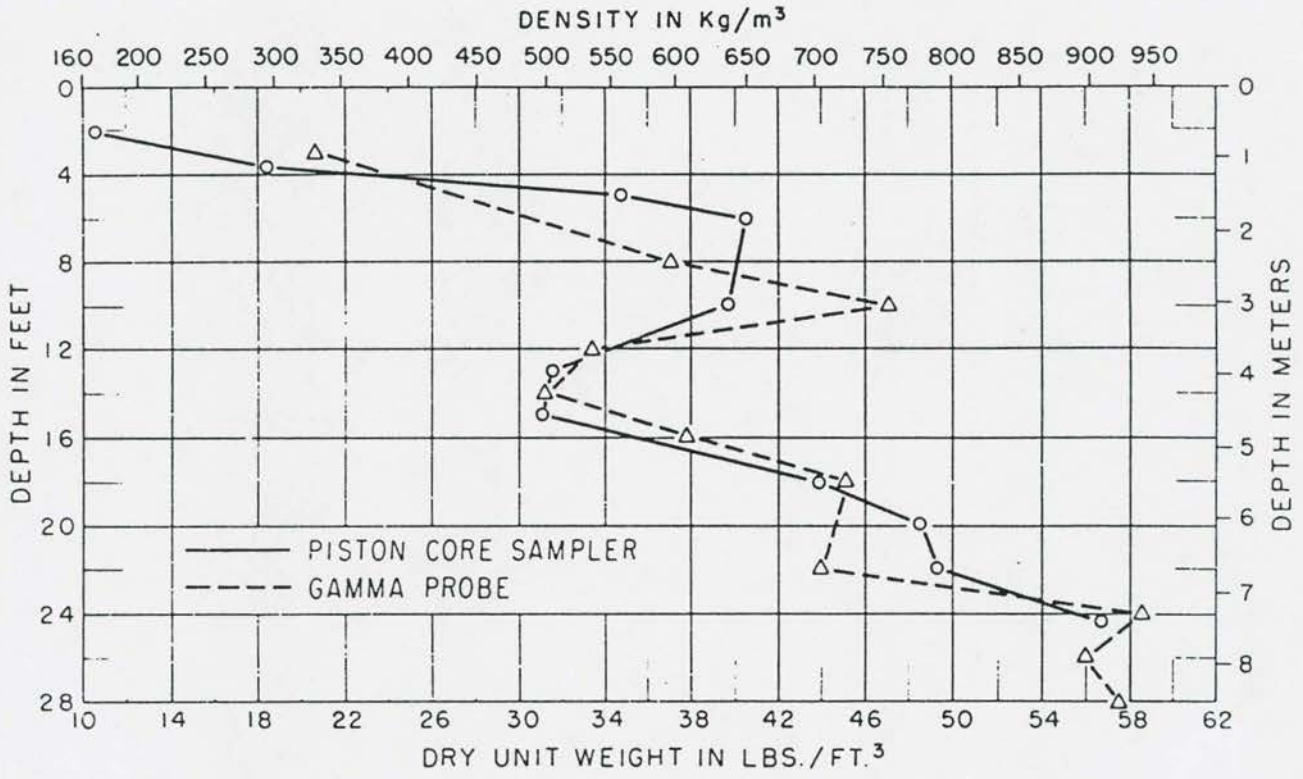

Figure 5.5-2 Observed sediment density changes with depth in Lake Mead

Most of the reservoirs evaluated by *Braune* are regularly exposed to air drying. Observed densities could be related to spatial sediment size distribution and reservoir operation. A summary of data for these reservoirs is given in **Figures 5.4-3** to **5.5-8**. Due to the very limited data base on South African reservoir sediment densities, the data will be discussed in more detail:

Krugersdrift Reservoir (1980) has a long narrow basin and is often empty. Twenty one samples were taken by Selby tube on both sides of the water to a maximum depth of 2,2 m with average penetration 75 % of the full depth **(Figure 5.5-3)**.

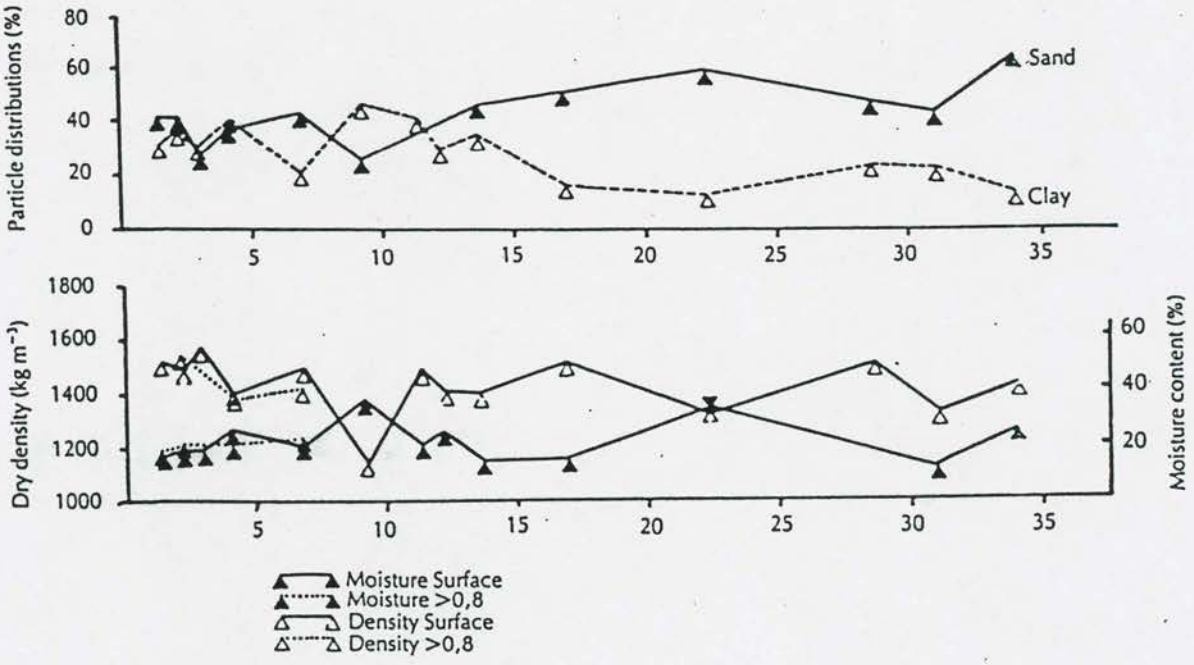

Figure 5.5-3 Observed bed sediment density at Krugersdrift Dam (1980)

Beervlei Reservoir (1980) was empty when sampled and 39 samples were taken to a maximum depth of 2,1 m, with 40 % penetration **(Figure 5.5-4)**.

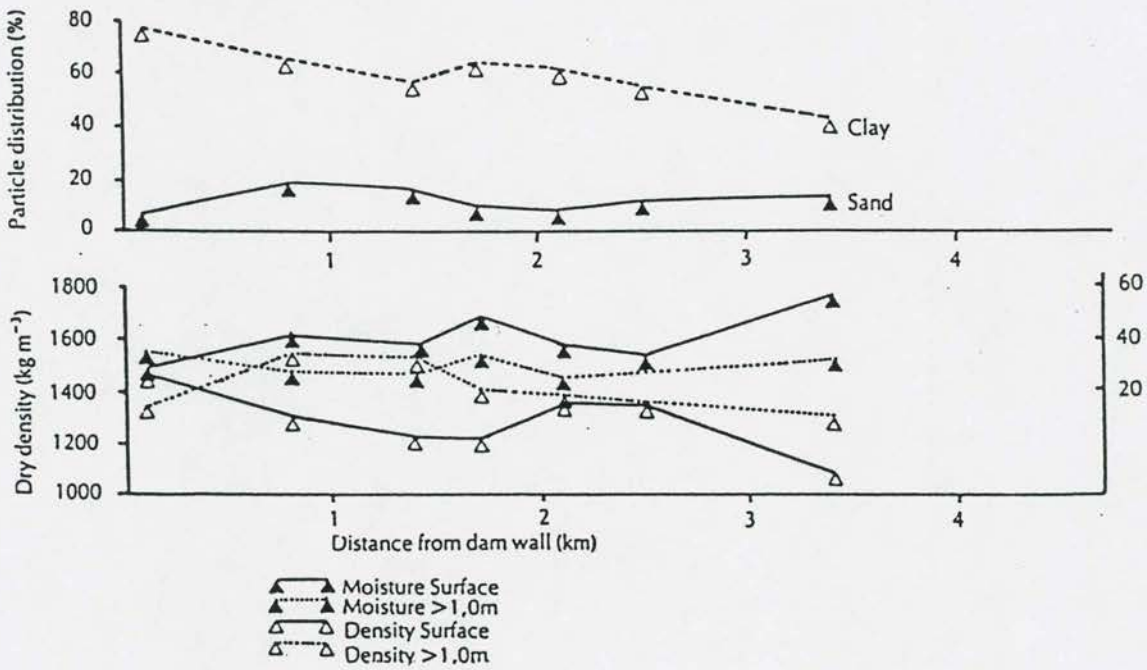

Figure 5.5-4 Observed bed sediment density at Beervlei Dam (1980)

Van Rynevelds Pass Reservoir (1980) was almost empty, and 42 samples were taken with penetration 15 to 50 % of total sediment depth **(Figure 5.5-5)**. Sampling was also carried out in 1960 with sediment densities depicted in **Figure 5.5-6**.

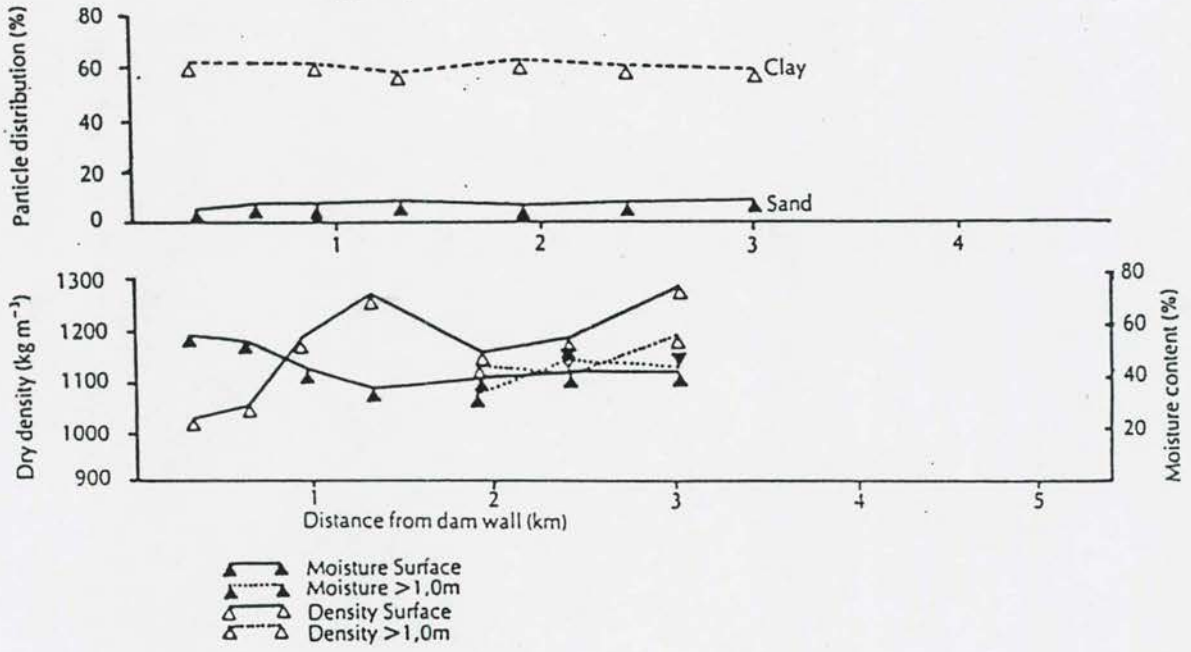

Figure 5.5-5 Observed bed sediment density at Van Rynevelds Pass Dam (1980)

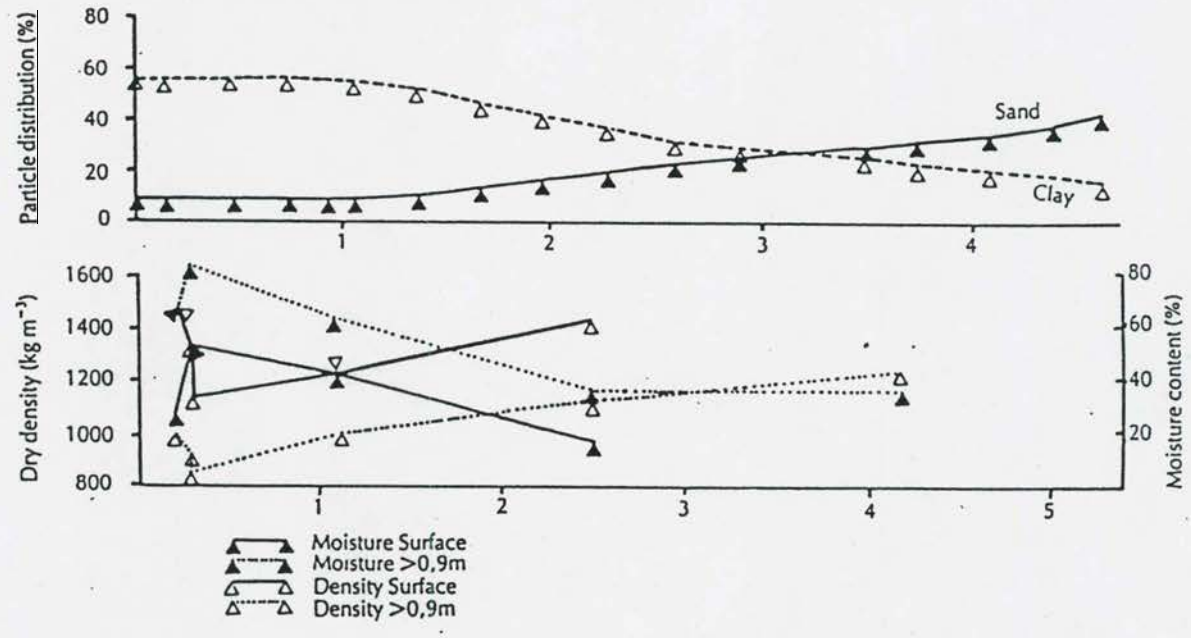

Figure 5.5-6 Observed bed sediment density at Van Rynevelds Pass Dam (1960)

Grassridge Reservoir *Rabie (1960)* sampled 22 positions to a maximum depth of 3 m, with 45 % penetration, only in the dried basin areas **(Figure 5.5-7)**.

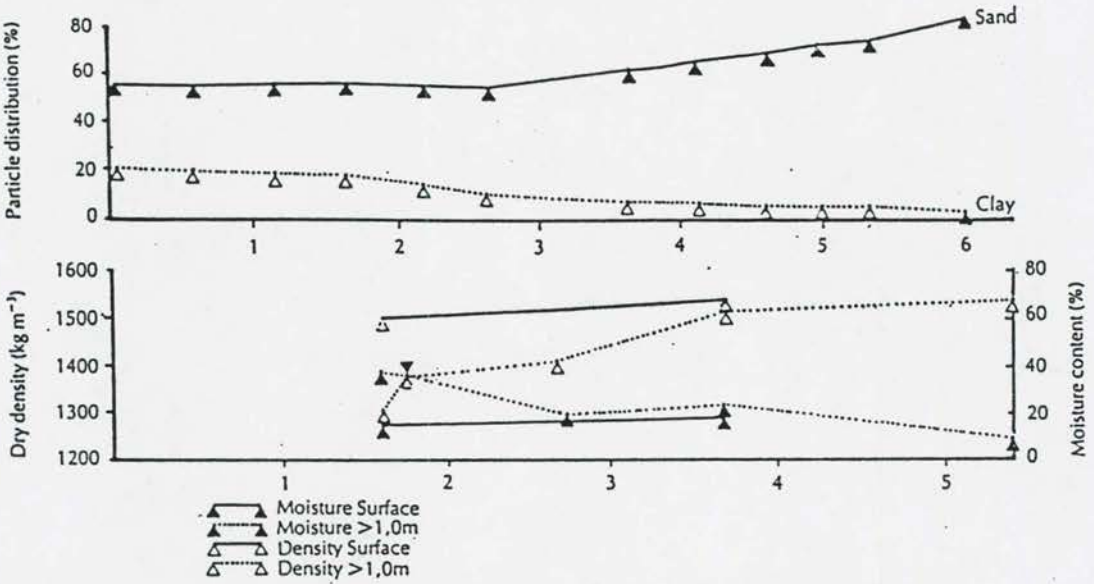

Figure 5.5-7 Observed bed sediment density at Grassridge Dam (1960)

Lake Arthur *Lewis, (1936)* obtained a maximum penetration of 10,4 m **(Figure 5.5-8)**.

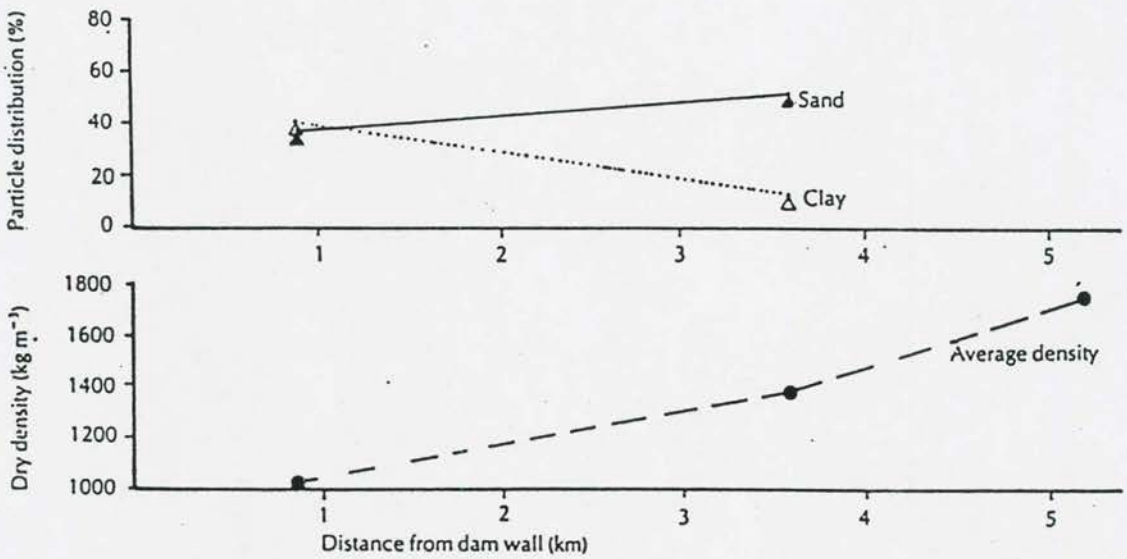

Figure 5.5-8 Observed bed sediment density at Lake Arthur (1936)

For a clay content of around 45 % in Lake Arthur, non-exposed surface samples had densities (1936) as low as 609 kg/m³, while deeper samples had consolidated to 900 kg/m³. Sandy samples at the upper basin (clay content < 10 %) had a density of 1 600 kg/m³.

Gariep Reservoir *(Potgieter, 1979)*

Based on observed sediment inflow and outflow over a period of 8 years and a basin survey in 1979, an average dry density of 1 060 kg/m³ was obtained.

As part of an attempt to relate soil mechanical characteristics to hydraulic behaviour of Welbedacht Reservoir's flushing channel, sediment densities were also obtained in this study, as described in **Chapter 6**. Owing to compression of sediment in the core pipes during sampling, true densities cannot be given, but they are lower than the "normal" long-term density of 1 350 kg/m³ generally assumed in South Africa. The sampled sediment had variable periods of consolidation of < 1 year to say 10 years, always saturated, with mostly fine sediment. Recent deposits and sand layers were also analysed and the variability of data is shown in **Figures 5.5-9** and **5.5-10**. (The locations of the sampling positions are indicated in **Figure 6.5-1**, **Chapter 6**.)

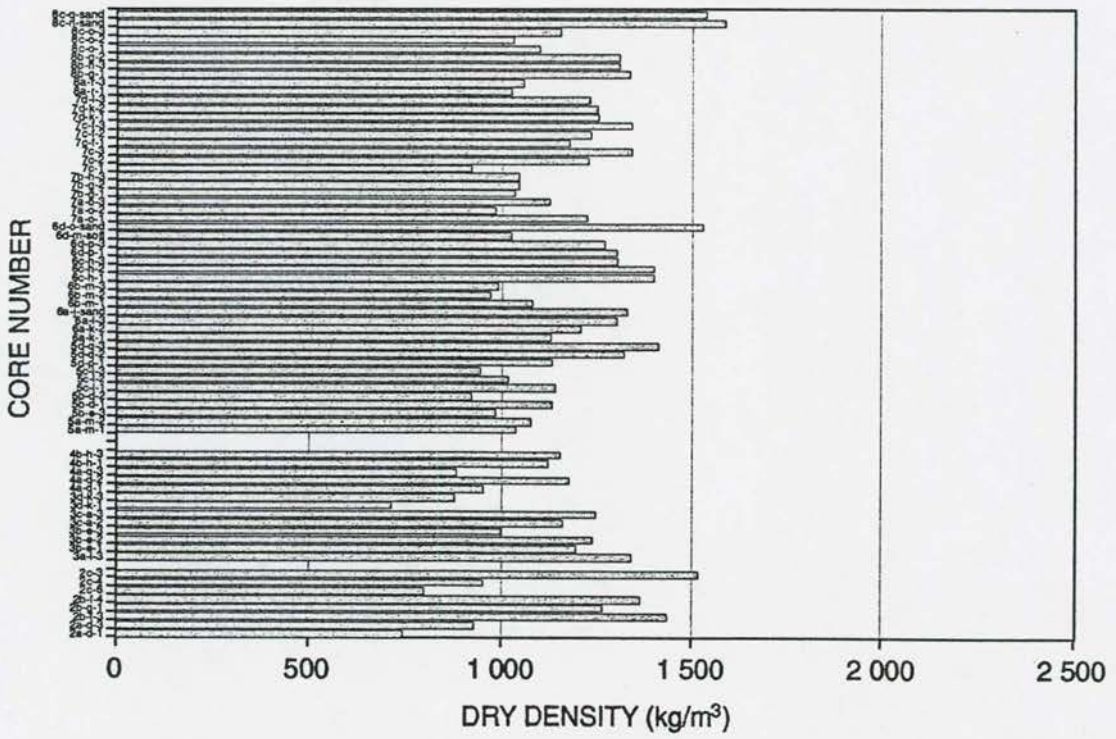

Figure 5.5-9 Welbedacht Reservoir sediment densities in flushing channel bed and banks

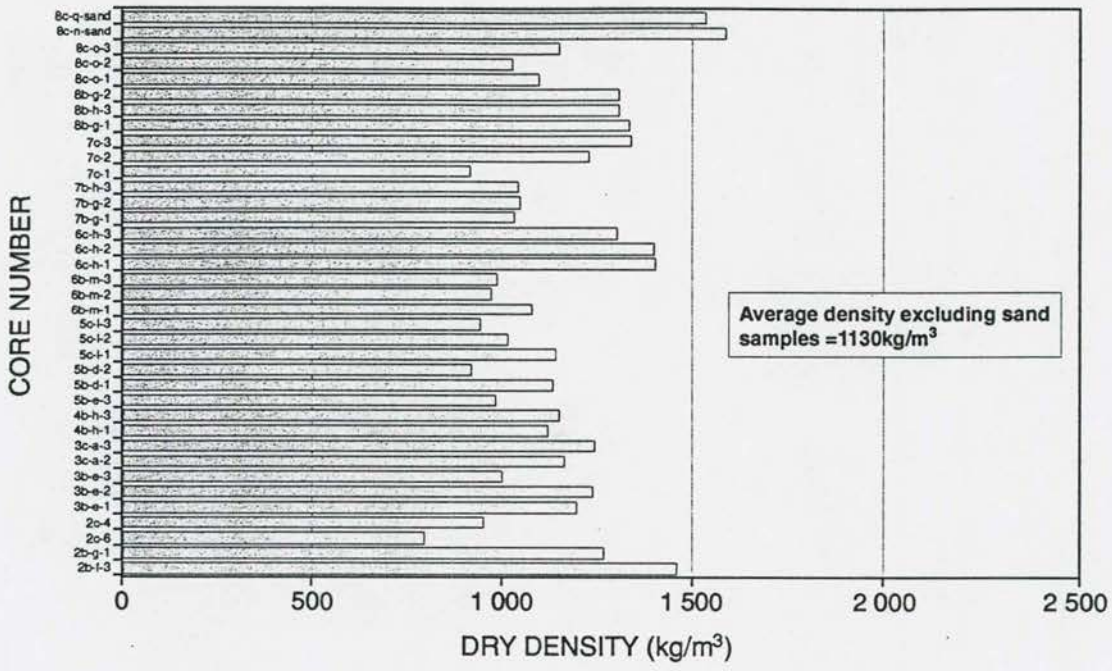

Figure 5.5-10 Welbedacht Reservoir sediment densities in flushing channel bed

5.6 Sediment consolidation

5.6.1 Review of available prediction methods

Bottom sediments undergo consolidation, an increase of bonding forces by overburden, and slow rearrangement of aggregates, so-called thixotropic effects. Overburden crushes the deposited weak aggregates, and their strength increases with depth. Rapid consolidation occurs in sediment formed from dilute suspensions, while hindered consolidation occurs when the bed is formed from suspensions with concentrations $> 10 g/\ell$ (and is caused by restricted upward movement of pore water by diminishing permeability and increasing path length) *(Sloff, 1991)*.

While compaction of cohesive beds is permanent, shrinkage is recovered upon submergence. Gelling and microbiological alteration of pore water composition occurs with time *(Krone, 1962)*.

Prediction of consolidation is presented by *Samogyi (1985), Hayter (1983), Thom and Parsons (1980)*, and *Owen (1970)*. Consolidation of deposits is included in some mathematical

models. *Hu (1990)* used the non-linear consolidation theory of *Gibson et al (1967, 1984)* in his model. This theory is widely used in sedimentation/consolidation problems.

The sediment density increase with time is given by:

$$\rho_T = \rho_0 + K\log_{10}T \qquad (5.6\text{-}1)$$

with ρ_T = density after T years of compaction
ρ_0 = initial density
K = constant dependent upon size analysis of the sediment

In order to accommodate continuous sedimentation and related different compaction times, *Miller (1953)* developed an approximation of the integral for determining the average density of all sediment deposited in years, assuming constant sediment input with time:

$$\rho_T = \rho_0 + 0{,}4343K_o\left(\frac{T}{T-1}\left(\log_e T\right) - 1\right) \qquad (5.6\text{-}2)$$

with K_0 = (K-Clay . clay fraction) + (K-silt . silt fraction) + (K-sand . sand fraction), and K_o-values presented in **Table 5.6-1**.

Table 5.6-1: Consolidation coefficients

Reservoir type	K-Clay	K-Silt	K-Sand
1	256	91	0
2	135	29	0
3	0	0	0

The sediment density up to a 100 year period can be estimated with this method.

Although the theory of consolidation has been well established in the geotechnical engineering field, practical application in the case of large reservoirs can be problematic due to a number of reasons:

- Consolidation calculations have to be carried out in terms of a two-dimensional plan view of the reservoir due to the variable depths of sediment.

- The sorting process and distribution of sediment during deposition, as well as scoured depths, need to be accounted for.

- The reservoir pool level and drying/wetting of the sediment should be taken into account.

- Consolidation of each layer as it was deposited needs to be modelled with time.

Although it is possible to incorporate all of the above in reservoir sedimentation and consolidation modelling, the process will take up considerable computing time, while calibration of such a model with field data (especially with high contents of silt and clay) will be very difficult considering the lack of accuracy with which sediment transport can be modelled.

Rooseboom (1975) plotted the change in sediment volume with time for different reservoirs, and found a logarithmic relationship with time as is generally found in consolidation processes. An arbitrary reference time of 50 years was selected as reference volume with assumed density to express the sediment volume as dimensionless relationship: Vt/V_{50} versus log t, with Vt = sediment volume after t years and V_{50} the sediment volume after 50 years. After 50 years the density does not change rapidly with time and can be estimated with some degree of reliability. Fifty years is also in many cases the approximate economic life of a reservoir, and a longer period was difficult to select owing to the limited number of reservoir basin data sets exceeding 50 years (even today).

The updated (1995) sediment volume changes of South African reservoirs with time still show features similar to those found in 1974, and are indicated in **Figures 5.6-1** and **5.6-2.**

Using the latest survey data for reservoirs with large trap efficiencies only, it is possible to derive Vt/V_{50} relationships as indicated in **Table 5.6-2.**

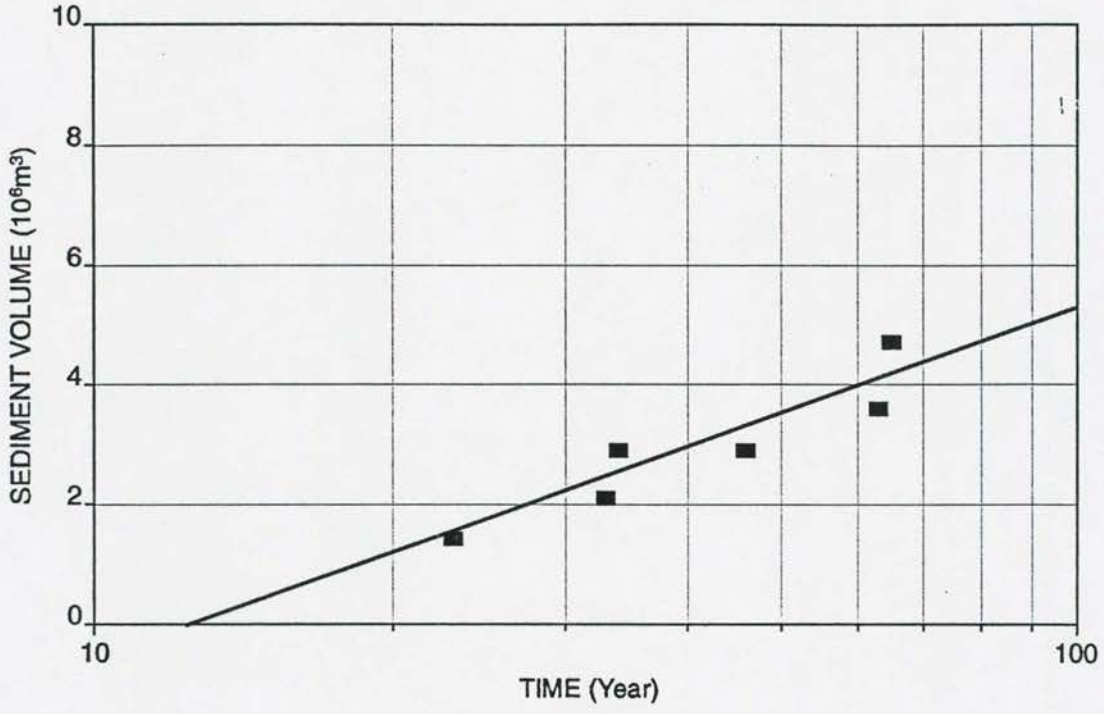

Figure 5.6-1 Sediment volume changes with time in Prinsrivier Reservoir

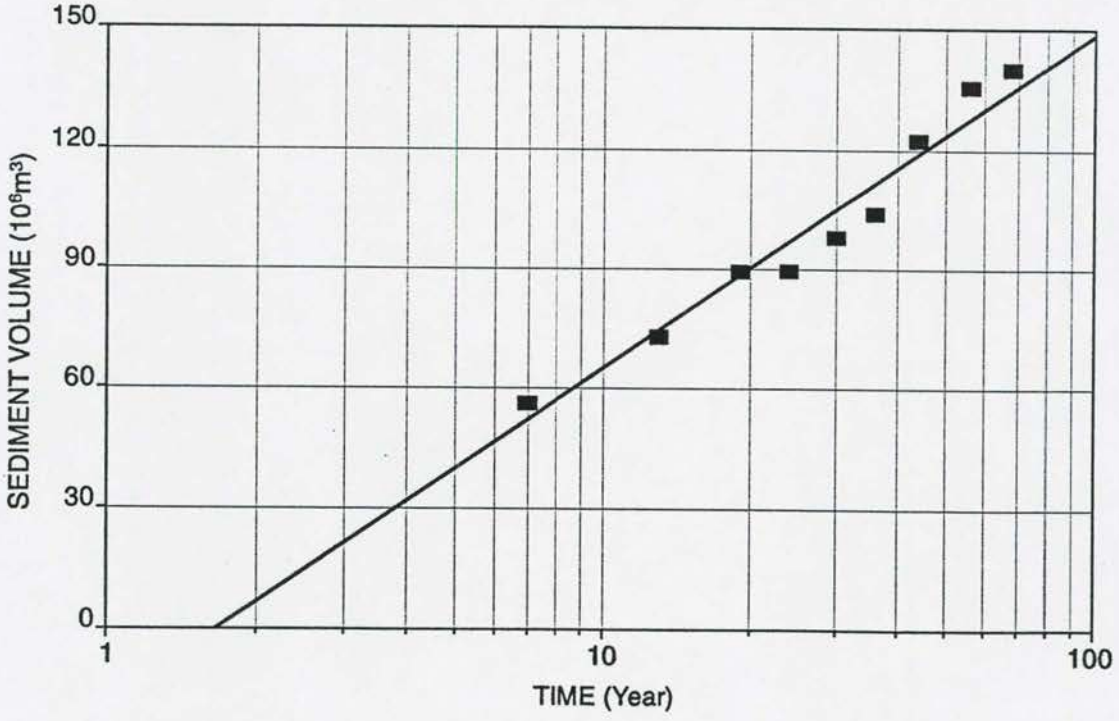

Figure 5.6-2 Sediment volume changes with time in Darlington Reservoir

Table 5.6-2: Sediment volume as fraction of the 50 year volume

Reservoir	Country	Original capacity* (million m³)	$\frac{V_{10}}{V_{50}}$	$\frac{V_{20}}{V_{50}}$
Darlington	RSA	328	0,49	0,72
Kommandodrift	RSA	74	0,33	0,62
Lake Arthur	RSA	105	0,29	0,60
Floriskraal	RSA	67	0,11	0,49
Grassridge	RSA	91	0,45	0,68
Beervlei	RSA	58	0,42	0,66
Kalkfontein	RSA	355	-	0,47
Nzhelele	RSA	62	0,29	0,54
Gamkapoort	RSA	55	0,44	0,69
Loskop	RSA	384	-	0,73
Olifantsnek	RSA	16	0,21	0,55
Prinsrivier	RSA	8	-	0,31
Laing	RSA	23	0,41	0,66
Van Ryneveldpas	RSA	79	0,29	0,62
Elephant Butte	USA	3 249	0,46	0,69
Theodore Roosevelt	USA	1 877	0,45	0,69
Lake MacMillan	USA	112	0,36	0,63
Guernsey	USA	91	0,36	0,64
Average values:				
- *Rooseboom (1975)*			0,39	0,65
- This study			0,36	0,61

* Gross Storage Capacity at current full supply level

Table 5.6-2 shows that fairly constant relationships, especially for the V_{20}/V_{50}, values can be obtained for the larger reservoirs. All the reservoirs in **Table 5.6-2** are however large in terms of the mean annual runoff. *Rooseboom (1975)* fitted a curve to the average volume ratios:

$$\frac{V_t}{V_{50}} = 0376 \ell n \frac{t}{3,5} \qquad (5.6\text{-}3)$$

which has been widely used in South Africa to date to make long-term forecasts of sediment volumes when short-term basin surveys are available, or to predict sediment yields from basin surveys assuming a 50-year density of 1 350 kg/m³. Recently updated South African regional sediment yield maps have also been calculated based on this approach *(WRC, 1992)*. When this map is used to predict sediment yields and a 50-year density of 1 350 h/m³ is used, any discrepancies due to possibly incorrectly assumed densities are cancelled out in the calculation of deposit volumes. It should be remembered that **Equation (5.6-3)** is only reliable when $t \geq 10$ years.

5.6.2 Verification of the methods of *Miller (1953)* and *Rooseboom (1975)* with reservoir data

Rooseboom (1975) rewrote the *Miller* method to a dimensionless $\frac{V_t}{V_{50}}$ format by assuming constant annual sedimentation of W weight units and by using $\frac{50W}{t.W} = \frac{\gamma_{50}.V_{50}}{\gamma_t.V_t}$

Then $$\frac{V_t}{V_{50}} = \frac{t\left(\gamma_1 + 0{,}4343K\left(\frac{50}{49}\ \ell n\ 50-1\right)\right)}{50\left(\gamma_1 + 0{,}4343K\left(\left(\frac{t}{t-1}\right)\ \ell n\ t-1\right)\right)} \qquad (5.6\text{-}4)$$

γ_1 and K-values depend on sediment grading and reservoir operation, but it seems that even if the highest realistic K-value and lowest γ_1 are used, the rate of consolidation seems to be overestimated by the method of *Miller (1953)*, as is shown in **Figure 5.6-3** and **Table 5.6-3** *(Rooseboom, 1975)*.

Table 5.6-3: Sediment consolidation predictor evaluation

t (year)	$\frac{V_t}{V_{50}}$ (*Miller*, 1953)	$\frac{V_t}{V_{50}}$ (*Rooseboom*, 1975)
10	0,28	0,39
20	0,48	0,65
40	0,84	0,92

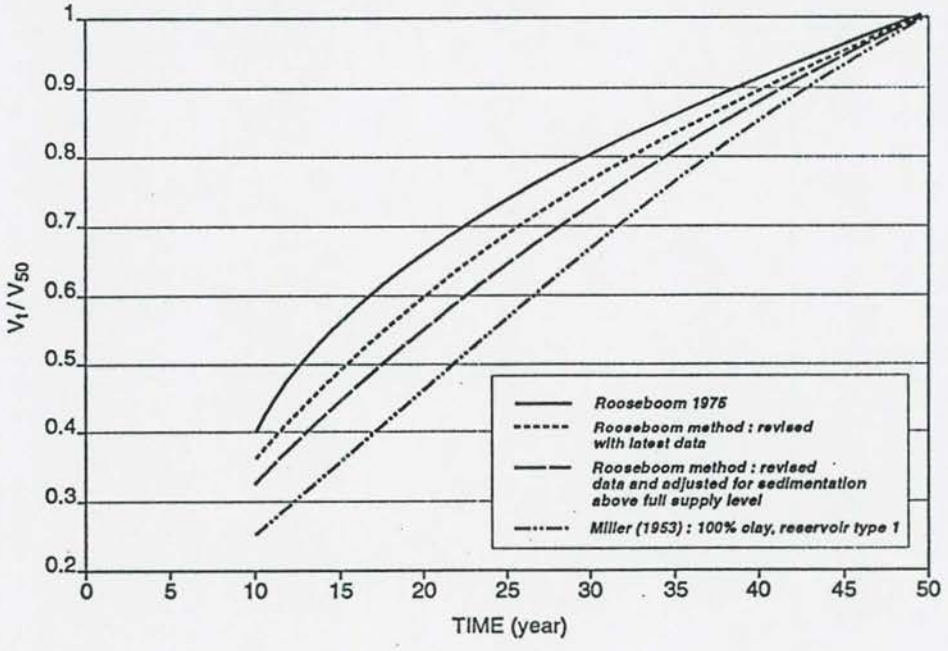

Figure 5.6-3 Comparison between consolidation predictors of Miller (1953) and Rooseboom (1975)

Rooseboom (1974) stated that based on the South African data, the method of *Miller (1953)* is unreliable.

Braune (1984) evaluated observed sediment densities, sediment size distribution, the time of consolidation and reservoir operation. Most sediment samples taken from South African reservoirs were, however, only obtained in dry basin parts and averaged reservoir sediment density conclusions will therefore generally overestimate the sediment densities. Sediment at deep levels and in wet parts of the reservoir will be saturated, with densities much lower than in the dried-out basin.

Compaction of the sediment is a function of the amount of re-adjustment of sediment particles and the rate at which water can escape from the voids. Sands achieve maximum consolidation in relatively short periods of time. Clay and silt deposits have greater porosity, but the low permeability of clay soils causes a slow water release rate and slow consolidation (if the sediment remains saturated with water). The water column on top of the sediment cannot affect the consolidation as long as the water pressure is taken up by the soil water and not the sediment itself.

Braune stated that a fine grained sediment will compact rapidly when exposed to air drying because of the effects of surface tension incident to evaporation. When the induced reactive stresses of the soil skeleton attain the magnitude of the capillary pressure, the menisci of the capillary moisture columns rupture and no further shrinkage occurs. Sediment shrinkage limits vary from about 10 to 15 % moisture per dry weight of sediment, giving maximum soil dry densities around 1 800 kg/m^3. Shrinkage of cohesive sediment is often related to surface cracks forming before the moisture content is exhausted. (See **Photograph 5.6-1**)

The observed and predicted sediment densities for South African reservoirs are shown in **Table 5.6-4**. The methods of *Lane and Koelzer (1943)* and *Lara and Pemberton (1965)* differ only in the initial sediment densities these methods are based on, and the calculation methodology is similar to the method of *Miller (1953)*. From **Table 5.6-4**, it would seem that the method of *Lara and Pemberton (1965)* underestimates dry densities of sediment with high clay content and considerable exposure, but considering that only relatively dry samples were analysed during 1980, thereby overestimating the average reservoir sediment density, such a conclusion cannot be proven here with the available data.

Photograph 5.6-1 **Cohesive sediment drying and shrinkage at Floriskraal Reservoir**

Table 5.6-4: Comparison of measured and calculated densities *(Braune, 1984)*

Reservoir	Krugersdrift	Beervlei	Van Rynevelds Pass	Grassridge	Lake Arthur	Gariep
Capacity (mill m^3) and date completed	78 1971	58 1958	81 1925	60 1924	79 1925	5952 1970
Measured dry density (kg/m^3)	1110-1430	1300	1140	1370	1100	1060
% clay	29	56	52	12	30	27
% silt	28	29	36	26	35	58
% sand	43	15	12	62	35	15
Dam operation type	3	4	3	3	3	1
Calculated initial density (kg/m^3)						
a) Lane & Koelzer (1943)	1275	1303	1135	1370	1250	956
b) Lara & Pemberton (1965)	1148	924	933	1325	1110	996
Compaction factor (K)	32	0	56	16	34	122
Record period	1970-1980	1958-1980	1924-1980	1924-1960	1925-1936	1970-1979
Record length (years)	10	12	56	36	11	9
Calculated dry density (kg/m^3)						
a) Lane & Koelzer	1 300	1300	1210	1390	1270	1030
b) Lara & Pemberton	1 170	920	990	1350	1130	1070

Other factors apart from sediment compaction can play a role in causing differences between the sediment density predictors as derived by *Miller (1953)* and *Rooseboom (1975)*:

a) **Decreased catchment sediment yield**

Rooseboom et al (1975) showed that the sediment load of the Orange River decreased by more than 50% from 1929 to 1969, attributed to a progressive decrease in available sediment. Decreased sediment yield from catchments could, however, be the reason for discrepancies at only some South African reservoirs used by *Rooseboom (1975)*.

b) **Decreased reservoir trap efficiency** with sedimentation cannot be a reason for differences, as large reservoirs (in terms of run-off and operation) were selected by Rooseboom.

c) **Increased deposition above full supply level of a reservoir**

Data used by Rooseboom did not account for sediment deposits above full supply level, but *Braune (1984)* estimates this error at 4 to 8% and therefore cannot account for the discrepancies under discussion.

At some reservoirs the sedimentation above full supply level can be high and should therefore always be considered when determining sediment yield from a basin survey, as indicated in **Table 5.6-5**.

Table 5.6-5: Sedimentation above reservoir full supply level

Dam	Sediment above FSL as % of sediment up to FSL
Prinsrivier Reservoir	10
Floriskraal	29
Pietersfontein	21

By taking the Welbedacht Reservoir data (only as example, owing to its small trap efficiency) above full supply level (FSL) into account, it can be shown that ignoring the sediment volume above FSL can lead to considerable overestimation of the accumulated volume relationship as shown in **Figure 5.6-4** and **Table 5.6-6**.

Table 5.6-6: Welbedacht Reservoir $\frac{Vt}{V_{50}}$ above full supply level

Height above FSL considered (m)	$\frac{V_{10}}{V_{50}}$	$\frac{V_{20}}{V_{50}}$
0	0,48	0,71
4	0,45	0,68
10	0,44	0,67

d) **Settling of the dam basin**

Initial settling of a reservoir basin when filling could be mistaken for negative sediment accumulation during a sediment resurvey, but indications are that typical settling for a large reservoir as Gariep is too small to be considered. Observed settling in Gariep Reservoir was in the order of 15 mm *(Braune, 1984)*.

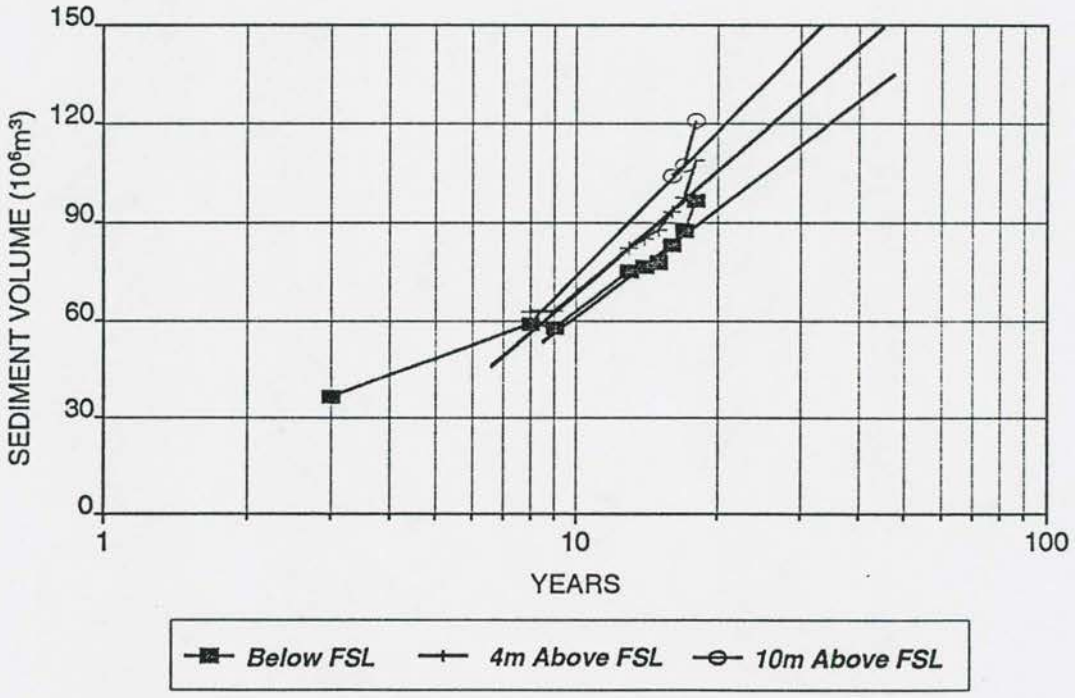

Figure 5.6-4 Sedimentation above reservoir full supply level and long-term capacity changes

e) **Variation in field data in determining Vt/V_{50}**

The data given in **Table 5.6-2** display much more variation of Vt/V_{50} values than the *Rooseboom* 1975 data. Although some evidence is found of reasons included under a - e for differences between the Rooseboom and Miller methods, it cannot explain all the differences when average values are considered. It is however believed that the most important reason lies in the reservoir operation type and associated K_o value **(Table 5.6-1)**.

In terms of consolidation prediction, a type 3 reservoir probably does not act like a reservoir which is normally empty from the beginning of operation, as -

- water demands are usually much less at the beginning than later on;
- total live plus dead storage is still available;
- the basin below FSL will contain mainly finer sediment, which will change with time and become coarser as sediment transport capacities into the reservoir basin increase; and
- even if the reservoir is drained regularly from the beginning of operation, consolidation depends on the degree of saturation, and quite often only the upper layer of deposits exposed to the sun is consolidated to high densities.

Therefore a reservoir will probably start as a type 1 (clay) and could later change to type 3 (silt/sand). Using these assumptions of changing operation type with time, prediction results based on the methods of *Miller and Rooseboom* are in agreement.

5.6.3 Proposed modelling of sediment consolidation

Having established what causes the differences between the *Miller and Rooseboom* consolidation prediction methodologies, it is proposed to use a combination of these methods in modelling spatial reservoir consolidation. The differences between the proposed and existing methods, such as the *Rooseboom* and *Miller* methods, are:

- Sediment inflow into a reservoir is not constant per time step and should be accounted for in determining consolidation

- ρ_o values can be based on sediment characteristics as described by *Strand (1974)*.

- K_o values can be based on the South African reservoir data.

- The methodology should not be so detailed that excessive computing time is required, or mathematical model instability occurs due to widely variable densities, or be too complicated without gaining prediction reliability.

A first attempt at establishing a simple consolidation methodology reads *(Olesen, 1995)*:

$$\rho_t = \rho_\infty + (\rho_o - \rho_\infty) \exp\left(\frac{-t}{T}\right) \qquad (5.6\text{-}5)$$

with ρ_∞ = long-term density of say 1350 kg/m^3 = ρ_{50}, with T = 50 years, often used in South Africa. Final sediment characteristics will, however, not be available when ρ_∞ is being predicted.

and ρ_o = initial density *(Strand, 1974)*. No RSA-data is available on ρ_o-values and therefore the relationship will be difficult to calibrate.

A further complication arises from the way in which consolidation is calculated with time and with deposition:

$$\rho\ (t + \Delta t) = \frac{z_d(t).\rho'(t + \Delta t) + \Delta z.\rho_o}{z_d(t) + \Delta z} \qquad (5.6\text{-}6)$$

with z_d = depth of previously deposited sediment

and Δz = depth of recent deposits

When constant sediment deposition rates and a similar equation as **Equation 5.6-5** (for example **Equation 5.6-1**) is used in **Equation 5.6-6**, it is found that:

- **Equation 5.6-6** overestimates sediment density;

- when trying to incorporate changing rates of deposition with time, **Equation 5.6-6** does not allow for the impact of deposition changes on future total densities.

The above possible problems related to **Equations 5.6-5** and **5.6-6** can be resolved by using:

- **Equation 5.6-1,**

- a similar relationship as **Equation 5.6-6**, and

- an effective time.

The procedure is as follows:

$$\rho_t = \rho_o + K_o \log t \qquad (5.6\text{-}1)$$

(a) $t = 1$: $\rho_1 = \rho_{01} + K_{01} \log 1$
$= \rho_{01}$

(b) $t = 2$: $\rho_2 = \dfrac{((\rho_{02} + K_{02} \log 2) \,.\, z_o\ (t = 1)) + (\rho_{02} . z_{02}))}{(z_{01} + z_{02})}$

(c) t effective $= 10^{((\rho(t = 2) - \rho_{02})/K_{02})}$

(d) $z\ \text{total}_2 = ((z_{01} \cdot \rho_{01}) + (z_{02} \cdot \rho_{02}))/\rho_2$

$$t = 3 : \rho_3 = \frac{[((\rho_{03} + K_{03} \log (\textit{teff.} + \Delta t\ (= 1))) \,.\, (z_{01} + z_{02}) + (\rho_{03} \cdot z_{03})]}{(z_{01} + z_{02} + z_{03})} \qquad (5.6\text{-}7)$$

Repeat steps (c) and (d)

$t = 4$: Repeat steps (b), (c) and (d) for further time steps.

The above method works with all USA ρ_o and K_o values and variable deposition, and can be related to the RSA-data through altered input K-values.

With the new approach, changes in ρ_o and deposition depth related to variable sediment inflow can be accounted for as indicated in **Figure 5.6-5**.

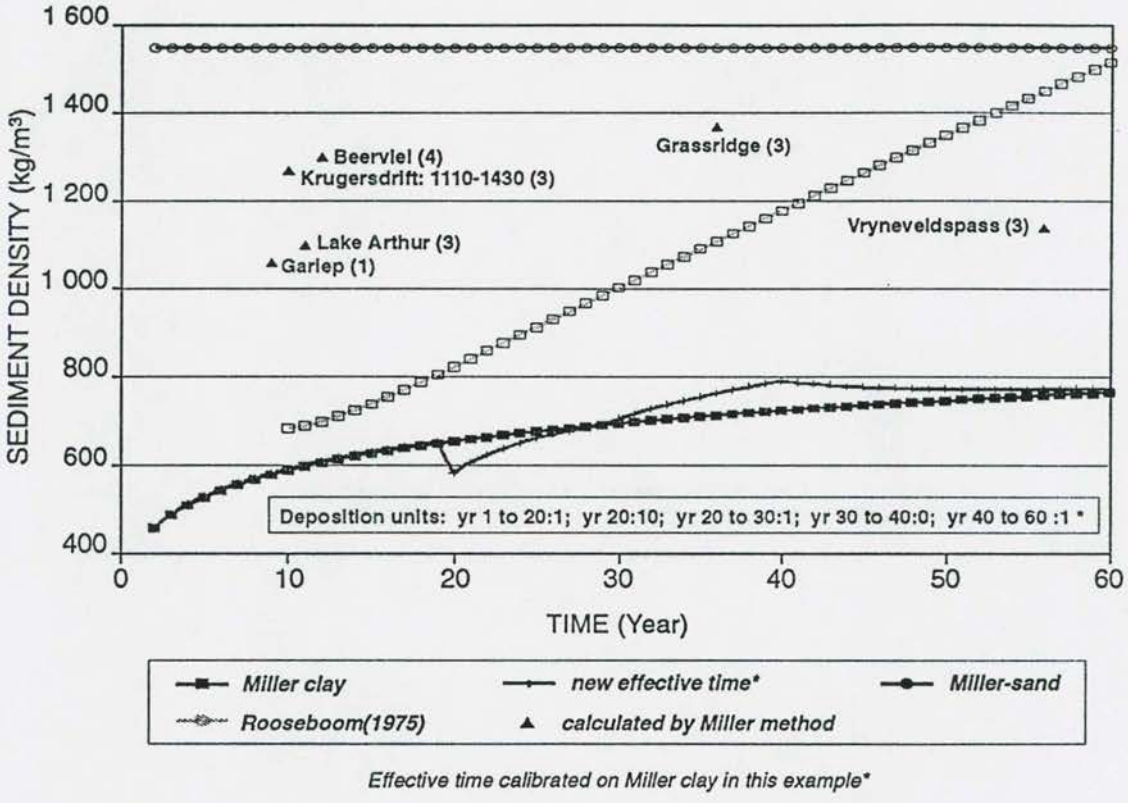

Figure 5.6-5 Effective time consolidation with variable deposition rates

2075H/sw

1996-11-20

6. SEDIMENT RE-ENTRAINMENT PROCESSES

6.1 Introduction

An understanding of the principles of entrainment of sediment particles is of great importance in the flushing of reservoirs. The parameter which defines the onset of sediment movement is, however difficult to define in reservoirs for sediment deposits with a very fine, cohesive nature and which are often consolidated. For non-cohesive sediments, incipient motion can be expressed mathematically, while laboratory tests have mostly been used to quantify incipient movement conditions for cohesive sediments.

During flushing operations, retrogressive erosion of the delta will result when the water level is drawn below the elevation of the apex point. Initially intensive erosion takes place downstream of a turning point (T) as indicated in **Figure 6.1-1**. This turning point keeps moving upstream as degradation continues and eventually disappears altogether. During this process the slope of the front-set is decreased and that of the top-set increased. The two parts finally merge to form a unified reach with a single gradient. Further erosion occurs in the form of progressive erosion with diminishing intensity. This process has been observed at several reservoirs as well as a physical model study *(Zhang Ren et al, 1985)*.

The process of retrogressive erosion can be illustrated by means of the sediment continuity equation:

$$\frac{\gamma . dA}{dt} = \frac{Q . dC}{dx} \qquad (6.1\text{-}1)$$

Plotting of the left hand term for conditions of erosion, along the length of a reservoir, yields **Figure 6.1-2**.

Figure 6.1-2 indicates that during erosion, the stream tries to minimize the rate of energy dissipation by first acting on and reducing the highest $\frac{QdC}{dx}$ values near the dam, followed by upstream erosion. Delta formation is the reverse of the retrogressive erosion process.

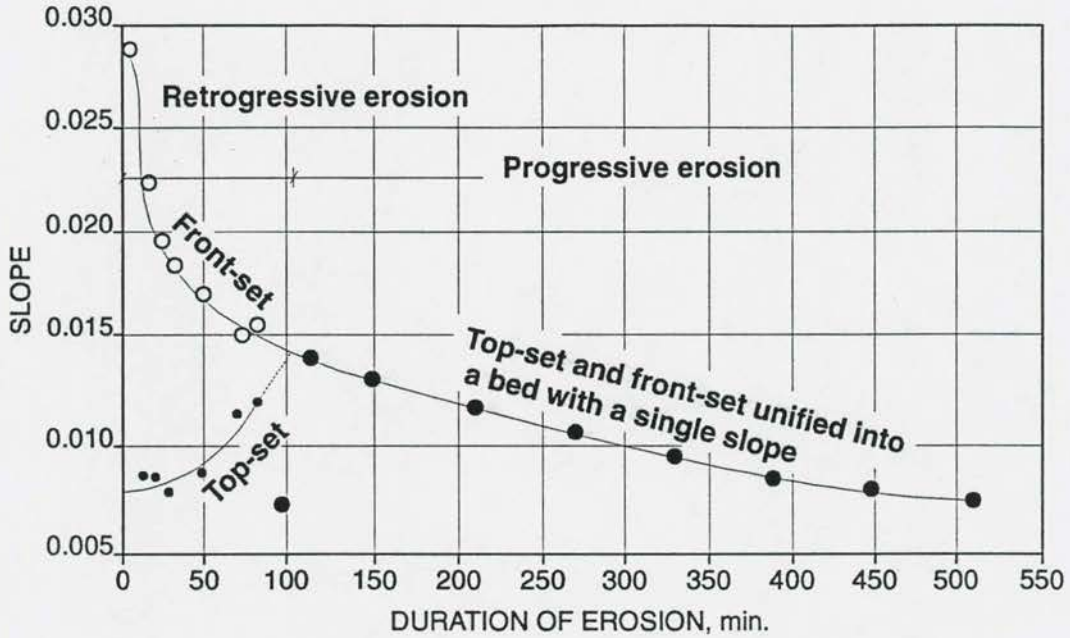

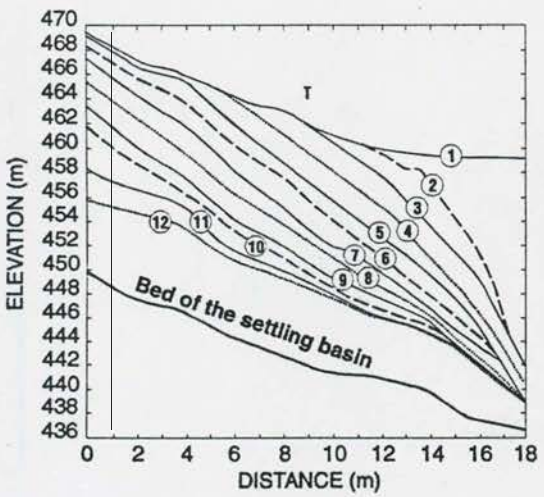

(a) Change in water surface

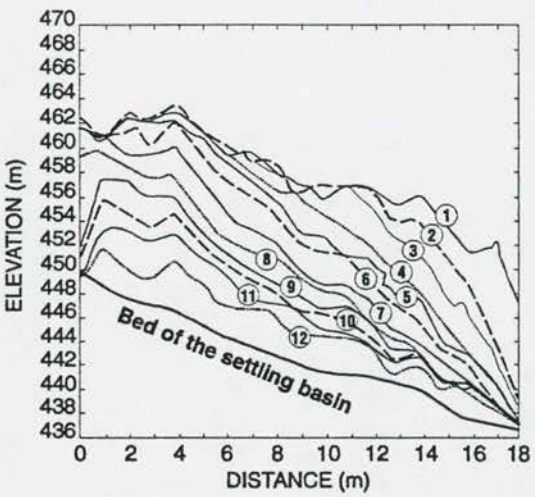

(b) Change in bed profile

Curve	*Duration of erosion, min.*
1	0
2	6
3	14
4	29
5	49
6	69
7	109
8	149
9	209
10	269
11	329
12	449

Figure 6.1-1 Retrogressive erosion

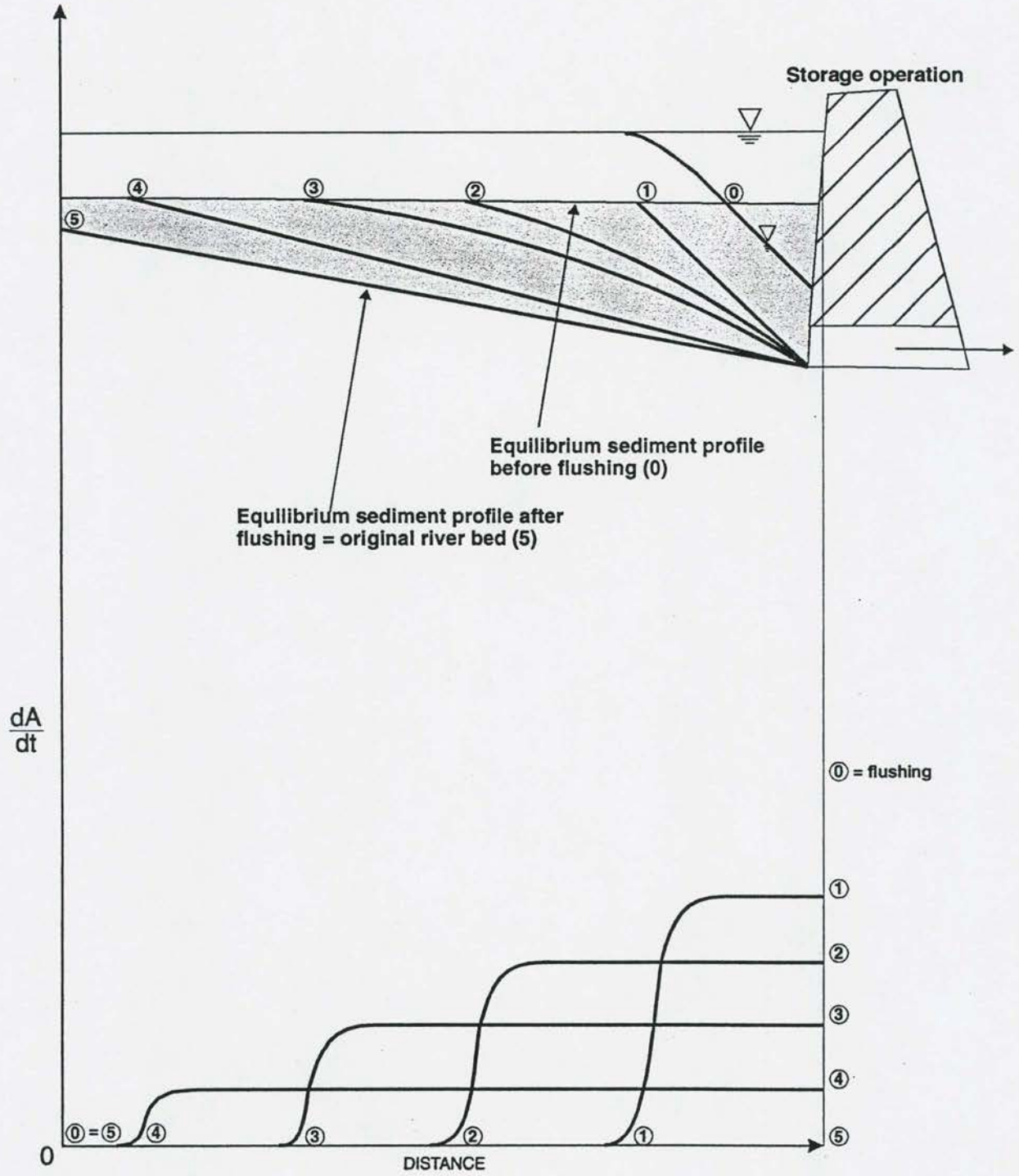

Figure 6.1-2 Retrogressive erosion and sediment continuity

When the sediment profile reaches equilibrium, whether for storage operation or drawdown flushing, the left and right-hand side terms of **Equation 6.1-1** approach zero values, and uniform flow conditions will prevail. This is of course a highly simplified explanation of the complex sedimentation processes within a reservoir.

In order to understand why consolidated, cohesive sediment deposits collapse after rapid water level drawdown, it is important to obtain some insight into the clay mineralogy of the sediments.

The clay mineralogy of a sediment sample taken from Welbedacht Reservoir is shown in **Table 6.1-1.**

Table 6.1-1: Clay mineralogy of Welbedacht Reservoir sediment sample

Smectite	21 %
Mica	21 %
Interstratified minerals	21 %
Kaolinite	13 %
Quartz	22 %

A normal soil with a composition as in **Table 6.1-1** will be highly erodible *(ISCW, 1995)*.

Kaolinite is composed of a succession of oxygen, silicone, hydroxyl and aluminium components, regularly stacked like "leaves" in a book. The layer bonds are strong and therefore little water can enter between the layers, and kaolinite does not disintegrate and split in water like other clay minerals *(Partheniades, 1971)*.

Montmorillonite has a structure similar to that of kaolinite; the main difference is that the bonding forces are much weaker. As a result, cations and water can enter between the sheets and montmorillonites can easily disintegrate into individual units. Montmorillonites are the finest and most active clays displaying swelling, cohesion and plasticity.

With rapid drawdown of a reservoir during high inflow flushing, the process of erosion occurs by the following mechanisms:

a) Local scour near the outlet is caused by 3-dimensional converging flow at high velocities.

b) Hydraulic cutting back of the delta from downstream to upstream, thus reducing the bed slope and the applied power. If the flushing duration is long enough, the river will erode to its original bed level.

c) Bank failure of the flushing channel creates relatively steep side slopes. These side slopes are constant for the same reservoir and sediment characteristics and can be well represented by assuming a trapezoidal channel form. Bank failure caused by hydraulic overpressures associated with rapid pool drawdown is very important in the flushing process, since it provides the sediment for saturated sediment transport within the channel.

d) Large flows have high erosive power and transporting capacity, and normally a wider channel will be created than with smaller flows. Smaller flows have the tendency to meander through the reservoir if left for some time. This was experienced in the Mbashe Reservoir during 1993 (See **Photograph 6.1-1**).

e) Erosion of the bed to a certain depth (associated with minimum required stream power). This equilibrium depth can be described with the applied power principle and is a function of the energy slope, unit discharge, bed roughness, energy dissipation and sediment transport. When this equilibrium depth is reached for a specific discharge, the flushing channel has an almost horizontal bed (across the width) at each cross-section, as observed at Phalaborwa Barrage, Welbedacht Reservoir and Windsor Reservoir. The width of scouring is related to the discharge. The scoured channel profile can be well represented by a trapezoidal profile.

Photograph 6.6-1 Mbashe Reservoir low flow flushing channel

6.2 Non-cohesive sediments

Criteria for determining the beginning of transport of sediment have been presented by *Hjulstrom (1935)* and *Shields (1936)*. Hjulstrom related critical velocity to particle diameter and does not provide an accurate criterion. Although the Shields diagram is widely used, its main shortcoming is the use of the particle diameter, which is not a representative or unique measure of transportability *(Rooseboom, 1975)*. The settling velocity of particles is a more significant criterion than particle diameter. *Mahmood et al (1985)* also found that due to pressure drag on bedforms, the average shear stress is smaller than the values given by the Shields diagram.

Rooseboom and Mülke (1982) showed that incipient motion can be analysed more comprehensively in terms of stream power.

The unit stream power (per unit volume) required to suspend a particle with mass density ρ_s and settling velocity w in a fluid with mass density ρ equals $(\rho_s-\rho)g.w$, while in rough turbulent flow, the unit stream power applied in maintaining motion along a plane bed consisting of particles with diameter d, is proportional *(Rooseboom et al, 1982)* to:

$$\frac{\rho g s D\sqrt{gDs}}{d} \tag{6.2-1}$$

with s = energy slope
D = depth of flow

A stream will begin to entrain particles when the power required to suspend the particles becomes less than the power required to maintain the status quo, and then

$$(\rho_s-\rho)gw \;\alpha\; \rho g s D\frac{\sqrt{gDs}}{d} \tag{6.2-2}$$

According to the general equation for settling velocity *(Graf 1971)*,

$$w \;\alpha\; \frac{\sqrt{(\rho_s-\rho)gd}}{\rho Cd} \tag{6.2-3}$$

If it is assumed that the drag coefficient Cd is a constant, which is true for larger diameters, then the condition of incipient motion under rough turbulent flow conditions is given by

$$\frac{\sqrt{gDs}}{w} = constant \tag{6.2-4}$$

This relationship fits measured data *(Yang, 1972)* well, as indicated in **Figure 6.2-1**. When $\frac{\sqrt{gDs.d}}{\nu} > 13$, the constant is 0,12.

Similarly, in smooth turbulent and completely laminar flow, the unit applied stream power equals

$$\frac{(\rho g s D)^2}{\rho \nu} \tag{6.2-5}$$

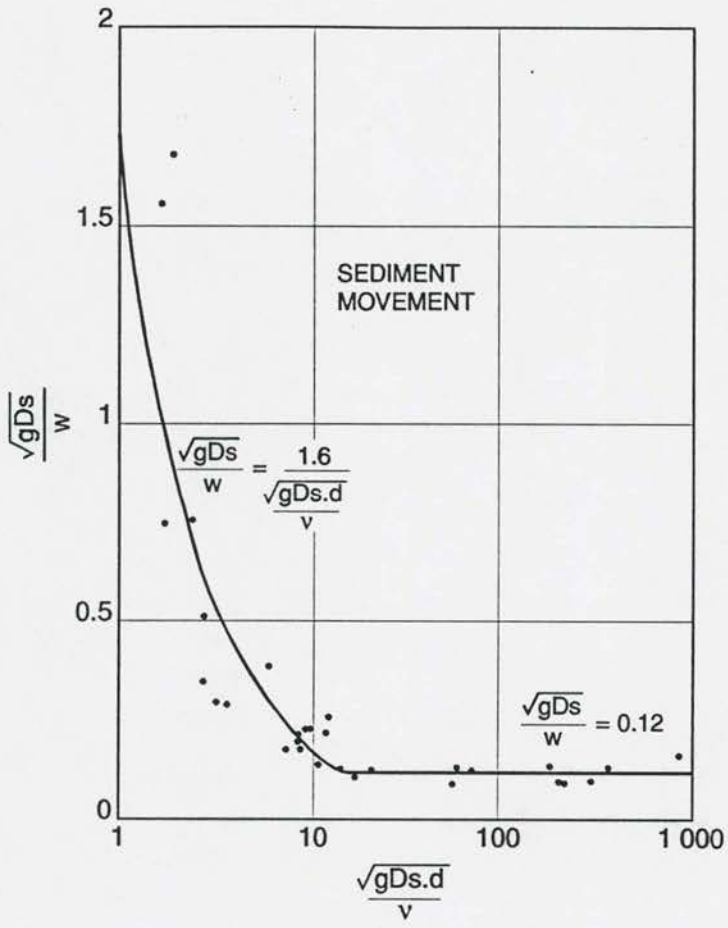

Figure 6.2-1 Incipient conditions for cohesionless sediment particles

with the corresponding settling velocity under viscous conditions (Stokes' Law):

$$w\alpha\frac{d^3g(\rho_s-\rho)}{\rho\nu} \tag{6.2-6}$$

The relationship for values of $\frac{\sqrt{gDs.d}}{\nu} < 13$ calibrated with data by *Grass (1970)* and *Yang (1972)* is found to be

$$\frac{\sqrt{gDs}}{w} = \frac{1{,}6}{\frac{\sqrt{gDs.d}}{\nu}} \tag{6.2-7}$$

The above analyses logically lead to a Liu type diagram (1957) and provide a complete mathematical explanation to describe the shape of this diagram. **(Figure 6.2-1)**

6.3 Cohesive sediment

6.3.1 General

In the case of cohesive sediments neither particle size nor settling velocity represents erodability, and relationships for incipient motion of non-cohesive sediments are no longer valid. For the erosion of cohesive sediments to take place it is necessary to break the interparticle bonds.

Two main types of erosion are described by *Partheniades (1965)* and *Krone (1962)*:

- Surface erosion of particles
- Bulk or mass erosion because the bulk shear-strength of deposits is exceeded.

Scour criteria are often assumed to be functions of particle diameter and cohesion coefficient, and empirical relations for critical shear force have been obtained, also for consolidated sediments *(Mehta et al, 1982; Migniot, 1981; Otshubo et al, 1986)*.

The resistance to erosion depends *(Ariathurai and Krone, 1976)* on:

- the type of clay
- the physical nature of the bed
- the chemical composition of pore and eroding fluids
- the stress history
- organic matter

Critical shear stresses for cohesive sediment have in most cases been obtained from laboratory tests carried out on estuarine clays *(Partheniades, 1972)*.

6.3.2 Surface erosion

Partheniades (1962, 1965, 1971, 1973) tested the effect of mass shear stresses on cohesive bed erodibility by remoulding one bed in a flume while a second bed was formed through deposition of suspended sediment. Although the microscopic strength of the latter was 1/100

of that of the former, the critical shear stress for erosion was found to be the same (0,098 N/m²). The erosion rate for the dense bed was constant and independent of the suspended sediment concentration, which suggests that surface erosion limits sediment availability and sediment transport. *Partheniades et al (1970)* also concluded that bulk density and mass shear strength cannot be used as a measure of soil erodibility as long as erosion takes place by removal of individual particles without any mass erosion.

Surface erosion of a deposited bed shows increasing resistance to erosion with depth, while a bed formed with uniform consistency is eroded at a constant rate *(Partheniades, 1985)*. The former situation can only be explained by an increase of the interparticle cohesive bonds with depth, which is inherent to the internal floc structure as flocs segregate during deposition.

For a given bed shear stress (τ_b), resuspension will proceed at decreasing rates until the total depth of erosion corresponds to a condition with $\tau_b = \tau_s$ (shear strength). The instantaneous resuspension rate, E, has been found to be a function of the excess bed shear stress ($\tau_b - \tau_s$):

$$\frac{E}{E_o} = \exp\left(\propto \frac{\tau_b - \tau_s}{\tau_s}\right) \qquad (6.3\text{-}1)$$

with E_o and $\propto$ empirical coefficients *(Partheniades, 1986)*.

The resuspension of cohesive sediment obviously depends greatly on the degree of consolidation. As an example, the critical shear strengths for surface erosion for different periods of consolidation (short in reservoir terms) is illustrated in **Figure 6.3-1**.

Migniot (1968) expressed the erosion rate of surface cohesive erosion as:

$$E = M(\tau - \tau_c) \qquad (6.3\text{-}2)$$

and related the yield shear stress of the mud, τ_c, to the bulk density of the sediment. The constant M is the erosion rate with units (s/m).

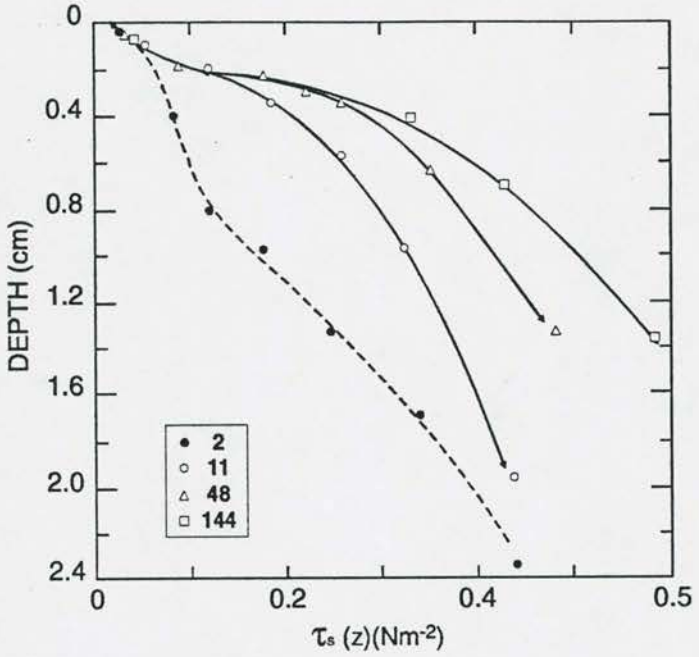

Figure 6.3-1 Variation of critical erosion stress with depth for various consolidation times (Mehta et al., 1982)

6.3.3 Critical conditions for mass erosion of cohesive, consolidated sediments: laboratory analysis

Critical conditions for resuspension of cohesive sediments have been established in the laboratory by various researchers who tried to relate it to the soil mechanical and physical properties of the sediment. The shear stress required to erode a cohesive sediment is significantly affected by the amount and type of clay mineral, microscopic and macroscopic clay properties, water content, pH and temperature of the eroding water as well as the pore water and the thixotropy and consolidation of the clay *(Kamphuis, 1983)*.

The results of laboratory studies vary widely. For example, for approximately similar cohesive sediment conditions, critical shear stress is given as 11,5 to 72 Pa, 5,7 to 23,5 Pa, 0,4 to 2,4 Pa, and 0,7 to 4,3 Pa in different studies *(Kamphuis, 1983)*. This large variation is a result of experimental error, variation in experimental techniques, an overly simplistic interpretation of sediment properties and different criteria for the onset of erosion. If such

large differences are obtained in the laboratory, the validity of such data in field applications is highly doubtful.

Kamphuis (1983) also conducted laboratory tests on cohesive sediments, consolidated to various densities and clay contents. The correlation with various soil properties is shown in **Figures 6.3-2 to 6.3-6**.

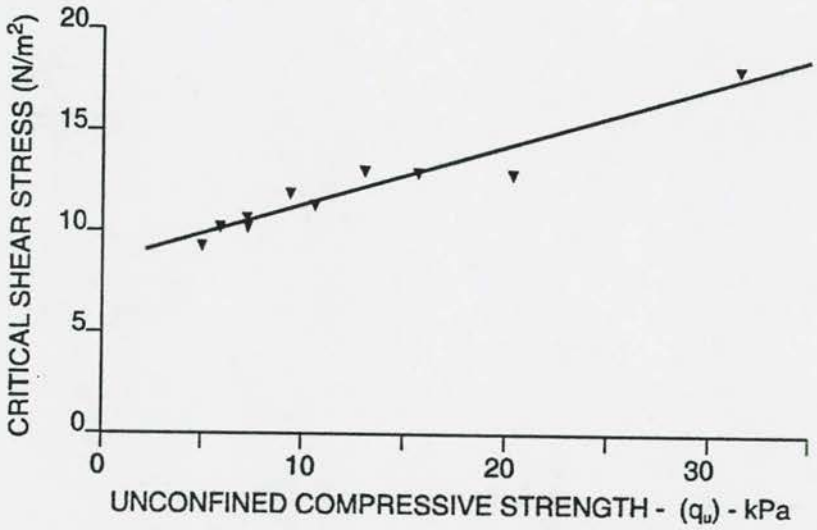

Figure 6.3-2 Critical shear stress and unconfined compressive strength

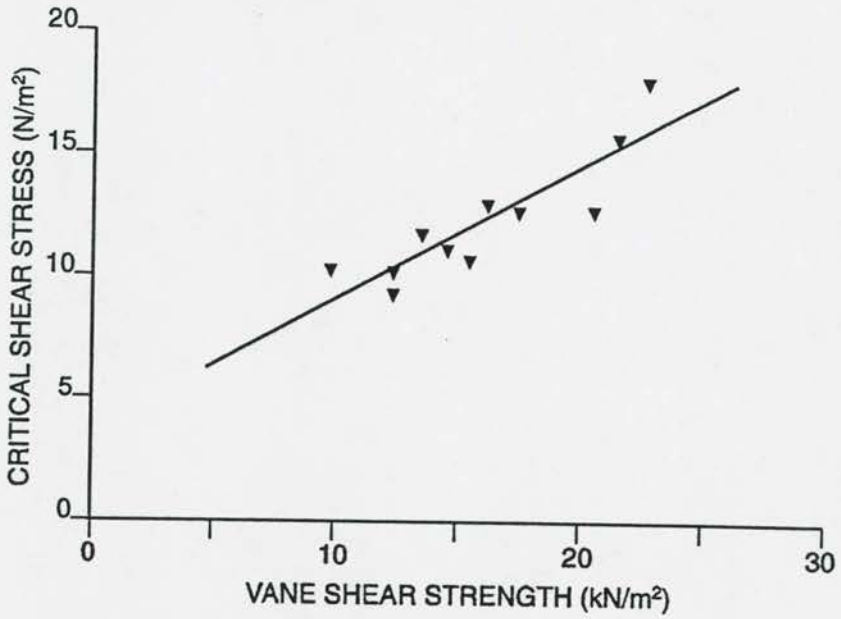

Figure 6.3-3 Critical shear stress and vane shear strength

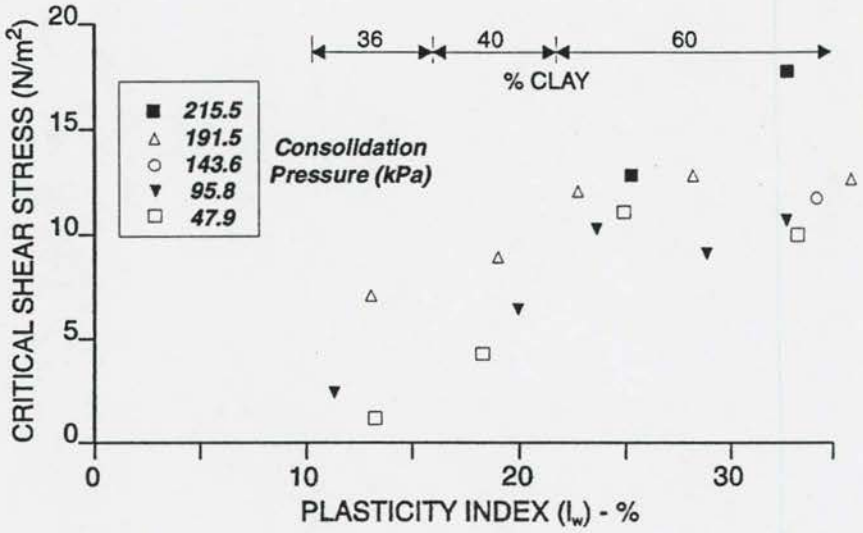

Figure 6.3-4 Critical shear stress and plasticity index

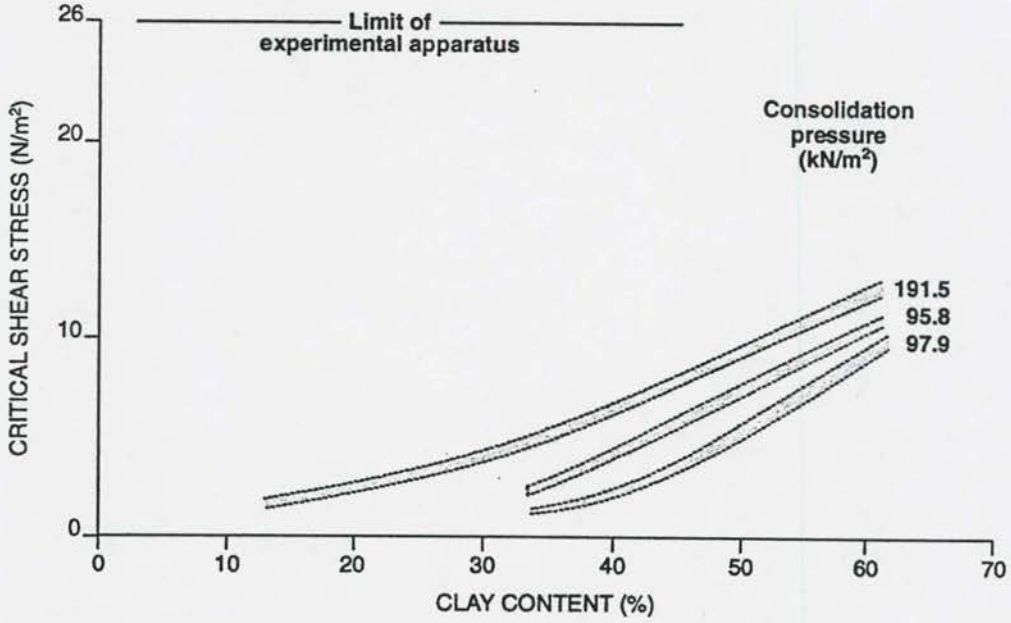

Figure 6.3-5 Critical shear stress and clay content

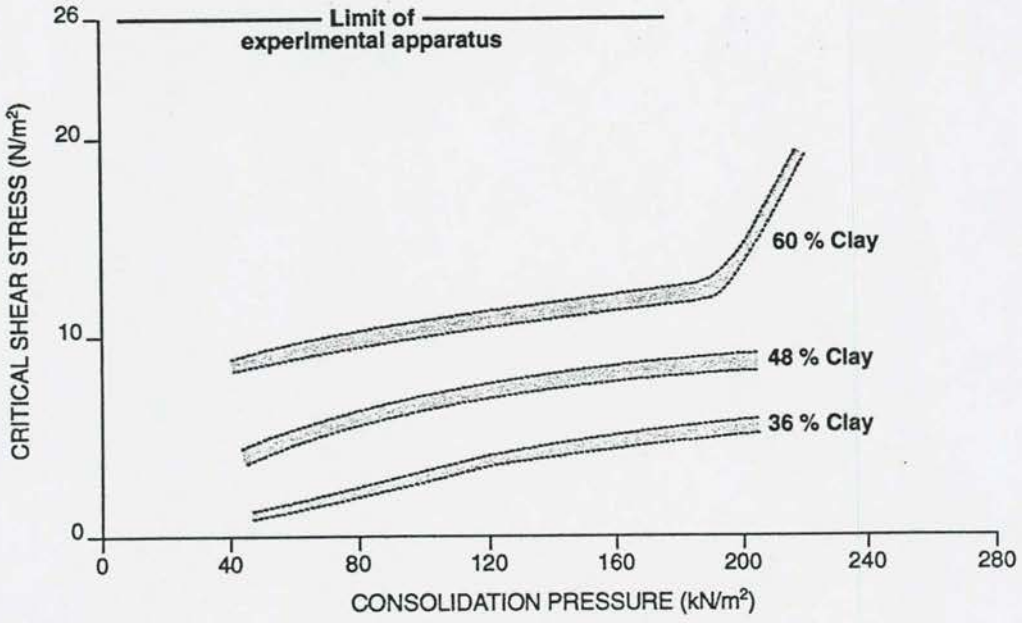

Figure 6.3-6 Critical shear stress and consolidation pressure

Kamphuis (1983) found a linear variation of critical shear stress with unconfined compressive strength and vane shear strength. The resistance to erosion increases with clay content and plasticity index. The shear stress required to initiate erosion of cohesive soil increases with consolidation pressure. Once critical conditions for a soil are reached, erosion progresses immediately (mass erosion).

The critical shear stress data, vane shear strength and clay fraction data of Kamphuis are shown in a combined graph in **Figure 6.3-7**.

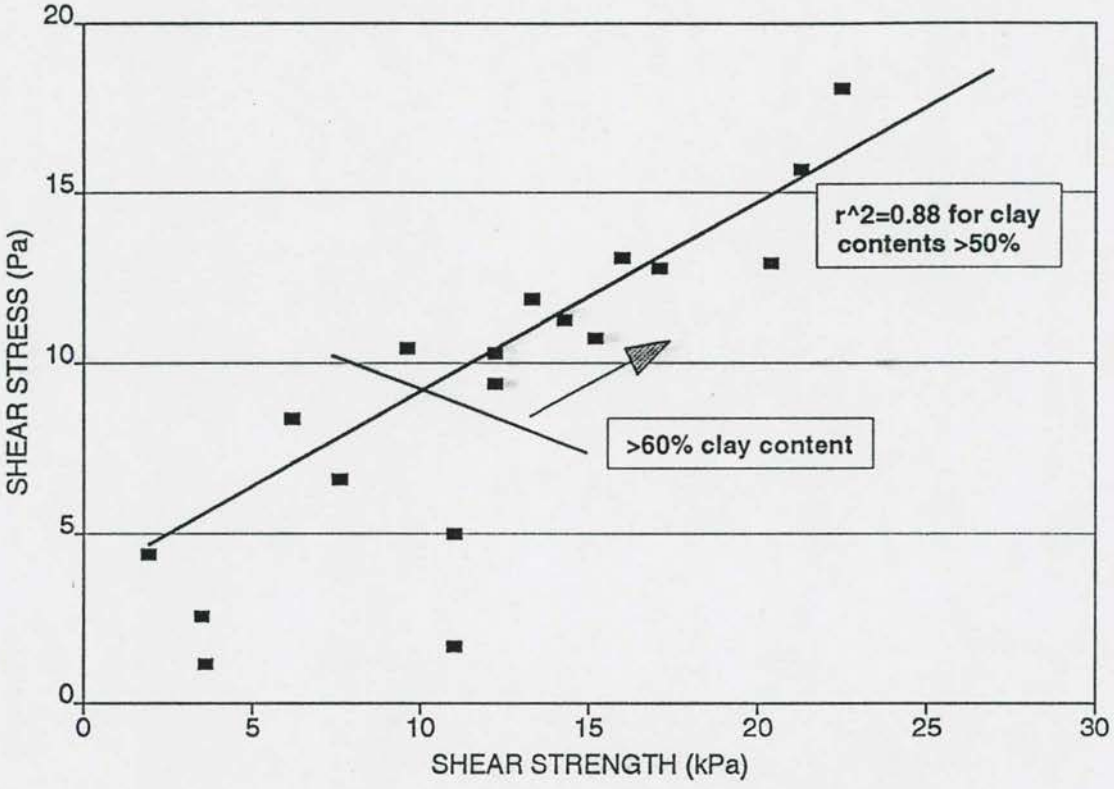

Figure 6.3-7 Critical shear stress versus vane shear strength and clay fraction

In stead of using the critical shear stress value τ at the bed, a theoretically more appropriate variable would be the applied power at the bed $\left(\tau\frac{dv}{dy}\right)_o$, which also reaches a maximum value at the bed:

$$\left(\tau\frac{dv}{dy}\right)_o = \frac{30\rho gsD\sqrt{gDs}}{\kappa k_s} \qquad (6.3\text{-}3)$$

By taking κ = 0,4 and $k_s = d_{50}$ = particle diameter in the experiments of Kamphuis (unfortunately not enough data is given by Kamphuis to calculate k_s), it is possible to derive **Figure 6.3-8**, relating critical stream power to shear strength, % clay and consolidation.

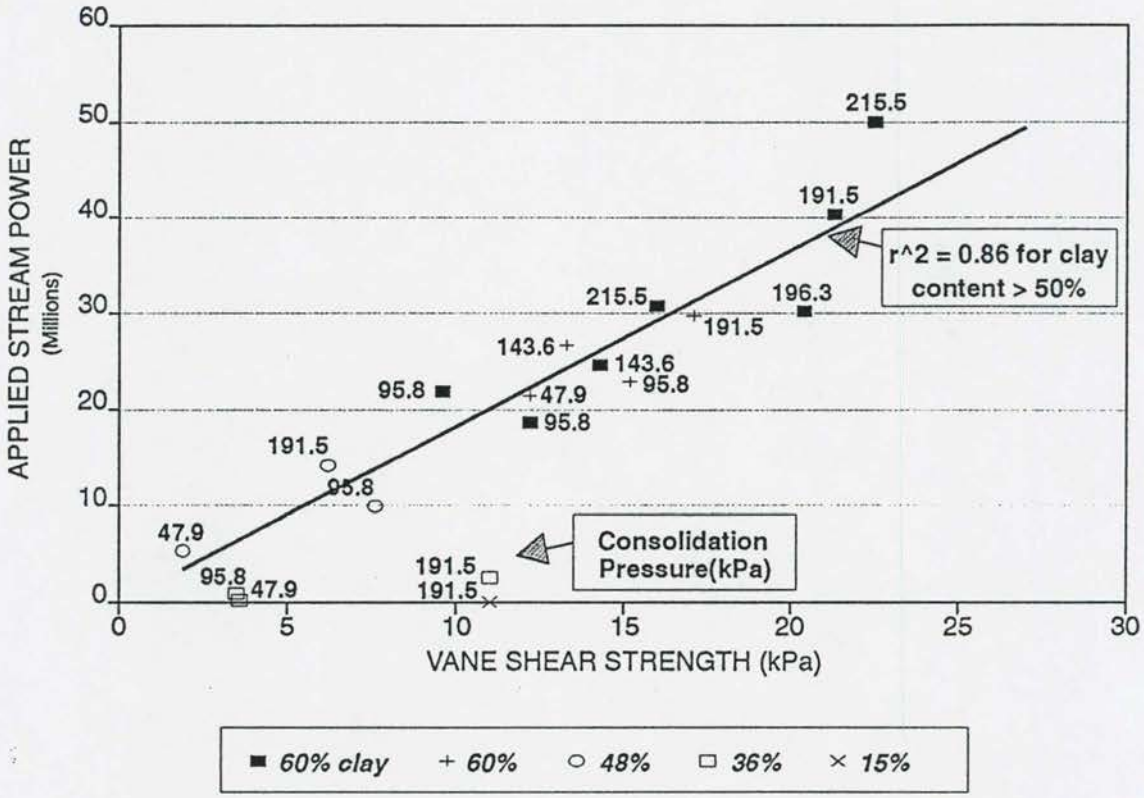

Figure 6.3-8 Critical applied stream power versus vane shear strength, clay fraction and consolidation

A linear regression analysis of applied power versus shear strength, % clay and consolidation

pressure was carried out and a correlation coefficient of $r^2 = 0,91$ was obtained. The best fit curve is shown in **Figure 6.3-9** which indicates that a remarkably good correlation is possible when considering the variables.

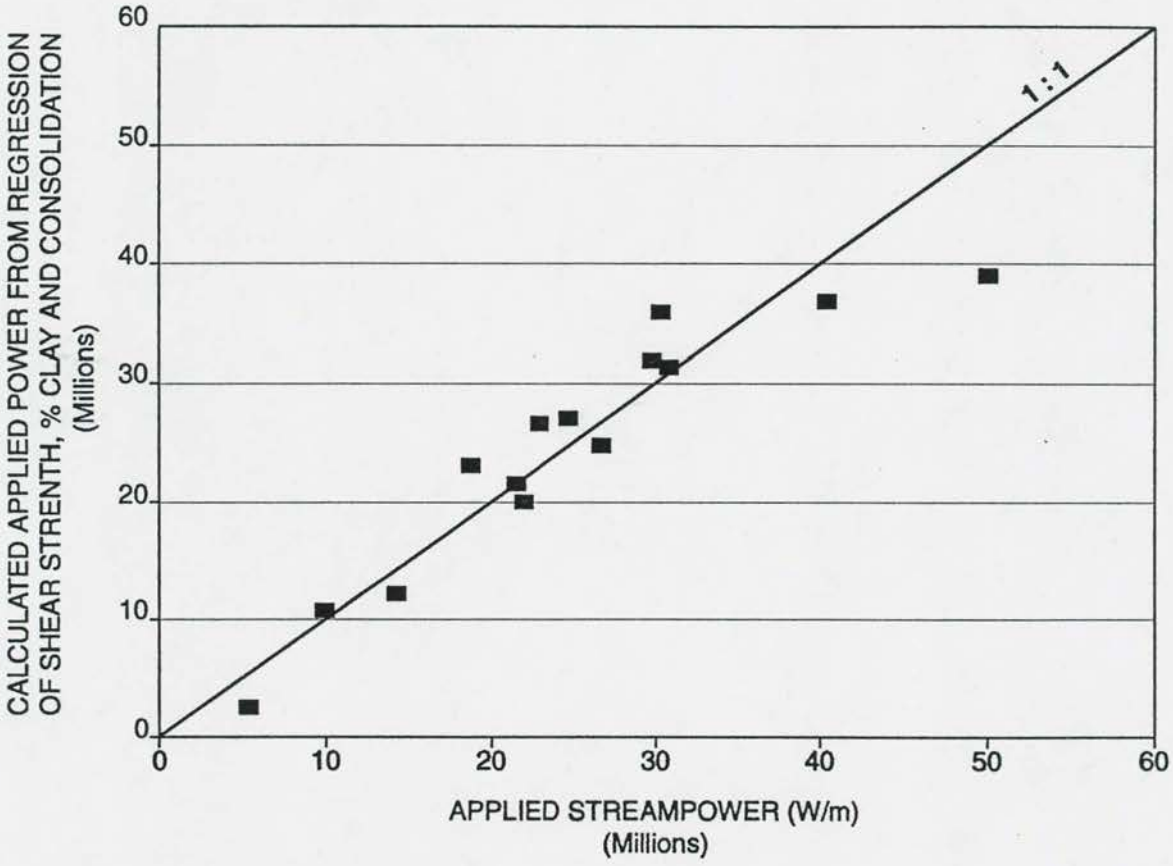

Figure 6.3-9 **Observed versus calculated shear strength: applied power, clay and consolidation**

Cai (1993) described critical conditions for cohesive soil erosion by relating stream power to soil shear strength. The stream power relationship of *Bagnold (1966)* was used ($\rho g R v s$) and good correlation as shown in **Figure 6.3-10** was found.

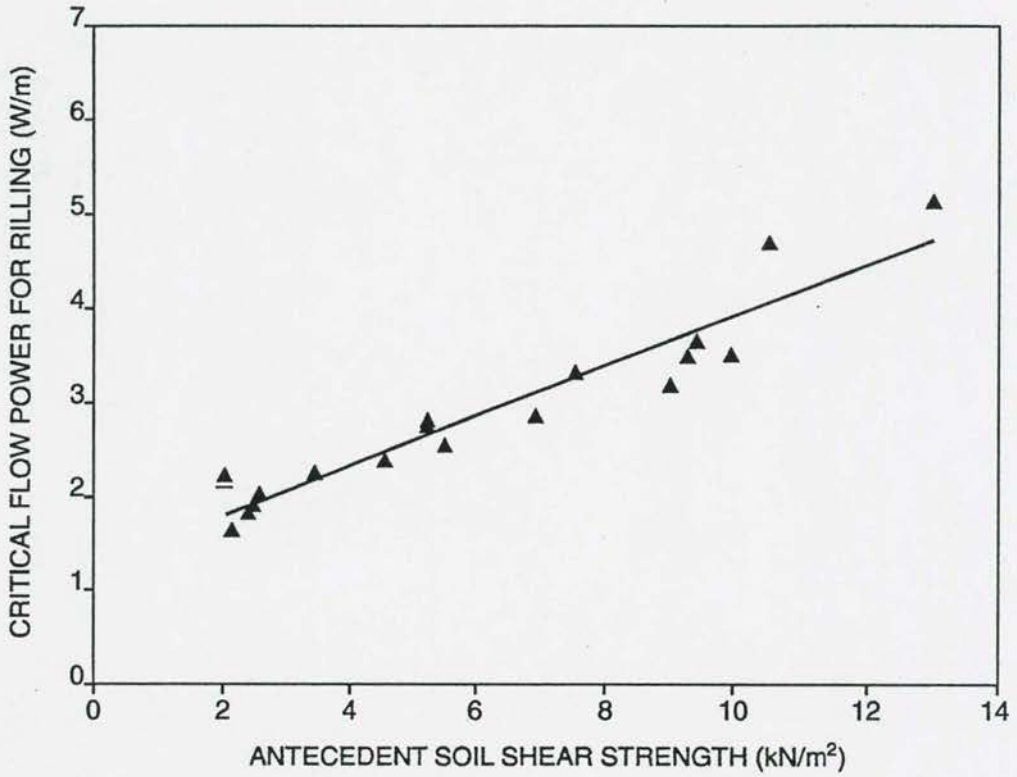

Figure 6.3-10 Critical unit stream power for rill initiation versus antecedent soil shear strength

Although the above relationship is not directly applicable to reservoir conditions, it is shown here that stream power can be a reliable predictor for describing critical erosion conditions.

Some tests have been carried out on reservoir sediments. *Du et al. (1987)* discusses tests carried out on sediment from the Shuizoazi Reservoir, China. Silt from the flood plain of the Yellow River and river bed sediments from Beijing were also used for comparison. The sediment was placed in a drop section in a flume, each sample prepared with a different dry

density. Results of the erosion tests indicated that the variation of critical shear stress (τ_o) was found to be related to dry density. Once the critical value of τ_o was reached, erosion progressed immediately and there was little or no dependence on the previous time history of the flow. A comparison test on an undisturbed reservoir sediment sample yielded the same test results as disturbed samples. The sediment characteristics and critical shear stress relationship are depicted in **Table 6.3-1** and **Figure 6.3-11** respectively. From **Figure 6.3-11** it is clear that critical shear stress is related to the dry density by straight lines (on a log scale) for each sediment sample. *Du et al. (1987)* related the experimental shear stresses to density with an exponential equation:

$$\tau_o = \alpha \gamma_o^5 \tag{6.3-4}$$

with α the erosion constant, found to be equal to 0,5 for Shuicaozi Reservoir.

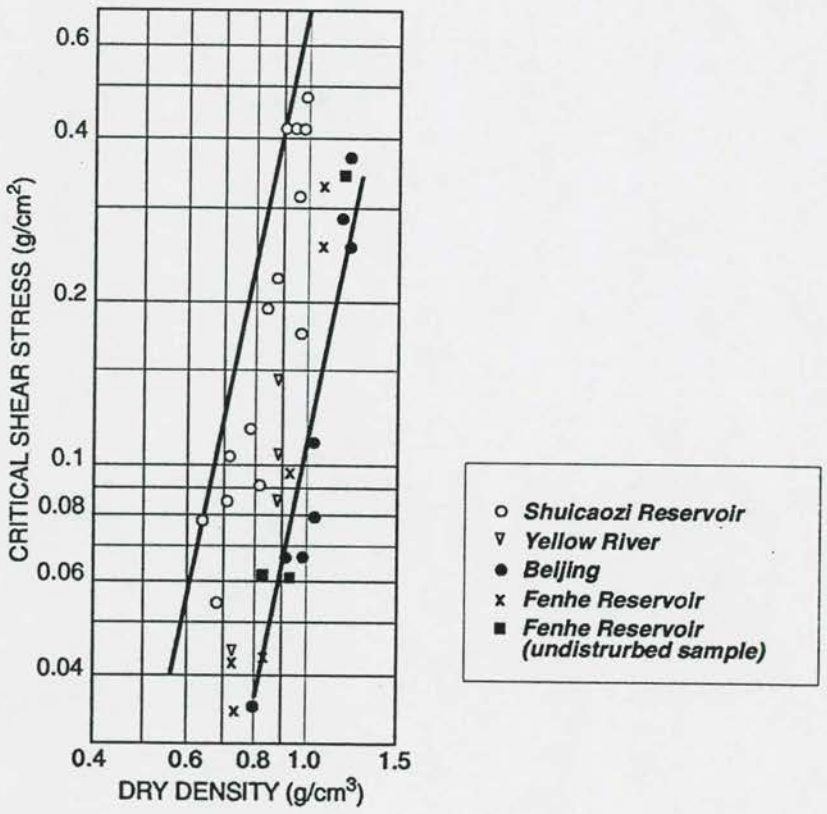

Figure 6.3-11 Incipient motion for cohesive sediment versus sediment density

Table 6.3-1: Characteristics of sediment samples

Sample	d_{50} (mm)	Dry density (g/cm³)	Liquid limit (%)	Plastic limit (%)	Plasticity Index (%)
Shuicaozi Reservoir	0,0058	0,64 - 0,98	51,95	30,00	22,95
Yellow River flood plain	0,004	0,51 - 1,0	43,39	24,76	18,63
Beijing	0,023	0,56 - 1,2	30,90	19,70	11,20

Bouchard et al. (1983) investigated critical erosion conditions within the Escale and St Lazare Reservoirs on the Durance River. Analysis of the density and sand fraction of 14 sediment cores, taken to a maximum depth of 3m into the sediment, indicated good correlation between shear strength (by viscometer) and sediment density. Flume tests established the critical stress of erosion between 6 and 27 N/m². No indication was, however, given whether this was for surface or mass erosion.

Rooseboom and Mülke (1982) derived a relationship for erosion of cohesive sediments in terms of unit stream power theory. In order to express both the transporting capacity of a stream and the characteristics of its bed sediment in equivalent scalar terms, they considered both fluid and sediment movement in directly comparable terms. Incipient movement of sediment is therefore treated as flow of a medium with high viscosity. Viscous flow is defined in terms of the Newtonian equation:

$$\tau = \mu \frac{dv}{dy} \qquad (6.3\text{-}5)$$

with τ the applied shear stress

μ the dynamic viscosity

$\frac{dv}{dy}$ the vertical velocity gradient, equal to velocity of rotation of a flowing element

In order to determine the applied unit power $\left(\tau \frac{dv}{dy}\right)$, it is necessary to determine the "viscosity" of the soil μ_s.

$$\mu_s = \frac{\tau}{\left(\frac{dv}{dy}\right)} \qquad (6.3\text{-}6)$$

By using a standard shear box test, the value of μ_s can be determined with τ known and $\frac{dv}{dy} = \frac{v_s}{d}$ with v_s the translation velocity and d = particle diameter.

The applied unit power equals $\tau\frac{dv}{dy} = \frac{\tau^2}{\mu_s}$ and the power required to dislodge a layer with thickness d and area A therefore is

$$\frac{\tau^2}{\mu}Ad \qquad (6.3\text{-}7)$$

with A representing the plan area of the sample and d the particle size.

The power required in the shear box is also Fv_a, but as v_a is constant, F may be taken to represent the applied power.

The power applied in maintaining fluid motion along a bed (rough turbulent flow) equals

$$\rho gsD\frac{\sqrt{gDs}}{\kappa y_o} \qquad \text{with} \quad y_o = \frac{k}{29{,}6} \text{ and } \kappa = 0{,}4$$

$$74\rho gsD\frac{\sqrt{gDs}}{k} = E \qquad (6.3\text{-}8)$$

A definite relationship was obtained between applied stream power (E) and mean shear force (F) for field data representing erosion of steep slopes. In this research a similar attempt was made to relate critical conditions for mass erosion to soil mechanical characteristics of the sediments (**Chapter 6.5**).

In mathematical modelling of reservoirs with a significant proportion of fine material load, two critical values are commonly defined: threshold of erosion and threshold of deposition with values of 5 - 10 N/m² and 0,5 - 1,0 N/m² respectively *(Mahmood, 1986)*. Once deposited, the shear strength required for re-entrainment of sediment is much higher than for deposition and increases with age and consolidation. Soil mechanical parameters such as shear strength, cohesion, dry density and Atterburg limits do not correlate with the erosion initiation conditions or rates of erosion, except in a limiting sense.

Shear strength is of course influenced by other soil properties such as bulk density and moisture content.

It has been found that soil shear strength is well correlated with soil erosion as obtained from analyses by *Rooseboom et al (1982), Wang et al (1992, 1994), Luk and Hamilton (1986), Rauws and Govers (1988)* and *Bradford et al (1987)* for both field and laboratory conditions.

6.3.4 Sand and clay mixtures

Sediment deposits in reservoirs often consist of sand and clay mixtures, or thin clay layers in sand. The presence of sand in clay deposits increases erodibility. Erosion of a clay bed with increased sand percentages mainly occurs as mass erosion instead of surface erosion. Increases of sand (5 to 30 %) causes a decrease in shear strength (50 to 80 %) *(Migniot, 1968).*

The presence of sand layers in clay as is often found in reservoirs complicates the determination of critical shear stresses for mass erosion. *Kamphuis (1989)* showed that for sand-clay mixtures, theoretical erosion conditions are related to resuspension conditions of the sand.

Results of other investigations of clay and sand mixtures have been published by *Terwindt et al (1966), Kamphuis and Hall (1983), Migniot (1989), Murray (1977), Kuti & Yen (1976), Ashida (1987).*

6.3.5 Critical mass erosion conditions for some South African reservoirs

The longitudinal distribution of critical bed shear stress ($\tau_{cme} = \rho g R s_f$) of mass erosion through a reservoir at the end of flushing has been determined for a number of reservoirs. Such distributions for Welbedacht Reservoir (front-set slope flushing channel with 1991 flushings), Phalaborwa Barrage with two historical flushings, and Windsor Reservoir (equilibrium flushing channel with dominant discharge), are shown in **Figures 6.3-12** to **6.3-14**. The τ_{cme} values in these figures are fairly constant for each case, indicating that equilibrium sediment transport and erosion conditions were approached, during the process of minimization of stream power.

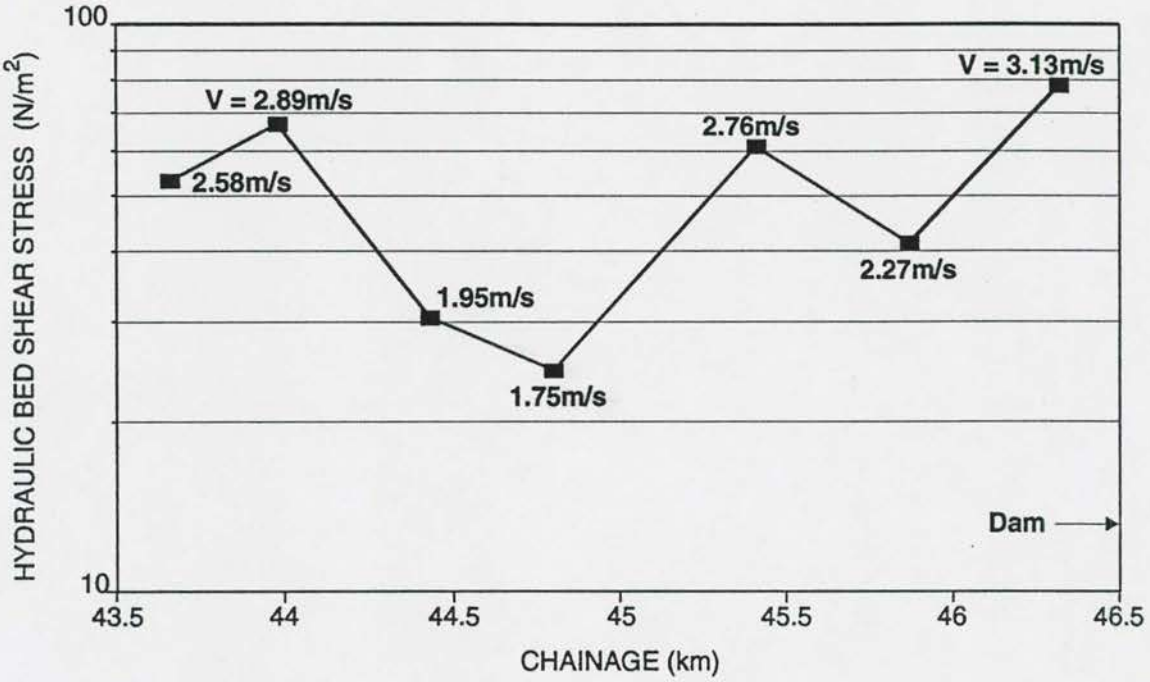

Figure 6.3-12 Bed shear stress variation: Welbedacht Reservoir flushing channel

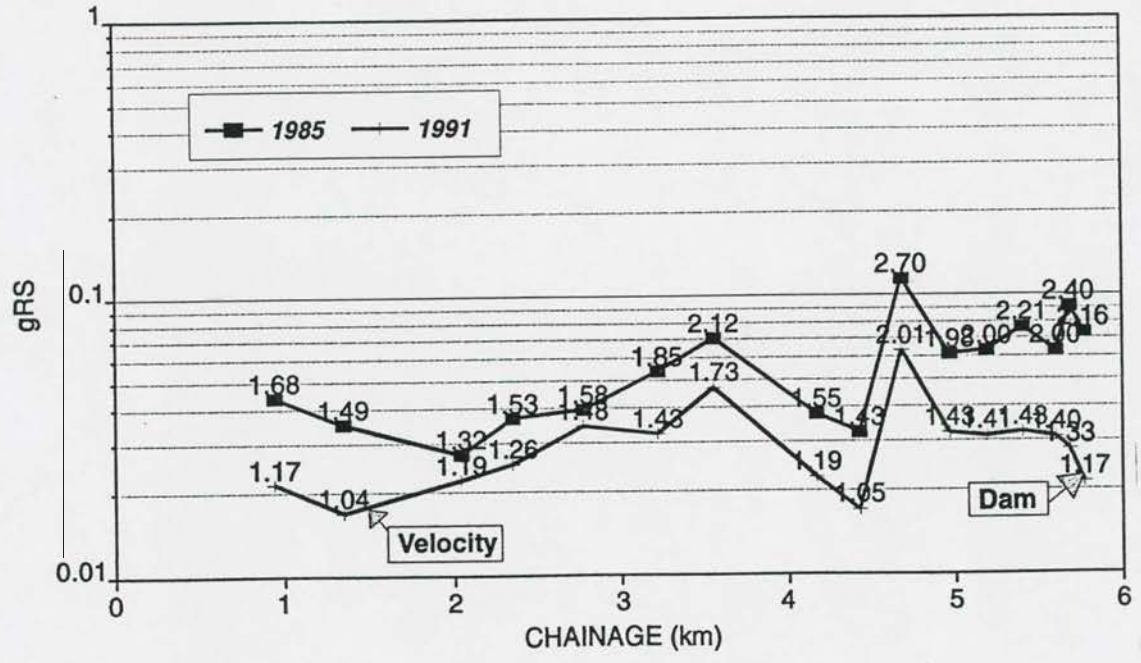

Figure 6.3-13 Bed shear stress variation: Phalaborwa Barrage

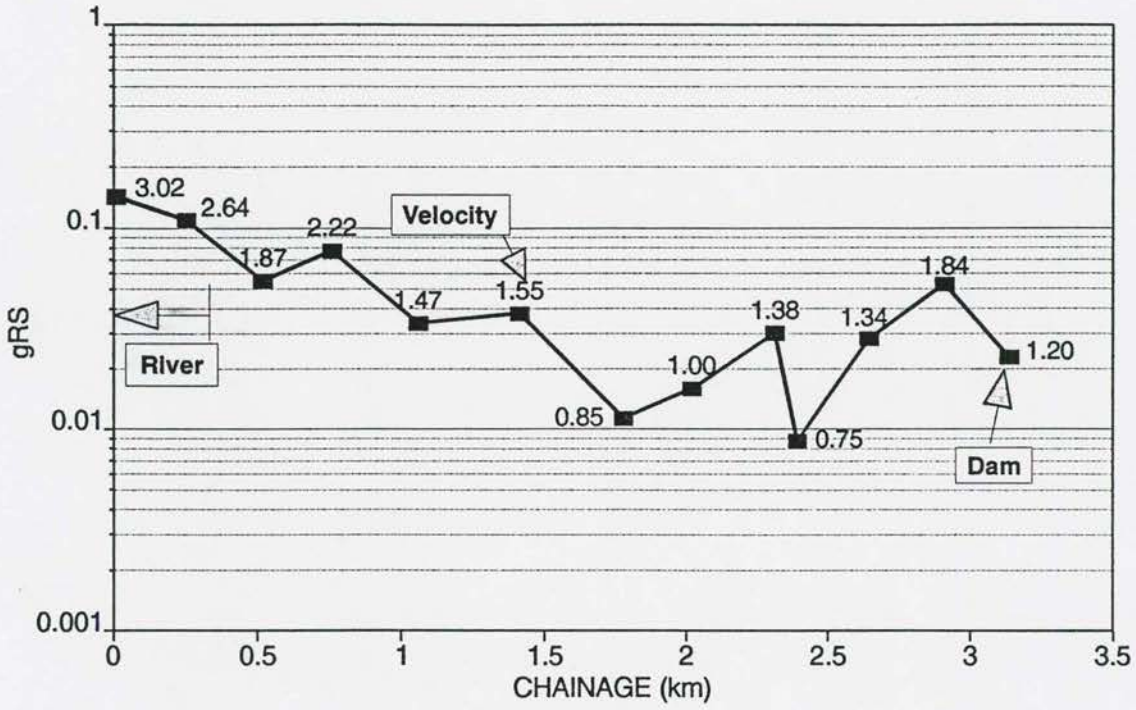

Figure 6.3-14 Bed shear stress variation: Windsor Reservoir

For Welbedacht, the maximum $\tau_{cme} \approx 80\ N/m^2$ as determined in this research, while much lower values have also been observed. During a mathematical model calibration (carried out as part of this dissertation **(Chapter 7)**), based on the 1991 canal scoured in Welbedacht Reservoir during flushing, it was found that a critical bed shear stress for mass erosion of 80 N/m^2 accurately represents the general field conditions.

In a previous study (*Rooseboom et al, 1986*) the critical conditions for erosion were determined by using the shear velocity $(gRs_f)^{0.5}$ variation through Boegoeberg Reservoir with a 1 in 2 year as well as a 1 in 10 year flood as dominant discharges. Boegoeberg Reservoir had reached near equilibrium, according to basin surveys, and deposition and scouring should be in equilibrium, and therefore it was felt appropriate to superimpose the Boegoeberg data on the Welbedacht Reservoir, which has a similar basin shape and sediment characteristics.

Figure 6.3-15 shows the Boegoeberg Reservoir shear velocities for the dominant flows. The maximum shear velocity converts to 10 N/m², compared to the 80 N/m² found from this research. The reasons for this serious underestimation in the earlier study might be the following:

- The maximum shear velocity at Boegoeberg is found at the upstream end of the reservoir, where conditions represent river, non-cohesive sediment conditions, with much lower critical resuspension criteria than at Welbedacht Reservoir, with cohesive sediment near the dam.

- The higher Welbedacht critical shear stresses were determined after erosion, while those of Boegoeberg were based on a survey which was undertaken after a long period of non-scouring conditions.

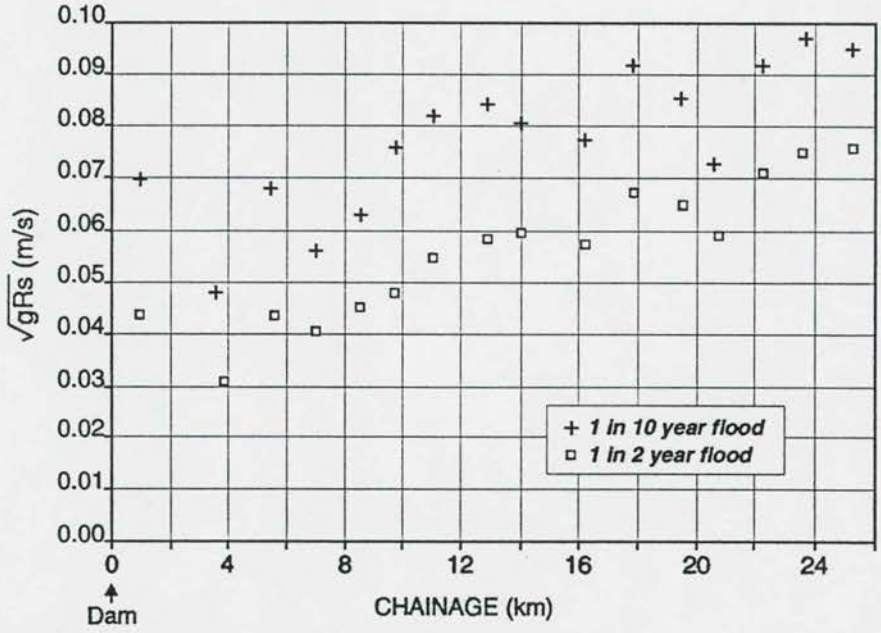

Figure 6.3-15 Boegoeberg Reservoir shear velocity variation

6.4 Width - depth relationships for reservoir flushing channels

6.4.1 General

Empirical relationships have often been used to describe the width and depth of a river in equilibrium. In a reservoir with flushing operation, South African as well as Chinese

reservoir data *(Guan, 1991)* indicate the formation of a main flushing channel with an almost trapezoidal shape. With drawdown flushing and a specific discharge, the channel is first eroded in depth until critical conditions for mass erosion (cohesive sediment, or incipient for non-cohesive sediment) are reached. This process is associated with bank failure as the channel deepens. Only when the equilibrium depth of scour is reached are the banks eroded further until width and depth equilibrium are reached. This gives the typical almost horizontal transverse bed profile of the flushing channel. Larger discharges will increase the equilibrium depth and width. Small discharges create a narrower channel, but if left long enough, meandering begins as the energy slope is decreased in the process of energy minimization, as was found at the Mbashe weir.

During retrogressive erosion, the top width (at water level) of an eroded channel was found to be dependent on the water discharge for a number of rivers and reservoirs in China, as indicated in **Figure 6.4-1** *(Bruk, 1985)*.

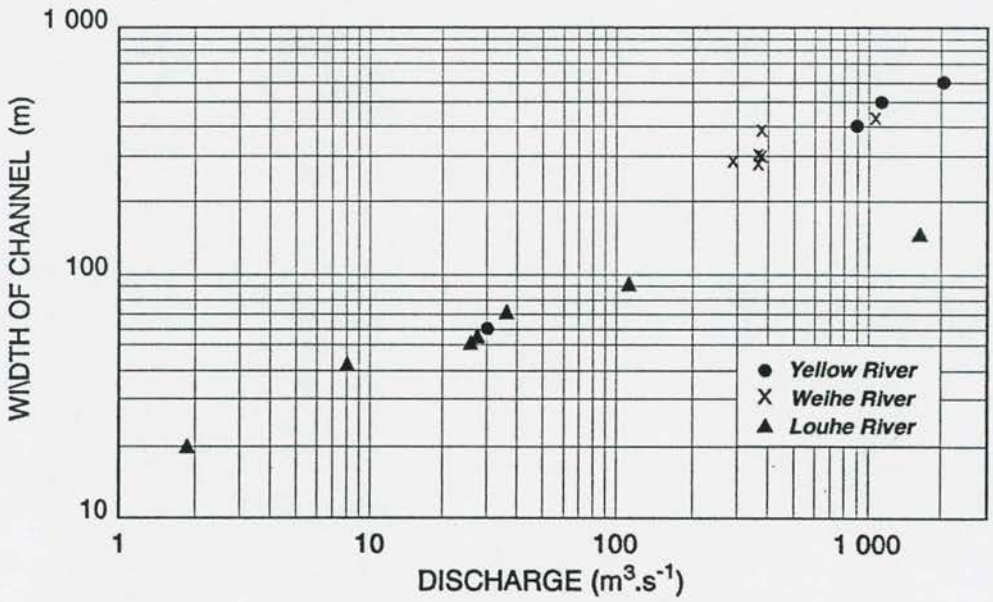

Figure 6.4-1 Relationship between flushing channel width and discharge

In order to describe the width-depth relationships of the flushing channel, the approach followed in this study was to relate depth of scour to critical conditions for re-suspension for non-cohesive, cohesive surface or mass erosion, while the width of scour is determined from an empirical relationship related to the discharge. The variability of sediment characteristics and lack of field data, however, limits the establishment of reliable empirical relationships.

Before establishing a new relationship for critical conditions for mass erosion, existing theories on the deformation of channels are evaluated and applied to flushing channel conditions.

6.4.2 Direct width-depth relationship *(Guan, 1991)*

Guan (1991) proposed an empirical width-depth relationship for modelling of the Fenhe Reservoir. Data from 4 cross-sections indicated the relationship:

$$B = 141.H^{0,15} \qquad (6.4\text{-}1)$$

with B = bed width of flushing channel
and H = depth of flushing channel

This relationship is shown graphically in **Figure 6.4-2**.

When the South African data are combined with the Fenhe reservoir data, the relationship shown in **Figure 6.4-3** is obtained.

The South African data consist of the flushing channel data for Welbedacht Reservoir (1991), Phalaborwa Barrage (1985, 1993) and Windsor Reservoir (dominant discharge taken as the 1 in 5 year flood).

Figure 6.4-3 indicates that the South African reservoir data show more or less the same trend as the Chinese reservoir data. Each reservoir has to be considered separately, and even then variable discharges/operation can alter the channel geometry.

The relationship in **Figure 6.4-3** is purely empirical, and the B-H correlation is in fact not as good as shown graphically in **Figures 6.4-2** and **6.4-3**, since H is used on both axes. More data for a range of discharges are required for each reservoir to obtain a reliable empirical relationship of channel width versus depth.

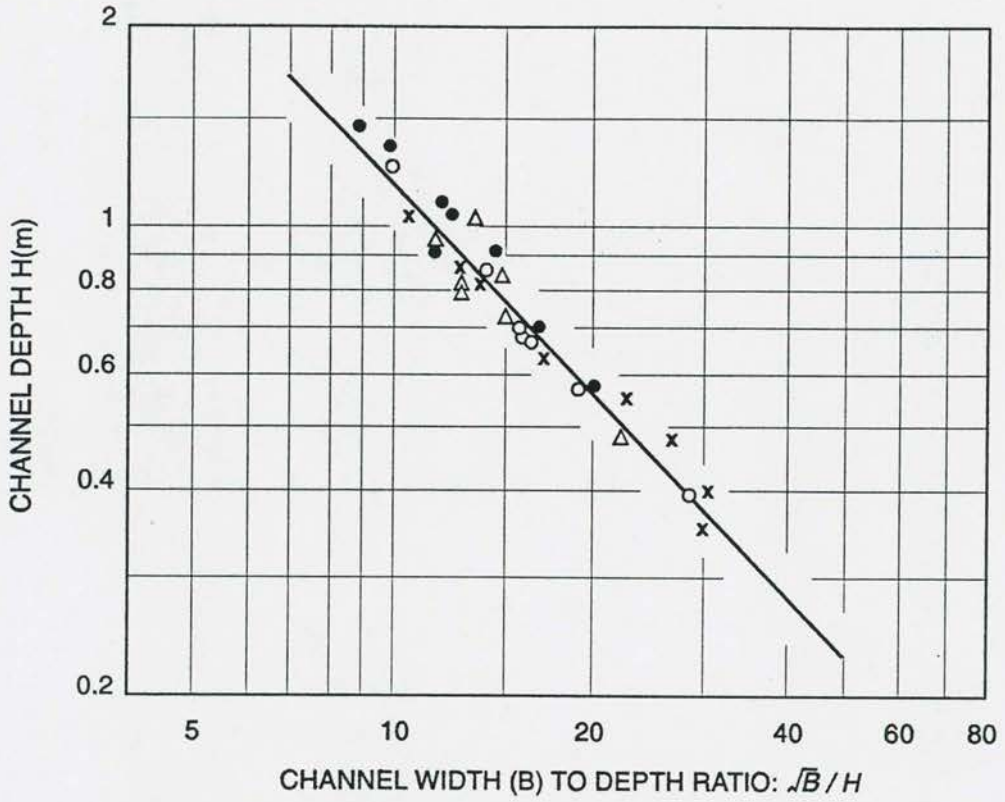

Figure 6.4-2 Flushing channel geometry relationship: Fenhe Reservoir, China

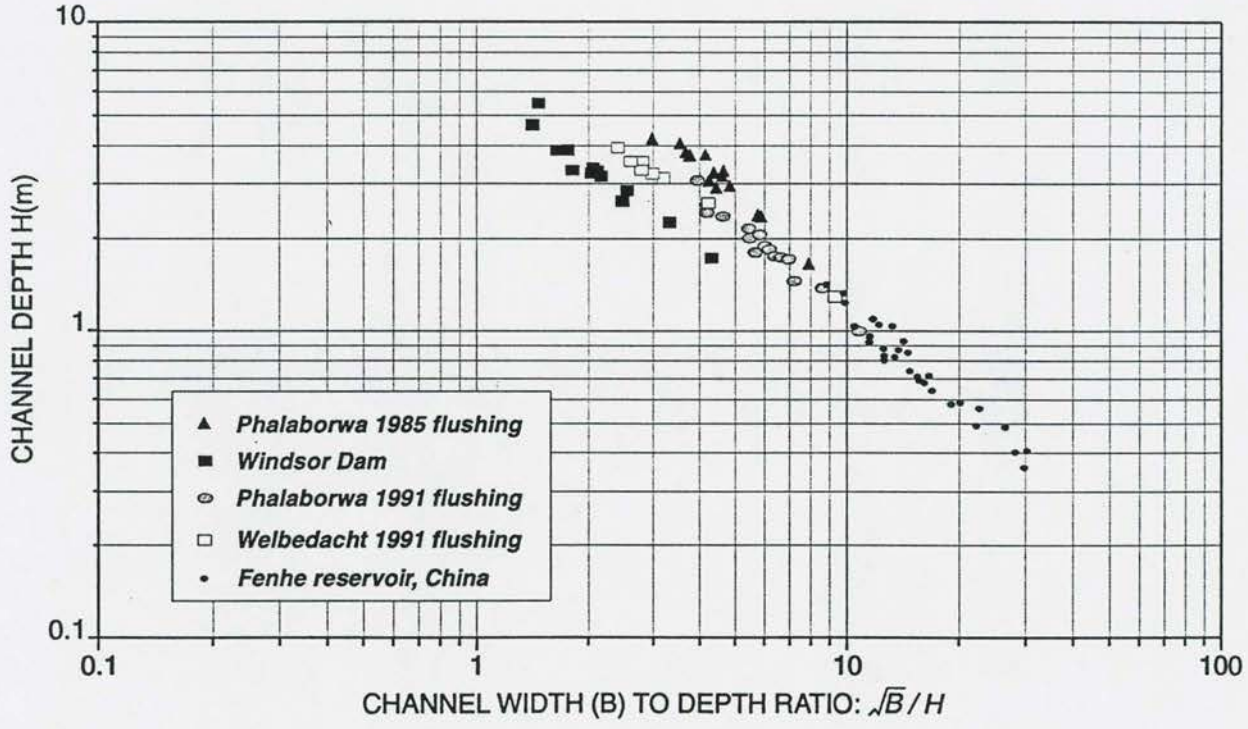

Figure 6.4-3 Flushing channel geometry relationship: South African and Chinese data

6.4.3 Morphometric equations

Three different types of morphometric equations have been established for rivers *(Batuca, 1986)*:

a) empirical (regime type)
b) semi-empirical (of the Altunin and Velikanov types)
c) theoretical (variational theory)

a) **Empirical regime equations**

Lacey (1930) derived empirical equations:

$$\begin{aligned} & v = 1{,}17\ (fR)^{0,5}\ ;\ Af^2 = 3{,}8\ v^2 \\ & P = 2{,}67\ Q^{0,5} \\ \textit{with}\quad & f = \textit{Lacey's silt factor} \end{aligned} \tag{6.4-2}$$

Lindley (1919) recognized that the type of bank material was an important factor in determining regime dimensions.

Blench (1957) used a silt factor (F_s), relating bank properties to velocity and channel width:

$$b = \frac{v^3}{F_s} \qquad \text{(English units)} \tag{6.4-3}$$

Simons and Albertson (1963) supported Blench's view:

$$P = F_s\ Q^{0,512} \tag{6.4-4}$$

The tractive force theory for stability of non-cohesive sediment was developed by *Lane (1952)*, relating shearing force of the fluid on the banks to the geometry of the cross-section and the weight of individual particles. *Henderson (1963)* used the theory to derive Lacey's **Equation 6.4-2**, modified to include particle size.

Leopold and Maddock (1953) proposed the relationships:

$$A = C_a.Q^a \quad (6.4\text{-}5)$$

$$v = C_v.Q^b \quad (6.4\text{-}6)$$

$$h = C_h.Q^c \quad (6.4\text{-}7)$$

$$B = C_b.Q^d \quad (6.4\text{-}8)$$

with A the cross-section wetted area, B = top width of flow, and C_a, C_v, C_h, C_b = constants and a, b, c, d = coefficients.

Calibrated equations with laboratory and field (river) data reveal remarkable consistency in the exponents, while the constants (C_a, ..., C_b) depend on the sediment characteristics such as particle size *(Batuca, 1986)* or cohesive nature. Typical exponent values are given in **Table 6.4-1**.

Table 6.4-1: Regime equation exponents calibrated with river and laboratory data *(Batuca, 1986)*

Author	Regime exponents				Data
	a	b	c	d	
Lacey (1930 - 1948) Blench (1957 - 1966) Nixen (1959)	0,83	0,17	0,33	0,50	River
Ribkin (1947)	0,79	0,21	0,22	0,57	River
Leopold-Maddock (1953)	0,90	0,10	0,40	0,50	River
Levi-Mostkov (1958)	0,75	-	0,22	0,50	River
Simons-Albertson (1960)	0,87	0,13	0,36	0,51	River
Ackers (1964)	0,86	0,15	0,43	0,43	Laboratory; theoretical
Langbein (1964)	0,90	0,10	0,37	0,53	Theoretical
Batuca (1980, 1981)	0,84	0,16	0,30	0,54	River

Figure 6.4-4 shows typical width relationships for Romanian rivers.

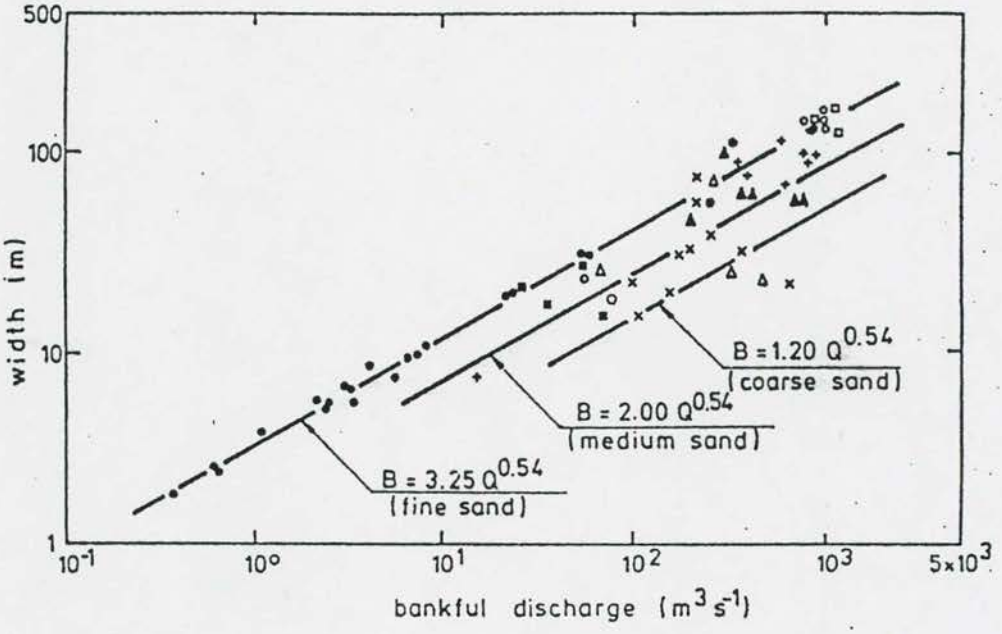

Figure 6.4-4 Regime morphometric equation calibration

b) **Semi-empirical morphometric equations**

The hydraulic geometry of stable channels was described by *Ghuskov (1926)*, later theoretically justified by *Altunin (1947, 1950, 1953)*:

$$B^m/h = k \tag{6.4-9}$$

with m = morphological stability of the channel from Orlov's equation (1952):

$$m = 0{,}72 \left(\frac{\rho_s - \rho}{\rho} \cdot \frac{d_{50}}{h.s_o} \right)^{0{,}10} \tag{6.4-10}$$

with recommended	m	=	1,0 for upper river reach,
values	m	=	0,54 for mean reach, and
	m	=	0,50 for lower reach.

The constant k's values range from 1,5 (coarse sediment) to 15, typically 2 to 4 for sand beds.

Velikanov (1954, 1958), using dimensional analysis, proposed a width relationship:

$$\frac{B}{d} = A_1 \left(\frac{Q}{d_{50}^2 \sqrt{gds}} \right)^{x_1} \tag{6.4-11}$$

which calibrated with river data typically gives A_1 = 5,6 to 7,3
and x_1 = 0,37 to 0,4 *(Batuca, 1986)*.

c) **"Theoretical" morphometric equations**

Variational concepts in river engineering were first introduced by *Velikanov (1958)*, who formulated the principles of minimum dissipation of flow energy during the formation of stable channels.

Hancu (1976) used the principle of maximum sediment transport, while *Yang (1980)* introduced the minimum unit stream power concept to describe stable river cross-sections and *Chang (1980)* also used a minimum stream power approach. *Chang* stated that the regime is established when the total stream power $\gamma Q s_o$ is a minimum, subject to constraints.

White et al (1982) used a hypothesis of maximization of sediment transport in establishing channel regime which they show is equivalent to the approach by Chang. No physical justification to support the extremal methods could be found.

Based on the principle of maximum entropy, *Deng (1994)* derived a relationship which is in good agreement with the statistical mean values of 260 sets of field data:

By assuming unit input stream power as the dominant factor in river channel formation *(Yang, 1972)*, Deng used:

$$\begin{aligned} \frac{d(vs)}{dx} &= \frac{d}{dx}\left(\frac{Q^3 n^2}{B^3 H^{13/3}} \right) \\ &= Q^3 n^2 \left(- \frac{3}{B^4 H^{13/3}} \cdot \frac{dB}{dx} - \frac{13}{3B^3 H^{16/3}} \cdot \frac{dH}{dx} \right) \end{aligned} \tag{6.4-12}$$

Therefore the increment of (vs) consists of two parts:

$$P_B = \frac{-3Q^3n^2}{B^4H^{13/3}} \cdot \frac{dB}{dx} \Big/ \frac{d(vs)}{dx} \tag{6.4-13}$$

and $$P_H = \frac{-3Q^3n^2}{3B^3H^{16/3}} \cdot \frac{dH}{dx} \Big/ \frac{d(vs)}{dx} \tag{6.4-14}$$

with $$P_B + P_H = 1 \tag{6.4-15}$$

Using the principles of maximum entropy, it was indicated that the self-adjustment of vs is equally compensated by the increments of B and H.

$$\therefore P_B = P_H \tag{6.4-16}$$

Qian (1987) reports an investigation at 165 gauging stations which found that a channel changes all its hydraulic parameters (B, H, s, v) in an even distribution among them.

Substituting **Equations 6.4-13** and **6.4-14** into **Equation 6.4-17**:

$$\frac{dB}{dx} = \frac{13B}{9H} \cdot \frac{dH}{dx} \tag{6.4-17}$$

and integrating:

$$\frac{B^{9/13}}{H} = k_{o_1} \tag{6.4-18}$$

similar to the Altunin equation.

Simultaneous solution of **Equation 6.4-18** and equations of continuity, resistance to flow and sediment transport, provide the morphologic equations for the cross-sectional geometry.

$$Q = \frac{BH^{5/3}S^{1/2}}{n} \tag{6.4-19}$$

If the dominant discharge is known, substitution of **Equation 6.4-18** into **Equation 6.4-19** gives:

$$B = k_B\, Q^{13/28}/J^{13/56} \quad (6.4\text{-}20) \quad \text{and} \quad k_B = n^{13/28}\, k_o^{65/84} \tag{6.4-22}$$

$$H = k_H\, Q^{9/28}/J^{9/56} \quad (6.4\text{-}21) \quad \text{and} \quad k_H = n^{9/28}\, k_o^{13/28} \tag{6.4-23}$$

and $$k_B = 0{,}5m_c \tag{6.4-24}$$

from river data and m_c = critical bank slope of v-shaped cross-section.

Substituting **Equation 6.4-24** into **Equations 6.4-22** and **6.4-23** gives:

$$k_o = k_B^{84/65}\, n^{3/5} = (0{,}5m_c)^{84/65}/n^{3/5} \tag{6.4-25}$$

$$k_H = (n/k_B)^{3/5} = \left[\frac{n}{(0{,}5\ m_c)}\right]^{3/5} \tag{6.4-26}$$

The primary morphological coefficient (k_o) is therefore inversely proportional to the roughness n and directly proportional to the bank slope m, also found by *Chang (1988)*.

Deng (1994) verified **Equations 6.4-20** and **6.4-21** with Chinese river and reservoir data as shown in **Figure 6.4-5** and **Table 6.4-2**.

Table 6.4-2: Value ranges of parameters used in the verification

Parameter	Range
Dominant discharge Q(m^3/s)	0,0055 - 60000
Channel slope J(10^{-4})	0,04 - 214,67
Sediment concentration S(kg/m^3)	0,06 - 196,5
Median diameter d_{50} of suspended load (mm)	0,0043 - 0,055
Median bed material size D_{50} (mm)	1,3 - 175,8
Roughness n ($s/m^{1/3}$)	0,0061 - 0,0727
Critical side slope m_c	0,9 - 12
Water surface width B (m)	0,40 - 3050
Mean flow depth H (m)	0,031 - 45
Mean velocity v (m/s)	0,28 - 4,00

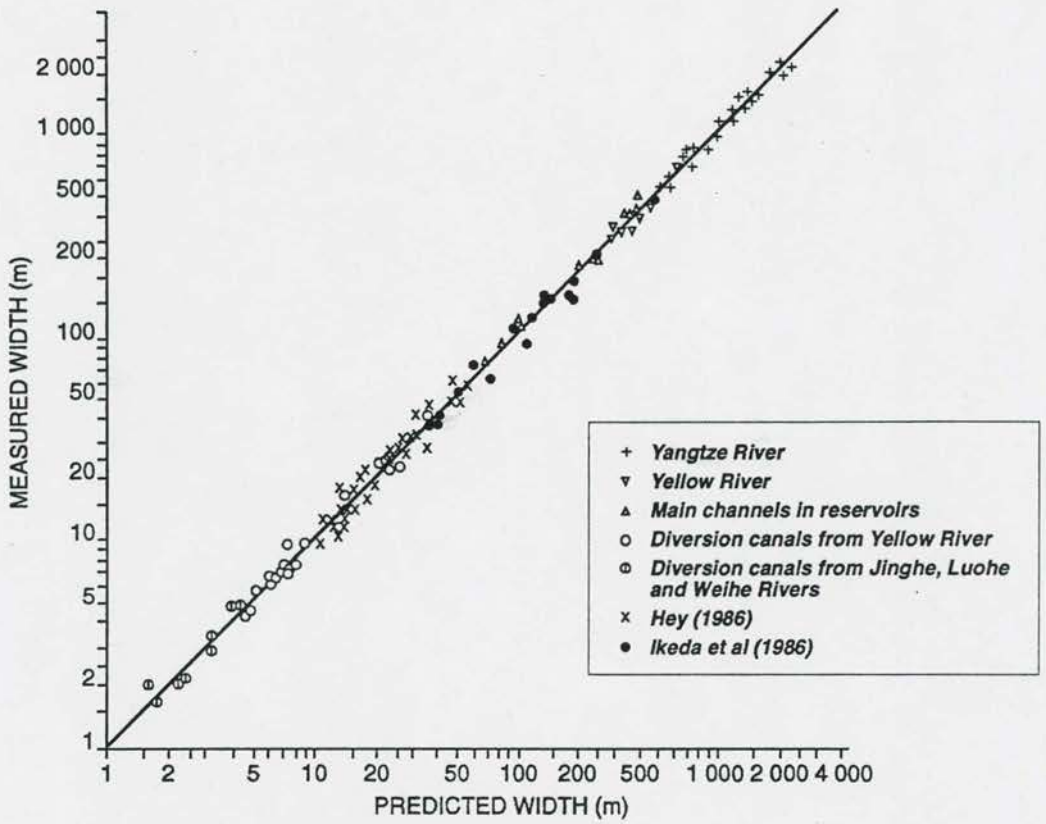

Figure 6.4-5 Comparison of measured and predicted water surface width

In a comparison of the accuracy of width formulas by *Lacey (1929), Schumm (1969), Chang (1983)*, and the Lacey divergence predictor *(Chitale, 1977)* with river data, the Lacey divergence predictor was found superior *(Chitale, 1995)*.

Bank stability has been used as a controlling factor in determining river widths. Different failure mechanisms can be considered based on soil mechanical principles *(Thorne, 1982)*.

The morphometric equations, although seemingly giving accurate predictions, are not based on fundamental theory and are highly empirical. Minimization of stream power or maximization of sediment transport to predict width-depth ratios have been applied successfully, but no theoretical explanations are given why or how these morphological changes occur. The applied stream power concept which has been used in this research to describe sediment transport and critical conditions for erosion of cohesive and non-cohesive sediments, can be used to describe equilibrium channel depths, while the channel width is

related to the discharge. The applied power theory provides the answers to why and how the river channel deforms in the process of minimization of stream power.

6.5 Relating flushing channel deformation to sediment and hydraulic characteristics

6.5.1 General

The trapezoidal flushing channel found in a number of reservoirs led to the use of soil mechanical relationships which can be empirically related to the side slope. Since the sediments are mostly of a cohesive nature, it is not possible to relate bank slope directly to the angle of repose of particles alone: cohesion also needs to be considered.

Prediction of the depth of scour for non-cohesive sediments can be related to minimization of applied power. The same would apply to cohesive sediments, but the cohesive nature of the sediment needs to be considered. It is therefore proposed that the critical shear stress for mass erosion on the flushing channel bed is related to cohesion (if applicable) and sediment size characteristics.

To analyse reservoir sediments in order to determine cohesive characteristics, a number of approaches can be followed:

a) Sediment can be removed from the reservoir bed, placed in a laboratory flume, and critical scouring conditions for different flow conditions can be established. It is, however, extremely difficult (if not impossible) to accurately simulate the cohesive and consolidated sediment conditions found in the field. Several researchers in the field of cohesive sediment have shown that repeatability of test results when working with cohesive sediments is extremely difficult to obtain. Results can vary by orders of magnitude. This is because the cohesion is determined by the flocculation process, which is affected by various factors such as duration of deposition, water quality, degree of consolidation etc.

b) Observed conditions critical to mass erosion in the field can be used, which is preferred, owing to the many uncertainties involved with cohesive and consolidated sediments.

c) When trying to relate bank slope and critical mass erosion conditions to sediment characteristics, again the approach of using undisturbed field conditions needs to be followed as far as possible. Tests can either be carried out directly in the field or "undisturbed" samples can be taken to be analysed in the laboratory under simulated field conditions using standard geotechnical methods.

6.5.2 Welbedacht Reservoir bed sediment sampling

Welbedacht Reservoir was selected for a core sampling exercise due to the regular basin surveys that are available, which made planning of the sampling much easier.

The available methods for field measurements are:

a) Penetrometer: Measurement of penetration rate, which can be related to consolidation.

b) Vane shear apparatus: From the surface, the sediment can be penetrated to the required depth, where the shear vane can be applied to establish the 3-dimensional shear stress characteristics. A drawback is, however, that a sediment sample for particle size analysis cannot be obtained in the same process.

c) Selby tube method: From the water surface (fixed float), a pipe is washed down into the sediment to the required depth. The Selby tube is then lowered down inside and a sample of (say) 500 mm can be taken at the bottom, raised to the surface and sealed for later analysis in the laboratory. (Or alternatively a vane shear test can be carried out in conjunction with the removal of sediment.) Possible problems related to the Selby tube method are:

- the difficulty of maintaining the same position on the surface and wave action also needs to be considered,
- unconsolidated sediments may drop from the bottom of the tube before reaching the surface.

d) In situ freezing of sediment: Although often used in the past to determine sediment density, it cannot be used to obtain undisturbed samples since the cohesive nature of the sediment is altered.

e) A sediment core can be obtained by mechanical equipment hydraulically driven from a fixed float on the surface. This is possibly the best method to use, but there is still the possibility that sediments can drop out of the bottom, although core catchers are often used. The method is, however, expensive due to the transport of heavy equipment and slow manoeuvrability and positioning on the reservoir.

f) Sediment core obtained by using divers: This approach was found to be the cheapest and most efficient method of obtaining sediment cores in this study. The method involved the insertion of a PVC pipe into the softer upper layers of sediment. The pipe is then rammed to the required depth by means of an underwater hammer mechanism by a diver. The core is lifted by the diver at the bed, assisted from the surface. The core is capped as soon as it is raised from the bed. The sediment core is, of course, not undisturbed, because of the way in which the core is obtained (most methods will cause some disturbance). At Welbedacht Reservoir it was found that the pipes could actually be inserted fairly easily, but greater difficulty was experienced with the extraction due to cohesion on the pipes.

Sediment cores (maximum length of pipes 6 m) were taken during 1995 in Welbedacht Reservoir. The aim was to obtain bottom sediments from the level of the first flushing (1991) in the main channel. From **Sections 2** to **8**, cores were obtained, one on each bank, of the flushing channel and two on the bed, giving 28 cores in total (**Figure 6.5-1** and **Photograph 6.5-1**). Laboratory analyses were carried out to relate hydraulic conditions with sediment size, cohesion and density.

During the planning phase of the field sampling programme, many uncertainties as to the nature of the sediment at depth made it difficult to decide on a procedure to obtain samples. Since the 1991 flushings, more than 2 m of deposits had accumulated on top of the scoured bed through which had to be cored. The Council for Geoscience's marine geology unit was contracted to conduct the Welbedacht sampling since they had had similar coastal and inland experience.

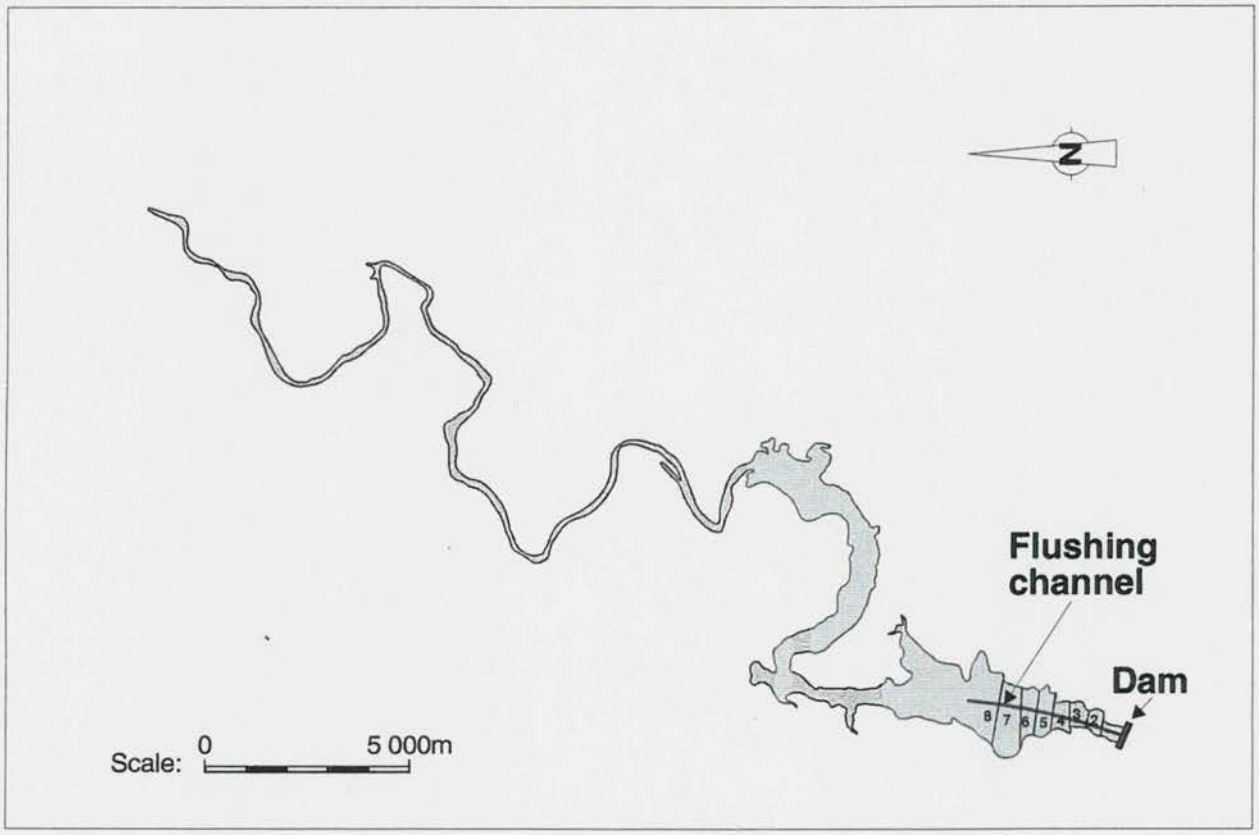

Figure 6.5-1 Welbedacht Reservoir basin layout

Photograph 6.5 - 1 Sediment core sampling at Welbedacht Reservoir

Sediments of low density were encountered in the first 0,5 m of the bed. Lower sediments were more consolidated, but layers of sand corresponding to high inflow conditions and/or flushing with high intensity were also found.

Once removed from the reservoir, the cores were sealed and transported to the laboratory upright and saturated.

One major problem with the sediment core sampling was that a significant degree of consolidation of the upper sediment was experienced due to cohesion between the pipe and the deposits. It is, however, believed that the impact of consolidation during sampling was incremented and that the deepest sediments to be sampled were not much influenced by the consolidation. When the cores were later opened before testing, it was found that the higher-density sediments to be tested actually expanded slightly in length as they were removed from the pipes, probably reversing the sampling consolidation process somewhat. Sediment densities thus obtained are not deemed to be reliable, while it is believed that other variables being tested were not significantly influenced by the sampling method.

The degree of consolidation found during sampling is indicated in **Table 6.5-1.**

Table 6.5-1: Depth of pipe insertion and core lengths

Reservoir Section	Pipe insertion depth from bed level (m)				Sediment core length in pipe (m)			
	Core position left to right bank							
	A	B	C	D	A	B	C	D
2	2,4	3,8	3,3	1,7	1,6	2,1	2,1	1,0
3	1,5	3,5	3,3	1,9	0,9	1,7	1,7	1,2
4	2,4	3,8	2,8	1,5	1,5	2,4	1,5	1,1
5	3,5	4,9	4,7	2,2	1,8	1,8	2,0	1,3
6	1,9	4,2	4,4	2,3	1,0	2,2	2,4	1,4
7	3,6	4,3	5,0	3,2	2,3	2,4	2,3	1,6
8	3,2	4,2	4,1	3,8	1,4	2,5	2,1	1,9

6.5.3 Relating soil mechanical and hydraulic characteristics to determine critical conditions for mass erosion - methodology

The bed shear stress (τ) is often used as a parameter in describing incipient conditions. *Rooseboom et al (1982)* related the applied power at the bed $\left(\tau \frac{dv}{dy}\right)_o$ to mechanical power ($F.v$) as determined in a shear box test (with F = applied force and v = velocity of shear box movement during test). Dry samples obtained from the field were compacted in the shear box and the test results could be used to describe when erosion of cohesive soil on steep slopes will occur.

It was thought to conduct similar tests on the reservoir sediment, with a few differences:

- the sediment sample had to be placed undisturbed in the shear box, which made it necessary to build a circular hole inside the usual square box in which the sample could be pushed directly from the core pipe,

- the force applied to the sample had to represent the water and sediment pressure as experienced in the field, and

- the sample had to be analysed under saturated conditions.

All of the above seemed easy to obtain in the laboratory and the shear box provided the horizontal failure mechanism one could expect from a horizontal shear stress acting on the bed. In practice, however, it was impossible to carry out the tests due to the fineness of the sediment. Since the sediment was saturated, the sediment was squeezed through the tiniest of openings of the shear box apparatus when the normal force was applied, and this was before the test even started. Smaller weights just to balance the instrument before the test also did not work and still led to rapid consolidation of the low density sediment. Eventually the shear box test method had to be abandoned and resort had to be taken to triaxial tests.

Triaxial tests are in fact more accurate than shear box tests, since cell pressures representing field pressures can be applied on the sample and the problem experienced with fine sediments in the shear box is overcome. The sediment still had to be stiff enough to stand alone in a plastic membrane. The biggest drawback of the triaxial test is that failure is not horizontal but rather along the weakest shear zone in the sediment, and the duration of a test is normally quite long.

Instead of relating critical scouring conditions (applied power) to mechanical power as was originally envisaged with the shear box tests, it was decided rather to relate it to cohesion (c), angle of friction (ϕ), percentage clay and sediment density of the layer of sediment where the 1991 flushing channel bed stopped scouring. The same variables could be used in establishing a relationship with the bank slopes at each cross-section.

After a number of trial and error runs on the triaxial instruments, it was decided to follow the following testing procedure:

- Saturated, undrained tests were carried out.

- Cell pressures representing full reservoir conditions (maximum) and drained drawdown conditions (as minimum) and an average pressure were applied.

- Each core was cut into approximately 30 cm lengths, the part to be tested identified, and sealed to be tested as soon as possible after opening. Compaction of the core sediment made it difficult to establish exactly how deep the sediment in the pipe to be tested is according to the reservoir cross-section surveys. It was, however, quickly discovered that the 1991 scoured bed level is overlain by coarse sand of 10 to 30 cm thickness in the core, and most often the recent deposition above the sand lens was of a much less dense nature than that below.

- As expected, the plastic nature of the clay-silt core, caused a slow change in strength during tests and no rapid breakage (as with "normal" soil) was experienced. Continuous monitoring was therefore necessary to establish a reliable material strength.

- In combination with the triaxial tests, hand-held vane shear tests were carried out on each 30 cm cut of core before it was removed from the pipe.

The test cell pressures used are indicated in **Table 6.5-2**.

Table 6.5-2: Test cell pressures

Reservoir Section	Sample	Cell Pressure (kPa)		
		Maximum	Mean	Minimum
2	A	122	81	40
	B	152	107	61
	C	164	117	70
	D	147	102	56
3	A	116	89	30
	B	162	114	66
	C	158	111	63
	D	127	83	38
4	A	106	67	27
	B	153	109	64
	C	153	109	64
	D	126	85	44
5	A	119	82	44
	B	146	106	65
	C	148	107	66
	D	126	89	51
6	A	104	70	35
	B	131	94	57
	C	130	93	56
	D	103	68	33
7	A	97	70	42
	B	107	79	50
	C	114	85	56
	D	85	59	33
8	A	75	56	36
	B	89	69	48
	C	91	70	48
	D	82	61	40

6.5.4 Discussion of test results : bed shear stress for mass erosion

Critical scouring conditions for mass erosion in the front-set delta region of Welbedacht Reservoir were analysed and a relationship was sought with shear strengths (from triaxial tests), percentage clay and density of the sediments.

Test results are depicted in **Table 6.5-3**, and include data for channel banks and bed.

Table 6.5-3: Triaxial test results

Sample	τ (kPa) (Triaxial)	% Clay	Dry density (kg/m^3)	τ (Observed hydraulic) (Pa)	Remarks
2A	5	49	834	-	
2B	19	-	1 353	78	
2C	5	-	871	78	
2D	-	-	-	-	too soft
3A	14	19	1 339	-	
3B	11	36	1 142	41	
3C	8	21	1 202	41	
3D	5	56	791	-	
4A	11	31	1 000	-	
4B	30	17	1 134	61	
4C	-	-	-	-	too soft
4D	-	-	-	-	too soft
5A	13	35	1 052	-	
5B	11	35	1 010	25	
5C	8	36	1 030	25	
5D	43	17	1 286	-	
6A	23	20	1 210	-	
6B	10	37	1 010	31	
6C	34	16	1 366	31	
6D	15	21	1 285	-	
7A	7	29	1 107	-	
7B	13	34	1 038	67	
7C	33	18	1 249	67	
7D	22	20	1 242	-	
8A	10	31	1 038	-	
8B	41	16	1 315	53	
8C	14	31	1 090	53	
8D	35	15	1 213	-	

The results of **Table 6.5-3** clearly indicate a direct relationship between soil mechanical shear strength and dry density **(Figure 6.5-2)**, and an inverse relationship with the percentage clay in the sample **(Figure 6.5-3)**.

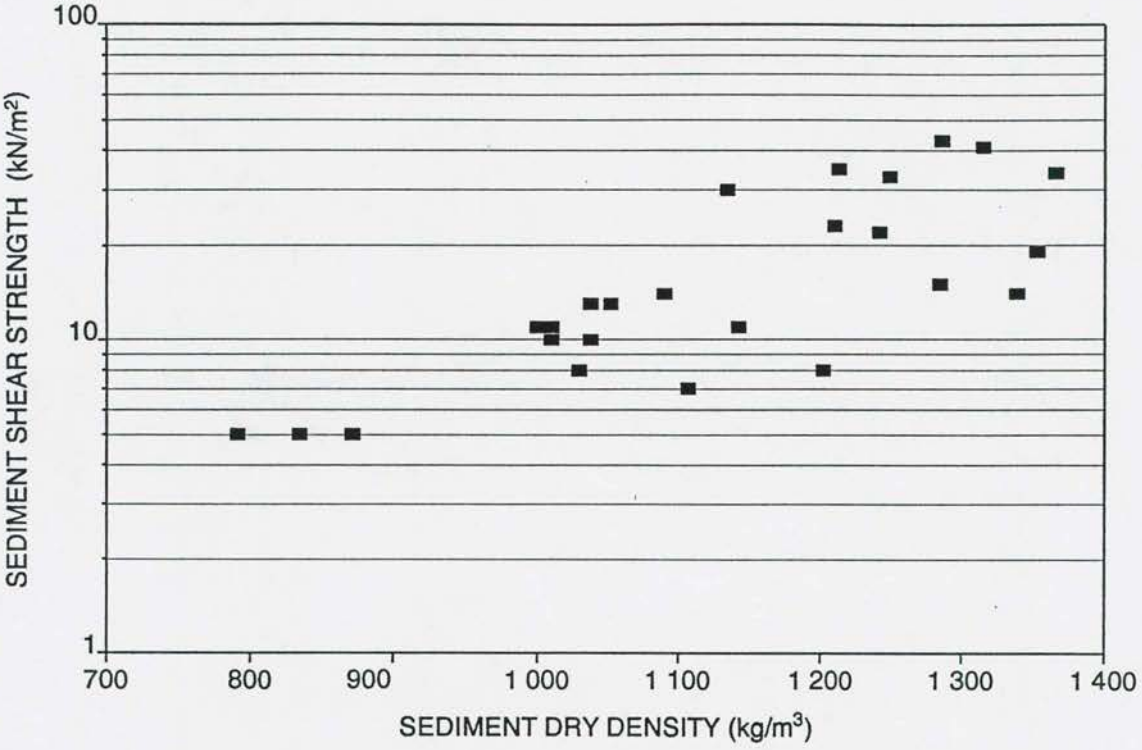

Figure 6.5-2 Shear strength versus sediment density: Welbedacht Reservoir

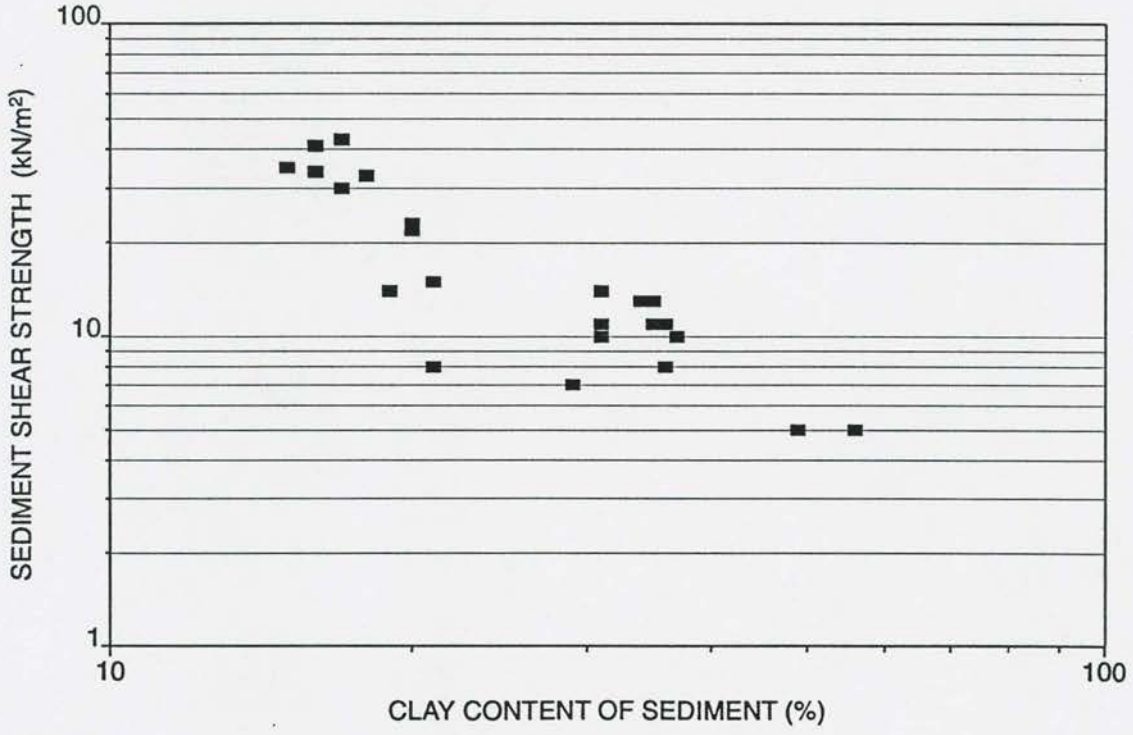

Figure 6.5-3 Shear strength versus % clay: Welbedacht Reservoir

The hydraulic bed shear stresses calculated for the 1991 flushing in Welbedacht Reservoir are also indicated in **Figure 6.3-12** and in **Table 6.5-3**.

Correlation between hydraulic and soil mechanical shear stresses, using only reliable triaxial data and averaging the bed shear stress data (triaxial) for each cross-section, yielded reasonably good results as shown in **Figure 6.5-4**. The correlation coefficient (r^2) is 0,72.

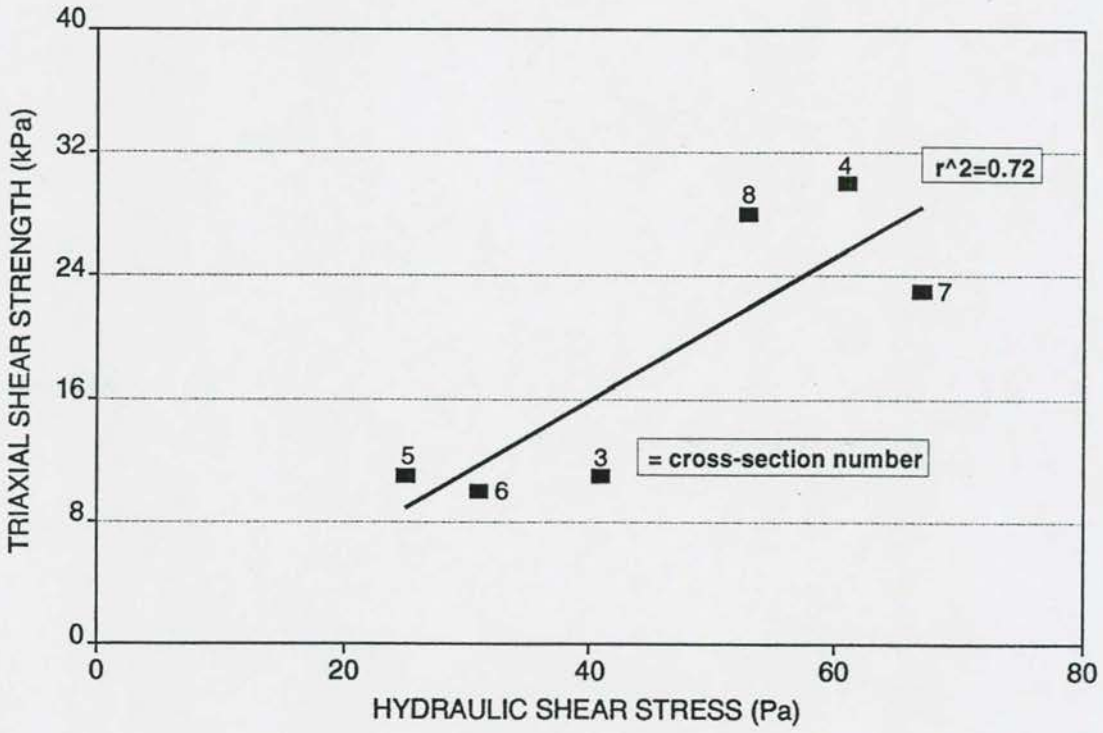

Figure 6.5-4 Shear stress correlation: Welbedacht Reservoir

The data set is too small to draw general conclusions, but the general trend seems to be that critical conditions for mass erosion can be related to the soil mechanical shear strength.

It has already been shown that the critical shear stress also depends on the percentage clay and is related also to the density of the sediment (**Figures 6.5-2** and **6.5-3**). It is therefore logical to expect that the shear stress correlation can be improved by also considering clay content and sediment density. This is indeed illustrated with the data when considering:

$$\tau_{hydraulic} = f(\tau_{triaxial;}\ 1/\%\ clay;\ dry\ density)$$

and the correlation is shown in **Figure 6.5-5** ($r^2 = 0,79$).

Figure 6.5-5 shows that if a good data base for various reservoir flushing channels can be established, quite reliable predictions of critical mass erosion conditions would be possible.

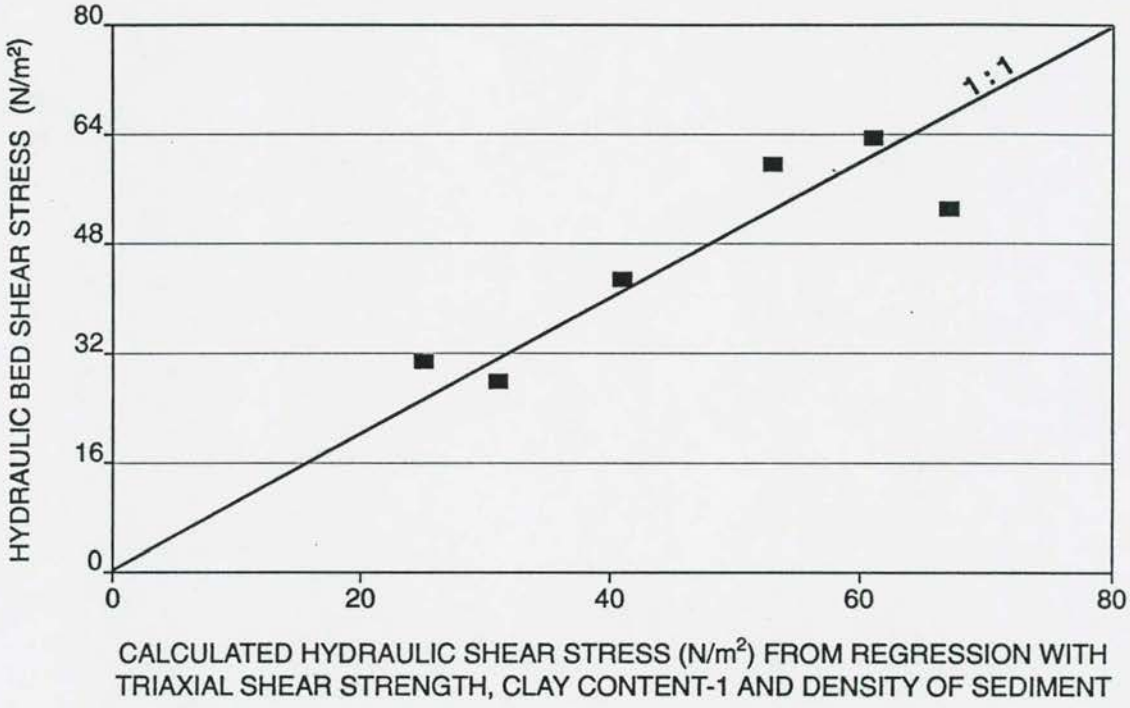

Figure 6.5-5 Shear stress as function of soil mechanical strength, % clay and density

What is very interesting from **Figure 6.5-5** is that the correlation of hydraulic shear stress versus % clay and density gives the same result as when the triaxial shear stress results are included. The particle size distribution seems to be the dominant factor in determining the degree of consolidation and the soil mechanical shear stress. *Rooseboom et al (1982)* observed the same phenomena when shear stress (from shear box tests) could be related to the fineness modulus of the material, even though the particles being tested were much coarser (fine sand) than reservoir sediments.

With an adequate hydraulic shear stress versus sediment density and particle size distribution data base, the theory can be utilised to determine critical conditions for mass erosion which vary with time and space.

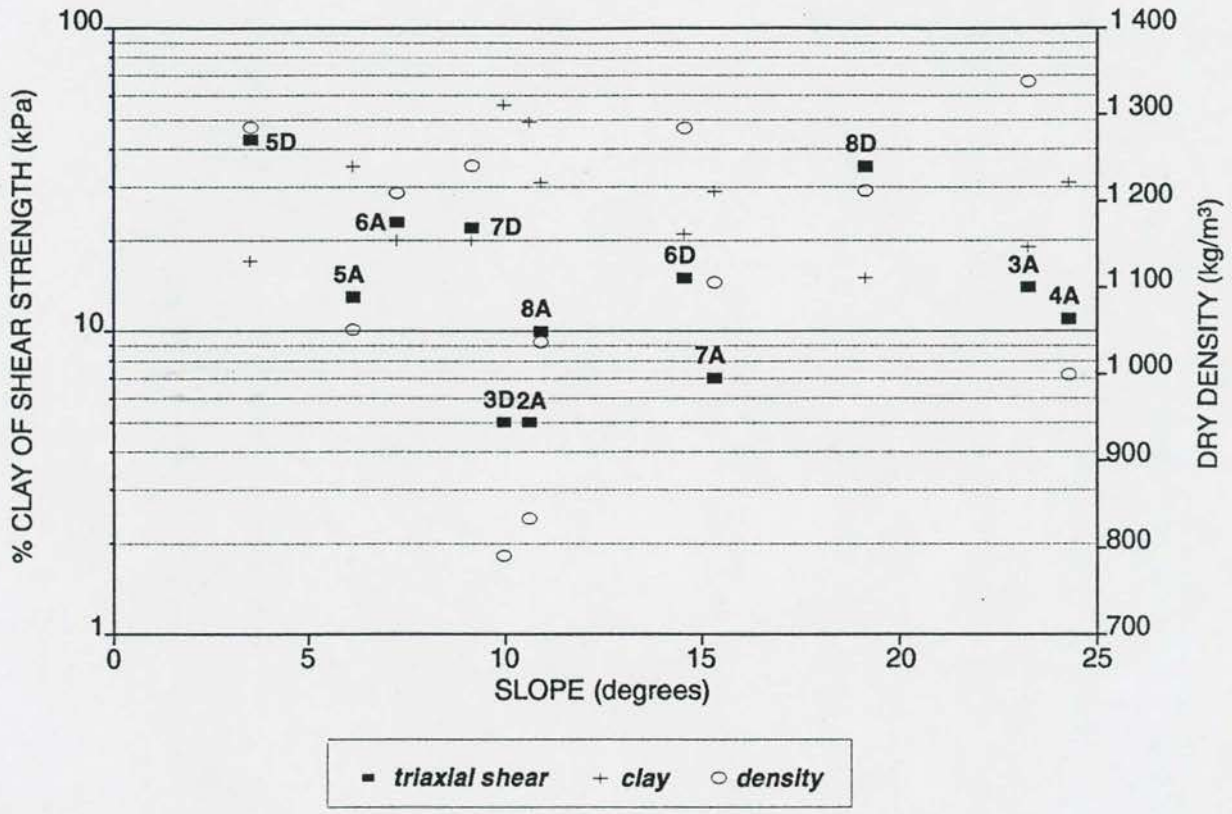

Figure 6.5-6 Flushing channel bank slope and other variables, Welbedacht Reservoir

6.5.5 Discussion of test results : prediction of flushing channel bank slopes

The nature of rapid reservoir drawdown, flushing and associated bank failure seems to indicate that the flushing channel bank slopes can be predicted by means of soil mechanical relationships.

Triaxial tests were therefore carried out on bank sediment (at 1991 scoured elevation) in an attempt to establish a possible correlation with the bank slope. The relationship between slope and shear strength, percentage clay and sediment density is shown in **Figure 6.5-6**, while the slope data are shown in **Table 6.5-4**.

Table 6.5-4: Observed flushing channel bank slopes, Welbedacht Reservoir

Section	Flushing channel bank slope (degrees)
2A	10,6
2D	19,0
3A	23,2
3D	9,9
4A	24,3
4D	14,3
5A	6,1
5D	3,5
6A	7,2
6D	14,5
7A	15,3
7D	9,1
8A	10,9
8D	19,1

The correlation between side slope and shear strength, % clay and sediment density is poor. The only conclusion that can be made is that other factors also played a role in establishing the observed bank slopes. These factors may include:

- the combined effect of flowing water and soil mechanical bank failure,
- layered deposition of coarse and fine sediment, which may lead to variable slopes,
- various bank failure mechanisms, which may produce different slopes, and
- tested samples that may not be representative of sediment eroded during the 1991 flushing.

Finally, the effect of the poor correlation in **Figure 6.5-6** is illustrated in **Figure 6.5-7**. Although the correlation coefficient (r^2) only equals 0,36, the accuracy of prediction of bank slope is such that it will over or underestimate the flow area by only + 11 % to - 7 %, when considering the extreme data.

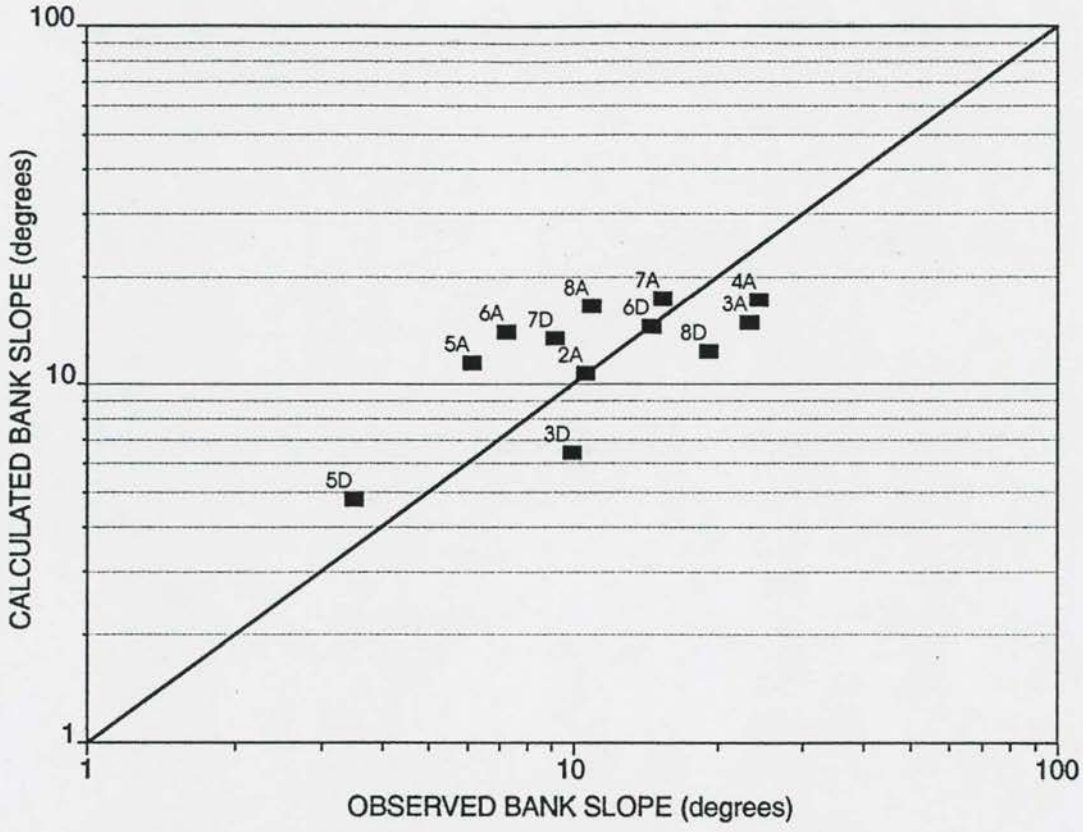

Figure 6.5-7 Flushing channel bank slope correlation: Welbedacht Reservoir

2076H/sw
1996-11-26

7. LONG-TERM EQUILIBRIUM SEDIMENTATION CONDITIONS

7.1 Introduction

The theory derived and discussed in Chapters 3 to 6 can now be combined to evaluate their joint use to determine long-term equilibrium reservoir sedimentation. Not only sediment deposition (storage operation), but also flood flushing with retrogressive erosion have to be evaluated in order to make accurate predictions of long-term sedimentation.

7.2 Minimization of stream power

One of the main points of concern in the design of a reservoir is the long-term equilibrium sediment profile which will be reached. Various mathematical models have been developed and used in conjunction with physical (and empirical) models to determine such profiles. In terms of stream power considerations, a stable sediment profile can be related to a constant shear velocity for a specific reservoir.

Rooseboom (1975) indicated that when alternative modes of flow exist, a fluid will always follow that mode that requires the least amount of applied stream power. Since most of the power is applied at the bed, only minimization of power at the boundary of flow is considered. Minimization of applied stream power at the bed can be expressed mathematically *(Rooseboom and Mülke, 1982)*:

$$minimize \left(\tau \frac{dv}{dy}\right)_{bed} \alpha \; minimize \; \rho g D s \frac{\sqrt{gDs}}{\kappa k} \tag{7.2-1}$$

Minimization is therefore possible by changing the channel geometry (D, s, k) and/or changing the fluid properties (κ). Under stable conditions, stability as regards sediment transport is also reached with κ approaching a constant value, therefore:

$$\left(\tau \frac{dv}{dy}\right)_{bed} = K \frac{(gDs)^{3/2}}{k} \tag{7.2-2}$$

Applied stream power at the bed of the channel will therefore be a minimum when

$$\frac{(gDs)^{3/2}}{k} = \text{minimum.} \tag{7.2-3}$$

Under stable conditions, k will assume a constant value of $\sqrt{gDs}$ = constant throughout the reservoir *(Annandale, 1994)*.

Under stable conditions, the exchange of sediment particles between fluid and channel boundary would also be stable, and by using stream power theory it can be shown theoretically and experimentally *(Rooseboom 1975; Yang, 1976)* that

$$\frac{\sqrt{gDs}}{w} = constant \qquad (7.2\text{-}4)$$

with w = settling velocity of sediment under conditions of incipient motion.

Assuming a direct relationship between w and k *(Graf, 1971)*, shear velocity is constant giving the same relation as **Equation 7.2-4**. Criteria for minimization of applied power and incipient motion therefore yield the same relationship for stable sediment profiles.

When equilibrium sedimentation is reached in a reservoir, the incoming sediment load equals the outgoing sediment load, with no further (net) deposition. In a reservoir operated for water and sediment control, the long-term capacity is determined by the flushing channel capacity, since flood plain deposits cannot be re-entrained. Normally (except in a gorge type reservoir) the flushing channel width is less than the width of the main river *(Zhou, 1995)*.

7.3 Proposed reservoir sedimentation model

Several mathematical models have been developed in the past to simulate reservoir sedimentation deposition processes, but only a handful have been designed to simulate sluicing/flushing with reservoir water level drawdown *(Han, 1973, 1990; Thomas and Prasuhn, 1977; Chollet and Cunge, 1980; Sanchez, 1982; Zhang, Q, 1983; Pitt and Thompson, 1984; Holly and Rahuel, 1990; Yang, 1992; Vasiliev et al, 1993; Wang, SSY, 1993; etc)*. Although most "river" mathematical models can simulate the latter condition, which closely relates to river flow conditions, there are factors such as fine sediment transport, cohesive sediment deposits, consolidation of the bed, as well as different modes of re-entrainment of sediment which all need to be accounted for.

For modelling of reservoir sedimentation processes, a model should be able to simulate both short-term (flushing) and long-term deposition events, with non-cohesive and cohesive sediments. It should be borne in mind that the "ideal" mathematical model is only as good as the theory it is based on.

The mathematical model MIKE 11 of the Danish Hydraulic Institute has been modified to incorporate the theory for reservoir sedimentation processes, which has subsequently been calibrated and verified with reservoir data.

The reservoir flushing model which has been developed has the following characteristics:

a) **One-dimensional (1D)**

One-dimensional models are mostly used in river and reservoir applications around the world, although computationally "heavy", two-dimensional (2D) and even 3D models have been developed. The main constraints in using a 2D model with sediment transport is often a lack of data for calibration of the model, and secondly the uncertainty of the sedimentation processes. It is generally believed that modelling with a 2D approach often does not give more accurate or reliable results. For flushing application, a 1D model should be adequate due to the narrow river-like flow conditions which prevail in the narrow channel which is formed when reservoir flushing is practised.

Two-dimensional models can be of specific benefit when considering:

- deposition outside the main channel across the wide open reservoir basins often encountered in South Africa;
- sediment built up at a specific position in a reservoir, such as at a tunnel intake; and
- modelling of flushing when sediment transport conditions vary across the main channel, as was found at Phalaborwa Barrage.

b) **St Venant equations for hydrodynamic simulation**

A fully hydrodynamic approach is required to describe the rapidly changing flow and bed level conditions during flushing. The model must also be able to simulate the supercritical flow conditions which can be encountered during drawdown flushing. Typical outflow conditions during flood flushing are indicated in **Photograph 7.3-1** as observed at Phalaborwa Barrage, 1996.

Photograph 7.3-1 Phalaborwa Barrage flood flushing (900m^3/s, February 1996)

c) **Sediment transport**

The unit (input) stream power equation *(Yang, 1973)* was implemented in the MIKE 11 model by using user-defined input parameters M and N in **Equation 7.3-1**:

$$\log(C) = M + N \log\left(\frac{VS}{w_i}\right) \qquad (7.3\text{-}1)$$

with	C	=	sediment concentration (ppm)
	M,N	=	values defined by user
	v	=	flow velocity
	s	=	energy slope
	w_i	=	settling velocity of fraction i.

Equation 7.3-1 has been calibrated with data from a number of South African reservoirs for flood flushing and storage operation conditions, with M = 4,31 and N = 0,343.

Several other well-known sediment transport equations are also available in the MIKE 11 model to simulate transport of coarse fractions.

d) **Coupled solution of flow and sediment equations, with sediment continuity**

A coupled solution is required due to the rapidly changing hydrodynamic and sediment transport conditions during flushing.

e) **Non-uniform sediment modelling**

It is essential in reservoir modelling that sediment transport calculations are carried out per size fraction in order to model the sorting process and related non-cohesive and cohesive deposits through the reservoir.

f) **Non-equilibrium sediment transport of fine sediment**

Non-equilibrium transport of fine sediment occurs, which means that transition to saturated sediment transport capacity conditions is not instantaneous as for coarser fractions, but a time and distance lag is involved. The multifraction model (MIKE 11) which has been developed in this study can operate with a traditional equilibrium transport equation for some fractions and a non-equilibrium formula for others.

The non-equilibrium modelling is based on solution of the unsteady advection-dispersion equation, with a source/sink term *(ss)* describing erosion and deposition:

$$\frac{\delta C}{\delta t} + u\frac{\delta C}{\delta x} - D\frac{\delta^2 C}{\delta x^2} = ss \qquad (7.3\text{-}2)$$

with D the dispersion coefficient,

u = flow velocity,
t = time,
x = distance in direction of flow

In case of non-cohesive sediments the source/sink term (ss) is represented by:

$$ss = \frac{(C^* - C)}{aT} \qquad (7.3\text{-}3)$$

with C* the equilibrium sediment transport calculated with a sediment transport formula,

"T" is the time scale defined as settling time (water depth divided by settling velocity),

"a" is a calibration parameter as described in **Chapter 3** and can be interpreted as a mean (relative) settling depth. In the model implementation, the coefficient "a" is different for various given size fractions, for erosion and deposition.

For non-cohesive sediments, incipient motion is determined according to the sediment transport model used. For cohesive sediment (fractions) the source/sink term should be represented by:

$$ss = 0 \quad ; \tau < \tau_{ce} \qquad \text{(No erosion)} \qquad (7.3\text{-}4)$$

$$ss = E(\tau - \tau_{ce}) \quad ; \tau_{ce} < \tau < \tau_{cme} \qquad \text{(Surface erosion)} \qquad (7.3\text{-}5)$$

$$ss = \frac{(C* - C)}{\Delta t} \quad ; \tau > \tau_{cme} \qquad \text{(Mass erosion, no lag)} \qquad (7.3\text{-}6)$$

with τ = bed shear stress,
τ_{ce} = critical shear stress for surface erosion,
τ_{cme} = critical shear stress for mass erosion,
E = erosion rate.

g) **Calculation of erosion**

The model combines theory for non-cohesive and cohesive sediment to model three cases of erosion: cohesive sediment, non-cohesive sediment and a mixture of the two. In the latter case, a linear combination of the cohesive and non-cohesive relationship is used. The erosion rate, assuming both cohesive and non-cohesive sediment, is calculated, and the actual rate determined via linear interpolation.

For surface erosion, the erosion rate is checked against sediment transport capacity in order not to exceed the capacity. Mass erosion modelling is based on the assumption that (instantaneous) erosion will take place to satisfy the sediment transport capacity.

The availability of sediment for erosion is checked. If the calculated erosion rate exceeds the available sediment supply, the rate is reduced to reflect the amount of available sediment.

h) **Cross-section deformation**

Solution of the bed continuity equation determines whether erosion or deposition will occur.

When deposition occurs it is assumed that:

$$dz = aD^b \tag{7.3-7}$$

with dz the change in bed level, a and b input calibration parameters and D the flow depth.

During erosion phases it is assumed that the cross section will be of a trapezoidal shape described by regime type equations (relating width and depth to the discharge). Bank slopes of the trapezoid are required as input parameters. The difference between the actual bed level and that of the trapezoidal section is integrated to determine what changes are required.

The following special cases have been identified:

- The trapezoidal section is "smaller" than the actual section : **Equation 7.3-7** is used for changing the bed level

- Erosion goes below the original (bedrock) section : increase width if bed is non-erodible and lower bed if sides are non-erodible; otherwise erosion is limited.

Typical surveyed cross sections of Welbedacht Reservoir are shown in **Figure 7.3-1**.

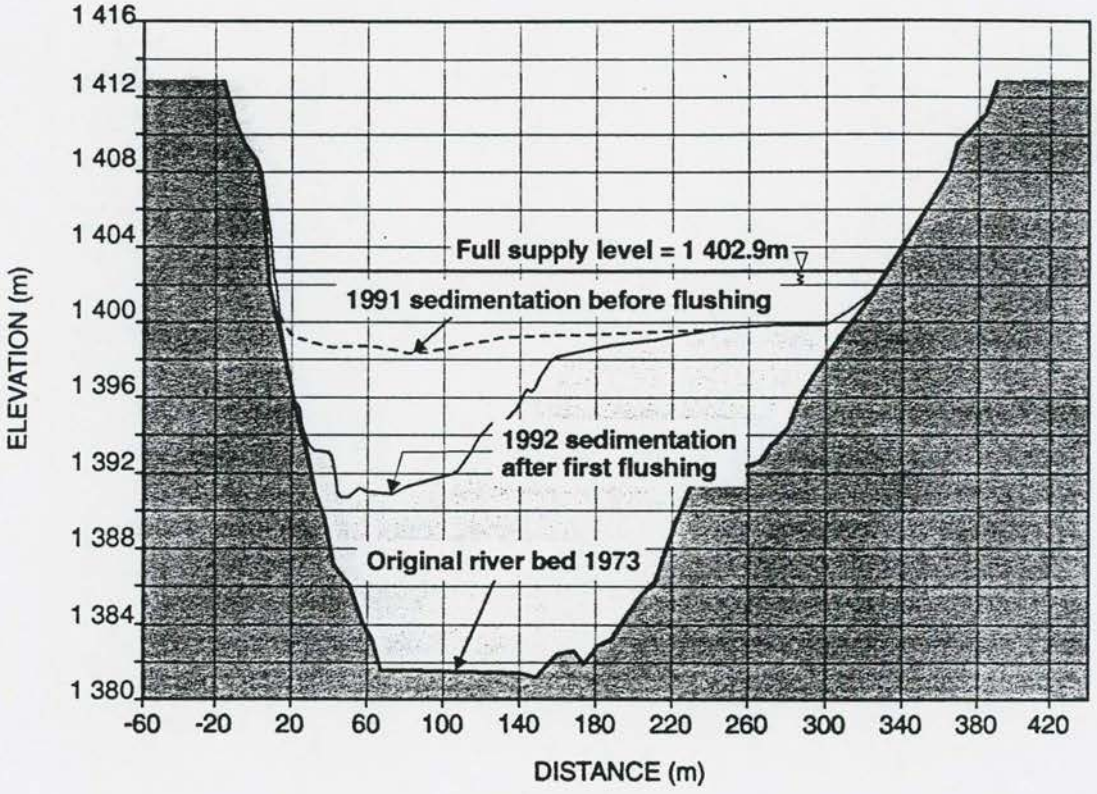

Figure 7.3-1 Welbedacht Reservoir flushing channel deformation

i) **Consolidation of sediment**

Modelling of consolidation is important when critical conditions for mass erosion are linked to sediment characteristics and density. A consolidation methodology as proposed by *Miller (1953)* which relates sediment density changes with time to reservoir operation and sediment characteristics was incorporated in the model, with certain changes:

- The consolidation constant used by *Miller (1953)* was calibrated with South African reservoir data based on reservoir basin surveys. This was necessary because it was found that sedimentation and changing water demands lead to changes in reservoir operation patterns in time.

- Erosion and deposition rates are not constant with time, and the integration method adopted by *Miller* had to be changed by incorporating an effective time approach which accounts for previous deposits as well as recent changes in the bed surface.

7.4 Calibration and verification of the reservoir flushing model (RFM) with South African reservoir data

7.4.1 General

A number of South African reservoirs have been monitored during flood flushing events since 1993 as part of a Water Research Commission project *(Basson et al, 1996)*. The data for Welbedacht Reservoir is used here to calibrate the RFM. Welbedacht Dam **(Photograph 7.4-1)** was completed in 1973 on the Caledon River and is located in a high sediment yield region. During the first three years of operation, it had lost 36 million m^3 of its original 114 million m^3 capacity due to sedimentation. By 1991 the full supply capacity was only 17 million m^3.

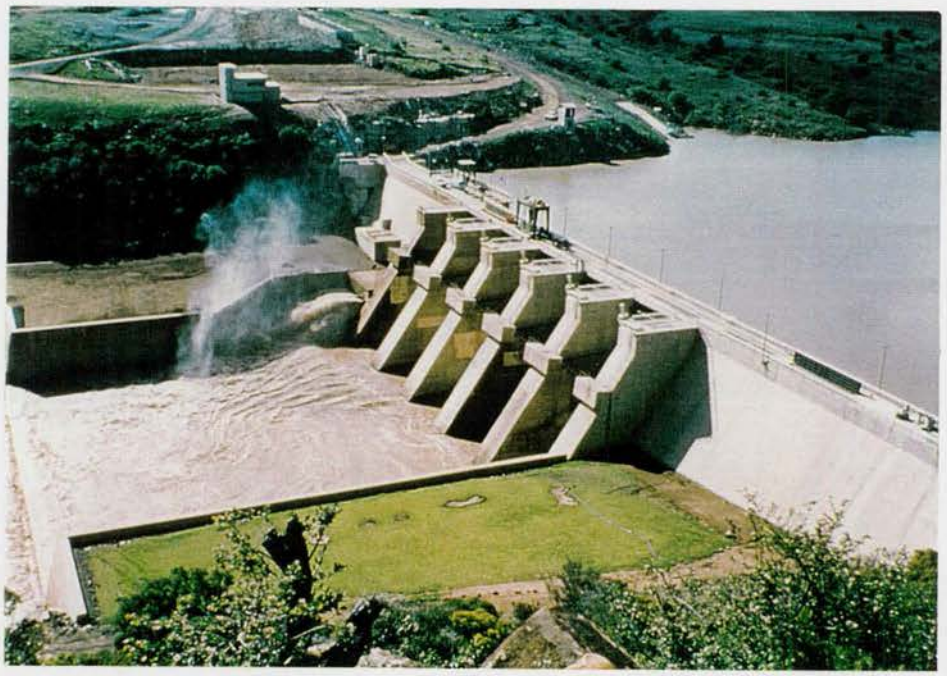

Photograph 7.4-1 Welbedacht Dam

During 1991 it was decided to use flood flushing in order to regain some of the storage capacity. The dam is equipped with five gates, but their elevation is 15 m above the original river bed. Two flushings during October 1991 managed to scour a channel with a bed width of approximately 50 m, and a longitudinal bed profile as indicated in **Figure 7.4-1**. During subsequent flood flushings during the rainy seasons of 1994 and 1995, additional field data was gathered with which the RFM was calibrated and verified.

7.4.2 Calibration of the RFM

The bed shear stress required for mass erosion was determined for two flood flushings during October 1991, using a trapezoidal flushing channel profile in the model and the 1991 sedimentation levels. The scoured bed profile as surveyed in 1992 after the flushings was compared with simulated profiles and a critical mass erosion bed shear stress of 80 N/m^2 was determined. This bed shear stress value agrees with the maximum value as calculated for the flushing channel.

Unfortunately, sediment transport loads were not measured during the 1991 flushings and the model could therefore only be calibrated in terms of bed shear stress to achieve the observed scoured bed profile. A sediment transport equation calibrated in this dissertation with existing data from a number of South African reservoirs (with flushing and storage operation) was used. The observed and calibrated bed profiles are shown in **Figure 7.4-1**. Observed inflows and water levels at the dam, with inflow suspended sediment concentrations based on a sediment load-discharge rating curve were used as boundary conditions in the model. The surveyed 1991 reservoir bed was used as the starting condition, and calibration was based on the surveyed 1992 reservoir bed profile.

7.4.3 Verification of the RFM

Using exactly the same model setup which had been used to determine shear stresses (1991 flushings), it was possible to simulate a 1995 flushing at Welbedacht Dam while using as input the stream power relationship which had been calibrated with South African reservoir data. The simulated curve of cumulative water discharge versus cumulative flushed sediment is shown in **Figure 7.4-2**, and excellent agreement with observed data was obtained. The

observed and predicted sediment transport versus time relationship is shown in **Figure 7.4-3**. The RFM prediction reliability has therefore been proven by the 1995 flushing event.

Although not calibrated for a wide range of flood events, the calibrated model for Welbedacht Reservoir might be used to investigate changes in the outlet configuration and operation to improve sluicing/flushing efficiency and to predict sustainable long-term equilibrium reservoir storage capacities.

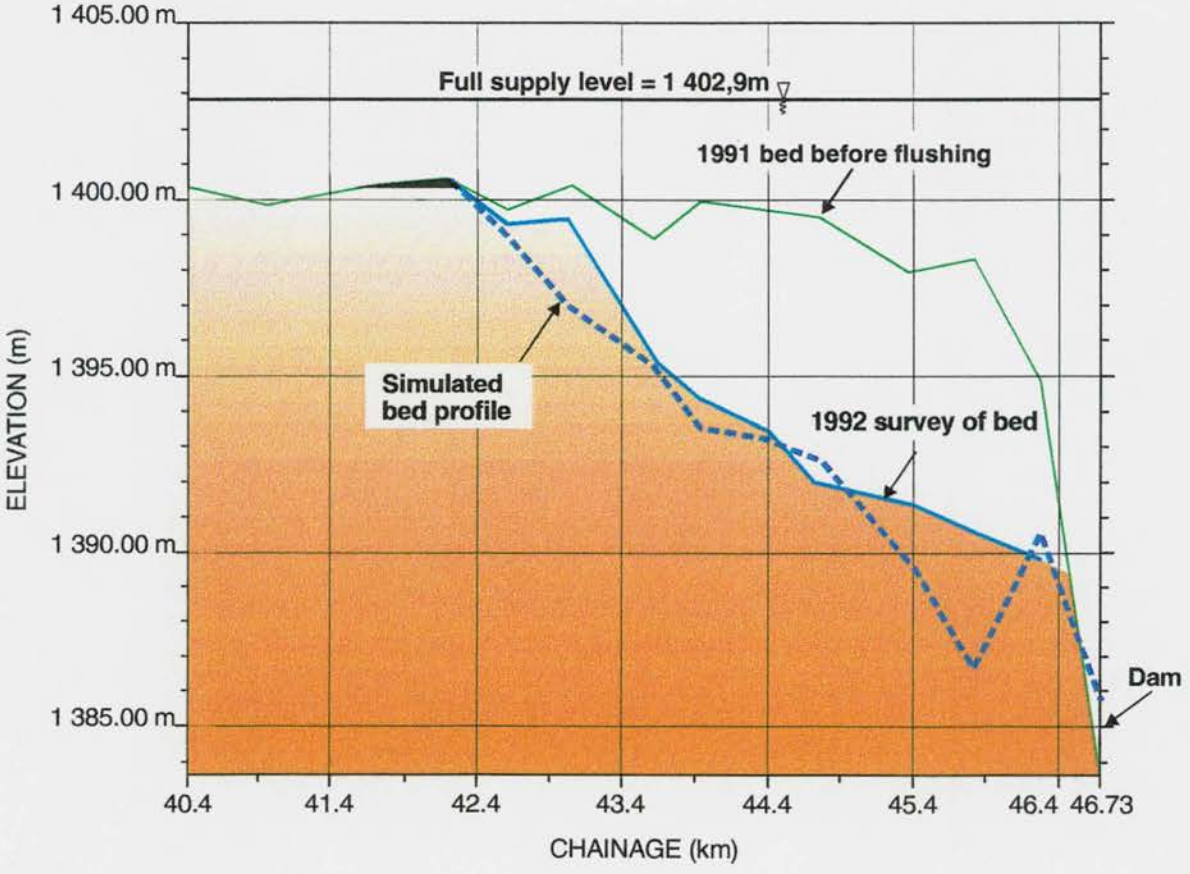

Figure 7.4 - 1 Calibrated and observed flushing channel bed profiles at Welbedacht Reservoir

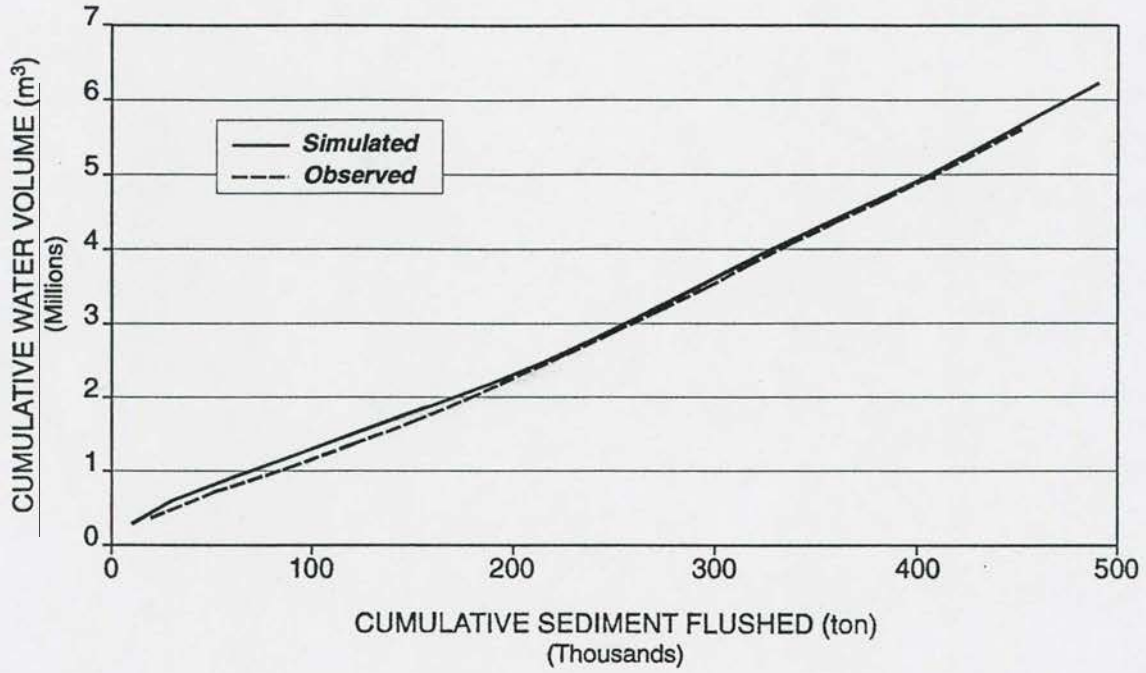

Figure 7.4-2 Welbedacht Reservoir 1995 flushing cumulative mass plot verification of sediment transport

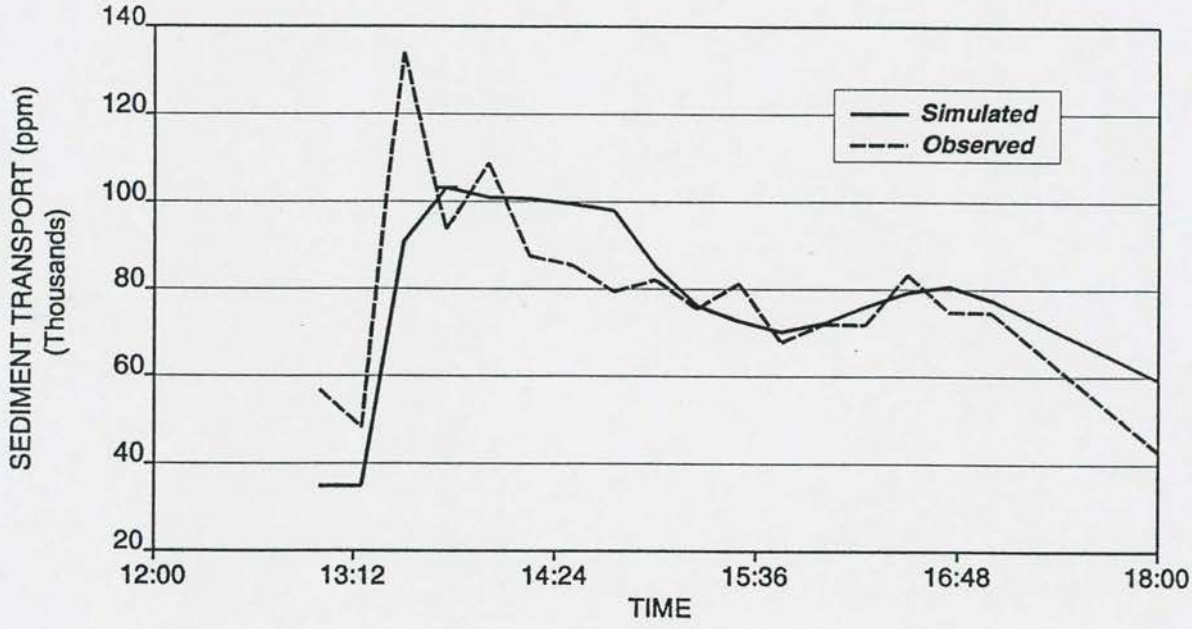

Figure 7.4-3 Welbedacht Reservoir 1995 flushing verification of sediment transport

7.4.4 Simulation of long-term Welbedacht Reservoir capacity

Using the same model configuration as calibrated and verified in the previous sections, simulation of the long-term reservoir capacity which could be achieved through flood flushing was carried out with the current outlets (at a high elevation), but also a scenario with hypothetical gates located at the original river bed.

With the estimated 1 in 2 year flood peak discharge at Welbedacht Dam equal to 800 m^3/s and the present reservoir capacity less than 1 percent of the mean annual runoff, sufficient excess water with high erosive power is available for flushing. Taking the dominant inflow at 500 m^3/s during floods (conservatively low) and inflow suspended sediment concentrations based on the sediment load-discharge rating curve, the long-term equilibrium bed profiles which have been found by simulation are indicated in **Figure 7.4-4**.

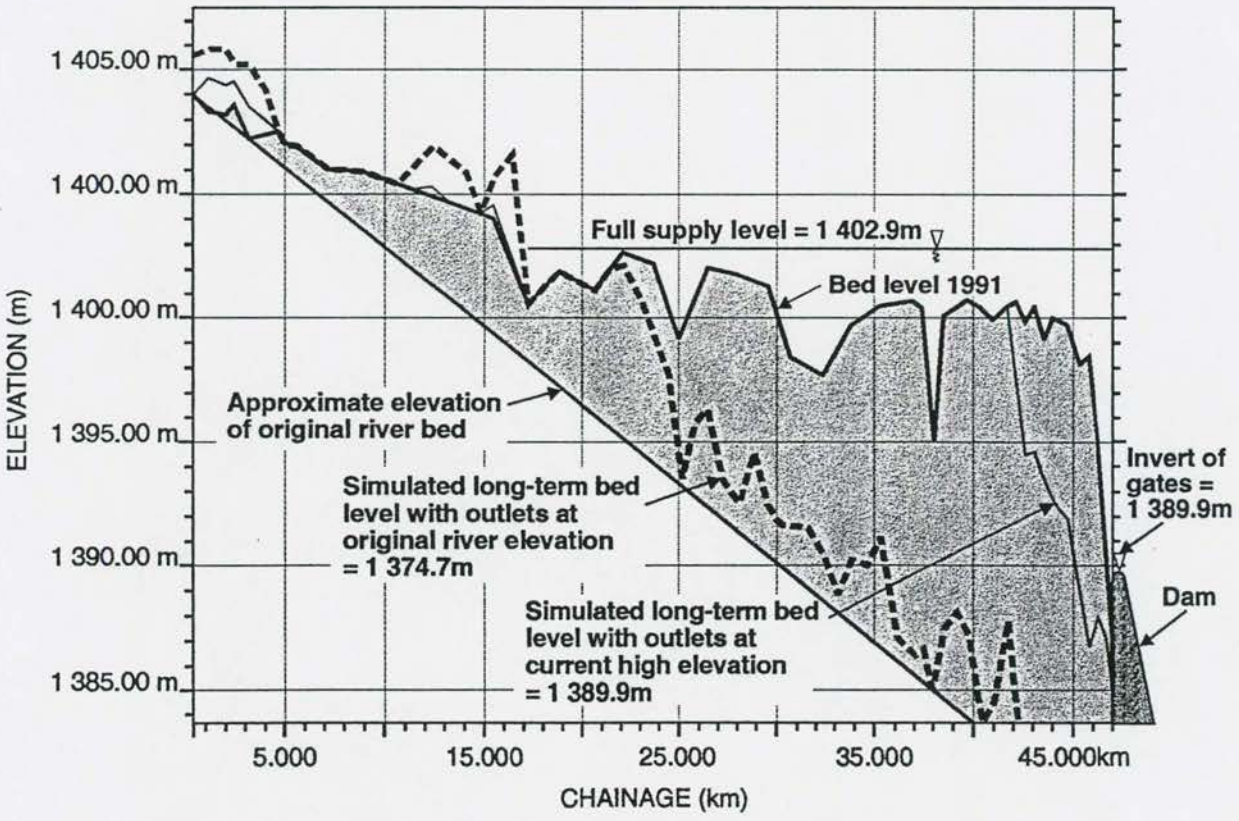

Figure 7.4-4 Simulation of long-term equilibrium sedimentation at Welbedacht Reservoir with flood flushing and different outlet configurations

The current high elevation of the outlets prevents retrogressive erosion far upstream from the dam. In the scenario with bottom outlets and water level drawdown, flushing will be much more efficient. According to **Figure 7.4-4** it looks as if a major part of the original 114 million m^3 reservoir capacity can be restored, but only the flushing channel will be scoured down to the original bed level with bottom outlets provided. The flushing channel shape determines the long-term storage capacity of the reservoir, and overbank sediment deposits will not be resuspended during flushing (unless if flushing duration is long and meandering of the flushing channel develops). The long-term equilibrium storage capacities simulated with high outlet (current) and bottom outlets, are 10 million m^3 and 30 million m^3, respectively.

8. CONCLUSIONS AND RECOMMENDATIONS FOR FURTHER RESEARCH

8.1 Conclusions

The research focussed on the hydraulics of sediment transport through reservoirs. The following key results have been obtained from the study:

- A new total load sediment transport equation was derived based on applied unit stream power principles. This relationship was calibrated with laboratory, river and reservoir data and its accuracy was found comparable with other often used international equations.

- The sediment transport through reservoirs was found to be significantly underestimated by any of the well-known sediment transport equations used internationally where such equations had been calibrated with flume and/or river data only. This explains the unrealistic typical delta formation in the upper reaches with almost no transport into the reservoir area as presented by most computer models based on such equations.

- An extensive field reservoir monitoring programme during high flow conditions and for operations varying from storage to drawdown flushing made it possible to establish a general relationship for sediment transport through reservoirs for South African conditions.

- Non-uniform sediment transport and the sorting process were evaluated with field data.

- A non-equilibrium sediment transport methodology is proposed, which has been calibrated with tests carried out in a canal with fine sediments.

- Re-entrainment of cohesive consolidated sediment was investigated theoretically and verified with laboratory data and by sampling bed sediment in the flushing channel of Welbedacht Dam. The critical shear stress for mass erosion could be related to soil mechanical shear strength, % clay and density of the sediment.

- Channel deformation during retrogressive erosion was investigated and a methodology for modelling was proposed.

- A theory for consolidation of sediment based on a combination of two generally used methods is proposed, with an allowance for non-constant sediment deposition/erosion as would be required in a mathematical model of the process.

- New methodologies for the hydraulic description of density current movement, formation and sediment transport are proposed. For the first time in South Africa, data on a density current in a reservoir formed by suspended sediment have been obtained, which could be used to verify density current sediment transport.

- The theory required for modelling of the reservoir sedimentation processes was incorporated in the existing 1D MIKE 11 river model of the Danish Hydraulic Institute. The model was tested, calibrated with field data, verified and simulations of structural and/or operational changes were carried out to determine long-term equilibrium reservoir sedimentation.

8.2 Recommendations for further research

A number of aspects need further investigation.

- The transport of fine sediments (silt and clay fractions) under uniform equilibrium transport conditions needs to be tested in the laboratory in order to calibrate a sediment transport equation which can be used in simulating the reservoir sedimentation sorting process more accurately.

- The minimization of stream power hypothesis as proposed in this study to describe the formation of a density current needs to be tested in the laboratory with a density current formed by suspended sediment.

- Non-equilibrium sediment transport relationships need to be calibrated for a wider range of conditions than could be evaluated in this research.

- The theory as developed and verified in this study should be incorporated in a two or three-dimensional mathematical model which can model reservoir drawdown flood flushing and sediment deposition processes.

9. REFERENCES

Ackers, P. (1964). "Experiments on small streams in Alluvium." Proc. Am. Soc. Civil Engrs., Vol. 90, No. HY4.

Ackers, P., and White, W.R. (1973). "Sediment Transport: New Approach and Analysis." JHD, Proc. ASCE, Vol. 99, No. HY-11.

Ackers, P., and Thompson, G. (1987). "Reservoir Sedimentation and Influence of Flushing." In: Thorne C.R., Bathurst, J.C. and Hey, R.D. (eds.) Sediment transport in gravel-bed rivers, John Wiley & Sons, Chichester, UK, pp. 845 - 868.

Akiyama and Stephan, J., and Stefan, H.G. (1987). "Onset of Underflow in Slightly Diverging Channels." J. Hydr. Engrg., ASCE, Vol. 113, No. 7, p. 825-844.

Altinakar, M.S., Graf, W.H., and Hopfinger, E.J. (1990). "Weakly depositing turbidity current on small slopes." J. Hydr. Res., Vol. 28, No. 1, NL.

Altunin, S.T. (1947). "Vîpravitelinîie, Zascitnîiei regulirovocinie soorujenia na rekah." Moscow.

Andrews, E.D. and Parker, G. (1987). "Formation of a coarse surface layer as the response to gravel mobility." In: Thorne, C.R., Bathurst, J.C. and Hey, R.D. (eds.) Sediment transport in gravel-bed rivers, Wiley, Chichester, UK, p.269-325.

Annandale, G.W. (1984). "Deposition of sediment in reservoir basins." (In Afrikaans). D. Eng. Thesis, University of Pretoria, South Africa.

Annandale, G.W. (1987). "Reservoir Sedimentation." Vol. 29, in Developments in Water Science, Amsterdam, Netherlands: Elsierivier Science Publishers.

Ariathurai, R and Krone, R.B. (1976). "Finite Element Model for Cohesive Sediment Transport." J. Hydr. Div., ASCE, Vol. 102, No. HY3, p.323-338.

Ashida, K., and Egashira, S. (1975). "Basic Study on Turbidity Currents." Japan Soc. of Civil Engrg., Vol. 237, pp. 37 - 50.

Ashida, K. (1980). "How to predict Reservoir Sedimentation." Proc. 1st International Symposium on River Sedimentation, Beijing, China.

Ashida, K. (1987). "Mountain Torrent Erosion." In: Thorne C.R., J.C. and Hey, R.D. (eds.) Sediment Transport in Gravel-bed River, Wiley, Chichester, UK. p. 513-544.

Athaullah, M. (1968). "Prediction of bed forms in erodible channels." Ph.D Dissertation, Dept. of Civil Eng., Colorado State Univ., Fort Collins, Colorado.

Bagnold, R.A. (1962). "Auto-suspension of transported sediment; Turbidity currents." Proc. royal Soc. of London, Ser. A., 265, p. 315-319.

Bagnold, R.A. (1966). "An approach to the sediment transport problem from general physics." Geol. Survey professional paper 422-I.

Barton, J.R., and Lin, P.N. (1955). "A study of the Sediment Transport in Alluvial channels." Colorado A & M College, Report No. 55JRB2.

Basson, G.R., and Rooseboom, A. (1996). "Dealing with Reservoir Sedimentation." Water Research Commission, South Africa. (to be published).

Bata, G., and Knezevich, B. (1953). "Some Observations on Density Currents in the Laboratory and in the Field." Proc. Minnesota int. Hydraul. Convtn.

Batuca, D. (1980). "Quantitative Aspects of Sediment Transportation Characteristics of some Romanian Watercourses." I.F.A.C. Symposium on Water and Related Land Resource Systems, Ohio.

Batuca, D. (1981). "Contributions to the solution of some morphological problems of the rivers and canals." Ph.D. Thesis, Bucharest, (In Romanian).

Batuca, D. (1986). "Morphometric Equations for Stable Channels of some Romanian Rivers." U.S. - Romanian Workshop on Water resources Engineering, Bucharest.

Bell, H.S. (1940). "Density Currents as agents for transporting sediments." J. of Geology, Vol. L.5.

Bell, H.S. (1942). "Stratified flow in reservoirs and its use in prevention of silting." Misc. Publication No. 491, US Dep. of Agriculture.

Belleudy, Ph and Rahuel, J.L. (1987). "CARICHAR - Mobile bed modelling of graded sediments in unsteady flow. In: Cunge, J.A. and Ackers, P. (eds.) Topics in hydraulic modelling, Proc. 22nd IAHR Congress, Lausanne, Switzerland, p. 138-143.

Bishop, A.A. (1965). Simons, D.B. and Richardson, E.V. "Total bed material transport." Jnl. of the Hydr. Div., ASCE., Vol. 91, HY2.

Blanton, J. (1980). "Reseires Dam." US Department of the Interior, Foreign Disaster Assistance.

Blench, T. (1957). "Regime Behaviour of Canals and Rivers." Bult. Sci. Pub.

Bolton, P. (1984). "Sediment deposition in major reservoirs in the Zambezi Basin." Challenges in African Hydrology and Water Resources, Proc. of the Harare Symposium, IAHS publ. No. 144, pp.559 - 567.

Bondurant, D.C., Garde, R.J., and Albertson, M.L., (1958). "Discussions of Laursen (1958).", JHD, Proc., ASCE, Vol. 84, No. HY-6, Nov.

Bondurant, D.C., et al. (1973). "Sediment Control Methods: D. Reservoirs." J. Hydraul. Div. Am. Soc. Civ. Engrs., Vol. 99, No. HY4, p.617-635.

Borland, W.M. (1971). "Reservoir Sedimentation. River Mechanics Vol. II." Edited and published by Shen, H.W., Colorado.

Bouchard, J.P., Cordelle, M., Labadie, G., and Lorin, J. (1983). Numerical simulation of Mud Erosion in Reservoirs by Floods: Application to Reservoirs of the Durance River."

Brabben, T.E. (1988). "Reservoir Desilting Methods." Hydraulics Research, Wallingford, Technical Note OD/TN 32, January '88.

Bradford, J.M., Ferris, J.E., and Ramley, P.A. (1987). "Interill Erosion Processes: 1. Effect of surface sealing on infiltration, runoff and splash detachment." Soil Sci. Soc. Am. J. 51, pp.1566-1570.

Braune, E. (1984). "Density of sediment in South African Reservoirs." Technical Report 119, Hydrological Research Institute, South African National Hydrogeological Symposium.

Braune E., and Looser, U. (1988). "Cost impacts of sediments in South African Rivers." Sediment and the Environment, IAHS - AISH Publication, pp. 131 - 143.

Breusers, H.N.C., Klaassen, G.J. Brakel, J. and Van Roode, F.C. (1982). "Environmental Impact and Control of Reservoir Sedimentation." 14th Congress on Large Dams, ICOLD, Rio de Janeiro, Q54, R23, p.353-372.

Brown, C.B. (1943). "The Control of Reservoir Silting." US Department of Agriculture, Miss. Publ. No. 521. Aug. '43.

Brown, C.B. (1958). "Sediment Transportation." IN: Rouse, H. (ed.) Engineering hydraulics, Wiley, New York.

Bruk, S. (Ed.) (1985). "Methods of Computing Sedimentation in Lakes and Reservoirs." Unesco, Paris. IHP-11 Project.

Brune, G.M. (1953). "Trap Efficiency of Reservoir." Trans. Am. Geoph. Union, Vol. 34, No. 3.

Bryan, R.B., Govers, G., Poesen, J. (1989). "The concept of soil erodibility and some problems of assessment and application." Catena, Vol. 16, pp.393-412.

Cai, Q., and Wang, G. (1993). "Rill initiation and erosion on hill loess in the hilly Press region, Western Shanxi province." Int. J. of Sed. Research., Vol. 8, No. 3, Dec.

Cao, R. (1992). "Experimental Study on Density Current with Hyperconcentration of Sediment." Int. J. of Sediment Research. Vol. 8, No. 1.

Chang, H.H. (1980). "Stable Alluvial Channel Design." Journal of the Hydr. Div., ASCE, Vol. 106, No. HY5.

Chang, H.H. (1982). "Fluvial Hydraulics of Deltas and Alluvial Fans". J. Hydr. Div., ASCE, Vol. 108, No. HY11, p. 1282-1295.

Chang, H.H. (1985). "River morphology and thresholds." J. Hydr. Engrg., ASCE, pp.509-519.

Chang, H.H. (1988). "Fluvial Processes in River Engineering." John Wiley and Sons, Inc., New York.

Chien, N. (1954). "The Present Status of Research on Sediment Transport." Proc. Am. Soc. Civ. Engrs. Vol. 80.

Chien, N. (1982). "Reservoir Sedimentation." Institute of fluvial processes, Fort Collins, Colorado.

Chikita, K. (1989). "A Field Study on Turbidity Currents Initiated from Spring Runoffs." Water Resour. Res., 25, pp. 257 - 271.

Chitale, S.V. (1977). "Sympathetic changes in river regime." Proc. Inst. of Civ. Engrg., Part 2, London, pp.613-623.

Chitale, S.V. (1995). "Comparison of width and friction factor predictors and implications." J. of Hydraulic Engineering, Vol. 121, No.5.

Chollet, J.P., and Cunge J.A. (1980). "Simulation of Unsteady flow in Alluvial Streams." Appl. Mathematical Modelling, Vol. 4.

Churchill, M.A. (1948) Discussion of "Analysis and use of Reservoir Sedimentation data" by L.C. Gottschalk, Proc. of the Federal Inter-Agency Sedimentation Conference, Washington DC., Jan. 1948, p. 139 - 140.

Colby, B.R. (1964). "Practical Computations of Bed Material Discharge." JHD, Proc. ASCE, Vol. 90, No. HY-2.

Crowder, B.M. (1987). "Economic Costs of Reservoir Sedimentation, a Regional Approach to Estimating Cropland Erosion Damage." J. Soil and Water Conservation 42, No. 3, pp. 194 - 197.

Day, T.J. (1980). "A Study of the Transport of Graded Sediments." HRS Wallingford, Rep. IT 190, April.

Delft Hydraulics (1992). "The Control of Reservoir Sedimentation - A Literature review." Ministry of Development Co-operation, Government of the Netherlands, Delft Hydraulics.

Deng, Z., and Zhang, K. (1994). "Morphometric Equations based on the Principle of maximum Enthropy." International Journal of Sediment Research, Vol. 9, No. 1, April.

Denton, R.A., Faust, K.M., and Plate, E.J. (1981). "Aspects of stratified flow in man-made reservoirs." Research Report ET-203, Sonderforschungs-bereich 80, Univ. of Karlsnike, Germany.

Diplas, P. (1986). "Bed-load transport in gravel-bed streams: Some properties." In: Wang, S.Y., Shen, H.W., and Ding, L.Z. (ed.) River Sedimentation Vol III proc. of the Third Int. Symp. on River Sedimentation, Univ. of Mississippi, USA, p. 925-934.

Diplas, P. (1987). "Bedload transport in gravel-bed streams." J. Hydr. Engrg., ASCE., 113(3), pp. 277-292.

Di Silvio, G., and Armanini, A. (1981). "Influence of the upstream boundary conditions of the Erosion-Deposition Processes in open channel." XIX IAHR Congress, Paper 22, sub. A(a), New Delhi, India, 1981.

Di Silvio, G. (1995). "River modelling." UNESCO IHP-IV Project H-1-2, Working Group on Erosion, Riverbed Deformation and Sediment Transport in River Basins as related to National and Manmade changes.

Dou, G. (1974). "Similarity theory and its application to the design of total sediment transport model. "Research Bulletin of Nanjing Hydraulic Research Inst., Nanjing, China.

Du, G., and Zhang, Z. (1987). "The Erosion of Cohesive Sediment in Retrogressive erosion in Reservoirs."

Duquennois, H. (1956). "New Methods of Sediment Control in Reservoirs." Water Power, pp. 174 - 180.

DWAF. (1995). "Reservoir Basin Survey Data." Department of Water Affairs and Forestry, South Africa.

DWAF. (1996). "Welbedacht Reservoir basin survey." South African Department of Water Affairs and Forestry.

Egiazaroff, J.V. (1965). "Calculation of Non-uniform Sediment Concentrations." J Hydraul. Div. ASCE, No. 4.

Einstein, H.A. (1950). "The bed load function for sediment transportation in Open Channel Flows." Technical Bulletin 1026, U.S. Dept. of Agriculture, Soil Conservation Serv., Washington, D.C., 70p.

Einstein, H.A., and Chien, N. (1953). "Transport of sediment mixtures with large ranges of grain sizes." Missouri River Division Sediment Series No. 2, Univ. of California, Inst. of Eng. Res., US. Army Eng. Div., Missouri River.

Einstein H.A. et al. (1954). "Second approximation to the solution of suspended load theory." Univ. of California, Inst. Res., No. 3.

Einstein, H.A., and Chien, N. (1955). "Effects of heavy sediment concentration near the bed on velocity and sediment distribution." Univ. Calif. Inst. Engrg. Res. No. 8, 1955.

Einstein, H.A., and Abdel-Aal F.M. (1972). "Einstein bed load function at high sediment rates." J. of the Hydraulics Div., ASCE, Vol. 98, No. HY, pp. 137-152.

Engelund, F., and Hansen, E. (1967). "A Monograph on sediment Transport in Alluvial Streams." Teknisk Forlag, Denmark.

Fan, J. (1960). "Experimental Studies on Density Currents." Scientia Sinica, 9(2), pp. 275 - 303.

Fan, J. (1985). "Methods of Preserving Reservoir Capacity." Lecture notes on the Training Course on Reservoir Sedimentation, IRTCES.

Fan, J. (1986). "Turbid Density Currents in Reservoirs." Water Int. 11(3), pp. 107 - 116.

Fan, J. and Morris, G.L. (1992). "Reservoir Sedimentation II. Reservoir desiltation and long-term Storage Capacity." J. Hydr. Engrg., Vol. 118, No. 2, ASCE.

Farrell, G.J., and Stefan, H.G. (1986). "Buayoncy induced plunging flow into Reservoirs and Coastal Regions." St Anthony Falls Hydraulic Laboratory, Univ. of Minnesota, Project Report No. 241.

Ford, D.E. and Johnson, M.C. (1980). "Field Observations of Density Currents in Impoundments." In: Stefan, H.G. (ed.) Surface Water Impoundments, Proc.of the symp. on-, ASCE, Vol.2, Minneapolis, Minnesota, p.1239-1248.

Fukuoka, S. and Fukushima, Y. (1980). "On Dynamic Behaviour of the Head of the Gravity Current in a Stratified Reservoir." Second Int. Symp. on Stratified Reservoir, Trondheim, Norway, Vol. 1, p. 164-173.

Galapatti, R. and Vreugdenhil (1985). "A Depth-integrated Model for Suspended Sediment Transport." J. Hydr. Res., IAHR, Vol.23, No. 4, p. 359-377.

Garde, R.J., and Albertson, M.L. (1958). "The Total Sediment Load of Streams." J. Hydraul. Div. Am. Soc. Civ. Engrs. No. HY6.

Garde, R.J., and Dattatri, J. (1963). "Investigations of the Total Sediment Discharge of Alluvial Streams." University of Roorkee, Research Journal, Roorkee, India, Vol. VI, No. II.

Garde, R.J. (1968). "Analysis of distorted river models with movable beds." (JIP, Vol. 2,5, No. 4, Oct.

Garde, R.J., and Ranga Raju (1977). "Mechanics of Sediment Transportation and Alluviul Stream Problems." Wiley Eastern Limited, New Delhi.

Gessler, J. (1971). "Critical Shear Stress of Sediment Mixtures." Proc. 14th Congress IAHR, Paris, Vol. 3. No. C1.

Gibson, R.E., England, G.L., and Hussey, M.J.L. (1967). "The theory of one-dimensional consolidation of saturated clays. Finite non-linear consolidation of thin homogeneous layers." Geotechnique, Vol. 17.

Gibson, R.E., Schiffman, R.L., and Cargill, K.W. (1981). "The theory of one-dimensional consolidation of saturated clays. II finite non-linear consolidation of thick homogeneous layers." Canadian Geotechnical Journal, Vol. 18.

Gilbert, G.K. (1914). "The transportation of debris by running water, based on experiments made with the assistance of E.C. Murphy." U.S. Geol. Survey Prof. Paper 86, 263p.

Gilbert, R. (1975). "Sedimentation in Lillooet Lake." British Columbia, Can. J. Earth Scis. 12, pp. 1697-1711.

Goldsmith, E, et al. (1985). "Sedimentation, the way for all Dams." The Social and Environmental effects of Large Dams, Vol. 1, pp. 226 - 239, European Ecological Action Group.

Graf, W.H. (1971). "Hydraulics of Sediment Transport." McGraw-Hill.

Graf, W.H. (1983). "The Hydraulics of Reservoir Sedimentation." Int. Water Power and Dam Construction. Vol. 35, no. 4, p.45-52, April.

Grass, A.J. (1970). "Initial instability of fine Bed sand." Proc. Am. Soc. Civil Engrs., Vol. 96, No. HY3.

Guan, Y., Rong, F., Wang, J., Yin, L., and Wang, H. (1991). "A numerical Model for sedimentation in Fenhe Reservoir and the Adjoining Reaches." Int. Journal of Sediment Research, Vol. 6, No. 1, IRTCES.

Guy, H.P., Simons, D.B., and Richardson, E.V. (1966). "Summary of Alluvial Channel data from flume Experiments, 1956 to 61. Sediment Transport in alluvial channels." Geological Survey Professional Paper 462-1.

Han, Q., et al. (1973). "Non-equilibrium Transportation of Sediment in Reservoirs." Collection of Reports on Reservoir Sedimentation, Yellow River Conservancy Commission (in Chinese).

Han, Q.W., and Tong, Z.J. (1982). "The Impact of Danjiangkou Reservoir on the Downstream River Channel and the Environment." 14th Congress on Large Dams, ICOLD, Rio de Janeiro, Brasil, Vol III, Q54, R13, pp. 189-200

Han, Q. and He, M. (1990). "A Mathematical Model for Reservoir Sedimentation and Fluvial Processes." Int. J. of Sediment Res., IRTCES, Vol. 5, No. 2, April, p.43-84.

Hancu, S. (1976). "Regulation of small rivers." Ed. CERES, Bucharest, (in Romanian).

Harleman, D. (1961). "Stratified flow." In Handbook of fluid dynamics, Edited by V. Streeter, McGraw Hill, New York, USA.

Hayter, E.J. (1983). "Prediction of Cohesive Sediment Transport in Estuarial Waters." Ph.D. disseration, Univ. of Florida, Gainesville, Florida.

He M., and Han Q. (1986). "Mechanism and Characteristics of Non-uniform Sediment Transport." In: Wang, S.Y., Shen, H.W. and Ding, L.Z. (ed.) River Sedimentation Vol. III, proc. of the Third Int. Symp. on River Sedimentation, Univ. of Mississippi, Mississippi, USA, p.844-853.

Heineman, H.G. (1972). "Volume-weight of reservoir sediment". J. Hydraul. Div., ASCE,88,5 pp. 188-197.

Henderson, F.M. (1963). "Stability of alluvial channels." Transactions, ASCE, 128(1), 657-720.

Hinze, J.O. (1960). "Turbulence." 1st ed., McGraw-Hill Book Company, Inc., New York, N.Y. pp. 64-66.

Hjulström, F. (1935). "The Morphological Activity of Rivers as illustrated by Rivers Fyris." Bull. Geol. Inst. Uppsala, Vol. 25.

Holley, F.M., and Rahuel, J.L. (1990). "New Numerical/Physical Framework for Mobile-bed Modelling.: J. Hydr. Res., IAHR, Vol. 28, No. 4-5.

Hu, S. (1990). "Self-weight Consolidation on Impervious Bases". M.Sc. Thesis H.H.42, Int. Inst. for Hydr. and Environ. Engrg., IHE, Delft, The Netherlands.

ICOLD. (1989). "World Register of Dams 1988 update." pp. 366.

Ippen, A.T. (1969). "A new look at sedimentation in turbulent streams." J Boston Soc. Civ. Engrs., Vol. 58, No. 3.

ISCW. (1995). Personal Communication, Institute of Soil, Climate and Water, Agricultural Research, South Africa.

Itakura, T., and Kishi, T. (1979). "Open channel flow with suspended sediments." J. of the Hydraulics Div, ASCE, Vol. 106, No. HY8.

Iwagaki, T. (1968). Applied Hydraulics, Marizen Book Co., Series II, Vol. 1 (Japanese) pp. 33.

James, S.C. (1990). "Prediction of Entrainment Conditions for Non-uniform, Non-cohesive Sediment." J. hydr. Res., IAHR, Vol. 28, no. 1, p. 25-42.

Jordaan, J.M. (1989). "The Sediment Problem in South African Reservoirs." Proceedings of the International Symposium on sediment transport modelling, USA pp. 795 - 800.

Kamphuis, J.W. and Hall, K.R. (1983). "Cohesive Material Erosion by Unidirectional Current." J. Hydr. Engrg., ASCE, Vol. 109, no. 1, p.49-61.

Kamphuis, J.W. (1989). "Influence of sand or gravel on the erosion of cohesive sediment." J. of Hydraulic Research, Vol. 28.

Kan, K., and Tamai, N. (1981). "On the plunging point and initial mixing of the inflow into reservoirs." Proc. 25th Japanese Conf. on Hydr., 631-636 (In Japanese).

Kereselidze, N.B., et al. (1985). "Silting and Flushing Mountain Reservoirs, Exemplified by the Rioni Series of Hydroelectric Stations." Hydotech. Constr. Vol. 19, No. 9.

Keulegan, G.H. (1938). "Laws of turbulent flow in open channels." J. natn. Bureau Stand., Washington, Research Paper 1151, Vol. 2.

Keulegan, G.H. (1958). "12th Progress Report on Model Laws for Density Currents." The motion of Saline fronts in still water, U.S. Nat. Bur. Std, Report No. 5831.

Keunen, P.H. (1952). "Estimated size of the Grand Banks Turbidity Current." Am. J. Science.

Krone, R.B. (1962). "Flume Studies of the Transport of Sediment in Estuarial Shoaling Processes." Final Rep., Hydr. Engrg and Sanitary Engrg. Res. Lab., Univ. of California, Berkely, Calif.

Krone, R.R. (1963). "A study of rheologic properties of estuarial sediment." Hyde Eng. Lab. and Soni Eng. Lab., Univ. of California, Berkely, 1963.

Krumdieck, A., and Chamot, P. (1979). "Sediment Flushing at Santo Domingo Reservoir." Water Power and Dam Construction, December, p.25-30.

Kuti, E.O. and Yen, C.L. (1976). "Scouring of Cohesive Soils." J. Hdr. Res., IAHR, Vol. 14, No. 3, p. 195-206.

Lacey, G. (1929). "Stable channels in alluvium." Proc. Inst. Civ. Engrg. Vol. 229, 259.

Lane, E.W., and Koelzer, V.A. (1943). "Density of Sediments Deposited in Reservoirs." Report No. 9, Publ., St. Paul US Engrg., District Sub-Office Univ. of IOWA, USA.

Lane, E.W. (1952). "Progress report on results of studies on the design of stable channels." Report No. HYA-352, U.S. Bureau of Reclamation, Denver, Colorado.

Langbein, W.B. (1964). "Geometry of river channels." J. of the Hydraulic Div. Proc. A.S.C.E., Vol. 90, No. HY4.

Lara, J.M. and Pemberton E.L. (1965). "Initial Weight of Deposited Sediments." Proc. of the Federal Inter-Agency Sedimentation Conference, Misc. Publication no. 970, U.S. of Agriculture, Agricultural Research Service, pp. 818 - 845.

Laursen, E.M. (1958). "The Total Sediment Load of Streams." Prov. Am. Soc. Civ. Engrs., No. HY1.

Le Moigne, G. (1990). "Dam Safety and the Environment." World Bank Technical Paper No. 115, pp. 174.

Le Grange, A. Du P. (1995). "Prediction of Sand-Bed river channel deformation as a result of floods and calibrated by the stage-discharge behaviour of Laboratory Data." Dissertation, University of Stellenbosch.

Leopold, L.B., and Maddock, T. (1953). "The Hydraulic Geometry of Stream Channels and some Physiographic implications." U.S. Geol. Survey, Prof. Paper 252.

Leopold, L.B. (1966). "Data from 146 individual river measurements." In: Bagnold, R.A. (1966). An approach to the Sediment Transport problem from general physics.

Levi, I.I. (1958). "Injenernaia Ghidrologhia." Moscow.

Lewis, A.D. (1936). "Silting of Four Large Reservoirs in South Africa." Communication No. 5, 2nd Congress on Large Dams, Washington.

Li Eding. (Ed.) (1987). "Large Dams in China: History, Achievement, Prospect." Chinese National Committee on Large Dams, pp. 249., China Water Resources and Electric Power Press, China.

Lindley, E.S. (1919). "Regime Channels." Proc. Punjab Eng. Congr., Vol VII.

Little, W.C. and Mayer, P.G. (1976). "Stability of Channel Bed by Armouring." J. Hydr. Div., ASCE, Vol. 102, No. HY11, P. 1647-1662.

Liu, H.K. (1957). "Mechanics of Sediment Ripple Formation." J. Hydraul. Div. Am. Soc. Civ. Engrs. No HY2.

Lu, X. (1991). "An Approximate Method for Calculating the Efficiency of Venting Density Current Through outlet, Proc. of the 5th ISRS, Vol. II, Germany.

Luk, S.H., and Hamilton, H. (1986). "Experimental effects of antecedent moisture and soil strength on rainwash erosion of two Luvisols." Ontario, Geoderma 37, pp. 29-43.

Mahmood, K., and Haque, M.I. (1985). "Boundary shear stress measurement and analysis." Proceedings, Third US-Pakistan Binational Symposium on Mechanics of alluvial channels, Lahore, Pakistan.

Mahmood, K. (1987). "Reservoir Sedimentation: Impact, Extent and Mitigation." World Bank Technical Paper, No. 71, The World Bank, Washington D.C.

McHenry, J.R., Ritchie, J.C., and Cooper, C.M. (1980). "Rates of recent sedimentation in Lake Pepin." Water Resources Bulletin, 16.6 pp. 1049-1056.

Mehta, A.J., and Partheniades, E. (1973). "Effects of physico-chemical properties of fine suspended sediment on the degree of deposition." Proc. of the International Symp. on River Mechanics, Bangkok, Vol. 1, Paper A-41, pp. 465-476.

Mehta, A.J., Parchure, T.M., Dixit, J.G. and Ariathurai, R. (1982). "Resuspension Potential of Deposited Cohesive Sediment Beds." In: Kennedy, V.S. (ed.) Estuarine Comparisons, Academic Press, New York, p.591-609.

Mehta, H.L., Awasthi, A.K. and Sharma, D.K. (1989). "Innovative Approach to Overcome Sediment Constraint of a Hydroelectric Project with small Capacity Storage Reservoir." Indian J. Power & River Valley Development, Vol. 39, No. 8/9, Aug./Sept., p. 231-234.

Meyer-Peter, E., and Müller, R. (1948). "Formulae for bed load transport." Proc. 2nd Congress IAHR, Stockholm, June.

Michon, X., Goddet, J., and Bonnefille, R. (1955). "Etude Théorique et Experimentale de Courants de Densité." Tome 1 et 2, Lab. Nat. d'Hydraulique, Chatou, France.

Middleton, G.V. (1966). "Experiments on Density and Turbidity Currents." Canadian J. of Earth Sciences, Vol. 3, No. 4.

Migniot, C. (1968). "Étude des propriétés de différents sédiment très fins et de leur compartements sous des actions bydrodynamiques." La Houille Blanch, No. 7, p. 591-620.

Migniot, C. (1981). "Erosion et sédimentation en mer et en rivière." In: La pratique des sols et des fondations, Edition Moniteur 1981, 103 pp.

Migniot, C. (1989). Tassement et rhéologie des vases:
Premiére partie. La Houille Blanche, No. 1, p. 11-29
Deuxieme partie. La Houille Blanche, No. 2, p. 95-111

Miller, C.R. (1953). "Determination of the Unit Weight of Sediment for use in Sediment Volume Computations." Memorandum, Bureau of Reclamation, U.S. Dep. of the Interior, Denver, Colorado.

Mitchell, R.J., Tsui, KK. and Sangrey, D.A. (1972). "Failure of Submarine Slopes under wave action." Proc. of the 13th Coastal Engineering Conference, ASCE, p.1515-1541.

Monin, A.S., and Obukhov, A.M. (1973). "Basic Relationships of turbulent Mixing in the surface layer of the Atmosphere." In: Buoyancy Effects in Fluids, Cambridge Univ. Press, Ed. Turner, J.S.

Murray, W.A. (1977). "Erodibility of Coarse Sand-clayey Silt Mixtures." J. Hydr. Res., IAHR, Vol. 14, No. 3, p. 195-206.

Nikuradse, J. (1932). "Gesetzmässigkeiten der turbulenten Ströming in Glatten Rohren." V.D.I. Forschungsheft No. 356.

Nixon, M. (1959). "A study of Bank-full discharge of rivers in England and Wales." Proc. Inst. Civil Engrs, Vol. 12.

Olesen, (1995). "Personal Communication." Danish Hydraulic Institute.

Ohtsubo, K., and Mroaka, K. (1986). "Resuspension of Cohesive Sediments by currents." In: Wang. S.Y., Shen, H.W., and Ding, L.Z. (Ed.), River Sedimentation Vol. III, proc. of the Third Int. Symp. on River Sedimentation, Univ. of Mississippi, Mississippi, USA, p. 1680-1689.

Owen, M.W. (1970). "Properties of consolidating mud." Rep. No. INT83, Hydraulics Res. Station, Wallingford, England.

Parker, G. and Sutherland, A.J. (1990). "Fluvial Armor." J. Hydr. Res., IAHR, Vol. 28, No. 5, p.529-544.

Partheniades, E. (1962). "A Study of Erosion and Deposition of Cohesive Soils in Salt Water." Thesis presented to Univ. of California, Berkeley in partial fulfilment of the requirements for the degree of Doctor of Philosophy.

Partheniades, E. (1965). "Erosion and Deposition of Cohesive Soils." J. Hydr. Div., ASCE, Vol. 91, No. HY1, p. 105-139.

Partheniades, E., and Paaswell, R.E. (1970). "Erodibility of channels with cohesive Boundary." J. of the Hydraulics Div., ASCE, Vol. 96, No. HY3, Proc. Paper 7156, pp. 755-771.

Partheniades, E. (1971). "Erosion and Deposition of cohesive Materials." River mechanics, H.W. Shen, Ed., Fort Collins, Colorado.

Partheniades, E. (1973). "Engineering Properties of Estuarie Sediments." Lecture No. 16, North Atlantic Treaty Organization, Advanced Study Inst. of Estuarine Dynamics, Lisbon, Portugal, June 1973.

Partheniades, E. (1986). "The Present State of Knowledge and Needs for Future Research on Cohesive Sediment Dynamics." In: Wang, S.Y., Shen, H.W. and Ding, L.Z. (ed.) River Sedimentation Vol. III, proc. of the Third Int. Symp. on River Sedimentation, Univ. of Mississippi, Mississippi, USA, p.3-25.

Paul, T.C., and Dhillon, G.S. (1988). "Sluice Dimensioning for Desilting Reservoirs." Intern. Water Power and Dam Construction, Vol. 40, No. 5, May, p. 40-44.

Philpott, W. (1978). "The plunging of density currents." Research Report, Dep. of Civil Eng., Univ. of Canterbury, Christchurch, New Zealand.

Pierce, T.J. and Williams, D.J. (1966). "Experiments on Certain Aspects of Sedimentation Basins." J. Hydr. Engrg., ASCE, Vol. 113, No. 1, p. 80-96.

Pitt, J.P., and Thompson, G. (1984). "The Impact of Sedimentation on Reservoir Life." Proc. Symp. on Challenges in African hydrology and Water Resources, IAHS, Harare, Zimbabwe, Publ. No. 144.

Postel, S. (1989). "Water for agriculture, facing the limits." World Watch Paper 93.

Potgieter, D.J. (1979). "Sedimentbalans in Hendrik Verwoerddam." Taak Nr. A1975, Department of Water Affairs and Forestry, South Africa.

Prandtl, L. (1925). "Essentials of Fluid Dynamics." Blackie (Ed), 1952.

Proffitt, G.T. and Sutherland, A.J. (1983). "Transport of Non-uniform Sediments." J. Hydr. Res., IAHR, Vol. 21, No. 1, p.33-43.

Qian, Ning et al. (1958). "Density Current." China Water Conservancy Press.

Qian, N. (1982). "Reservoir Sedimentation and Slope Stability Technical and Environmental Effects." 14th Int. Congress on Large Dams, ICOLD, Rio de Janeiro, Brasil, Vol. III, O54, G.R. 54, p.639-960.

Qian, Y., et al. (1993). "Influence of the Upstream Reservoirs on the Adjustment of Downstream Alluvial Channel, Intern. J of Sediment Research, Vol. 8, No. 3.

Qian, Z, and Zhang, K. (1994). "Morphometric equations based on the principle of maximum entropy. "Int. Journal of Sediment Research, Volume 9, No. 1, April.

Quinn, M.J. (1980). "A scanning Electron Microscope study of the microstructure of dispersed and flocculated Kaolinite Clay taken out of suspension." A thesis presented to the University of Florida in partial fulfillment of the requirement for the degree of Master of Science.

Rabie, A.L. (1960). "Sedimentgradering en digtheidstudies: Van Ryneveldspas- en Grassridge-damme." Tegniese verslag Nr. 45, Department of Water Affairs and Forestry, South Africa.

Rauws, G., and Govers, G. (1988). "Hydraulic and Mechanical aspects of Rill Generation on agricultural soils." J. of Soil Science 39, pp. 111-124.

Ribberink, J.S. (1987). "Mathematical Modelling of One-dimensional Morphological Changes in Rivers with Non-uniform Sediment." Comm. on Hydr. and Geotech. Engrg., Rep. No. 87-2, Delft, The Netherlands. (Doctoral thesis).

Ribkin, S.I. (1947). "Morfometricescaia clasificatia rek." Moskva.

Rooseboom, A. (1975). "Sediment Transport in Rivers and Reservoirs." D.Eng dissertation, University of Pretoria, (In Afrikaans). (Later published by Water Research Commission, South Africa, Report No. 297/1/92, 1992, English).

Rooseboom, A., and Mülke, F.J. (1982). "Erosion Initiation". Proc. symp. on recent developments in the explanation and prediction of erosion and sediment yield, IAHS Publication No. 137.

Rooseboom, A. (1985). "Sediment transport in Rivers and Reservoirs." Lecture notes, University of Pretoria.

Rooseboom, A., et al. 1986. "Welbedacht Reservoir - The Effect of Different Operating Rules on the Sedimentation Rate and Reservoir Yield with Reference to off-channel Storage in the Proposed Knelpoort Reservoir." South African Department of Water Affairs and Forestry.

Rooseboom, A. (1992). "Sediment transport in rivers and reservoirs. A South African perspective." Water Research Commission Report No. 297/1/92, South Africa.

Rottner, J. (1959). "A formula for bed load transportation." La Houille Blancke 4, No. 3.

Rouse, H. (1937). "Engineering Hydraulics." John Wiley & Sons, New York, p. 797.

Sánchez, J.C. (1982). "Mathematical Model for Simulation of Delta Formation and Erosion Downstream of a Reservoir." 14th Int. Congress on Large Dams, ICOLD, Rio de Janeiro, Brasil, Vol. III, Q54, R8, p.117-129.

Savage, S.B., and Brimberg, J. (1975). "Analysis of Plunging Phenomena in Water Reservoirs." J. of Hydr. Research, IAHR, Vol. 13, No. 2 p.187-204.

Schälchi, U. (1987). "Reservoir Sedimentation and Flushing in a Hydraulic Model." In: Topics in Hydr. Modelling, Proc. 22nd IAHR Congress, Lausanne, Switzerland, p. 240-245.

Scheuerlein, H. (1987). "Sedimentation of Reservoirs - Methods of Prevention, Techniques of Rehabilitation." First Iranian Symp. on Dam Engrg., Teheran, Iran, June "87.

Scheuerlein, H. (1993). "Estimation of flushing efficiency in silted reservoirs." Proc. of the 1st. ICHE, Vol. 1, Part A, USA.

Shen, H.W., and Hung, C.S. (1971). "An Engineering approach to total bed material load by regression analysis." Proc. Sedimentation Sym., Berkeley, 1971.

Shields, A. (1936). "Anwendung der Aehnlichkeits-mechanik und der Turbulenz for schung auf die Geschiebe beweging." Mitteilungen der Preuss. Versuchsanstalt für Wasserbau und Schiffsbau, Berlin.

Simons, D.B., and Albertson, M.L. (1963). "Uniform Water Conveyance in Alluvial Material." Trans. Am. Soc. Civil Engrs., Vol. 128/1.

Simons, D.B., and Sentürk. F. (1977). "Sediment transport technology." Water Resources publications, Colorado.

Singh, B. and Shah, C.R. (1971). "Plunging Phenomenon of Density Currents in Reservoirs." La Houille Blanche, Vol. 26, No. 1, p. 59-64.

Singh, K.P. (1987). "Lake Sedimentation Reduction Techniques." Public Works, Vol. 118, No. 9.

Sloff, C.J. (1991). "Reservoir Sedimentation, a Literature Survey." Communications on Hydraulic and Geotechnical Engineering, Report No. 91-2.

Smil, V. (1987). "Land reclamation in China: an ancient problem getting worse." Land Degradation on Society, Blaikie and Brookfield eds. pp 214 - 223.

Stein, R.A. (1965). "Laboratory Studies of total load and apparent Bed-load." J. of Geophysical Research, Vol. 70, No. 8, pp. 1831-1842.

Stevens, J.C. (1936). "The silt problem." (with discussion by Messrs F.E. Banner, M.P. O'Brien, W.W. Waggener, and Bisschop), Trans. Am Soc. Civil Eng., V.101, p.207-288.

Strand, R.I. (1974). "Sedimentation" in Design of Small Dams, Bureau of Reclamation, U.S. Dep. of the Interior, Revised reprint.

Streeter, V.L. (1971). "Fluid mechanics." McGraw-Hill, New York.

Sundborg, A., (1964). "The importance of the Sediment problem in the technical and economic development of river basins." Ann. Acac. Reg. Sci. Uppsala, 8, pp. 33-52.

Takasu, S. (1982). "Hydraulic design and model tests on sediment release facility of Unazuki Dam." Q54, R3, 14th ICOLD Congress, Rio de Janeiro.

Tan, Y. (1994). "Reservoir Design and Management to Control Sediment." Topic VI, Russia.

Terwindt, J.H.J., Breusers, H.N.C., and Svasek, J.N. (1966). "Experimenteel onderzoek naar de erosie van zand-klei laminaten." Nota K241, WL Delft (In Dutch).

Thomas, W.A., and Prasuhn, A.L. (1977). "Mathematical modelling of sediment transport, scour and deposition in river channels". 17th Congress IAHR, Germany.

Thorn, M.F.C., and Parsons, J.G. (1980). "Erosion of cohesive sediments in estuaries: An engineering guide." Proc. Third Int. Symp. on Dredging Technol., Paper F1, Bordeaux, France.

Thorne, C.R. (1982). "Processes and Mechanics of River Bank Erosion." In: Hey, R.D., Bathurst, J.C. and Thorne,C.R. (eds.) Gravel-bed rivers, Wiley, Chichester, UK, p. 227-272.

Toffaletti, F.B. (1968). "A procedure for computation of the total river sand discharge and detailed distribution beds to surface." Committee on channel stabilization, Corps of Engineers, U.S. Army Technical Report No. 5, Vicksburg, Mississippi, November.

Turner, J.S. (1973). "Buoyancy Effects in Fluids." Cambridge University Press, Cambridge, England.

Turner, J.S. (1979). "Buoyancy Effects In Fluids." Cambridge Univ. Press, London, England.

Un Groupe De... (1982). "Controle de l'alluivonnement des retenues." Q54 - R34, 14 th ICOLD Congress, Travail du Comite' Francois de Grand Barrages, Rio de Janeiro. FAO. (1975).

Van Rijn, L.C. (1982). "Computation of Bed-Load and Suspended Load." Report S487-11, Delft Hydraulics Laboratory, Delft, The Netherlands.

Van Rijn, L.C. (1984). "Sediment transport, Part I: Bed load transport." Journal of Hydraulic Engineering. Vol. 110, No. 10.

Van Rijn, L.C. (1984). "Sediment transport, Part II: Suspended sediment load transport." Journal of Hydraulic Engineering, Vol. 110, No. 11.

Vanoni, V.A., and Namicos, G.N. (1960). "Resistance properties of sediment-laden streams." Trans. ASCE, Vol. 125, 1960.

Vanoni, V.A. (Ed.) (1975). "Sedimentation Engineering." ASCE Task Committee for the Preparation of the Manual on Sedimentation, USA, New York.

Vanoni, V.A. (1977). "Sedimentation Engineering" ASCE, New York, p. 587-604 and p. 616-618.

Vasiliev, O.F., et al. (1993). "Mathematical modelling of sedimentation in deep reservoir." Proc. of 1st ICHE, Vol. I, Part A, USA.

Velikanov, M.A. (1954). "Principle of the Gravitational Theory of the movement of sediments." Acad. of Sci. Bul., USSR, Geophy. Series, No. 4, pp. 349-359.

Velikanov, M.A. (1958). "Ruslovoi Protess." Moscow.

Von Kármán, Th. (1948). "Progress in the statistical theory of turbulence." Proc. Nat. Acad. Sci. Washington, 34, p.539.

Wallace, R. (1994). Personal communication, Tescor, South Africa.

Walling, D.E. (1989). "The erosion problem." Intern J. Sediment Research, Vol. 4, No. 1, pp. 1 - 11.

Wang, S. and Zhang, R. (1989). "Sediment Transport Rate for Non-uniform Sand." In: Wang, S.S. (ed.) Sediment Transport Modelling, Proc. Int. Symp., New Orleans, USA.

Wang, X., and Qian, N. (1992). "Velocity profiles of sediment-laden flow." Int. Journal of Sediment Research, Vol. 7, No. 1, March.

Wang, G.P., Zang, B.Q., Luk, S.H., and Chen, H. (1992). "Prediction of soil erosion on the hillslopes in the hilly Loess Region, West Shanxi." Interrill erosion. Soil and Water Conservation in China, No. 5.

Wang, S.S.Y. (1993). "Advances in Hydro-Science and Engineering." Proc. of the 1st ICHE, USA.

White et al. (1975). Sediment transport equation accuracies. In: Randkivi, A.J. Loose Boundary Hydraulics, 1992, Publisher R. Maxwell.

White, W.R., Bettess, R., and Paris, E. (1982). "Analytical approach to river regime." J. Hydr. Div., ASCE, 1179-1193.

White, W.R., and Bettes, R. (1984). "The Feasibility of Flushing Sediments through Reservoirs." Proc. Symp. on Challenges in African Hydrology and Water Resources, IAHS, Harare, Zimbabwe, Publ. No. 144.

Wu, D. (1994). Personal Communication, IRTCES, China.

Wu, D. (Ed.) (1994). "Movement of Density Current in Reservoir." International Research and Training Centre on Erosion and Sedimentation.

Xu Muju (1990). "Sediment problems at Dujiangyan Project." International Journal of Sediment Research, Vol. 5, No. 2. April.

Yang, C.T. (1972). "Unit Stream Power and Sediment Transport." Proc. Am. Soc. Civ. Engrs. Vol. 98, No. 10, 1972.

Yang, C.T. (1973). "Incipient motion and sediment transport." Proc. Am. Soc. Civ. Engrs, Vol. 99, No. HY10.

Yang, C.T. (1976). "Minimum unit stream power and fluiral hydraulics." Jnl. of the Hydr. Div. ASCE., Vol. 102, HY7.

Yang, C.T. (1979). "Unit Stream Power Equations for Total Load." J. of Hydrology, Vol. 40, 1979, pp. 123-138.

Yang, C.T., and Molinas, A. (1982). "Sediment Transport and Unit stream power function." J. of the Hydraulics Division, ASCE, Vol. 108, No. HY6, June, pp. 774-793.

Yang, C.T. (1984). "Unit Stream Power Equation for Gravel." J. of the Hydraulics Div., ASCE, Vol. 110, No. HY12.

Yang, C.T., and Kong, X. (1991). "Energy dissipation rate and sediment transport." Journal of Hydraulics Research, Vol. 29, No. 4.

Yang, G. (1992). "Mathematical Modelling of Alluvial Rivers." (in Chinese).

Yoon, Y.N. (1991). "The State and the Prospects of the Direct Sediment Removal Methods from Reservoirs." Proc. of Intern. Symp. on Special Problems of Alluvial Rivers, including those of Intern. Rivers, Korea.

Zanke, U. (1977). "Berechnung der Sinkgeschwindigkeiten von Sedimenten." Mitt. des Franzius - Instituts für Wasserbau, Heft 46, Seite 243, Technical University, Hannover, West Deutschland.

Zhang, Q., and Long, Y. (1980). "Sediment problems of Sanmenxia Reservoir, Proceedings of International Symp. on River Sedimentation, China."

Zhang, Q., et al. (1983). "A mathematical model for the prediction of the sedimentation process in rivers." Proc. of the 2nd ISRS, China.

Zhang, R. (1959). "A study of the sediment transport capacity of the Middle and Lower Yangtze River, J. of Sediment Research, Vol. 4, No. 2, Beijing, China (In Chinese).

Zhang, R., and Qian, N. (1985). "Reservoir Sedimentation", Lecture notes on the Training Course on Reservoir Sedimentation. IRTCES (Int. Research and Training Centre on Erosion and Sedimentation), Sed. Research Lab. of Tsinghua Univ., Beijing, China, sponsored by UNESCO and PRC.

Zhou, B., et al. (1989). "Regulating Water and Sediment for preserving storage capacity in Hengshan Reservoir, Proc. of the 4th ISRS, Vol. 2.

Zhou, Z. (1994). "Impacts of Sediment Control." Int. Workshop on the State of the Research needs of Reservoir Sedimentation, ICCORES, Russia.

Zhou, Z. (1995). "Preservation of reservoir storage capacity - experience of China." Proc. The 1995 International Workshop on Reservoir Sedimentation, San Francisco, California.